CERN-2008-006
CARE-Conf-08-001-HHH
25 August 2008

ORGANISATION EUROPEENNE POUR LA RECHERCHE NUCLEAIRE
CERN EUROPEAN ORGANIZATION FOR NUCLEAR RESEARCH

CARE-HHH-APD Workshop on

Interaction Regions for the LHC Upgrade, DAFNE, and SuperB

"IR'07"

Frascati, Italy, 6 - 9 November 2007

PROCEEDINGS

Editors:
W. Scandale
F. Zimmermann

GENEVA
2008

CERN – 250 copies printed – August 2008

ABSTRACT

This report contains the Proceedings of the CARE-HHH-APD Mini-Workshop "IR'07," which was held in Frascati, Italy, from 7 to 9 November 2007.

The central theme of the IR'07 Mini-Workshop was the upgrade of the LHC interaction region (IR). A second topic was the experience with the upgraded DAFNE IR as well as the ongoing plans and studies for SuperB, plus possible applications of crab-waist collisions for the LHC upgrade. Discussions during the workshop addressed the performance and limitations of the IR-upgrade optics performance, the optimization of new LHC triplet magnets, the US-LARP magnet strategy (response to Lucio Rossi's "challenge"), heat deposition, early-separation dipoles, detector-integrated quadrupoles, strategy for crab cavities, beam–beam wire compensators, and crab-waist collisions.

At IR'07 all auxiliary systems, e.g. wires and crab cavities, received a strong boost. Energy deposition was shown to add an important criterion to the optics requirements—in a first attempt a 2-cm thick stainless-steel liner was considered; more realistic configurations will need to be explored in the future. Improved upgrade designs presented at IR'07 promise higher and better luminosity than earlier scenarios. Some remaining uncertainties for Nb_3Sn magnets were identified, for example concerning field quality and temperature margin. Only two IR upgrade optics versions were retained from a larger number of earlier proposals, namely the so-called "low β-max" and "symmetric" optics. Conflicting time scales were evidenced: the accelerator input to the experiments is requested almost immediately, while the experiments require first LHC physics results to determine the boundary conditions for the accelerator upgrade. Finally, IR07 confirmed the three principal LHC high-luminosity upgrade paths: (1) early separation, (2) full crab crossing, and (3) large Piwinski-angle scheme.

PREFACE

The CARE-HHH-APD Mini-Workshop on Interaction Regions, "IR'07", was held at INFN, Frascati, Italy, from 7 to 9 November 2007 (see http://care-hhh.web.cern.ch/CARE-HHH/IR07/). The workshop was sponsored by the European accelerator network for high-energy high-brightness hadron beams, CARE-HHH. It was attended by 39 participants, about half of whom came from CERN. The workshop scope and programme were drafted by Walter Scandale and Frank Zimmermann (both CERN) with input from Marica Biagini (INFN), Jean-Pierre Koutchouk (CERN), and Stephen Peggs (LARP & BNL).

The workshop scope extended from the upgrade of the LHC interaction region, to the rebuilt DAFNE IR and the IR plans for SuperB. Key topics addressed at IR'07 included:

- the **LHC IR-upgrade optics** performance and limitations;
- the optimization of **new LHC triplet magnets**;
- the **US-LARP magnet strategy** (Lucio Rossi's challenge);
- **heat deposition**;
- **early-separation** dipoles;
- **detector-integrated quadrupoles**;
- **crab cavities, wire compensators, and crab-waist collisions.**

The three main goals were to narrow down the possible LHC IR optics options and to converge on magnet parameters; to identify ingredients for the two LHC upgrade phases; and to strengthen the collaboration with DAFNE/SuperB studies and to explore the applicability of advanced IR concepts to LHC.

Intermediate discussion sessions focused on a number of open questions, related to (1) synergy or divergence between phase-1 and phase-2 magnets, (2) the need to complement a β^* reduction by crab cavities, (3) possible US-LARP and US magnet contributions, (4) the streamlining of the Q0 and D0 efforts, (5) advantages and drawbacks of a mixed triplet combining Nb_3Sn and NnTi magnets, (6) the crab cavity experience at KEK, (7) experimental tests of various types of levelling, (8) tradeoff between luminosity upgrades via current increase and via β^* reduction, (9) the minimum acceptable luminosity lifetime, (10) off-momentum beta beating, (11) the maximum tolerable number of low-distance long-range collisions, and (12) the collimator settings with larger physical aperture.

The final round-table discussion debated the following questions:

- strategy for scenarios,
- levelling & large Piwinski angle — where, how, real test?
- when & where trade-off between experiments and accelerator?
- strategy for magnets,
- strategy for wires,
- strategy for crab cavities, and
- strategy for crab waist in hadron colliders.

The main outcome of IR'07 can be summarized as follows: All auxiliary systems (e.g. wire compensators and crab cavities) received a strong boost. Energy deposition was shown to add an important criterion to the optics requirements — a 2-cm thick stainless-steel liner was considered in a first attempt; more realistic configurations will need to be explored in the future. Improved upgrade designs and scenarios presented at IR'07 promise higher and better luminosity than earlier scenarios. For Nb_3Sn magnets, some uncertainties still exist, for example concerning their field quality, and temperature margin. Only two IR upgrade optics were retained from a larger number of earlier proposals, namely the so-called "low β-max" and the "symmetric" scheme. Conflicting time scales for the upgrades of the experiments and accelerator were highlighted: the accelerator input to the experiments is requested almost immediately, while the experiments need first LHC physics results to determine the boundary conditions for the accelerator upgrade.

Further information on the workshop can be accessed from its home web site,
http://care-hhh.web.cern.ch/CARE-HHH/IR07/ .

The IR'07 workshop schedule was structured in nine sessions spanning over the full three days. In total 42 talks were given, complemented by 4 heated round-table discussions. The workshop also included a tour of the rebuilt DAFNE IR with large crossing angle, guided by Catia Milardi. The proceedings are structured according to the nine plenary sessions:

- Session 1: **Introduction** (convener W. Scandale), with presentations by M. Calvetti, C. Milardi, M. Biagini, W. Scandale, S. Peggs, E. Todesco, and D. Tommasini

- Session 2: **IR Triplet Magnets** (convener J. Strait), with presentations by P. Wanderer, G.L. Sabbi, G. Ambrosio, A. Zlobin, and R. Ostojic

- Session 3: **Early Separation** (convener C. Milardi), with presentations by J.-P. Koutchouk, P. Limon, G. Sterbini, W. Scandale, and F. Zimmermann

- Sessions 4: **Optics** (convener S. Peggs), with presentations by M. Giovannozzi, R. De Maria, R. Tomas, E. Laface, and G. Robert-Demolaize

- Session 5: **Energy Deposition** (convener J.-P. Koutchouk), with presentations by F. Broggi, and E. Wildner

- Session 6: **D0 and Q0 Detector Interface** (convener P. Limon), with presentations by M. Nessi, J. Nash, E. Tsesmelis, and S. Peggs

- Session 7: **Beam–Beam Compensation, Crab Cavities** (convener F. Zimmermann), with presentations by U. Dorda (2), C. Milardi, U. Dorda, R. Calaga, and F. Zimmermann

- Session 8: **Crab Waists, Flat Beams** (convener M. Biagini), with presentations by M. Zobov, E. Levichev, and P. Raimondi

- Session 9: **Final Round Table and Conclusions** (conveners W. Scandale and F. Zimmermann).

These proceedings have been published in paper and electronic form. The paper copy is in black and white; the electronic version contains colour pictures. Electronic copies can be retrieved through:
`http://care-hhh.web.cern.ch/CARE-HHH/IR07/Proceedings`

The compilation of these proceedings would not have been possible without the help of the conveners and speakers. The organizational support by the workshop secretaries Claudine Bosteels and Muriel Macchi is also gratefully acknowledged, as is the help of Lauriane Bueno for completing the final proceedings. In particular, we would like to thank all the participants for their stimulating contributions and lively discussions.

The IR'07 workshop was sponsored and supported by the European Community-Research Infrastructure Activity under the FP6 "Structuring the European Research Area" programme (CARE, contract number RII3-CT-2003-506395).

Geneva, 1 June 2008

W. Scandale and F. Zimmermann

CONTENTS

Preface v

SESSION 1: INTRODUCTION
(convener: W. Scandale)

Welcome *M. Calvetti*

DAΦNE Interaction Regions Upgrade
C. Milardi 1
The SuperB-Factory Accelerator Project
M.E. Biagini 6
Scenarios for the LHC Upgrade[1)]
W. Scandale, F. Zimmermann 10
News from the U.S. LHC Accelerator Research Program, LARP
S. Peggs 19
Nb-Ti Symmetric Triplets for the LHC Luminosity Upgrade
E. Todesco 21
CERN Plans on High Field Magnets Development
D. Tommasini 25

SESSION 2: IR TRIPLET MAGNETS
(convener: J. Strait)

U.S. LARP Magnet Program
P. Wanderer 26
High Field Niobium-Tin Quadrupoles
G.L. Sabbi 31
LARP Long Nb_3Sn Quadrupole
G. Ambrosio 33
LARP Joint IR Studies
A.V. Zlobin 36
Phased Approach to the LHC Insertion Upgrade and Magnet Challenges
R. Ostojic 38

[1)] The same paper was submitted to the proceedings of the CARE-HHH-APD BEAM'07 workshop, *http://care-hhh.web.cern.ch/CARE-HHH/BEAM07*.

SESSION 3: EARLY SEPARATION
(convener: C. Milardi)

New Results on the Early Separation Scheme
J.P. Koutchouk, G. Sterbini 40
Integrating Early-Separation Dipoles in CMS
P.J. Limon 43
D0 Design and Beam–Beam Effect
G. Sterbini, J.-P. Koutchouk 46
Round Table Magnet Discussion and Conclusions[2] *W. Scandale, F. Zimmermann*

SESSION 4: OPTICS
(convener: S. Peggs)

Optics Issues for Phase 1 and Phase 2 Upgrades
M. Giovannozzi 51
Phase 1 Optics: Merits and Challenges
R. de Maria 56
Correction of Multipolar Field Errors in Insertion Regions for the Phase 1 LHC Upgrade and Dynamic Aperture
R. Tomás, M. Giovannozzi, R. de Maria 62
Q0 Status
E. Laface, W. Scandale, C. Santoni 67
Update on US LARP Optics Studies *G. Robert-Demolaize*[3]

SESSION 5: ENERGY DEPOSITION
(convener: J.P. Koutchouk)

Energy Deposition in the Triplet and TAS Issues
F. Broggi 71
Are Large-Aperture NbTi Magnets Compatible with 1e35?
E. Wildner, C. Hoa, E. Laface, G. Sterbini 74

SESSION 6: D0 AND Q0 DETECTOR INTERFERENCE
(convener: P. Limon)

SLHC and ATLAS, Initial Plans
M. Nessi 81
CMS' View on D0 and Q0 *J. Nash*[2]
LHC Interaction Region Upgrades and the Machine–Experiment Interface
E. Tsesmelis 83
Round Table Discussion[2] *S. Peggs*

[2] A paper was not submitted to the proceedings. However, the slides presented are available in electronic form at *http://care-hhh.web.cern.ch/CARE-HHH/IR07*.

[3] A paper was not submitted to the proceedings. However, the slides presented are available in electronic form at *http://care-hhh.web.cern.ch/CARE-HHH/IR07*. For a description of recent US-LARP optics studies for the LHC upgrade also see: T. Sen, J. Johnstone, "Analysis of Optics Designs for the LHC IR Upgrade," Proc. PAC'07 Albuquerque, pp. 1718.

SESSION 7: BEAM–BEAM COMPENSATION AND CRAB CAVITIES (convener: F. Zimmermann)

Beam–Beam Issues for LHC Upgrade Phases 1 and 2
U. Dorda, F. Zimmermann 86
DAΦNE Lifetime Optimization with Octupoles and Compensating Wires
C. Milardi, D. Alesini, M.A. Preger, P. Raimondi, M. Zobov, D. Shatilov 92
Wire Compensation: Performance, SPS MDs, Pulsed System[4)]
U. Dorda, F. Zimmermanna 98
Small Angle Crab Crossing for the LHC[4)]
R. Calaga, U. Dorda, R. Tomás, F. Zimmermann 102
Discussion on Beam–Beam Compensation and Crab Cavities[2)] *F. Zimmermann*

SESSION 8: PHASE-2 - CRAB WAISTS, FLAT BEAMS (convener: M. Biagini)

Crab Waist Collision Studies for e^+e^- Factories
M. Zobov, P. Raimondi, D. Shatilov, K. Ohmi 110
Dynamic Aperture Studies in e^+e^- Factories with Crab Waist
S. Glukhov, E. Levichev, P. Piminov, D. Shatilov 114
Crab Waist Options for LHC[2)] *P. Raimondi*

SESSION 9: FINAL ROUND TABLE AND CONCLUSIONS (conveners: W. Scandale, F. Zimmermann)

Summary of CARE-HHH IR'07
W. Scandale, F. Zimmermann 117

List of Participants 125

[2)] A paper was not submitted to the proceedings. However, the slides presented are available in electronic form at *http://care-hhh.web.cern.ch/CARE-HHH/IR07*.

[4)] This paper also contains the material presented by the same authors at the CARE-HHH-APD BEAM'07 workshop, *http://care-hhh.web.cern.ch/CARE-HHH/BEAM07*.

DAΦNE INTERACTION REGIONS UPGRADE

C. Milardi, INFN/LNF, Frascati (Roma), Italy for DAΦNE Collaboration Team[1].

Abstract

DAΦNE, the Frascati Φ-factory, has recently completed experimental runs for the three main detectors, KLOE, FINUDA and DEAR achieving 1.6x10^{32} cm^{-2}s^{-1} peak and 10 pb^{-1} daily integrated luminosities.

Improving these results by a significant factor requires changing the collision scheme. For this reason, in view of the SIDDHARTA detector installation, relevant modifications of the machine have been realized, aimed at implementing a new collision scheme based on a large Piwinski angle and *crab-waist*, together with several other hardware modifications involving injection kickers, bellows and beam pipe sections.

INTRODUCTION

DAΦNE [2] is a lepton collider, working at the c.m. energy of the Φ resonance (1.02 GeV). It provided high K meson rates to three different experiments: KLOE, DEAR and FINUDA, taking data one at a time.

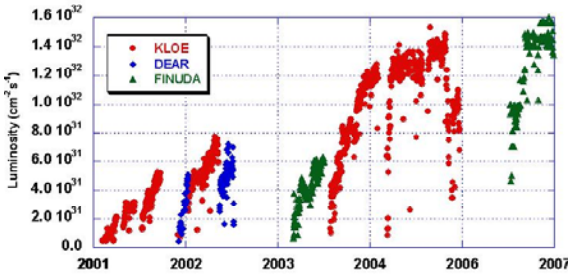

Figure 1: DAΦNE daily peak luminosity trend.

In its original configuration the collider consisted of two independent rings, each ~ 97m long, sharing two interaction regions IR1 and IR2 where the KLOE [3] and DEAR [4] or FINUDA [5] detectors were respectively installed. A full energy injection system, including a S-band linac, 180 m long transfer lines and an accumulator/damping ring, provides the e^+ and e^- beams with the required emittance and energy spread.

The DAΦNE complex runs also a beam test facility, providing e^-/ e^+ beams from the linac in the energy range 25÷725 MeV with tunable intensity from 10^{10} to a single particle per pulse.

A synchrotron radiation facility with three independent beam lines, collecting the radiation emitted in one wiggler and two bending magnets of the e^- ring, is also available.

In these years DAΦNE has undergone several progressive upgrades [6,7,8], aimed at improving the collider performances (see Fig.1), implemented during the shut-downs for detectors changeover.

ESTABLISHED PERFORMANCES

Since 2001 the DAΦNE accelerator complex has been delivering luminosity to three experiments, improving, at the same time, its performances in terms of luminosity, lifetime and backgrounds.

The DEAR experiment has been done in less than 5 months during 2002-2003, collecting about 200 pb^{-1}, with a peak luminosity of 0.7x10^{32} cm^{-2}s^{-1}.

The KLOE experimental program has been completed in 2006, more than 2 fb^{-1} have been acquired on the peak of the Φ resonance, while more than 0.25 fb^{-1} have been stored off-resonance [7], to perform a high statistics resonance scan. The best peak luminosity obtained has been 1.5x10^{32} cm^{-2}s^{-1}, with a maximum daily integrated luminosity about 10 pb^{-1}.

The second run of FINUDA, which collected 1.2 fb^{-1}, started in April 2006. During the operation a peak luminosity of 1.6x10^{32} cm^{-2}s^{-1} has been achieved, while a maximum daily integrated luminosity similar to best during the KLOE run has been obtained with lower beam currents, lower number of bunches and higher beta functions at the collision point [8].

However, these performances were the best obtainable with the DAΦNE original collision scheme.

Long-range beam-beam interactions (parasitic crossings) [9, 10] lead to a substantial lifetime reduction of both beams in collision, limiting the maximum storable current and, as a consequence, the achievable peak and integrated luminosity.

The minimum value of β^*_y at the IP is set by the longitudinal bunch size to avoid destructive effects coming from the *hourglass* effect. The bunch length in the DAΦNE main rings is presently, after a careful coupling impedance optimization [11], 25 mm for both beams at the operating bunch current (~ 15 mA). Moreover the horizontal crossing angle at the IP must be lower with the Piwinski limit of 30 mrad.

A new conceptual approach is necessary to push the luminosity towards 10^{33} cm^{-2}s^{-1}. After long studies and discussions involving the Accelerator Division Team and the international accelerator community, a new collision scheme based on large Piwinski angle and *crab-waist* has been adopted for the DAΦNE collider.

NEW COLLISION SCHEME

The new collision regime [12] devised for DAΦNE is based on a large Piwinski angle Φ obtained by increasing the collision angle θ and reducing the transverse horizontal beam size σ_x.

$$\Phi \approx \frac{\sigma_z}{\sigma_x}\frac{\theta}{2}$$

Luminosity and tune-shift depend on the number N of particles in the colliding bunches, on the transverse beam sizes $\sigma_{x,y}$ and the vertical betatron function β^*_y according to the following formulas [13]:

$$L \propto \frac{N\xi_y}{\beta_y^*}; \quad \xi_y \propto \frac{N\sqrt{\beta_y^*}}{\sigma_z\theta}; \quad \xi_x \propto \frac{N}{(\sigma_z\theta)^2}$$

A first luminosity gain can be obtained, while keeping the vertical tune shift constant, by increasing N proportionally to ($\sigma_z\theta$).

Moreover the length of the overlap region of the colliding bunches drops as:

$$\Sigma \propto \frac{\sigma_x}{\theta}$$

Being $\Sigma << \sigma_z$, β^*_y can be made as small as Σ and further advantages can be envisaged in terms of higher luminosity, vertical tune shift reduction and synchrobetatron resonance reduction. However collider operation with large Piwinski angle requires a compensation mechanism for the new beam-beam resonances introduced by the configuration itself and limiting the maximum achievable vertical tune-shift value.

Table 1: DAΦNE beam parameters.

	DAΦNE (KLOE)	**DAΦNE (Upgrade)**
I_{bunch} (mA)	13	13
N_{bunch}	110	110
β^*_y (mm)	17	6
β^*_x (mm)	1.7 *10^3	0.2 *10^3
σ^*_y (μm)	5.4	2.6
σ^*_x (μm)	0.7	0.2
σ^*_z (mm)	25.	20.
$\Theta_{cross}/2$ (mrad)	12.5	25.
$\Phi_{Piwinski}$	0.36	2.5
***L* ($cm^{-2}s^{-1}$) * 10^{32}**	**1.5 measured**	**10. expected**

This compensation is provided by a couple of sextupoles installed in symmetric positions with respect to the IP, in phase with it in the horizontal plane and at π/2 in the vertical one: they are called the *crab-waist* sestupoles. They mainly suppress the betatron and sinchrobetatron resonances coming from the vertical motion modulation due to the horizontal oscillation.

The beam parameters adopted to implement the new collision regime at DAΦNE are listed in Table 1. According to the theoretical simulations the new collision scheme should provide a peak luminosity of the order of 10^{33} cm^{-2} s^{-1}.

INTERACTION REGIONS EVOLUTION

Large collision angle, crab-waist and small β^*_y require important changes in the design criteria of the mechanical and magnetic layout of IR1 [14], see Fig. 3.

The second interaction region has been also completely rebuilt in order to provide full beam separation and in order to be ready, with minor modifications, for a future FINUDA run based on the new collision scheme.

Four beam position monitors, installed both halves of the IR1 and of the ring-crossing region, after the pipe separation, provide beam independent closed orbit measurement even in collision.

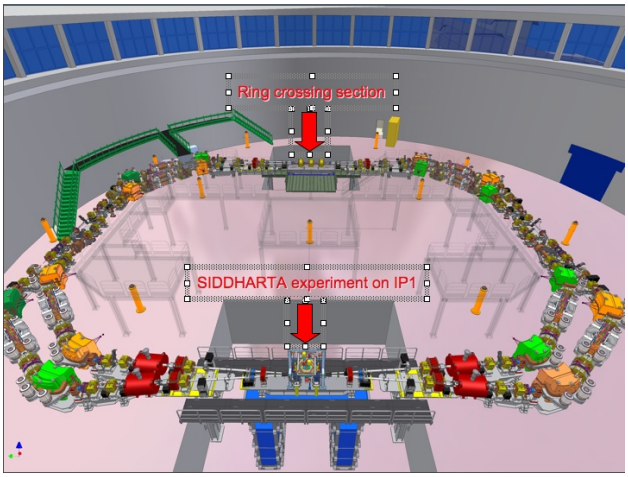

Figure 2: New Main Rings layout

Interaction region for the SIDDHARTA experiment

Removing the splitter magnets and rotating the two sector dipoles in the long and short arcs adjacent to the interaction regions of both rings has doubled the horizontal crossing angle in IR1.

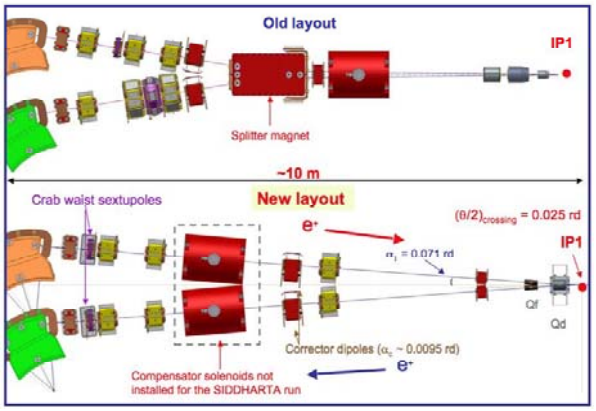

Figure 3: Half view of old IR1 (top) and new (bottom) layout.

The bending fields have been changed, according the values reported in Table 2, in order to meet the new layout angles.

Table 2: Bending dipole parameters; old values are shown in parenthesis.

	α [rd]	ρ [m]	B [T]
Sector long	0.7874 (0.8639)	1.53(1.40)	1.11
Sector short	0.7834 (0.7069)	1.27(1.40)	1.34

Four additional corrector dipoles have been used to match the vacuum chamber in the arcs [15].

The *low-beta* section in the SIDDHARTA IR is based on permanent magnet quadrupole doublets. The quadrupoles are made of SmCo alloy and provide gradients of 29.2 T/m and 12.6 T/m for the first one from the IP and the second one respectively. The first is horizontally defocusing and is shared by the two beams; due to the off-axis beam trajectory, it provides strong beam separation. The second quadrupole, the focusing one, is installed just after the beam pipe separation and is therefore on axis see Fig. 4. The new configuration almost cancels the problems related to beam-beam long range interactions, because the two beams experience only one parasitic crossing inside the defocusing quadrupole where, due to the large horizontal crossing angle, they are very well separated ($\Delta x \sim 20\ \sigma_x$). It is worth reminding that in the old configuration the colliding beams had 24 parasitic crossing in the IRs and in the main one the separation at the first crossing was $\Delta x \sim 7\ \sigma_x$ [9].

The crab-waist sextupoles are installed at both ends of the interaction region. They are electromagnetic devices and the required integrated gradient k_s [16] is:

$$k_s = \frac{1}{2\theta}\frac{1}{\beta_y^* \beta_y^{sext}}\sqrt{\frac{\beta_x^*}{\beta_x^{sext}}}$$

In the case of the optics for the SIDDHARTA operation $k_s = 36.74\ m^{-2}$, more than a factor 5 larger than the average required for the normal sextupoles used for chromaticity correction.

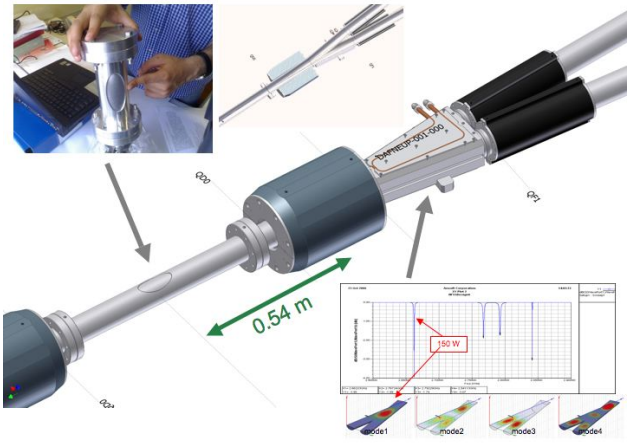

Figure 4: IR1 low-beta section (center), detail of the thin window at IP1 (upper left), vacuum chamber cross section view (upper right) and HOM analysis in the *y-section* (bottom right).

Four electromagnetic quadrupoles have been installed on both sides of IP1 to get the proper phase advance between the *crab-waist* sestupoles and the interaction point.

The compensator solenoids, present in the original setup, have been removed since there is no solenoid around the SIDDHARTA detector. However there is room to reintroduce them for a possible future KLOE run. In a such case, due to the new geometrical layout of IR1, two compensator solenoids will be necessary for each ring, requiring an upgrade of the cryogenic transfer lines.

The DAΦNE main rings layout evolution is shown in Fig. 2.

Ring crossing region

A new crossing section providing complete separation between the two beams has replaced the second interaction region [15]. It is geometrically symmetric to IR1 and its vacuum chamber is based on the same design criteria. Independent beam vacuum chambers are obtained by splitting the original pipe in two *half-moon* shaped sections, see Fig. 5, providing full vertical beam separation

This aspect is quite relevant because it cancels completely the problems coming from the beam-beam long range interaction [10], allowing at the same time to relax the ring optics requirements imposed by beam separation at the unused interaction point.

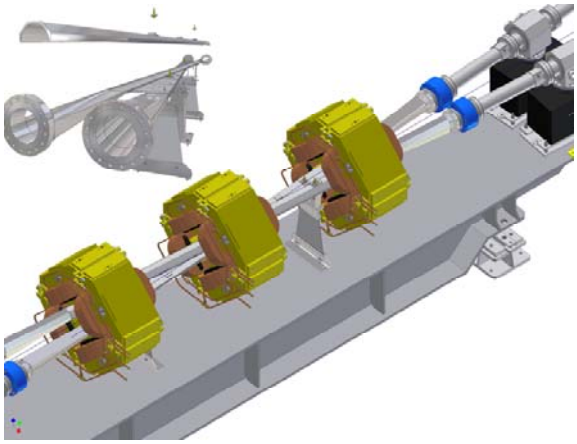

Figure 5: Quadrupole triplet in the ring crossing region (bottom) and *half-moon* vacuum chamber design (top).

The magnetic layout of the ring crossing region is the same as in IR1, but for the missing *crab-waist* sextupoles. and the central focusing section. It is based on a single large aperture electromagnetic quadrupoles triplet, allowing for wide operation flexibility in terms of betatron functions.

IR Vacuum chamber

The design criteria of the new vacuum chamber for IR1 and the ring crossing region are very simple. All the possible discontinuities have been avoided in order to keep the ring coupling impedance low. The number of bellows has been also limited to the strict necessary to compensate thermal strain and mechanical misalignments; there are four bellows per ring both in IR1 and in the second crossing region.

The vacuum chamber of IR1 consists of straight pipes merging in a *Y* shaped section. The pipe is aluminum (AL6082) made and is equipped on IP1 with a thin 0.3 mm window.

Special attention has been paid to the *Y-section* design since beam induced electromagnetic fields can generate trapped high order modes (HOM). Simulations have pointed out four possible HOMs, among them only the first is trapped and even in the worst case, when the beam spectrum is in full coupling with the mode, the released power is less than 200 W. Nevertheless the *Y- section* has been equipped with a cooling system to remove the heating due to the HOM [17].

Bellows

New bellows have been developed and installed in the new IR1 and in the ring crossing section. Presently four new bellows are used in each one of the previous sections.

They connect circular cross section pipes of 88 mm diameter. The inner radius of bellows convolutions is ≈ 65 mm, the outer one 80 mm and the length ≈50 mm, see Fig. 6. Their innovative component is the RF shield [17], necessary to avoid the discontinuity acting as a cavity for the beam. The new RF shield is implemented by means of Ω shaped Be-Cu strips, installed all around two cylindrical aluminum shells fixed at the bellows ends.

Figure 6: Copper-Beryllium strip shielded bellows, mechanical design (left) and real device (right).

The shield in the old design was realized by using contiguous mini bellows. Experience with the old devices has shown that they were loosing elasticity while aging; moreover they might no longer provide shield contour uniformity when compressed.

HFSS simulations in the frequency range from DC to 5 GHz have shown that the new design reduces bellows contribution to the ring coupling impedance.

OTHER UPGRADES

New fast injection kickers

The injection kickers, two in each Main Ring, have been replaced with new devices [18] based on tapered strips embedded in a rectangular cross section vacuum chamber allowing injection rate up to 50 Hz. The deflecting field is provided by the magnetic and the electric fields of a TEM wave traveling in the structure, which generates 5.4 ns flat top pulses, perturbing only three bunches out of 110 usually colliding. This new injection scheme represents a relevant improvement with respect to the old one, which was based on injection kickers having 150 ns pulse length perturbing almost half of the bunch train.

Figure 7: New fast injection kicker under test (left) and installed on the electron ring (right).

Moreover a smooth beam pipe and tapered transitions reduce the kickers contribution to the total ring coupling impedance. All these features should improve the maximum storable currents, colliding beams stability and background on the experimental detector during injection.

Control System

A new commercial processor (Pentium/Linux) has been implemented in the control system; this will progressively replace the original home designed front-end processor now seventeen years old.

Removed and repositioned elements

Few ion clearing electrodes still installed on the electron ring and no longer necessary have been removed.

The transverse horizontal position of two wigglers in the long arcs has been moved (-2.5 mm) for both rings in order to reduce the non-linear term in the magnetic field predicted by simulations and affecting the beam dynamics.

Positions of the electromagnetic quadrupoles, in the long straight sections on both rings, have been changed to allow the installation of the new injection kickers and to provide a flexible configuration for tuning the phase advance between the two injection kickers themselves.

RF cavity working frequency

The new ring layout is ~10 cm shorter than the original one due to the removal of the splitter magnets and the requirement to keep the position of the arcs unchanged in order to minimize the implementation work. As a consequence, the frequency of the RF cavities has been changed by ~ 400 KHz. The variation is well within the tune range of the main rings cavities, but imposes some modifications on the damping ring operating conditions. In fact its RF cavity operates on a sub-multiple frequency of the Main Rings one and the energy variation has to be corrected by changing the dipole field. The tuner range of the cavity has been also adapted in order to be compatible with the new operating conditions.

The front-end electronics used to acquire signals from the beam position monitors required also some

modifications in order to work properly with the new frequency value.

Luminosity monitors

The new luminosity monitor for the collider consists of three different devices: a small angle Bhabha tile calorimeter split into 20 sectors (30 degrees each) made of alternating lead and scintillating tiles, covering a vertical acceptance between 17.5 and 27 degrees; a GEM (Gas Electron Multiplier) tracker placed in front of the tile calorimeters allowing a redundant measurement of Bhabha events to minimize background; two Single Bremsstrahlung gamma detectors [19].

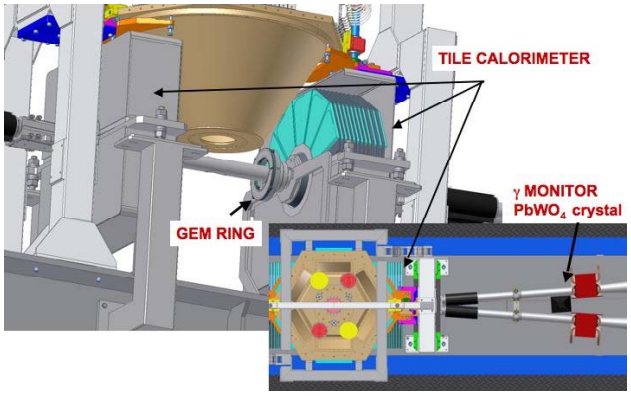

Figure 8: Three-dimensional (top) and top (bottom) view of the SIDDHARTA detector and the luminosity monitors installed around the IP1.

Redundancy in the luminosity measurement is required by the need to best quantify the luminosity gain obtained by adopting the new collision approach. In fact it is of interest not only for DAΦNE but also for the other lepton colliders and even for the LHC hadron collider expected to come in operation soon at CERN.

CONCLUSIONS

In a five months shutdown the DAΦNE collider has been upgraded to implement a new collision scheme based on large Piwinski angle and *crab-waist*. Commissioning started at the end of November 2007.

Presently the two beams have been stored, all the diagnostic and the new systems have been debugged and put in operation, the new injection kickers and the bellows behave well as espected .

Measurements on the bunch length show a 15% percent reduction at 10 mA per bunch, in agreement with the lower ring impedance.

Preliminary tests with the beams in collision have been also done and look quite promising.

Detailed results and measurements will be published as soon as possible after careful analysis.

REFERENCES

[1] David Alesini, Maria Enrica Biagini, Caterina Biscari, Roberto Boni, Manuela Boscolo, Fabio Bossi, Bruno Buonomo, Alberto Clozza, Giovanni Delle Monache, Theo Demma, Enrico Di Pasquale, Giampiero Di Pirro, Alessandro Drago, Alessandro Gallo, Andrea Ghigo, Susanna Guiducci, Carlo Ligi, Fabio Marcellini, Giovanni Mazzitelli, Catia Milardi, Fabrizio Murtas, Luigi Pellegrino, Miro Preger, Lina Quintieri, Pantaleo Raimondi, Ruggero Ricci, Ugo Rotundo, Claudio Sanelli, Mario Serio, Francesco Sgamma, Bruno Spataro, Alessandro Stecchi, Angelo Stella, Sandro Tomassini, Cristina Vaccarezza, Mikhail Zobov (INFN/LNF, Frascati (Roma)), Ivan Koop, Evgeny Levichev, Pavel Piminov, Dmitry Shatilov (BINP SB RAS, Novosibirsk), Victor Smaluk (BINP, Novosibirsk), Simona Bettoni (CERN, Geneva), Marco Schioppa (INFN Gruppo di Cosenza, Arcavacata di Rende (Cosenza)), Paolo Valente (INFN-Roma, Roma), Kazuhito Ohmi (KEK, Ibaraki), Nicolas Arnaud, Dominique Breton, Patrick Roudeau, Achille Stocchi, Alessandro Variola, Benoit Francis Viaud (LAL, Orsay), Marco Esposito (Rome University La Sapienza, Roma), Eugenio Paoloni (University of Pisa and INFN, Pisa), Paolo Branchini (Roma3, Rome).
[2] G. Vignola et al., Frascati Phys.Ser.4:19-30,1996; C. Milardi et al., Frascati Phys.Ser.16:75-84,1999.
[3] KLOE Coll., Nucl. Inst. Meth. A 482, 363-385 (2002).
[4] DEAR Coll., Physics Letters **B**, Vol. 535 (2002) 52.
[5] FINUDA Coll., Proc. HYP2000 (Torino, 2000).
[6] C. Milardi et al., e-print: physics/0408073
[7] A. Gallo et al., Edimburgh 2006, EPAC p. 604-606.
[8] C. Milardi et al., PAC07, p. 1457.
[9] C. Milardi et al., e-Print: physics/0607129.
[10] C. Milardi et al., this workshop.
[11]M.Zobov et al., *Journal of Instrumentation* 2: P08002, 2007, e-Print: arXiv:0705.1223.
[12]P.Raimondi, D.Shatilov, M. Zobov, physics/0702033.
[13]D. Shatilov and M. Zobov, ICFA BDN 37, 99 (2005).
[14]D. Alesini et al, LNF-06/033 (IR), 2006.
[15]S. Tomassini et al., PAC07, p. 1466.
[16]C.Zobov et al., this workshop , arxiv:0802.2667
[17]F. Marcellini, PAC07, p. 3988.
[18]D. Alesini et al, DAΦNE Tech. Note I-17, 2006.
[19]G. Mazzitelli, et al., Nucl. Instr. and Meth. A 486 (2002) 568.

THE SUPERB-FACTORY ACCELERATOR PROJECT

M.E. Biagini*, INFN, Laboratori Nazionali di Frascati, 00044 Frascati, Italy.

Abstract

An international collaboration on the design of a Super B-Factory aiming at a 10^{36} cm^{-2} s^{-1} luminosity is in progress. The design relies on a new collision scheme with large Piwinski's angle and very small IP beam sizes, where possible harmful resonances will be cancelled by the newly proposed "crab waist" method.

A Conceptual Design Report has been published in April this year. A review of the design principles and of the project status will be given.

INTRODUCTION

A Super B-Factory like *SuperB*, an asymmetric energy e^+e^- collider with a luminosity of the order 10^{36} $cm^{-2}s^{-1}$, can provide a uniquely sensitive probe of New Physics in the flavour sector of the Standard Model.

The PEP-II and KEKB [1,2] asymmetric colliders have produced unprecedented luminosities, above 10^{34} $cm^{-2}s^{-1}$, taking our understanding of the accelerator physics and engineering demands of asymmetric e^+e^- colliders to a new parameter regime.

Furthermore, the success of the SLAC Linear Collider and FFTB [3], and the subsequent work on the ILC [4] allow a new Super collider to incorporate linear collider techniques.

The implementation of a new colliding scheme with the combination of "large Piwinski angle", low β*, and "*crab waist*" will enable the design of a Super B-Factory with a target luminosity two orders of magnitude higher than presently achieved, by overcoming some of the issues that have plagued earlier super $e+e^-$ collider designs, such as very high beam currents and very short bunches.

An international *SuperB* study group has been formed in the past year to work on the physics case, the accelerator, and the detector. An International Steering Committee has been established, with members from Canada, France, Germany, Italy, Russia, Spain, UK, US, and close collaboration with Japan. Five workshops have been held at Frascati, SLAC and Paris, to focus on the physics case and the detector and accelerator feasibility. As a result, a Conceptual Design Report [5] was published in March 2007, describing the project and including costs estimates. About 85 Institutions worlwide have partecipated to this document, with the contribution of 320 scientists.

An International Review Committee, with experts in the fields, has also been appointed to review the whole project before spring 2008. More detailed informations on this project can be found at: www.pi.infn.it/SuperB.

*On behalf of the *SuperB* Accelerator Team

B-FACTORIES OUTLOOK

The construction and operation of multi-bunch e^+e^- colliders have brought about many advances in accelerator physics in the area of high currents, complex interaction regions, high beam-beam tune shifts, high power RF systems, controlled beam instabilities, rapid injection rates, and reliable uptimes (~95%). The present B-Factories have proven that their design concepts are valid, since asymmetric energies work well, the beam-beam energy transparency conditions are weak, high currents can be stored and the electron cloud instability (ECI) can be managed. On the detector-machine side the IR backgrounds can be handled successfully and Interaction Regions with two energies can work. Moreover unprecedented values of beam-beam parameters have been reached (0.06 up to 0.09), and continuous injection in production has helped increasing the integrated luminosity. Remarkably, SuperB would produce this very large improvement in luminosity with circulating currents and wall plug power similar to those of the current B-Factories.

On the other hand lessons learned from SLC and subsequent studies for the International Linear Collider (ILC) Damping Ring (DR) as well as experiments (FFTB, ATF, ATF2) have also shown new successful concepts: small beam emittances can be produced in a DR with a short damping time and very small beam spot sizes and β-functions can be achieved at the Interaction Region. All of the above techniques can be incorporated in the design of a future *SuperB* collider. There is clear synergy with ILC R&D; design efforts have already influenced one another, and many aspects of the ILC-R and Final Focus would be operationally tested at *SuperB*.

A NEW COLLISION SCHEME

Past approaches of collider optimization - the so called "brute force" methods followed over several decades, - have now run into a dead end. These approaches were mainly based on an increase of beam currents and a decrease of β_y* at the Interaction Point. However, β_y* cannot be made much smaller than the bunch length σ_z without incurring an "hourglass" effect, since particles in the head and tail of bunches would experience a larger β_y*. So, the bunch must be shortened accordingly with an increase in RF voltage, beam pipe overheating, instabilities and power costs. Other side effects related to the high currents are raising HOM instabilities and detector backgrounds increase.

The novel collision scheme [6, 7] uses frozen variables in parameter space to ascend to a new luminosity scale, by effectively exchanging the roles of the longitudinal and

transverse dimensions. The design is based on a new collision scheme, with "large Piwinski angle" and small beam sizes with "*crab waist*".

In the new scheme, the Piwinski angle ϕ defined as:

$$\phi = \frac{\sigma_z}{\sigma_x}\tan\frac{\theta}{2} \approx \frac{\sigma_z}{\sigma_x}\frac{\theta}{2}$$

(σ_x being the horizontal rms bunch size, σ_z the rms bunch length and θ the horizontal crossing angle) is increased by decreasing the horizontal beam size and increasing the crossing angle. In this way, the luminosity is increased, and the horizontal tune shift due to the crossing angle decreases. The most important effect is that the overlap area of colliding bunches is reduced, as it is proportional to σ_x/θ. Thus, if β_y^* can be made comparable to the overlap area size several advantages are gained, as small spot size at the IP, i.e. higher luminosity, a reduction of the vertical tune shift, and suppression of vertical synchro-betatron resonances. Moreover the problem of parasitic collisions (PC) is automatically solved by the higher crossing angle and smaller horizontal beam size, which makes the beam separation at the PC larger in terms of σ_x.

However, a large Piwinski angle itself introduces new beam-beam resonances and may strongly limit the maximum achievable tune shifts. This is where the "*crab waist*" innovation is required, boosting the luminosity mainly by suppression of betatron and synchro-betatron resonances that usually arise, through vertical motion modulation by horizontal beam oscillations [8]. A sketch of the new collision scheme is shown in Fig.1. The "*crab waist*" correction can easily be realized in practice with two sextupoles magnets in phase with the IP in the x plane and at π/2 in the y plane, on both sides of the IP.

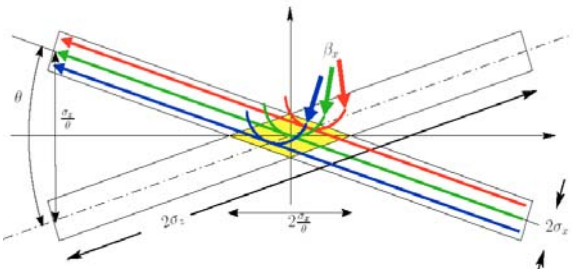

Figure 1: Large Piwinsky angle and crab waist scheme. The collision area is shown in yellow.

In summary, the main advantages of this new scheme are:

- manageable HOM heating;
- no coherent synchrotron radiation of short bunches;
- less power consumption;
- higher luminosity with same currents and bunch length;
- less severe beam instabilities;
- lower beam-beam tune shifts;
- negligible parasitic collisions due to higher crossing angle and smaller σ_x.

BEAM PARAMETERS AND LATTICE

Two beams will circulate in two separate rings at 4 and 7 GeV, colliding in only one Interaction Region, where the Super-BaBar detector will be installed. The Final Focus section design is similar to that designed for FFTB/ILC. The rings design is based on recycling all PEP-II hardware, magnets, and RF system, with a total RF power needed of 17 MW, lower than the PEP-II one. Fig. 2 shows a sketch of the layout with expanded arc cell and Final Focus section.

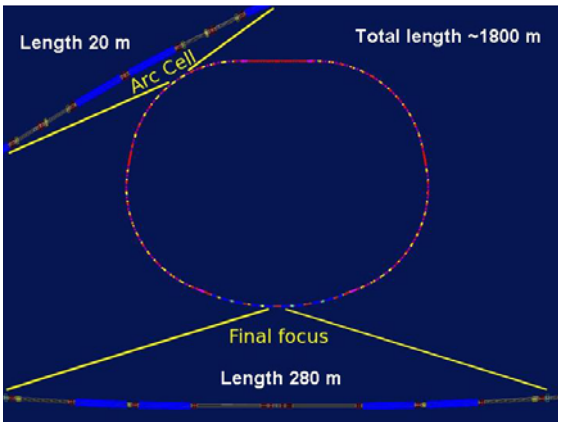

Figure 2: Layout of one ring with close up of one arc cell and Final Focus

The *SuperB* parameters have been optimized based on several constraints. The most significant are:

- maintaining wall plug power, beam currents, bunch lengths, and RF requirements comparable to present B-Factories;
- planning for the reuse as much as possible of the PEP-II hardware;
- requiring ring parameters as close as possible to those already achieved in the B-Factories, or under study for the ILC-DR or achieved at the ATF ILC-DR test facility [9];
- simplifying the IR design as much as possible. In particular, reduce the synchrotron radiation in the IR, reduce the HOM power and increase the beam stay-clear. In addition, eliminate the effects of the parasitic beam crossings;
- relaxing as much as possible the requirements on the beam demagnification at the IP;
- designing a Final Focus system to follow as closely as possible already tested systems, and integrating the system as much as possible into the ring design.

Table 1 shows the main parameter set that closely matches these criteria.

Table 1: *SuperB* Main parameters list

C (m)	1800	ε_y (pm-rad)	7/4
E (GeV)	4/7	β_y* (mm))	0.22/0.39
I (A)	2	β_x* (mm)	35/20
N_{bunch}	1342	σ_y* (mm)	0.039
N_{part}/bunch	$5.5x10^{10}$	σ_x* (mm)	10/6
θ (rad)	2x24	σ_z (mm)	5
ε_x (nm-rad)	2.8/1.6	RF Power (MW)	17
Peak luminosity ($cm^{-2}s^{-1}$)		$1.x10^{36}$	

Many of the nominal *SuperB* design parameters could, in principle, be pushed further to increase performance. This provides an excellent upgrade path after experience is gained with the nominal design. The upgrade parameters can be based on the following assumptions:

- the beam currents could be raised to the levels that PEP-II should deliver in 2008;
- the vertical emittance at high current could be reduced to the ATF values;
- the lattice supports a further reduction in β_x^* and β_y^*;
- the beam-beam effects are still far from saturating the luminosity.

In principle, the design supports these improvements, so luminosity higher than nominal may well be feasible. In addition, it should be pointed out that, since the nominal design parameters are not pushed to maximum values, there is flexibility in obtaining the design luminosity by relaxing certain parameters, if they prove more difficult to achieve, and pushing others.

BEAM-BEAM STUDIES

Beam-beam studies have been performed in order to verify the validity of the new scheme. Numerical simulations performed with LIFETRAC [10] have shown that the design luminosity of 10^{36} $cm^{-2}s^{-1}$ is achieved already with $2\text{-}2.5x10^{10}$ particles per bunch.

According to the simulations, for this bunch population the beam-beam tune shift is well below the maximum achievable value. Indeed, as one can see in the left plot of Fig. 3, the luminosity grows quadratically with the bunch intensity till about $7.5x10^{10}$ particles per bunch. This safety margin has been used to significantly relax and optimize many critical parameters, including damping time, crossing angle, number of bunches, bunch length, bunch currents, emittances, beta functions and coupling, while main-taining the design luminosity of 10^{36} $cm^{-2}s^{-1}$.

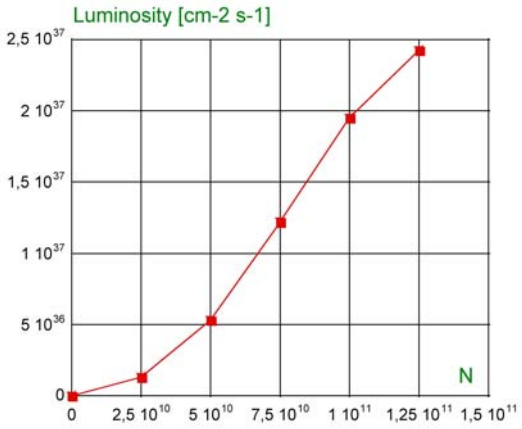

Figure 3: *SuperB* luminosity versus bunch intensity.

In order to define how large is the "safe" area with the design luminosity, a luminosity tune scan has been performed for tunes above the half integers, which is typical for the operating B-factories. The resulting 2D contour plot is shown in Fig.4, individual contours differing by 10% in luminosity, where the effect of the betatron resonances suppression by the "*crab waist*" becomes obvious. It is clear that the design luminosity can be obtained over a wide tune area, allowing for large operation freedom. It has also been found numerically that for the best working points the distribution tails growth is negligible.

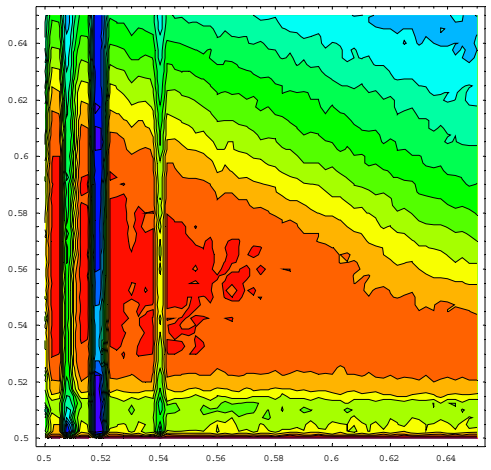

Figure 4: *SuperB* luminosity tune scan (horizontal axis: ν_x from 0.5 to 0.65; vertical axis: ν_y from 0.5 to 0.65).

CONCLUSIONS

The new large Piwinski angle collision scheme will allow for peak luminosity well beyond the current state-of-the-art, without a significant increase in beam currents or shorter bunch lengths. The use of the "*crab waist*" sextupoles will add a bonus for suppression of dangerous resonances. This scheme will be first tested at the DAΦNE Φ-Factory in Frascati, so helping in discovering

possible issues. There is a growing international interest and participation to the *SuperB*, with R&D proceeding on various items. A Conceptual Design Report (CDR) was published and is being reviewed by an International Review Committee.

REFERENCES

[1] KEKB Status report PAC 2005 Knoxville, TN.
[2] PEP-II Status report PAC2005 Knoxville, TN.
[3] The SLC Design Handbook, SLAC November 1984.
[4] ILC Technical Review Committee, Second Report 2003, ICFA SLAC-R-606.
[5] *SuperB* Conceptual Design Report, INFN/AE-07/2,SLAC-R-856, LAL 07-15, March 2007, also at http://arxiv.org/abs/0709.0451.
[6] P. Raimondi, "Status on SuperB effort", 2nd *Super* Workshop *B*, LNF Frascati, 16-18 March 2006, http://www.lnf.infn.it/conference/superbf06/.
[7] P. Raimondi, M. Zobov, D. Shatilov, Proc. of PAC2007, Albuquerque (US), June 2007.
[8] P. Raimondi, D. Shatilov, M Zobov, LNF-07/003 (IR), Jan.2007.
[9] Y. Honda et al, Phys. Rev. Lett. 92, 054802 (2004).
[10] D. Shatilov, Particle Accelerators 52, 65 (1996).

Scenarios for the LHC Upgrade

W. Scandale, F. Zimmermann, CERN, Geneva, Switzerland

Abstract

The projected lifetime of the LHC low-beta quadrupoles, the evolution of the statistical error halving time, and the physics potential all call for an LHC luminosity upgrade by the middle of the coming decade. In the framework of the CARE-HHH network three principal scenarios have been developed for increasing the LHC peak luminosity by more than a factor of 10, to values above 10^{35} cm^{-2}s^{-1}. All scenarios imply a rebuilding of the high-luminosity interaction regions (IRs) in combination with a consistent change of beam parameters. However, their respective features, bunch structures, IR layouts, merits and challenges, and luminosity variation with β^* differ substantially. In all scenarios luminosity leveling during a store would be advantageous for the physics experiments. An injector upgrade must complement the upgrade measures in the LHC proper in order to provide the beam intensity and brightness needed as well as to reduce the LHC turnaround time for higher integrated luminosity.

1 MOTIVATION AND TIME FRAME

The Large Hadron Collider (LHC) will collide two proton beams with a centre-of-mass energy of 14 TeV at design and "ultimate" luminosities of 10^{34} cm^{-2}s^{-1} and 2.3×10^{34} cm^{-2}s^{-1}. The LHC proton beams will cross each other at the four detectors of the two high-luminosity experiments ATLAS and CMS, the B physics experiment LHCb, and the ion experiment ALICE. The LHC is set to explore an extremely rich physics landscape, spanning from the Higgs particle, over supersymmetry, extra dimensions, black holes, precision measurements of the top quark, the unitarity triangle, to the quark-gluon plasma [1].

Simple models for the LHC luminosity evolution over the first few years of operation [2] indicate that the IR quadrupoles may not survive for more than 8 years due to high radiation doses, and that already after 4–5 years of operation the halving time of the statistical error may exceed 5 years. Either consideration points out the need for an LHC luminosity upgrade around 2016. Actually there exists even a third reason for an LHC upgrade, which is extending the physics potential of the LHC: A ten-fold increase in the luminosity will increase the discovery range for new particles by about 25% in mass [1]. Detailed physics examples can be found in Ref. [3]. The particle-physicists' goal for the upgrade is to collect 3000 fb^{-1} per experiment in 3–4 years of data taking. Simlar upgrades were performed at previous hadron colliders, where, for example, the Tevatron upgrade has resulted in an integrated Run-II luminosity about 50 times larger than that of Run I.

The LHC upgrade could consist of a series of improvements, e.g. two stages – the first one consolidating the nominal performance and providing a luminosity of up to 3×10^{34} cm^{-2}s^{-1} and the second one increasing the luminosity by more than an order of magnitude from nominal, to values above 10^{35} cm^{-2}s^{-1}.

Possible LHC upgrade paths were first examined around 2001 [4]. They have been further developed by the CARE [5] HHH network [6], in collaboration with the US LARP [7].

2 LHC CHALLENGES

Three major challenges faced by the LHC are *collimation and machine protection* [8] including issues such as damage levels, quench thresholds, cleaning efficiency, and impedance; *electron cloud* [9] involving the heat load inside the cold magnets, instabilities, and emittance growth; and *beam-beam interaction* [10], including head-on effects, long-range collisions, weak-strong and strong-strong phenomena. All these effects tend to be more severe for an upgrade.

Another LHC challenge is related to the crossing angle, which, together with the finite bunch length ("hourglass effect"), introduces a geometric luminosity reduction factor [11]

$$R(\phi,\sigma_z,\beta^*) = \frac{1}{\sqrt{\pi}\sigma_z}\int_{-\infty}^{\infty} ds \left\{\frac{1}{1+\frac{s^2}{\beta^{*2}}} \exp\left(-\frac{s^2}{\sigma_z^2}\left\{1+\phi^2\frac{1}{1+\frac{s^2}{\beta^{*2}}}\right\}\right)\right\} \quad (1)$$

where β^* designates the IP beta function, σ_z the rms (Gaussian) bunch length, and $\phi \equiv \theta_c\sigma_z/(2\sigma_x^*)$ the so-called "Piwinski angle", with θ_c being the full crossing angle and σ_x^* the rms transverse beam size at the interaction point (IP).

For bunches much shorter than β^* the reduction factor (1) can be approximated as

$$R(\phi,\sigma_z,\beta^*) \approx R(\phi,0,\beta^*) \equiv R(\phi) = \frac{1}{\sqrt{1+\phi^2}} \quad (2)$$

The reduction factor $R(\phi)$ decreases steeply as ϕ is raised beyond nominal, e.g. for smaller β^* and larger crossing angle, as is illustrated in Fig. 1. The nominal LHC operates at $R(\phi) \approx= 0.84$.

If a crab cavity is present, Eq. (1) is modified to

$$R_{\rm cc}(\phi,\sigma_z,\beta^*) = \frac{1}{\sqrt{\pi}\sigma_z}\int_{-\infty}^{\infty}\left\{\frac{1}{1+\frac{s^2}{\beta^{*2}}}\exp\left[-\frac{s^2}{\sigma_z^2} -\frac{\theta_c^2(-k_{\rm cc}s+\sin(k_{\rm cc}s))^2}{4k_{\rm cc}^2\sigma_x^{*2}\left(1+\frac{s^2}{\beta^{*2}}\right)}\right]\right\}, \quad (3)$$

where $k_{\rm cc} \equiv 2\pi/\lambda_{\rm cc}$ denotes the wave number of the crab-cavity rf.

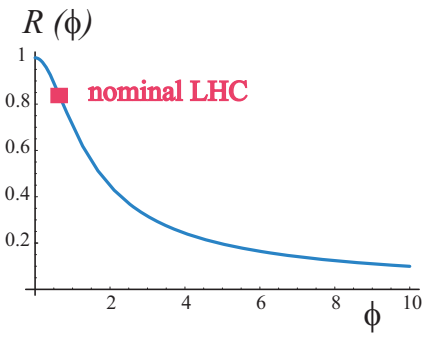

Figure 1: Geometric luminosity reduction factor $R(\phi)$ due to the crossing angle (2), as a function of the Piwinski angle ϕ. The nominal LHC operating point is also indicated.

3 BEAM PARAMETERS

The crossing angle reduces not only the luminosity, but also the beam-beam tune shift, and, thanks to this, for alternating planes of crossing at two interaction points (IPs), the luminosity can be expressed as [11]

$$L \approx \frac{f_{\rm rev}\gamma}{2r_p} n_b \frac{1}{\beta^*} N_b \, \Delta Q_{\rm bb} \, F_{\rm profile} F_{\rm hg} \ , \qquad (4)$$

where $\Delta Q_{\rm bb}$ denotes the total beam-beam tune shift, limited to about 0.01 according to experience at previous hadron colliders, $f_{\rm rev}$ the revolution frequency, N_b the number of protons per bunch, $F_{\rm profile}$ a form factor that depends on the longitudinal profile (about 1 for a Gaussian and $\sqrt{2}$ for a uniform profile) and $F_{\rm hg}$ the reduction factor due to the hourglass effect, which is relevant for bunch lengths comparable to, or smaller than, the IP beta function. In (4) the collision of two round beams has been assumed. Other variables are defined in Table 1, which compares parameters for the nominal and ultimate LHC with those for three upgrade scenarios (abbreviated "ES", "FCC" and "LPA"). The upgrade parameters in (4) which differ from the ultimate LHC configuration are $1/\beta^*$ ($\times 2$), N_b ($\times 2.9$), $\Delta Q_{\rm bb}$ ($\times 1.15$), $F_{\rm profile}$ ($\times\sqrt{2}$) and n_b ($\times 1/2$) for LPA, and $1/\beta^*$ ($\times 6.3$), $\Delta Q_{\rm bb}$ ($\times 1.25$) and $F_{\rm hg}$ ($\times 0.86$) in the ES or FCC schemes, yielding total increases in peak luminosity by factors of 15.5 and 10.6 above nominal, respectively.

Another important consideration for the upgrade is the luminosity lifetime, which can be written

$$\tau_{\rm lum} = \frac{1}{2}\frac{N_b}{\dot{N}_b} = \frac{n_b N_b}{L\sigma} = \frac{4\pi\epsilon\beta^*}{f_{\rm rev} N_b \sigma} \ . \qquad (5)$$

The luminosity lifetime is inversely proportional to the luminosity, or proportional to β^*. The lifetime can be increased only via a higher total beam current, proportional to $n_b N_b$. This implies either more bunches n_b (e.g. a previously considered scheme with 12.5-ns bunch spacing, which was ruled out at the CARE-HHH LUMI'06 workshop in view of excessive heat loads [12]) or a higher charge per bunch N_b, e.g. the LPA scheme. The effective luminosity lifetime can also be increased via "luminosity leveling," namely by suitably varying the beta function, the bunch length, or the crossing angle during a store.

4 EARLY SEPARATION SCHEME

In the **"early-separation" (ES) scenario** [13, 14, 15] one stays with the ultimate LHC beam, squeezes β^* down to about 0.1 m in ATLAS and CMS; and adds early-separation dipoles inside the detectors starting a few metres from the IP. Optionally, ES could also include a quadrupole doublet at about 13 m from the IP [16]. The ES scenario implies installation of new hardware inside the ATLAS and CMS detectors, as well as, most likely, the first ever hadron-beam crab cavities. The latter would gain a factor 2 to 5 in luminosity [15] by ensuring an effective Piwinski angle equal to zero. Their presence is assumed in Table 1. The maximum bunch intensity N_b is linked to the limit on the total beam-beam tune shift for two IPs, via $|\Delta Q_{\rm bb}| = N_b r_p \beta^*/(2\pi\gamma\sigma^{*2}) = N_b r_p/(2\pi(\gamma\epsilon))$, where σ^* denotes the transverse rms beam size at the IP. A maximum beam-beam tune shift of $|\Delta Q_{\rm tot}| = 0.01$ then translates into a maximum bunch population $N_b \approx 1.6 \times 10^{11}$. An IR layout for the ES scheme is sketched in Fig. 2.

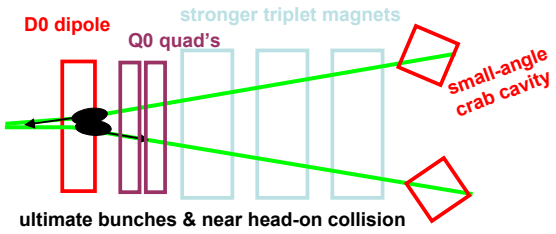

Figure 2: Possible interaction-region layout for the early-separation (ES) scheme, with highly squeezed optics ($\beta^* \approx 0.08$ m).

The merits of the ES scheme are the negligible effect of most long-range collisions thanks to the early separation, the absence of any geometric luminosity loss except for the hourglass effect, and no increase in the beam current beyond ultimate. Challenges include the early separation dipoles 'D0' deep inside the detector, the optional s.c. quadrupole doublet 'Q0', which would also be embedded, strong larger-aperture low-β quadrupoles based on Nb_3Sn, the use of crab cavities for hadron beams [17], the remaining 4 parasitic collisions at 4–5σ separation, a significant off-momentum beta beating (50% at $\delta = 3\times10^{-4}$), which may degrade the collimation efficiency plus low beam and luminosity lifetimes (proportional to β^*). Luminosity leveling via the crossing angle or crab voltage may alleviate this last concern [18].

Table 1: Parameters for the (1) nominal and (2) ultimate LHC compared with those for the three upgrade scenarios with (3) more strongly focused ultimate bunches at 25-ns spacing with either early separation and crab cavities [ES] or full crab crossing [FCC], and (4) longer intense flat bunches at 50-ns spacing in a regime of large Piwinski angle [LPA]. The numbers refer to the performance without luminosity leveling.

parameter	symbol	nominal	ultimate	ES or FCC	LPA
number of bunches	n_b	2808	2808	2808	1404
protons per bunch	N_b [10^{11}]	1.15	1.7	1.7	4.9
bunch spacing	$\Delta t_{\rm sep}$ [ns]	25	25	25	50
average current	I [A]	0.58	0.86	0.86	1.22
normalized transverse emittance	$\gamma\epsilon$ [μm]	3.75	3.75	3.75	3.75
longitudinal profile		Gaussian	Gaussian	Gaussian	uniform
rms bunch length	σ_z [cm]	7.55	7.55	7.55	11.8
beta function at IP1&5	β^* [m]	0.55	0.5	0.08	0.25
(effective) crossing angle	θ_c [μrad]	285	315	0	381
Piwinski angle	ϕ	0.4	0.75	0	2.01
hourglass factor	$F_{\rm hg}$	1.00	1.00	0.86	0.99
peak luminosity	$\hat{L}$ [10^{34} cm^{-2}s^{-1}]	1.0	2.3	15.5	10.6
events per crossing		19	44	294	403
rms length of luminous region	$\sigma_{\rm lum}$ [mm]	45	43	53	37
initial luminosity lifetime	$\tau_{\rm L}$ [h]	22.2	14.3	2.2	4.5
average luminosity ($T_{\rm ta} = 10$ h)	$L_{\rm av}$ [10^{34} cm^{-2}s^{-1}]	0.5	0.9	2.4	2.5
optimum run time ($T_{\rm ta} = 10$ h)	$T_{\rm run}$ [h]	21.2	17.0	6.6	9.5
average luminosity ($T_{\rm ta} = 5$ h)	$L_{\rm av}$ [10^{34} cm^{-2}s^{-1}]	0.6	1.2	3.6	3.5
optimum run time ($T_{\rm ta} = 5$ h)	$T_{\rm run}$ [h]	15.0	12.0	4.6	6.7
e-cloud heat load for $\delta_{\rm max} = 1.4$	$P_{\rm ec}$ [W/m]	1.07	1.04	1.0	0.4
e-cloud heat load for $\delta_{\rm max} = 1.3$	$P_{\rm ec}$ [W/m]	0.44	0.6	0.6	0.1
SR heat load	$P_{\rm SR}$ [W/m]	0.17	0.25	0.25	0.36
image-current heat load	$P_{\rm ic}$ [W/m]	0.15	0.33	0.33	0.70

Complementary Crab Cavities

In the ES scheme the geometric luminosity loss for a large crossing angle can be reduced either by bunch shortening rf or by crab cavity rf. It is instructive to compare the voltage required for the two cases [19].

The voltage required for bunch shortening is

$$V_{\rm rf} \approx \left[\frac{\epsilon_{||,\rm rms}^2 c^3 C\eta}{E_0 e\pi f_{\rm rf}}\right]\frac{1}{\sigma_z^4} \approx \left[\frac{\epsilon_{||,\rm rms}^2 c^3 C\eta}{E_0 e\pi f_{\rm rf}}\right]\frac{\theta_c^4}{\phi^4\ 16\ \sigma_x^{*\,4}}\ . \tag{6}$$

Equation (6) reveals an unfavorable scaling of the rf voltage with the 4th power of the crossing angle and the inverse 4th power of the IP beam size. The voltage can be decreased, to some extent, by reducing the longitudinal emittance (but limits come from intrabeam scattering, loss of Landau damping, and the injectors) and by increasing the rf frequency (the voltage scales inversely with the rf frequency).

By contrast, assuming horizontal crossing, the crab cavity voltage required is

$$V_{\rm cc} = \frac{cE_0\tan(\theta_c/2)}{e2\pi f_{\rm rf,cc}R_{12}} \approx \frac{cE_0}{e4\pi f_{\rm rf}R_{12}}\,\theta_c\ . \tag{7}$$

It is linearly proportional to the crossing angle and independent of the IP beam size. The voltage scales with $1/R_{12}$, where R_{12} is the (1,2) transport matrix element from the location of the crab cavity to the IP. As in the case of the bunch shortening rf, the crab-cavity voltage is also inversely proportional to the crab-rf frequency.

Figure 3 illustrates the voltages required for bunch shortening and for crab cavities, respectively, as a function of the crossing angle. The attractivity of crab cavities is evident. Figure 4 highlights the luminosity gain from a crab cavity for the ES and FCC schemes with an IP beta function β^* of 0.11 m. The residual $\sim$15% luminosity reduction at zero crossing angle is due to the hourglass effect, as β^* is comparable to the bunch length.

5 FULL CRAB CROSSING SCHEME

Crab cavities with sufficiently large total voltage could provide the same luminosity, and would allow for identical beam parameters, as the early separation (ES)) scheme, while avoiding the need for accelerator magnets inside the detectors. Possible beam parameters for such **"full crab crossing" (FCC) scenario** are identical to those of the ES scheme, as is indicated in Table 1. A corresponding IR layout is sketched in Fig. 5.

In the FCC scheme the crossing angle could be raised to any value supported by the triplet aperture and the crab-

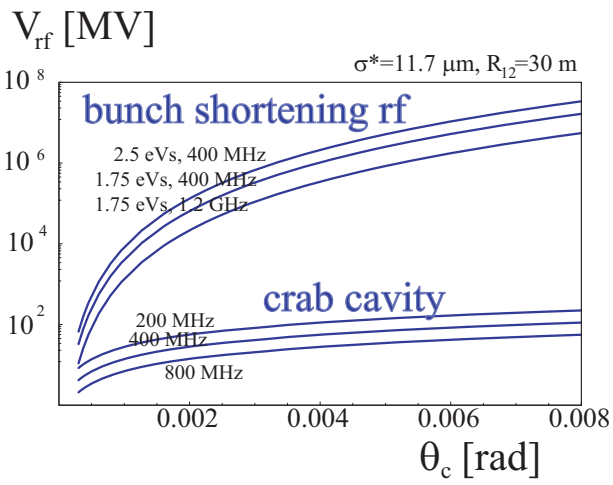

Figure 3: Bunch shortening rf voltage required to maintain a constant value $R(\phi) = 0.68$ and crab-cavity voltage as a function of the full crossing angle, for different rf frequencies and longitudinal emittances. The curves are computed from Eqs. (6) and (7). An IP beam size of 11.7 μm and $R_{12} = 30$ m from the crab cavity to the IP are assumed [19].

cavity system. For example, a transverse beam-beam separation of 8σ at the parasitic collisions is likely to be sufficient for avoiding performance degradation due to long-range beam-beam effects, provided a long-range wire compensation is also put in place.

The merits of the FCC scheme are the absence of any geometric luminosity loss except for the hourglass effect, no parasitic collisions at reduced separation, the absence of accelerator elements inside the detector, and no increase in the beam current beyond ultimate. A few of the ES challenges remain for FCC, namely the required strong larger-aperture low-β quadrupoles based on Nb_3Sn, the use of crab cavities for hadron beams (with 60% higher crab voltage than for ES), a significant off-momentum beta beating (50% at $\delta = 3 \times 10^{-4}$), plus low beam and luminosity lifetimes. Luminosity leveling via the crab voltage would be an option.

As an illustration, we consider an IP beta function $\beta^* = 0.08$ m, a crab cavity operating at 400 MHz and a typical (1,2) transport matrix element $R_{12} \approx 30$ m between the crab cavity and the IP. In this case the crossing angle needed for ES would be about 0.4 mrad (with 5σ separation), compared with 0.64 mrad for FCC (8σ separation). Using (7) these numbers translate into local crab-cavity voltages of 5.6 MV for ES and 9.0 MV for FCC. In other words, a 60% increase in the total crab voltage would be equivalent to the early-separation dipole.

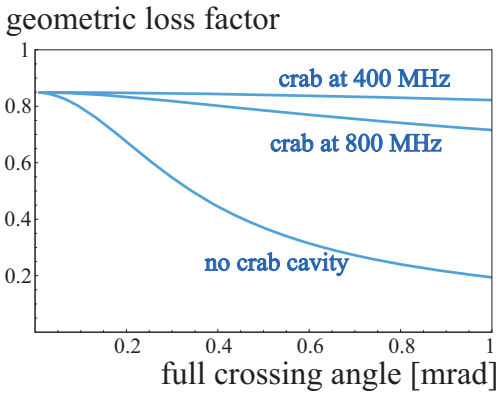

Figure 4: Luminosity reduction factor as a function of crossing angle without a crab cavity, and with a crab cavity operated at 400 MHz and 800 MHz, respectively, assuming $\beta^* = 0.11$ m. A crossing angle of 5 times the rms divergence (5 σ separation at the closest long-range encounters) would be 0.34 mrad, while 8σ separation at the closest parasitic encounters would translate to a 0.54-mrad crossing angle.

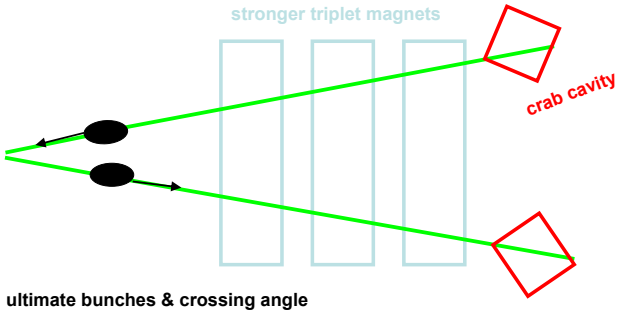

Figure 5: Possible interaction-region layout for the full crab-crossing (FCC) scheme, with highly squeezed optics ($\beta^* \approx 0.08$ m).

6 LARGE PIWINSKI ANGLE SCHEME

In the **"large Piwinski angle" (LPA) scenario** the bunch spacing is doubled, to 50 ns; longer, longitudinally flat, and more intense bunches are collided with a large Piwinski angle of $\phi \equiv \theta_c \sigma_z/(2\sigma^*) \approx 2$; the IP beta function is reduced by a more moderate factor of 2 to $\beta^* \approx 0.25$ m; and long-range beam-beam wire compensators [20] are installed upstream of the inner triplets. This regime of large ϕ and uniform bunch profile allows raising the bunch intensity N_b in (4) and thereby the luminosity, since lengthening the bunches in proportion to N_b maintains a constant value of $\Delta Q_{\rm bb}$. Figure 6 illustrates the IR layout for this upgrade option.

The merits of the LPA scheme are the absence of accelerator elements inside the detector, no crab cavities, reduced IR chromaticity, and relaxed IR quadrupoles. For

$\beta^* \approx 0.25$ m various possible optics solutions based on large-aperture NbTi quadrupoles exist [21], though the survival of the latter at high luminosity still remains to be demonstrated. Challenges are the operation with large Piwinski angle, unproven for hadron beams, the high bunch charge, in particular the beam production and acceleration through the SPS, the larger beam current, the (almost established) wire compensation, and an off-momentum beta beating of about 30% at $\delta = 3 \times 10^{-4}$. The level of off-momentum beta beating is about half that of the ES scheme, but approximately two times larger than for the nominal LHC, and likely to impact the collimation cleaning efficiency.

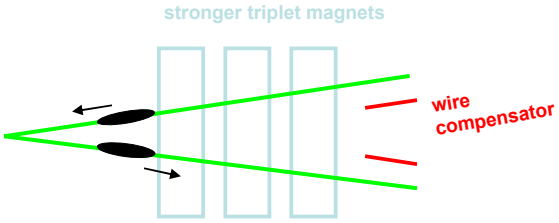

Figure 6: Interaction-region layout for large-Piwinski-angle (LPA) upgrade with an IP beta function of 0.25 m.

FLAT BUNCHES AND LARGE ϕ

The merits of longitudinally "flat" bunches and a large Piwinski angle can be unveiled more clearly by rewriting the luminosity expression in terms of the maximum beam-beam tune shift (which is taken to be the same and constant) for bunches with both Gaussian and uniform profiles.

As before and as appropriate for the LHC upgrade, we consider two interaction points (IPs) with alternating crossing. If the crossing angle is small, $\theta_c \ll 1$, the transverse IP beam size smaller than the bunch length, and the latter smaller than the IP beta function, $\sigma^* \ll \sigma_z \ll \beta^*$, and if furthermore the Piwinski angle is larger than 1, $\phi \gg 1$, the luminosity for bunches with Gaussian longitudinal profile can approximately be written [22]

$$L_{\rm gauss} \approx \frac{1}{2} \frac{f_{\rm rev} n_b \gamma}{r_p \beta^*} \Delta Q_{\rm bb} N_b \ , \qquad (8)$$

where $\Delta Q_{\rm bb}$ denotes the total linear beam-beam tune shift from the two interaction points, experienced at the center of the bunch.

Also for our second case of longitudinally "flat" bunches we assume a reasonably small crossing angle, $\theta_c \ll 1$. If in addition, the crossing angle is larger than the rms beam divergence, $\theta_c \gg \sqrt{\epsilon_N/(\gamma\beta^*)}$ (a logical requirement if the crossing angle is meant to separate the beams at the next parasitic encounter), and if the total bunch length l_b is larger than the effective extent of the beam intersection, $l_b \gg \sigma^*/\theta_c$, we can re-express the luminosity for bunches with flat longitudinal profile as [22]

$$L_{\rm flat} \approx \frac{1}{\sqrt{2}} \frac{f_{\rm rev} n_b \gamma}{r_p \beta^*} \Delta Q_{\rm bb} N_b \ . \qquad (9)$$

Comparison of (8) and (9) shows that, for the same number of particles per bunch N_b, and the same total tune shift from two IPs $\Delta Q_{\rm bb}$, the luminosity will be $\sqrt{2} \approx 1.4$ times higher with a "flat" distribution. The above assumptions were implicitly made when we earlier quoted the value of the form factor $F_{\rm profile}$ in (4).

As an additional merit, it is only in the regime of large Piwinski angle and for flat bunches that the number of particles N_b can be increased independently of the total tune shift $\Delta Q_{\rm bb}$, by lengthening the bunches.

7 CRAB WAIST COLLISIONS

All upgrade scenarios, LPA, ES and FCC, could conceivably be adapted for crab-waist collisions [23] by operating with flat beams with $\beta_x^* \gg \beta_y^*$, which would also make optimum use of the available aperture in the low-beta quadrupoles [24], and preferably with higher intensity and higher brightness. In addition, crab-waist collisions require a large Piwinski angle, such as the one for the LPA scheme, a small beta function comparable to σ_x^*/θ_c such as as for the ES or FCC scheme, and crab-waist sextupoles [25].

A possible approach for implementing crab-waist collisions at the LHC, therefore, is to adopt flat beams, combine some key ingredients of the ES, FCC and LPA schemes, and add suitable sextupoles in the IRs.

8 LUMINOSITY EVOLUTION

Figure 7 compares the luminosity evolution for the three scenarios. A turn-around time (the time between the end of a collision run and the start of the next collisions) of 5 h and the corresponding optimum run durations from Table 1 are assumed. The dashed lines indicate the respective time-averaged luminosities.

Without leveling the instantaneous luminosity decays as

$$L(t) = \frac{\hat{L}}{(1 + t/\tau_{\rm eff})^2} \ , \qquad (10)$$

with

$$\tau_{\rm eff} \equiv \frac{n_b N_b(0)}{\hat{L} \sigma_{\rm tot} n_{IP}} \qquad (11)$$

denoting the effective beam lifetime due to burn-off at the collision points, $\sigma_{\rm tot} \approx 100$ mb the relevant total cross section, n_{IP} the number of IPs, and $\hat{L}$ the initial peak luminosity. The optimum average luminosity is

$$L_{\rm av} = \frac{\hat{L} \tau_{\rm eff}}{(\tau_{\rm eff}^{1/2} + T_{\rm ta}^{1/2})^2} \ , \qquad (12)$$

where T_{ta} denotes the turn-around time. The optimum run time $T_{\rm run}$ is the geometric mean of effective lifetime and

turn-around time:

$$T_{\rm run} = \sqrt{\tau_{\rm eff} T_{\rm ta}} \, . \qquad (13)$$

In Fig. 7 it can be seen that the luminosity for the ES or FCC scenarios starts higher, but decays faster than for the LPA case, leading to shorter runs. The average luminosity values are nearly identical. The high initial peak luminosity for ES or FCC may not be useful for physics in view of possibly required set-up and tuning periods. On the other hand, the average event pile up for the ES and FCC options is about 30–40% lower than that for the LPA case, since there are twice as many bunches and collisions.

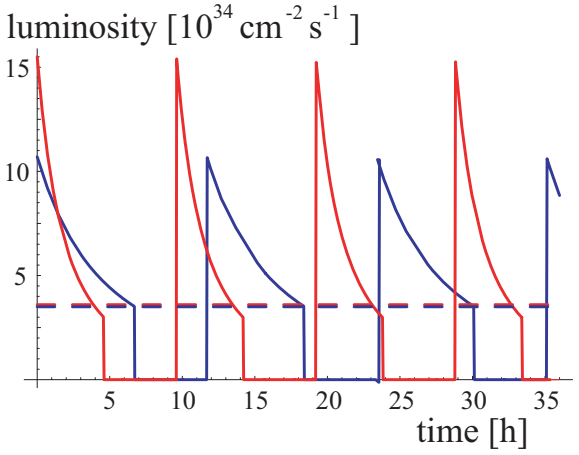

Figure 7: Ideal luminosity evolution without leveling for the ES or FCC (red) and LPA scenarios (blue), assuming the optimum run duration for a turn-around time of 5 h. The dashed lines indicate the corresponding time-averaged luminosities.

Smaller pile up at the start of a physics run, and higher luminosity at the end of each run would be desirable. Such luminosity leveling could be accomplished by dynamic β^* squeeze, crossing angle variation [18] for ES, or changes in the crab rf voltage for ES or FCC, and equally by dynamic β^* squeeze or via bunch-length reduction for LPA.

Leveling provides a constant luminosity, equal to L_0, and the beam intensity then decreases linearly with time t as

$$N_b = N_{b0} - \frac{L_0 \sigma_{\rm tot} n_{IP}}{n_b} t \, . \qquad (14)$$

The accessible intensity range $\Delta N_{b,\rm max}$ is limited, for example, by the range of the leveling variable, e.g. by the minimum value of β^*, so that the length of a run amounts to

$$T_{\rm run} = \frac{\Delta N_{b,\rm max} n_b}{L_0 \sigma_{\rm tot} n_{IP}} \, , \qquad (15)$$

and the average luminosity with leveling becomes

$$L_{\rm av,lev} = \frac{L_0}{1 + \Delta N_{b,\rm max} n_b T_{ta} / \left(L_0 \sigma_{\rm tot} n_{IP} \right)} \, . \qquad (16)$$

Table 2: Event rate, run time, and average luminosity for the three upgrade scenarios with leveling. Highlighted in bold are two promising examples.

	ES or FCC	LPA
events/crossing	300	300
optimum run time	N/A	2.5 h
av. luminosity [10^{34} cm^{-2}s^{-1}]	N/A	2.6
events/crossing	150	150
optimum run time	2.5 h	**14.8 h**
av. luminosity [10^{34} cm^{-2}s^{-1}]	2.6	2.9
events/crossing	75	75
optimum run time	**9.9 h**	26.4 h
av. luminosity [10^{34} cm^{-2}s^{-1}]	2.6	1.7

Table 2 compares event rates, run times, and average luminosity values achievable in the ES or FCC and LPA schemes. In case of β^* variation, the tune shift decreases during the store, while for leveling via the bunch length or crossing angle the tune shift increases. With leveling, the sensitivity of the average luminosity to the accessible range of the leveling parameter (β^*, bunch length or crossing angle) greatly depends on the chosen number of events per crossing, as is illustrated in Fig. 8.

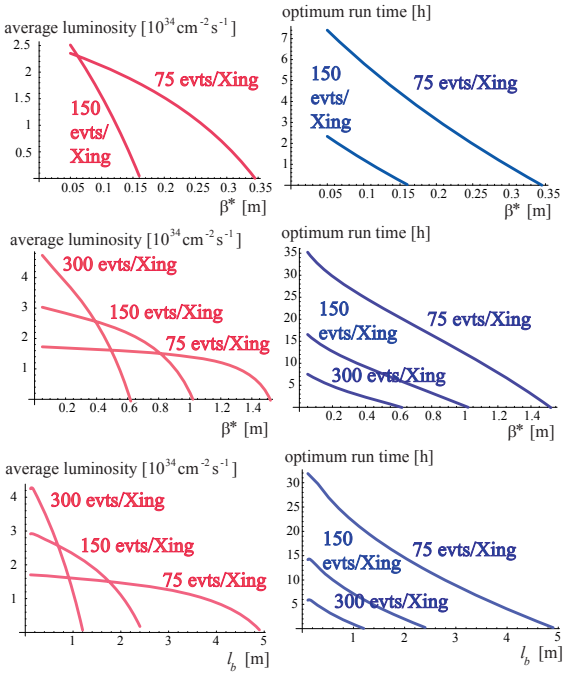

Figure 8: Average luminosity (left) and optimum run time (right) as a function of final β^* for ES or FCC with β^* leveling (top) and for LPA with β^* leveling (center), and as a function of l_b [total bunch length] for LPA with l_b leveling (bottom).

9 LUMINOSITY REACH

Figure 9 illustrates the dependence of the geometric luminosity reduction on the IP beta function. The two lower curves refer to a crossing angle of 9.5 or 5 times the rms IP beam divergence, respectively. The top curve represents both the early separation scheme with complementary crab cavity and also the full crab crossing scheme. The crab cavity restores most of the geometric overlap, except at very small β^* values, where the hourglass reduction becomes significant.

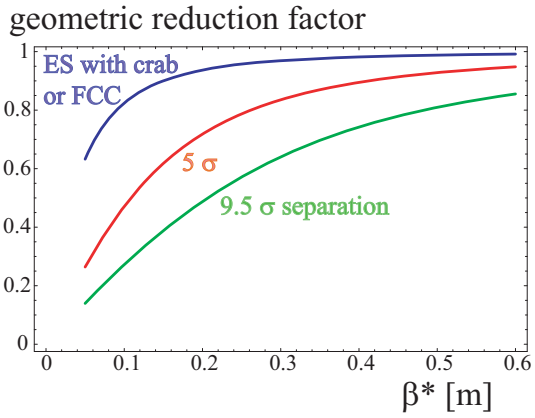

Figure 9: Geometric luminosity reduction as a function of β^* with 9.5σ (nominal) and 5σ separation (ES scheme without crab cavity) at the closest long-range encounters, as well as for arbitrary separation including crab crossing (ES with crab cavity or FCC).

Figure 10 shows the average luminosity as a function of β^* for four scenarios: the large-Piwinski angle (LPA) scheme, the early-separation (ES) scheme with either 9.5σ or 5σ beam-beam distance at the nearest long-range encounters if no crab cavity is employed, as well as ES with crab cavity or full crab crossing (FCC). The average luminosity shown is the ideal value (12), with an assumed turnaround time of 5 hours that could be provided by an upgraded LHC injector complex. For comparison, the average luminosities and β^* values corresponding to the nominal and the "ultimate" LHC with 10-h turnaround time are also indicated by plotting symbols.

The figure demonstrates that the performance of the ES scheme is considerably boosted by a crab cavity, but that both ES with crab cavity and FCC require β^* values below about 0.1 m in order to achieve the same average luminosity as obtained for the LPA scheme with a relaxed beta function of $\beta^* \approx 0.25$ m.

The LPA parameters in this example were chosen so that $|\Delta Q_{\rm tot}| \approx 0.011$ at $\beta^* \approx 0.25$ m. The magnitude of the LPA tune shift decreases if β^* is squeezed towards smaller values, a feature which could be exploited to further raise the integrated LPA luminosities for $\beta^* < 0.25$, e.g. by shortening the bunches. On the other hand, for constant normalized separation and constant bunch length, the total tune shift grows with increasing β^*, which may reduce the average LPA luminosity achievable for $\beta^* > 0.25$ m.

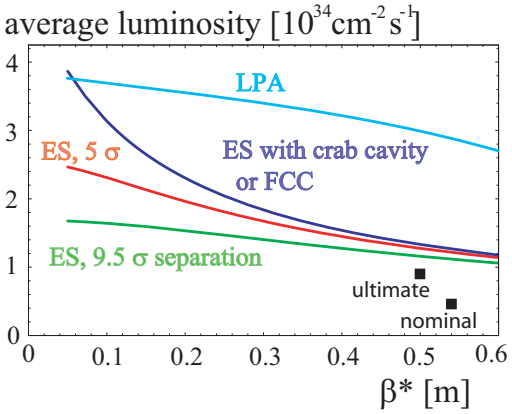

Figure 10: Average luminosity as a function of β^* for the large-Piwinski angle (LPA) scheme with a constant normalized separation of 8.5σ and a constant bunch length; for the early separation (ES) scheme with constant 9.5σ or 5σ separation and no crab cavity; and for ES with crab cavity or full crab crossing (FCC).

10 LHCB COMPATIBILITY

An upgrade of LHCb to Super-LHCb is planned, in order to exploit luminosities up to 2×10^{33} cm^{-2}s^{-1}, or 2% of the luminosity delivered to ATLAS and CMS. The LHCb detector is special due to its asymmetric location in the ring, which opens up a new possibility of supplying LHCb with its target possibility.

In the LPA case with 50-ns spacing between successive bunches in a train, we can arrange to have either collisions between the 50-ns bunches or no collisions at all in LHCb [27], depending on the distance in multiples of 25 ns which we choose between the various groups of bunch trains distributed around the ring. At 50-ns spacing, satellite bunches can be added in between the main bunches, as is illustrated in the bottom part of Fig. 11, displaying possible bunch patterns for various LHC configurations. Such satellites may be produced by asymmetric bunch splitting in the PS (possibly large fluctuation). In LHCb these satellites can be made to collide with main bunches at 25-ns time intervals. The intensity of the satellites should be lower than about 3×10^{10} protons per bunch in order to add less than 5% to the total tune shift and also to avoid electron-cloud problems. A beta function of about 3 m would result in the desired luminosity equivalent to 2×10^{33} cm^{2}s^{-1}. This value of β^* is easily possible with the present LHCb IR magnets and layout, which allows β^* squeezes down to 2 m [28].

For the ES or FCC scenarios with 25-ns bunch spacing, as well as for a different LPA filling with main-bunch collisions at LHCb, the resulting head-on collisions at Super-LHCb would contribute to the beam-beam tune shift of the

bunches colliding in ATLAS and CMS, which would lower the peak luminosity for the latter. Two ways out are (1) colliding only during the second half of each store when the beam-beam tune shifts from IP1 and 5 have sufficiently decreased below the beam-beam limit, or (2) introducing a transverse collision offset, albeit the latter raises concerns about offset stability, interference with collimation, poor beam lifetime, background etc. Requiring an LHCb contribution to the total tune shift of less than 10% implies transverse beam-beam offsets larger than 4.5σ, and $\beta^* \approx 0.08$ m, which is incompatible with the present LHCb IR configuration. For either option, the average luminosity delivered to Super-LHCb is considerably lower than for the LPA case with satellites.

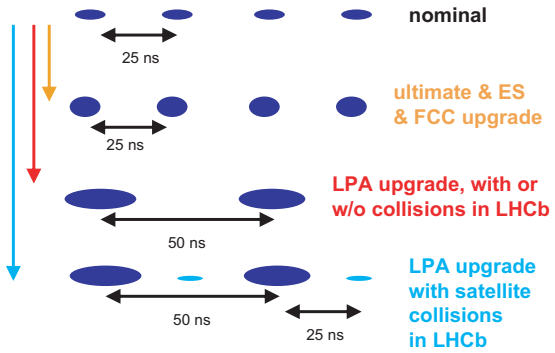

Figure 11: Bunch structures for nominal LHC, ultimate, ES or FCC upgrade, LPA upgrade, and LPA with satellite-bunch collisions at LHCb.

11 INJECTOR UPGRADE

An LHC injector upgrade is the central component of the CERN DG's White Papers [26]. The injector upgrade is already needed to produce the ultimate LHC beam (1.7×10^{11} protons per bunch with nominal beam emittance). In the context of the LHC upgrade, it will also provide a reduced turnaround time and, thereby, a higher integrated luminosity.

In order to provide the needed beam quality and intensity the existing 50-MeV proton Linac2 will be replaced by a 160-MeV "Linac4", and in the longer-term future extended by a 5-GeV s.c. proton linac (SPL). This will not only render the 1.4-GeV PS booster obsolete, but in addition it will raise the injection energy of the following storage ring PS2. The PS2 is a proposed successor of the present PS with twice the circumference and about twice the top energy (50 GeV). The next and last machine in the LHC injector chain is the Super Proton Synchrotron (SPS), which, though remaining, will be enhanced to cope with stronger electron-cloud effects and higher beam intensity.

The upgraded injector complex is designed to deliver to the LHC a beam with a maximum bunch intensity of 4×10^{11} at 25-ns bunch spacing. With this injector, the beam production for the ES scheme is straightforward. The LPA beam, requiring a slightly higher bunch population of 5×10^{11} at 50-ns bunch spacing, might be obtained by omitting the last double splitting in the PS, or in the future PS2 if the PS2 beam is still manipulated in a similar fashion as the present SPS. Numerous techniques for bunch flattening are at hand [29].

In the much longer term the SPS could be replaced by a higher-energy s.c. machine that would feed a higher-energy version of the LHC. R&D for an LHC energy upgrade is discussed in Refs. [30, 31], while the conceptual design for an energy tripler magnet can be found in [32].

12 CONCLUSIONS

We have presented three scenarios of the LHC luminosity upgrade, all promising a peak luminosity in excess of 10^{35} cm^{-2}s^{-1} with acceptable heat load and pile-up rate. Luminosity leveling should be seriously considered for the increased pile-up rates of the upgraded LHC, as it would provide a more regular flow of events at the possible expense of a moderate decrease in average luminosity.

The early separation (ES) and full crab-crossing (FCC) schemes both push β^*. ES requires slim magnets inside the detector, crab cavities, and Nb_3Sn quadrupoles. Also a "Q0" doublet inside the detector could optionally be added to achieve minimum β^* values. FCC requires 60% stronger crab cavities and wire compensation of residual long-range beam-beam effect. The ES and FCC schemes are particularly attractive if the total beam current in the LHC is limited. Luminosity leveling for ES and FCC can be realized by varying β^*, θ_c or the crab voltage. An open issue for ES is the effect of a few long-range collisions with reduced separation, which is avoided for FCC.

The large Piwinski angle (LPA) scheme entails fewer bunches of higher charge and an only moderately decreased β^*. It can conceivably be realized with NbTi magnet technology if necessary. The "Q0" doublet may also be an option for this scenario. LPA is more flexible in regard to collisions at LHCb. The LPA luminosity can be leveled by varying the bunch length or β^*. Open issues for LPA are the beam production, transport and acceleration through the SPS, and also hadron beam-beam effects at large Piwinski angle.

The off-energy beta beating compromises the collimation cleaning efficiency. This is a common concern for the three scenarios, but more severe for the lower β^* value of ES or FCC. The crab-waist scheme is yet another promising upgrade path that should further be explored for the LHC.

The first two or three years of LHC operation will clarify the severity of the electron cloud, long-range beam-beam collisions, collimator impedance, etc. On the same time scale, the first LHC physics results will indicate whether or not magnetic elements can be installed inside the detectors. Also around 2011, the LHC crab-cavity R&D, which — motivated by CARE-HHH discussions — is now being set up in a broad international collaboration, will have reached

a conclusion on the feasibility of LHC crab cavities and a solid cost estimate. The outcome from all these activities will finally decide the choice of the upgrade path.

13 ACKNOWLEDGEMENT

Many colleagues contributed to the ideas presented in this paper.

14 REFERENCES

[1] A. de Roeck, "Physics at the Next Colliders," Third National Turkish Accelerator Congress (UPHUK3), Bodrum, Turkey, 2007.

[2] J. Strait, private communication (2003).

[3] Physics Potential and Experimental Challenges of the LHC Luminosity Upgrade, F. Gianotti, M.L. Mangano, T. Virdee (conveners), CERN-TH/2002-078 (2002).

[4] O. Brüning et al, "LHC Luminosity and Energy Upgrade: A Feasibility Study," LHC-PROJECT-Report-626 (2002).

[5] *http://esgard.lal.in2p3.fr/Project/Activities/Current*

[6] *http://care-hhh.web.cern.ch/CARE-HHH*

[7] *http://www.agsrhichome.bnl.gov/LARP*

[8] *http://lhc-collimation-project.web.cern.c/lhc-collimation-project*

[9] *http://ab-abp-rlc.web.cern.ch/ab-abp-rlc-ecloud*

[10] *http://lhc-beam-beam.web.cern.ch/lhc-beam-beam*

[11] F. Ruggiero, F. Zimmermann, "Luminosity Optimization Near the Beam-Beam Limit by Increasing Bunch Length or Crossing Angle," PRST-AB 5, 061001 (2002).

[12] L. Tavian, "Cryogenic Limits," CARE-HHH LUMI'06 workshop, Valencia, 16–20 October 2006; *http://care-hhh.web.cern.ch/CARE-HHH/LUMI-06/*; and W. Scandale, F. Zimmermann, "IR Ranking Proposal and New Beam Parameter Sets for the LHC Upgrade — The View of HHH," Proc. CARE-HHH LUMI'06, Valencia, CERN Yellow Report CERN-2007-002, p. 99 (2006)

[13] J.-P. Koutchouk, "Possible Quadrupole-First Options with $\beta^* \leq 0.25$ m," Proc. CARE-HHH LHC-LUMI-05, Arcidosso, CERN Yellow Report CERN-2006-008, p. 41 (2006)

[14] J.-P. Koutchouk, "Strong Focusing Insertion Solutions for the LHC Luminosity Upgrade," Proc. CARE-HHH LHC-LUMI-06, Valencia, CERN Yellow Report CERN-2007-002, p. 43 (2007)

[15] E. Todesco, R.W. Assmann, J.-P. Koutchouk, E. Metral, G. Sterbini, F. Zimmermann, R. De Maria, "A Concept for the LHC Luminosity Upgrade Based on Strong Beta* Reduction Combined with a Minimized Geomtrical Luminosity Loss Factor," PAC'07, Albuquerque (2007).

[16] E. Laface et al, private communication; see also E. Laface, "Q0 Status," CARE-HHH IR07 workshop, Frascati, 6-8.11.2007, *http://care-hhh.web.cern.ch/CARE-HHH/IR07*

[17] R. Calaga, K. Akai, K. Ohmi, K. Oide, U. Dorda, R. Tomas, F. Zimmermann, "Small Angle Crab Compensation for LHC IR Upgrade," PAC'07, Albuquerque (2007).

[18] G. Sterbini, J.-P. Koutchouk, "A Luminosity Leveling Method for LHC Luminosity Upgrade Using an Early Separation Scheme," LHC-Project-Note-403 (2007).

[19] F. Zimmermann, U. Dorda, "Progress of Beam-Beam Compensation Schemes," Proc. CARE-HHH-APD Workshop LUMI'05, Arcidosso, CERN Yellow Report CERN-2006-008, p. 55 (2005).

[20] U. Dorda, W. Fischer, V.D. Shiltsev, F. Zimmermann, "LHC Beam-Beam Compensation Using Wires and Electron Lenses," PAC'07, Albuquerque (2007).

[21] O. Brüning, R. De Maria, R. Ostojic, "Low Gradient, Large Aperture IR Upgrade Options for the LHC Compatible with Nb-Ti Magnet Technology," LHC-PROJECT-Report-1008 (2007).

[22] F. Ruggiero, G. Rumolo, F. Zimmermann, Y. Papaphilippou, "Beam Dynamics Studies for Uniform (Hollow) Bunches or Super-Bunches in the LHC: Beam-Beam Effects, Electron Cloud, Longitudinal Dynamics, and Intrabeam Scattering," Proc. RPIA2002, Tsukuba, Japan, CERN-LHC-Project-Report-627 and KEK Proceedings 2002-30 (2002)

[23] P. Raimondi, "New Developments in Super B Factories," Proc. PAC'07, Albuquerque (2007).

[24] S. Fartoukh, "Flat Beam Optics," LHC MAC, 16.06.2006 *http://cern.ch/mgt-lhcmac*

[25] P. Raimondi, M. Zobov, D. Shatilov, "Beam-Beam Simulations for Particle Factories with Crabbed Waist," Proc. PAC'07, Albuquerque (2007).

[26] CERN DG White Papers, June 2006.

[27] M. Ferro-Luzzi, private communication, January 2008.

[28] W. Herr, Y. Papahilippou, "Alternative Running Scenarios for the LHCb Experiment," LHC-Project-Report-2009 (2007).

[29] F. Zimmermann, "Generation and Stability of Intense Long Flat Bunches," CARE-HHH BEAM'07, CERN, 1-5 October 2007, *http://care-hhh.web.cern.ch/CARE-HHH/IR07*, these proceedings (2008).

[30] LBNL S.c. Magnet Program Newsletter, no. 2 "HD-1 Sets New Dipole Field Record" (2003).

[31] *http://lt.tnw.utwente.nl/project.php?projectid=9*

[32] P. McIntyre et al, "On the Feasibility of a Tripler Upgrade for LHC," PAC'05, Knoxville (2005).

News from the U.S. LHC Accelerator Research Program, LARP

S. Peggs, BNL, Upton, NY, USA

INTRODUCTION

LARP Magnet R&D strategy aims at Nb_3Sn magnets in the Theme-3/Phase-2 IR Upgrade. However, the magnet R&D plan also supports the Theme-2/Phase-1 IR Upgrade activities. Accelerator Systems topics may include Theme-1 Paper Studies, for example in support of the PS2 conceptual design. Always, LARP R&D should enable U.S. contributions to LHC accelerator components in a Construction Project, if and when the DOE decides to fund such a project. These contributions could include:

1. Cold masses
2. Rotatable collimators
3. Crab cavities
4. Electron lenses ...

Contributions could commence well before 2016.

POTENTIAL UPGRADE CONTRIBUTIONS

U.S. contributions to LHC IR Upgrades are being considered in the context of some basic assumptions:

1. The Phase-1 upgrade is expected to lead to "ultimate" luminosities well beyond "nominal", in the range 2×10^{34} to 3×10^{34} cm^{-2} sec^{-1}.
2. Any contributions, in Phase-1 or -2, would need additional funding to a construction project separate from LARP.
3. Launching a construction project is synonymous with achieving a "Critical Decision 0" (CD-0), which crucially requires a clear official "statement of mission need" from CERN.
4. Efforts towards CD-0 for a construction project should begin immediately, even though the challenge may need to be declined.
5. Not only magnets but also accelerator components such as Rotatable Collimators could be delivered for the Phase-1 upgrade.

Coldmasses

In Rossi's "hybrid proposal" the U.S. would provide 4 or 8 Nb_3Sn quads out of the 16 required for the Phase-1 upgrade, with the NbTi complement made at CERN. The hybrid proposal is an exciting challenge, but must receive careful evaluation and discussion (CERN, DOE, LARP) before any commitment can be made. Some LARP R&D re-programming would be necessary if the hybrid proposal is accepted, beyond current LARP budget guidance from the DOE.

LARP magnet R&D has a single strategic goal: making Nb_3Sn magnet technology fully mature for use in the Phase-2 upgrade. Any LARP magnet R&D for Phase-1 must enhance progress towards this goal, rather than compromising it. Nb_3Sn magnets provided in Phase-1 would have to perform at least as well as NbTi magnets, otherwise they would not be worth installing. While Phase-1 tin magnets would be state-of-the-art in 2012, they would be intermediate R&D prototypes on the path to Phase-2.

It is not clear that the U.S. can commit to delivering even just 4 Nb_3Sn quads, absolutely guaranteed to be ready and reliable, to begin installation on the December 2012 date, even in scenarios unconstrained by funding limits. Nonetheless, LARP will immediately begin to evaluate the delivery of (at least) 4 Nb_3Sn quadrupoles, or Nb_3Sn D1 dipoles. A clear U.S. response to the hybrid proposal challenge should be possible by June 2008.

Rotatable collimators

Second generation collimators will also be required to achieve "ultimate" luminosities. Parallel R&D paths are being pursued in LARP and at CERN, in preparation for the construction of as many as 30 such collimators, to be installed on the Phase-1 upgrade timescale. Rotatable Collimator prototype RC2 is scheduled for beam tests alongside CERN's design soon after delivery to CERN in January, 2009. The U.S. will consider delivering many such RCs as part of a Phase-1 construction project.

Crab cavities

A recent DOE review of LARP stated that:

"The crab cavity effort seems well matched to the LARP program, and should be given sufficient resources to move forward."

Crab cavities are required for one of the two Phase-2 schemes. They also increase luminosity in any stand-alone installation. LARP could be the basis for U.S. participation in this strategic emerging enabling technology. Current LARP funding prohibits significant R&D participation, beyond maintaining observer status in the nascent international collaboration, and despite strong and growing interest at CERN.

Much crab cavity R&D remains to be performed. Nonetheless, the U.S. should consider delivering crab cavities. LARP would like to take a significant role in crab cavity R&D, with explicit support from CERN, and additional funds from DOE.

A Small Business (SBIR) proposal has been submitted by Advanced Energy Systems (AES), to build a prototype LHC crab cavity (800 MHz). This could be installed in the LHC in about 2011, in order to perform beam dynamics tests that would definitively resolve the practicality of a crab cavity construction project.

Evaluation process

A final commitment to Phase-1 deliverables will only occur after a stringent independent cost and schedule review. Different potential formats for this review include LARPAC, Lehman, and a joint review with CERN. The LARP Magnet Systems group will perform most of the magnet cost and schedule analyses, with the goal of releasing a report at about the same time as the LIUWG report.

2007	
Nov 7-9	CARE-HHH-APD IR07, Frascati
Dec 5	DOE Mini-Review, Germantown
Dec 6	Executive Committee meeting, Fermilab
Dec 18	CERN-U.S. Meeting, CERN
2008	
April 23-25	LARP Collaboration Meeting 10
June	CERN LIUWG report
June	LAUC report release
June	DOE full-scale review
June	Phase-1 construction project review.

Table 1: Milestones in the preparation and evaluation of a U.S. funded LHC Accelerator Upgrade Construction project (LAUC).

"JOINT IR STUDIES" WORKING GROUP

The recent DOE review also stated:

"The importance of establishing closer relations between the magnet and accelerator sectors of LARP cannot be overstated, especially in view of the fact that it is not clear what should follow the completion of the LQ magnet."

In response, the "Joint IR Studies" (JIRS) working group has been created within LARP (see Fig. 1), merging Magnet and Accelerator Systems people and activities. Sasha Zlobin leads JIRS. Ranko Ostojic chairs CERN's "LHC Insertions Working Group", evaluating all aspects of the Phase-1 upgrade. JIRS and LIUWG will maintain broad and unrestricted communications, but will work independently.

One of the JIRS goals is to define and evaluate a short list of potential locations for early Nb_3Sn magnets. According to de Rijk:

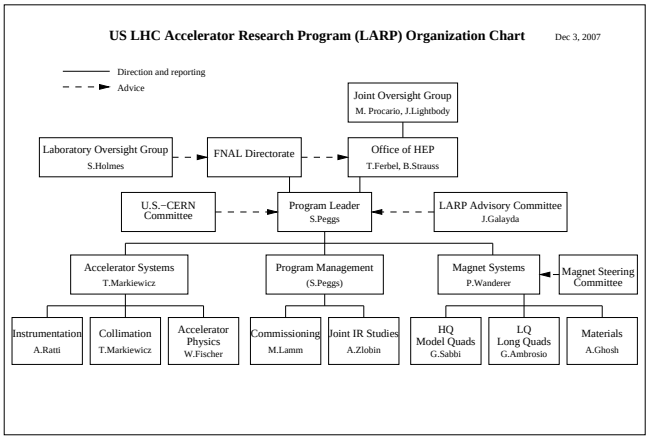

Figure 1: The organizational structure of LARP, the U.S. LHC Accelerator Research Program", in December 2007.

"New magnets are needed for the LHC phase 2 upgrade in about 10 years" [in the following potential locations:]

1. Quadrupoles for the low-beta insertions
2. Corrector magnets for the low-beta insertions
3. Dogleg dipoles for the cleaning insertions
4. Q6 for cleaning insertions
5. 10 m dipoles for the dispersion suppressors
6. Early separation dipole (D0)

Initial JIRS activities do not include crab cavity issues, although a crab task may be added to JIRS, eg in FY09

SUMMARY

LARP must move with "speed but not haste" to present to DOE possibilities for U.S. deliverables on the Phase-1 timescale. Rotatable collimators and crab cavity activities are gaining momentum. Potential Nb_3Sn cold mass locations include triplet quads and collimation quads. D1 dipoles are a significant alternative. CERN will definitively state upgrade parameters, on a timescale perhaps informed, but not driven, by LARP R&D. LARPs JIRS Working Group must work closely with LARP Magnet Liaison (Rossi), CERN-AB and AT divisions, and with the "LHC Insertions Upgrade Working Group" (Ostojic).

Mantra: LARP Magnet R&D strategy focuses on Nb_3Sn magnets for Phase-2, in collaboration with CERN/CARE.

What will beam say?

Nb-Ti SYMMETRIC TRIPLETS FOR THE LHC LUMINOSITY UPGRADE

E. Todesco, CERN, Geneva, Switzerland

Abstract

We study a Nb-Ti lay-out for the triplet in the low-beta interaction regions of the Large Hadron Collider, based on a stretched version of the present baseline. The triplet length is increased from the present value of 32 m up to about 60 m. The quadrupoles are based on a two layer coil made with the LHC main dipole cable. A parametric analysis of the dependence of the optics and magnet performances on the triplet length and aperture is carried out.

INTRODUCTION

The possibility of increasing the focusing in the interaction point of the Large Hadron Collider using a wider and longer Nb-Ti triplet has been considered in several studies [1,2,3]. In this paper we update the results of a parametric analysis developed according to the approach proposed in [4], and presented in [5] and [6]. The triplet lay-out is a stretched version of the today baseline, with quadrupoles of equal gradient and aperture, and different lengths ("symmetric option"). We extend the analysis up to triplet lengths that are ~25 m longer than the baseline, and we consider quadrupoles made up of two layers of the LHC main dipole cable. Moreover, we improved our analysis in a few points, namely i) we correct an overestimate of the LHC cable performance as given in [6], ii) we use a stronger focusing to have smaller beam size in Q4, iii) we increase the distance between Q2a and Q2b to take into account of the interconnection space needed for magnets in separate cryostats, and iv) we include a scaling of the cold bore thickness with the magnet aperture. The paper presents plots giving the main magnetic and optic properties as a function of the length of the triplet, which is taken as the free parameter.

OPTICS CONSTRAINTS

Triplet structure

We consider a triplet whose structure is similar to the LHC baseline [7], i.e., is made up of two focusing quadrupoles Q1, Q3 of equal length l_1, and with two defocusing quadrupoles Q2a and Q2b, each of length l_2, in between. We use the nominal distance l^*=23 m of Q1 from the interaction point (see Fig. 1). With respect to the calculations presented in [5] and [6] we increase the distance between Q2a and Q2b from 1 to 1.6 m to take into account the fact that the two magnets will have a separate cryostat, and not a common one as it is today in the baseline.

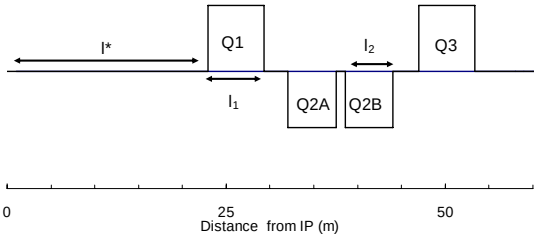

Fig. 1: Lay-out of the triplet close to the IP, nominal case of the LHC.

As in the previous work, we assume that

- all the quadrupoles have the same operational gradient;
- the gap between Q1-Q2 and Q2-Q3 is set to the actual values for the nominal LHC baseline (2.7 m between Q1 and Q2A, and 2.9 m between Q2B and Q3), i.e., we assume that the same structure and length of corrector magnets and instrumentation is kept.

The parametric analysis is carried out using the triplet length as the free parameter. All the following plots will be given in terms of the total quadrupole length, i.e. the length of the triplet minus the length of the gaps (2.7+1.6+2.9=7.2 m).

Approximated matching conditions

With respect to previous work, [5,6] we impose a larger focusing (up to 5%) to have smaller values of the beta functions in Q4 to avoid aperture bottlenecks in these magnets [8]. The obtained approximated matching has β functions in Q4 smaller than 1000 m for β^*=0.25 m. We keep the condition of approximately equal maxima of the β functions in the x and y planes (within a few percent) to determine the relative lengths of Q1-Q3 and Q2. Results are shown in Fig. 2, as a function of the total quadrupole length.

We use a quadratic fit for the inverse of the gradient G as a function of the total quadrupole length as proposed in [6] (see Fig. 3)

$$G = \frac{1}{f l_q^{\,2} + h l_q} \tag{7}$$

with f=2.33×10^{-6} [T^{-1} m^{-1}] and h=1.51×10^{-4} [T^{-1}] and we extended the fit analysis to total quadrupole lengths up to 55 m. The fit is very precise over the selected range. The obtained gradients are 3-4% larger with respect to the previous analysis [5,6].

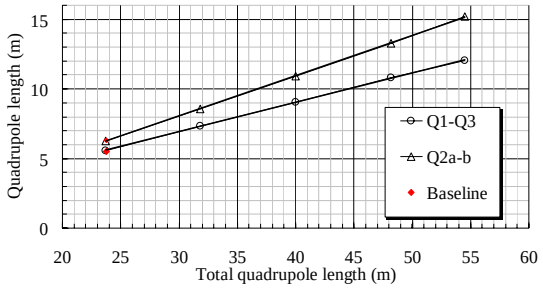

Fig. 2: Length of Q1-Q3 and Q2a-b versus total quadrupole length.

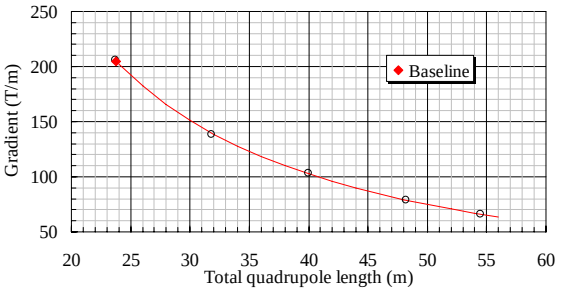

Fig. 3: Inverse of the quadrupole gradient versus total quadrupole length.

MAGNET CONSTRAINTS

Quadrupole aperture versus gradient

We considered two-layer quadrupole lay-outs having the inner and outer layer cable of the main LHC dipole for the inner and for the outer layer respectively, as presented in [6,9]. We used a revised estimate of the parameters of the critical surface of the superconductor

$$j_{sc}(B) = c(B^*_{c2} - B), \qquad (1)$$

i.e., c=575 A/mm^2 and B^*_{c2}=13.0 T. These values give a critical current density of 2300 A/mm^2 at 9 T and 1.9 K, which is an average of the measured values in FRESCA test station of 2200-2400 A/mm^2 for the outer layer cables [10]. We use the outer layer values since due to the strong grading the magnet performance is limited by the outer layer [9].

We calculated the critical gradient for quadrupole lay-outs with a aperture ranging from 100 to 220 mm. Results are shown in Fig. 4, where they are compared to the scaling law [11] using that values of c and B^*_{c2}. As in the previous works, we assume that the quadrupoles operational current is set at 80% of the loadline, i.e. a 20% operational margin. A parabolic fit is valid in this range (see Fig. 4). For the same aperture, the gradients are ~10% lower than what presented in [6,9].

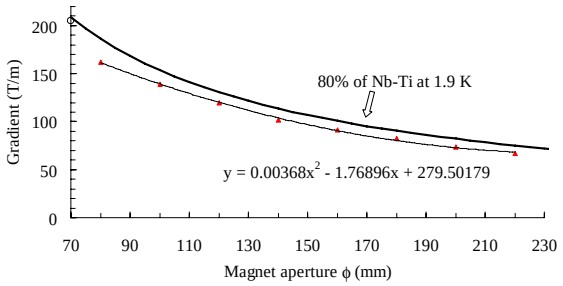

Fig. 4: Quadrupole gradient versus aperture: semi-analytical approach (solid line) and two-layer quadrupoles made with MB cable (markers).

Quadrupole aperture versus triplet length

Putting together Fig. 1 and Fig 4 we obtain in Fig. 7 the largest aperture reachable versus the total quadrupole length. With respect to the previous analysis [6] one obtains, for the same aperture, a ~10% longer total quadrupole length.

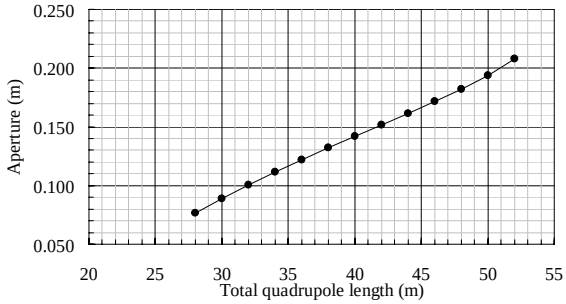

Fig. 7: Aperture of the quadrupole reachable for a matched triplet in Nb-Ti with LHC main dipole cable, two layers, versus triplet length.

Constraints due to the length of the MB cable

Using the estimate of the aperture required for a given triplet length given in Fig. 7, one can compute the cable needed to wind one pole for the longer quadrupoles Q1-Q3. In case of a total quadrupole length of ~41 m, corresponding to an aperture of ~150 mm, one needs a cable length equal to the unit length for the dipoles (see Fig. 8). Beyond these values one has to split each magnet in two cold masses, i.e., go for a modular option [12].

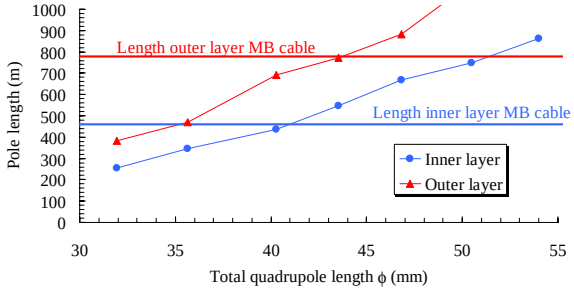

Fig. 8: Needed pole length to wind one pole of the Q1-Q3 magnets, versus triplet length.

Operational current versus triplet length

The operational current is a relevant parameter of the lay-out. Here we present its dependence on the triplet length It ranges between 11 and 9 kA, and decreases with larger apertures and longer triplets.

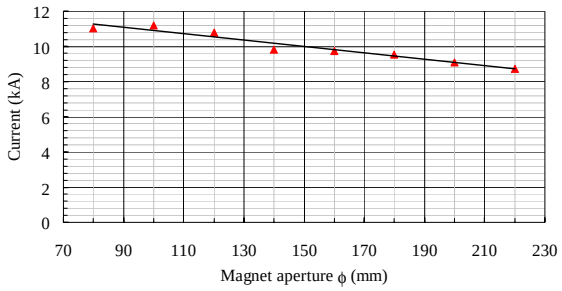

Fig. 9: Operational current in the triplet versus triplet length.

APERTURE CONSTRAINTS

β function

The fit of the maximum beta function in the triplet versus the triplet length is shown in Fig. 9. We use the linear function

$$\beta_{\max} = \frac{l^{*2} + a l_q}{\beta^*}. \qquad (4)$$

which holds well on the rather large domain of quadrupole lengths, with a=81 m. Due to the longer gap between Q2a and Q2b the increase of the beta function with respect to [6] is about 5%.

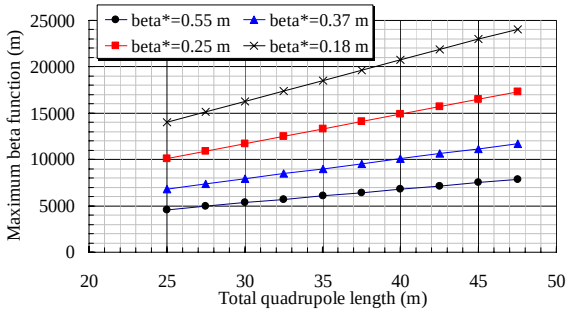

Fig. 10: Maximum beta function versus triplet length.

Aperture requirements

We assume a beam size of 10 sigma and the empirical scaling for the crossing angle with β^* [13], to work out the aperture requirements. In order to have a β^* =0.25 m one needs a total quadrupole length of 34.5 and an aperture of 115 mm (see Fig. 10). An aperture margin of 3 additional σ, which could ease the collimation, can be obtained with a total quadrupole length of 40 m and an aperture of 142 mm (see Fig. 10). This second option is very close to the solution that allows to reach the stronger possible focusing compatible with the chromaticity correction system β^* =0.18 m without margin on the aperture (total quadrupole length of 39.5 m and aperture of 140 mm, see Fig. 11).

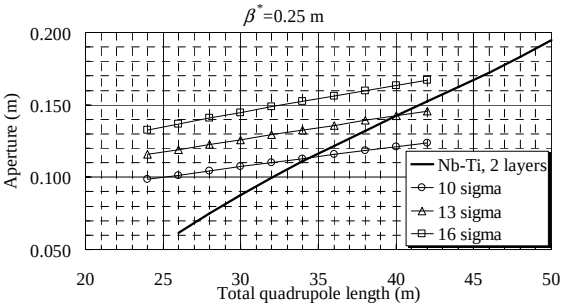

Fig. 11: Aperture requirements for 10, 13 and 16 sigma versus total quadrupole length, β^*=0.25 m.

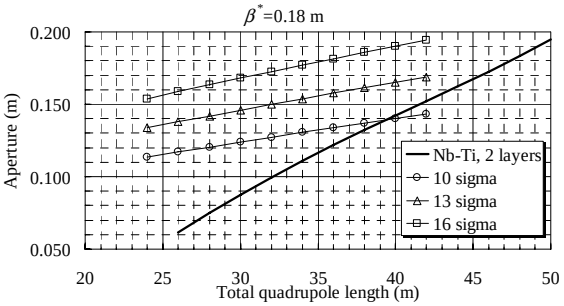

Fig. 12: Aperture requirements for 10, 13 and 16 sigma versus total quadrupole length, β^*=0.18 m.

DISCUSSION

One has two extreme cases: i) a first solution aiming at β^*=0.25 m and no aperture margin, with a total quadrupole length of 34.5 m and aperture of 115 mm, and ii) a second case giving either the largest possible focusing β^*=0.18 m without margin, or the β^*=0.25 m with ~3σ of margin. This second option, with a total quadrupole length of 40 m and aperture of 140 mm, is at the limit of the cable length of the dipoles, i.e. a lay-out with longer quadrupoles should be modular and at least double the number of cold masses. Results are summarized in Table I.

Table I: Quadrupole length, aperture, gradients and maximum beta function at β^*=0.25 m in 2 extreme cases.

l_t	l_1 (m)	l_2 (m)	ϕ (mm)	G (T/m)	β_{max} (Km)
34.6	7.9	9.4	115	125	13.0
40.0	9.0	11.0	140	103	15.0

Margin in aperture is welcome not only for the collimation issues but also to recover performance in case of impossibility of reaching nominal parameters. For

example, an emittance blow-up would need a larger aperture with respect to the nominal one to reach the foreseen beam focusing in the IP.

CONCLUSIONS

We updated the parametric analysis carried out in the last years [4,5,6] to find out the solutions for a Nb-Ti triplet made of two layers quadrupole with the LHC main dipole cable. A revised estimate of the cable performances, of the matching conditions, of the gaps in the triplet, and of the aperture clearance needed for the cold bore has been presented. The solution giving the possibility of reaching β^*=0.25 m with here additional sigma for collimation has an aperture of ~140 mm and a quadrupole length of 9/11 m, with respect to previous values of 130 mm, and 8/9 m given in [6].

For the present lay-out, an aperture of ~140 mm appears as a maximum value since i) it corresponds to the maximal length of the available dipole cable and ii) it corresponds to the maximum focusing of 0.18 m without having additional space for collimation. An aperture of ~135 mm would allow to keep basically the same level of performance and would have the advantage of being fully compatible with the large aperture Nb_3Sn quadrupoles foreseen for the LHC Accelerator Research Program [14]. This would keep open the possibility of having a mixed option Nb-Ti and Nb_3Sn for the phase I upgrade, as recently proposed [15].

ACKNOWLEDGMENTS

We acknowledge the support of the European Community-Research Infrastructure Activity under the FP6 "Structuring the European Research Area" program (CARE, contract number RII3-CT-2003-506395). I would like to thank J. P. Koutchouk for relevant comments on this study and for stimulating this work.

REFERENCES

[1] F. Ruggiero, et al., *EPAC* (2004) 608-10.
[2] R. Ostojic, et al., *PAC* (2005) 2795-7.
[3] R. De Maria, O. Bruning, *EPAC* (2006) 574-6.
[4] J.P. Koutchouk, LHC Project Report **973** (2006).
[5] E. Todesco, J.P. Koutchouk, LUMI-06 CARE-HHH proceedings (2006).
[6] J.P. Koutchouk, L. Rossi, E. Todesco, *LHC project Report* **1000** (2007).
[7] AA. VV. "LHC Design Report", CERN **2004-003** (2004).
[8] S. Fartoukh, *LHC Project Report* **10??** (2007).
[9] F. Borgnolutti, E. Todesco, *PAC07* ??? (2007).
[10] A. Verweij, and A. Gosh, *IEEE Trans. Appl. Supercond.* **17** (2007) 1454, in press, and T. Boutboul, private communication.
[11] L. Rossi, E. Todesco, *Phys. Rev. STAB* **9** (2006) 102401.
[12] O. Bruning, *LHC Project Report* **1008** (2006).
[13] F. Zimmermann, Y. Papahilippou, *Phys. Rev. STAB* **5** (2002) 074001.
[14] G. L. Sabbi, et al, *IEEE Trans. Appl. Supercond.* **17** (2007) 1051.
[15] L. Rossi, talk at LARP collaboration meeting, October 2007.

CERN PLANS ON HIGH FIELD MAGNETS DEVELOPMENT

D. Tommasini, CERN, Geneva, Switzerland

Abstract

The talk covered a short status of the LHC installation, an overview of R&D directions on superconducting magnets beyond the start of the LHC specifically addressing high field magnets, and an overlook of already on-going activities at CERN.

SUPERCONDUCTING MAGNETS ACTIVITIES BEYOND THE LHC START

Introduction

We can distinguish the activities on superconducting magnets beyond the LHC start as :

- Needed & funded activities
  - magnet R&D in "The White Paper" 2008-2011 (6 year-version under study);
  - 20.5 MCHF + 73 FTE-Y in High Field Magnets (primarily Nb_3Sn but HTS also considered);
  - 1.5 MCHF + 7 FTE-y for Fast Cycled Magnets
  - magnet R&D in the FP7;
  - installation of "long" magnets facilities in 2008-2009.
- Desirable, not funded (yet) activities
  - triplet upgrade with NbTi
- Being considered
  - D0;
  - Q0;
  - undulators for beam diagnostics with lead ions;
  - wigglers for CLIC damping ring;
  - cycled magnets for PS2.

We will here specifically focus on high field magnet development.

High Field Magnets

There is a variety of needs for high field magnets, which can be summarized as follows :

- large aperture, high peak field low-beta insertion quadrupoles Q1-Q2-Q3;
- large aperture, high peak field correctors for low-beta insertions;
- high field (< 15 T) , any cost, dipole for Fresca upgrade;
- high field, compact, any cost, D0 dipole (with 2 beam-beam LR at 5 σ, > 7 m);
- very high field (15-25 T), low cost, dipole (LHC energy upgrade);
- use of temperature margin for large heat deposition (D1, Q0, D0);
- high peak field undulators for LHC lead ions beam diagnostics;
- high peak field wigglers for CLIC damping rings;
- open mid-plane dipoles for neutrino factories

R&D programs & topics

The High Field program at CERN, coordinated by G. de Rijk, involves the CERN White Paper Program, the FP7-IA-HFM program and collaborations with several research institutes worldwide CEA, CIEMAT, INFN, STFC-RAL, UNIGE, TWENTE UNIVERSITY, WROCLAW UNIVERSITY and the LARP laboratories.

The R&D topics under consideration are :

- Conductor
  - Develop stable, high Jc conductors
  - Magnetization
- Enabling technologies & support studies
  - Electromagnetic layouts
  - Mechanical structures
  - High thermal transfer insulation
  - Radiation resistant insulation
  - Model coils (solenoid-racetrack) to study insulation & thermal treatment
  - Prospect HTS possibilities (design and build a 20 T insert)
- Model magnets
  - Design build and tests short models (dipole, quad and corrector)
- Prototype magnet
  - Design build and test 4 m prototype (dipole or quad)

On-going activities

The are at least four R&D activities already on-going at CERN concerning high field magnets :

- development of an industrial European wire with a target Jc of 3000 A/mm2 @ 12 T at 4.2 K. In Europe two technologies having the potential of reaching the target are being explored : powder in tube (contract awarded to SMI) and internal tin diffusion (contract awarded to Alstom). The progress on both fronts are promising and allowed achieving a Jc of 2500 A/mm2 @ 12 T and 4.2 K with the powder in tube technology, and a Jc of 2100 A/mm2 @ 12 T and 4.2 K with the internal tin technology;
- "fast" thermal treatment of OST wires, showing enhanced stability and excellent Jc values (~3000 A/ mm2 @ 12 T and 4.2 K) with a treatment of only 17 hours at 695°C;
- development of Nb3Sn undulators as synchrotron radiation sources for the beam profile monitors of the LHC run with lead ions. The short magnet period of only 14 cm, associated to a large aperture of 60 mm, requires a coil peak field of about 10 T to produce a magnetic field on the beam axis of 3 T;
- development of new concepts of Nb3Sn wire insulation, being experimented on mini dipole split-coils. The use of advanced ceramic insulations allowed the manufacture of a mini dipole reaching a short sample field of 12 Tesla at 4.2K with no training quenches. This insulation has the particularity to get fully hardened before the high temperature thermal treatment of the superconductor.

U.S. LARP MAGNET PROGRAM*

Peter Wanderer#, Brookhaven National Laboratory, Upton, NY, U.S.A.

Abstract

Progress and plans for the U.S. LARP R&D work are summarized. Results to date for work on materials and model magnets are presented in more detail.

INTRODUCTION

The primary goal of the LARP R&D effort is to demonstrate a "long, strong" superconducting quadrupole made with Nb3Sn by the end of 2009. Up to the present time, the focus has been on the development of the essential "building blocks" for Nb_3Sn magnets: materials, model magnets, supporting R&D, and IR design studies. The goal of the work on materials has been to establish a production method for Nb_3Sn that yields a superconductor that has high current density and stability against flux jumps. The goal of the work on model magnets has been to test 1 m versions of quadrupoles that reach 200 T/m using two different support structures. The supporting R&D has led to the early test of long (3.6 m) racetrack coils in one of the support structures, as a test for possible effects of magnet length on performance. It has also covered insulation and quench protection. The IR design studies have covered radiation studies, cryogenics, heat transfer issues, and magnet designs for several possible versions of IR optics (e.g., dipole first), as well as quadrupole designs for larger aperture and higher gradient.

Plans for R&D to reach the 2009 goal include the following: Construction and test of one to three 3.6 m, 90 mm quadrupoles, called LQ, with at least one test of both support structures. The plans for LQ R&D in general, and the support structures in particular, were reviewed by an external committee at the end of November. The LQ work has the highest priority in the LARP magnet R&D. The materials work is now directed toward increasing the diameter of the strand, additional studies of instability, and measurements of the strain sensitivity of the strand and the cable. Work toward a design which could test both high gradient and large aperture magnets is now concentrated on the large aperture (130 mm) version, with the possibility that the design might be close to the design needed for magnets that would be installed during the Phase I upgrade. A new task force, called JIRS (Joint IR Studies), has been established to pull together both magnet and accelerator physics work toward a Phase I upgrade.

This talk presents details of the LARP work on materials and model magnets. Other aspects of current LARP magnet work are presented in [1,2,3].

*Work supported by the U.S. Department of Energy
#wanderer@bnl.gov

MATERIALS

Starting several years ago, R&D has led to the development of Nb_3Sn strand that has been used in recent LARP model 90 mm quadrupoles that reached 200 T/m. This material, manufactured by Oxford Superconducting Technology, is designated RRP (rod restack process) [4]. Development has been supported by the U.S. DOE Conductor Development Program and by purchases by the "base" programs of the DOE labs. Design studies for larger aperture quadrupoles indicate that a larger diameter strand is desirable. Allowing the filament diameter to increase with the strand diameter is undesirable for stability, so studies of strand with an increased number of filaments are underway. The present strand, designated 54/61, has 54 filaments, with a copper core having the area of seven filaments. The strand has been drawn to a diameter of 0.7 mm for use in the LARP magnets made thus far. The 108/127 configuration has been selected for use in larger-diameter (0.8 mm – 1.0 mm) strand.

The work of the materials group has also included considerable effort on standardizing strand testing at the three labs. Consistency has been achieved at the level of ±5%. The materials group works with a month-by-month plan showing materials purchase and use. So far it has achieved its goal that cable be available when needed for use in magnets.

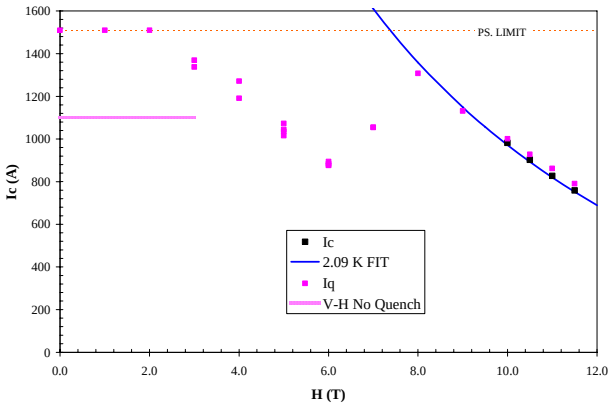

Fig. 1. Short-sample tests of 0.7-mm diameter RRP Nb_3Sn strand at 2.09 K.

The strand I_c measurements shown in Fig. 1 indicate the focus of stability studies now underway. At high field (H_0 > 9T), the strand I_c falls with increasing H_0 in the expected manner. At low field (H_0 < 3 T), the strand I_c is more than a factor of two greater than the current in individual strands in the magnets, indicating that the conductor will be stable in the low-field regions of the coils. However, at medium field, I_c drops to a value much less that its value at low field. This behavior is now under study. It may be the cause of quenching in the model

magnets (see below). However, even the minimum I_c, at 6 T, is still a factor of two greater than the strand current in these magnets.

MODEL QUADRUPOLE PROGRAM

Several model quadrupoles, called Technology Quadrupoles (TQ), have been made and tested. These models are approximately 1 m long and have a coil aperture of 90 mm. The coils have been made jointly at Fermilab and LBNL. The coils have been assembled using one of two support structures, denoted collar (TQC) and shell (TQS). A cross section of a collared magnet is shown in Fig. 2 [5]. The azimuthal preload is applied primarily during the assembly process via the collars and (through the yoke) the stainless steel shell. The end preload is modest – sufficient to keep the coil in contact with the end support. A cross section of a magnet assembled with the shell support structure is shown in Fig. 3 [6]. In this case, some of the azimuthal preload is applied via bladders (made of thin stainless steel) which are inflated during assembly. When the desired room temperature preload has been achieved, keys are inserted between the yoke and the iron pads and the bladders removed. An aluminum shell surrounds the yoke and provides the remainder of the preload during cooldown. High axial preload is achieved via rods which run the length of the magnet (Fig. 4).

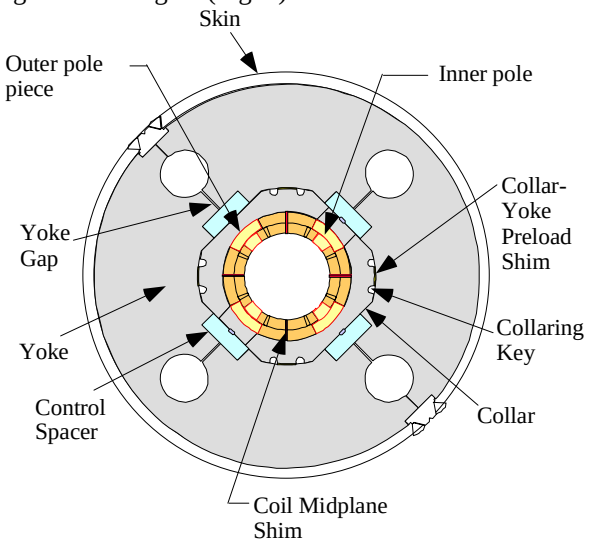

Fig. 2. Cross section of a TQC quadrupole cold mass

The most direct comparison of the collar and shell support structures was made by testing the same set of coils in both structures. The coils were made using 54/61 RRP strand. The coils were initially tested in a shell support structure (TQS02a). Starting from an initial quench gradient of 180 T/m, the magnet trained to ~90% of the expected conductor limit (220 T/m) at 4.4 K (Fig. 5). The magnet did not train to a higher gradient when further tested at 1.9 K. This behavior is not yet understood.

The coils were then reassembled in a collar support structure (TQC02E, where E stands for "exchange"). TQC02E also trained to ~90% of the expected conductor limit (200 T/m), from an initial quench gradient of ~ 165 T/m at 4.5 K (Fig. 6). Its quench performance at 1.9 K was slightly below that at 4.4 K, similar to the 1.9 K performance of TQS02a. (At the same fraction of the short-sample limit the two magnets have different gradients because of different yoke dimensions.)

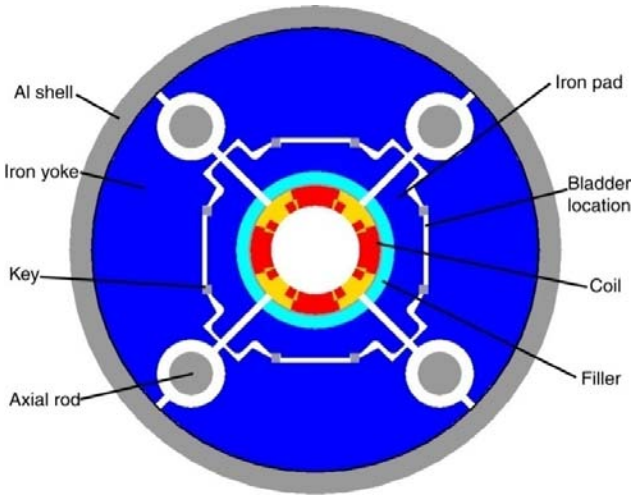

Fig. 3. Cross section of TQS quadrupole cold mass

Fig. 4. Photograph of a TQS quadrupole cold mass

Quench test data are also available from one additional magnet made with each of the support structures. In this case, the coils were made with MJR (modified jelly roll) Nb_3Sn, the predecessor of the RRP. Quadrupole TQS01 was tested in three versions (Fig. 7): TQS01a (standard assembly), TQS01b (reassembly with the limiting coil in version a replaced); and TQS01c (with reduced end preload). TQS01a quenched initially at ~ 180 T/m and advanced to ~ 195 T/m (~90% of the expected conductor limit) at 4.4 K. Its one quench at 3.2 K was higher than the quenches at 4.4 K. The 4.4 K training data of TQS01b lie below the training data of TQS01a, but the magnet did train to a higher gradient at 1.9 K.

TQC01 was tested in two versions. TQC01a, with a preload that was much lower than planned, and TQC01b, with satisfactory preload and two coils from TQS01. Given the low preload, it is not surprising that the initial

quench was at a low gradient, 130 T/m, and that it trained only to 150 T/m at 4.5 K (Fig. 8). What is interesting is that, at 1.9 K, it trained to 200 T/m (~ 86% of the expected conductor limit). The performance of TQC01b at 4.5 K was better than that of TQC01a. At 1.9 K, it reached 200 T/m (~90% of the expected conductor limit).

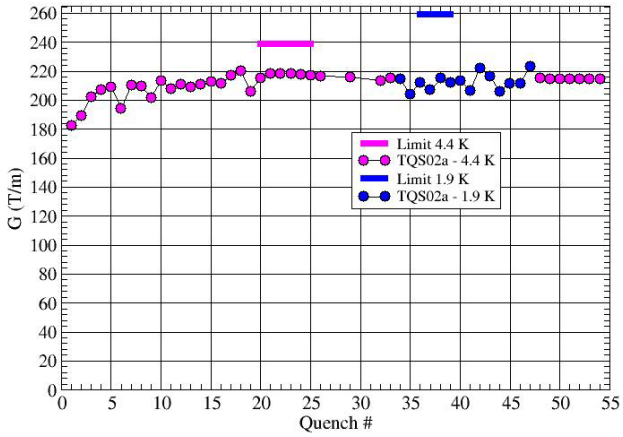

Fig. 5. Quench test data for TQS02a.

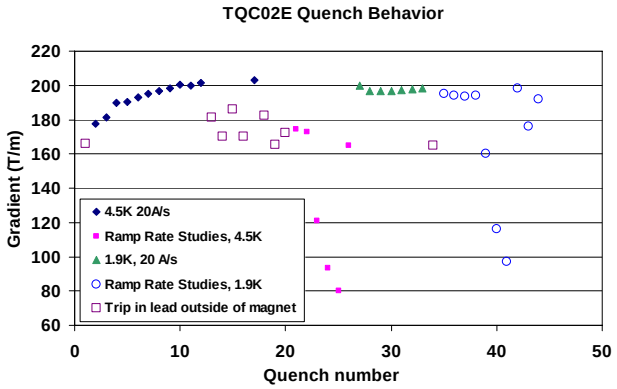

Fig. 6. Quench test data for TQC02E. (E denotes "exchange" – the coils were initially tested in the TQS support structure.)

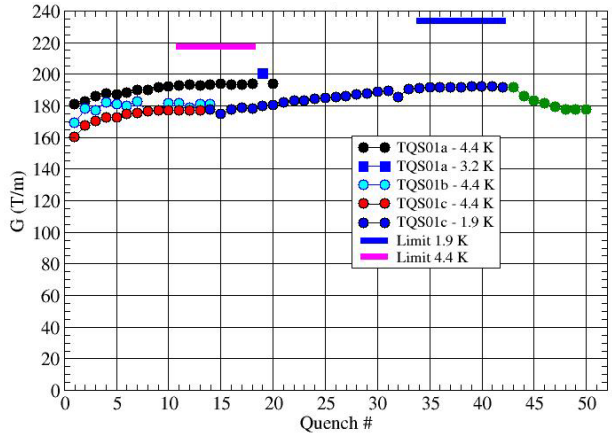

Fig. 7. Quench test data for the three versions of TQS01.

Overall, the 90 mm model quadrupoles reliably reach 200 T/m (~ 90% of the expected conductor limit) at 4.5 K. However, the factors affecting quench performance at 1.9 K are not yet fully understood.

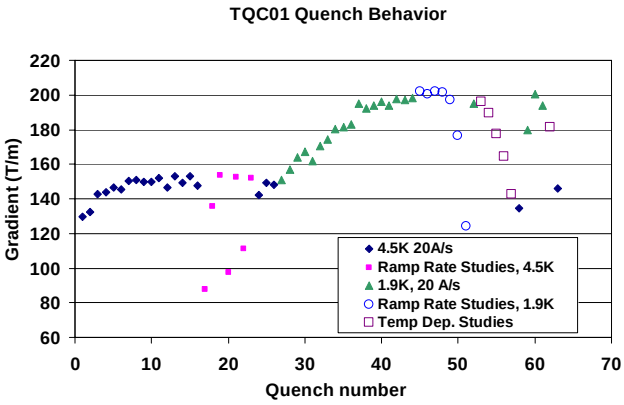

Fig. 8. Quench test data for TQC01.

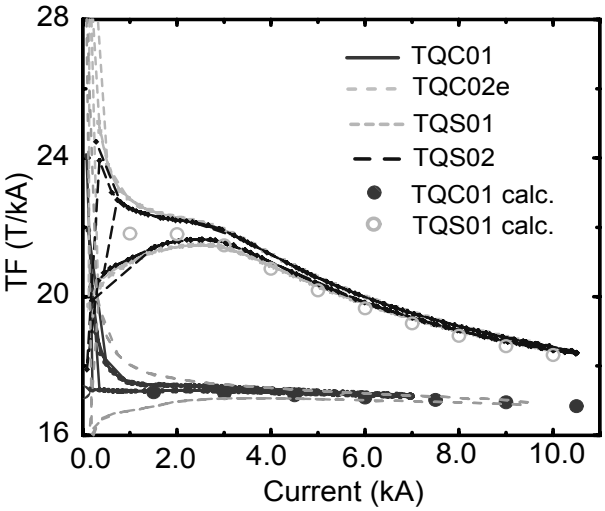

Fig. 9. Transfer function G/I calculations and measurements for the four TQs made thus far.

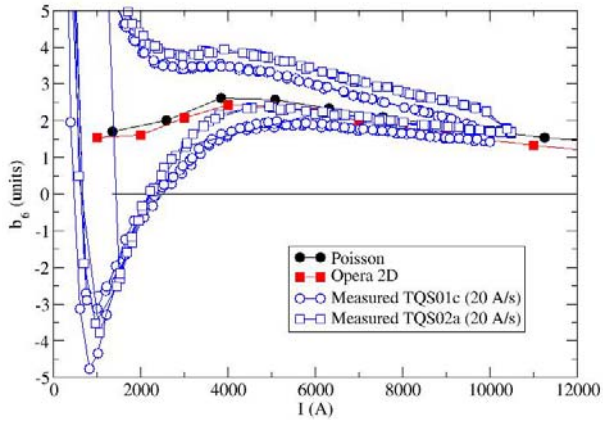

Fig. 10. Measurements and calculation of the first allowed harmonic for TQS01. The calculations do not include magnetization effects.

Field quality measurements of the TQs have been made [7]. Measurements of the transfer function (Fig. 9) are in agreement with the calculation for both the collar and shell structures (except for hysteresis at low current, which was not included in the calculation). The same is true of the measurements of the first allowed harmonic, b_6 (Fig. 10). Interestingly and surprisingly, measurements of this harmonic during a cycle which roughly simulates that of the LHC show no change with time during the ~ 1000 seconds when the current is held constant at the nominal value for injection (Fig. 11).

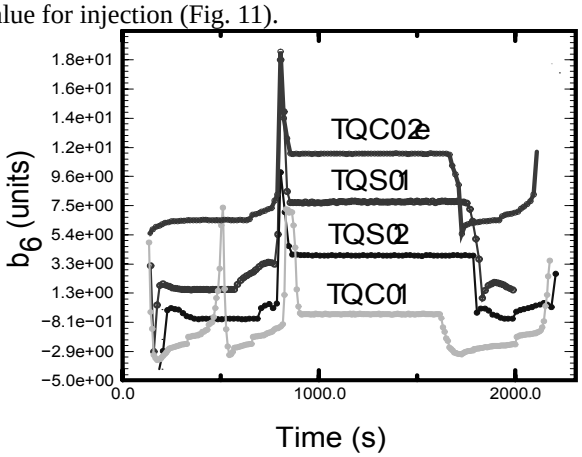

Fig. 11. Time dependence of the first allowed harmonic in the four TQs made thus far.

TECHNOLOGY SCALE UP

Another part of the LARP program focused on a test for length effects using a simple coil structure with a shell support structure, LRS01 (long racetrack shell). The goal was to make a (relatively) quick check for length effects. The 3.6 m coils, made from RRP conductor, were wired in the "common coil" mode (Fig. 12) [8]. The coils were preloaded using bladders and keys in the one direction with significant Lorentz force (Fig. 13). To maximize the Lorentz force, the coils were assembled with no gap between them. For this magnet, the coils were made at BNL, the support structure made at LBNL, and other components at Fermilab.

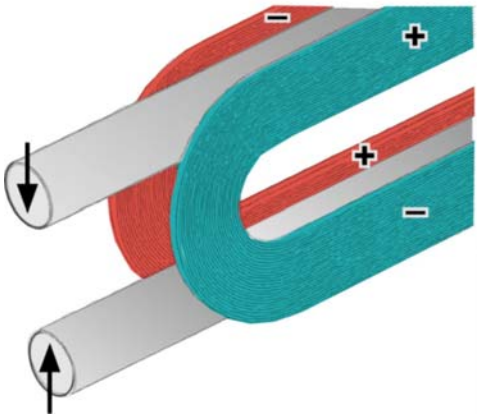

Fig. 12. Racetrack coils powered in the "common coil" mode for LRS01.

The magnet quenched initially at ~ 10 T and trained to 11 T at 4.5 K (~ 91% of the expected conductor limit, Fig. 14) [9]. The training performance was quite similar to that of a 0.3 m version of this magnet [10], although the short version, made with RRP, reached a slightly higher fraction of the conductor limit.

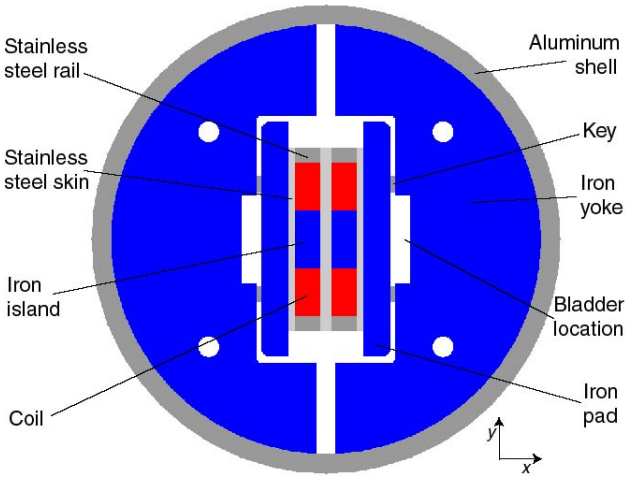

Fig. 13. Cross section of LRS01 coils and support structure.

To monitor the performance of shell support structure, strain gauges were mounted along the length of the shell. The gauges indicated that the assembly was as expected, as was the effect of cooling the support structure loaded with dummy coils (aluminum bars) to 77 K (Fig. 15) [11]. However, the gauges showed that the axial tension in the aluminum shell that arises during cooldown (because of the different thermal contraction coefficients of aluminum and iron) significantly relaxed when the coil was powered to 6 kA. After a thermal cycle, a similar slippage was observed during excitation to 3 kA. Given the good performance of the 1 m TQS quadrupoles, it was decided to segment the shell into 1 m sections. The reconfigured shell support will be tested with the same coils.

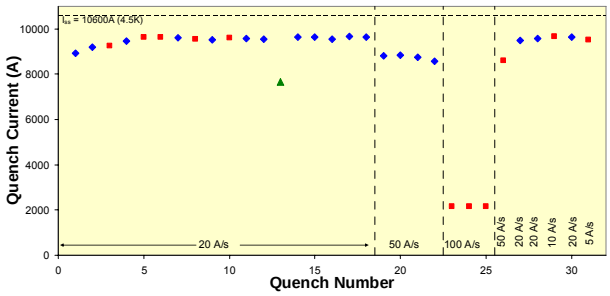

Fig. 14. Quench test data for the 3.6m common coil magnet LRS01.

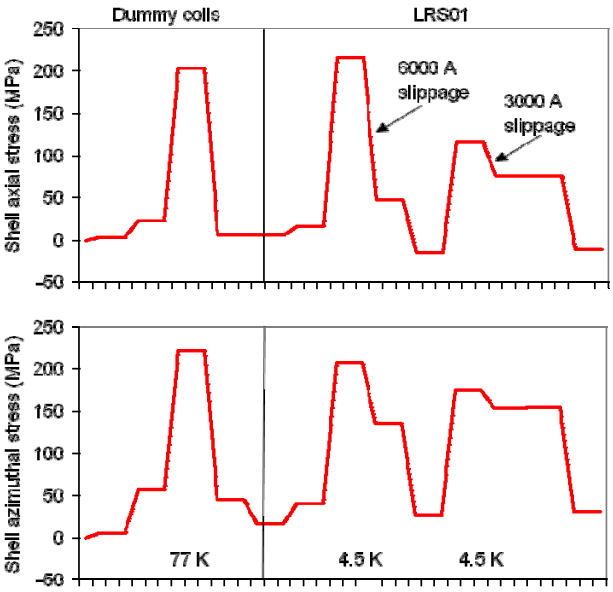

Fig. 15. Axial and azimuthal stress measurements made on the shell of LRS01 during cooldown and excitation.

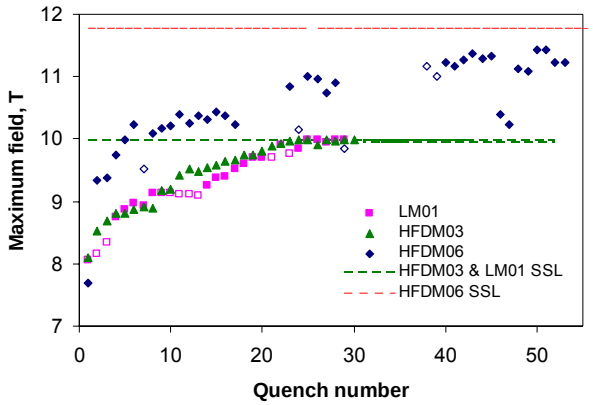

Fig. 16. Quench test data for 1m and 1m mirror dipoles.

Nb_3Sn mirror dipoles made under the Fermilab base program are also part of the data now available [12]. Models with length 1 m and 2 m (HFDM03 and LM01) made with PIT (power in tube) conductor had nearly identical quench performance, reaching the expected conductor limit at ~ 10 T (Fig. 16). A 1 m mirror dipole made with 108/127 RRP conductor reached 97% of its expected limit at 11 T. A 4 m long mirror model LM02 with 108/127 RRP strand has been fabricated and was tested in December reaching 10 T or ~90% of its expected conductor limit [13].

CONCLUSIONS

The "building blocks" – materials, model quadrupoles, 3.6 m racetrack coils and support structure – are in place. The LARP R&D program is ready to move to quadrupoles with longer length and greater aperture.

AKNOWLEDGEMENTS

I am grateful to my LARP colleagues for assistance in gathering the data presented in this paper.

REFERENCES

[1] G. Sabbi, "High Field Nb_3Sn Magnets," presented at this workshop (IR07, Frascati, November, 2007).
[2] G. Ambrosio, "Long Nb_3Sn Magnets," presented at this workshop (IR07, Frascati, November, 2007.
[3] A. Zlobin, "LARP Joint IR Studies," presented at this workshop (IR07, Frascati, November, 2007).
[4] Oxford Superconducting Technology Inc., Carteret New Jersey USA.
[5] R. C. Bossert et al., "Test of TQC02, LARP technological quadrupole magnet, " accepted for publication in IEEE Trans. Applied Superconductivity.
[6] S. Caspi et al., "Test results of TQS02, a second Nb_3Sn quadrupole magnet model for LARP," accepted for publication in IEEE Trans. Applied Superconductivity.
[7] G. V. Velev et al., "Field quality measurements and analysis of the LARP technological quadrupole models," accepted for publication in IEEE Trans. Applied Superconductivity.
[8] R.C. Gupta, "A common coil design for high field 2-in-1 accelerator magnets," Proc. 1997 Particle Accelerator Conference, Vancouver, Canada.
[9] P. J. Wanderer et al., "Construction and test of 3.6 m Nb_3Sn racetrack coils for LARP," accepted for publication in IEEE Trans. Applied Superconductivity.
[10] P. Wanderer et al., "LARP long Nb_3Sn racetrack coil program," IEEE Trans. Applied Superconductivity, Vol. 17, No. 2, pp. 1140-1143 (June 2007).
[11] P. Ferracin et al., "Assembly and test of a support structure for 3.6 m long Nb_3Sn racetrack coils," accepted for publication in IEEE Trans. Applied Superconductivity.
[12] F. Nobrega et al., "Nb_3Sn magnet technology scale-up using cos-thera dipole coils," accepted for publication in IEEE Trans. Applied Superconductivity.
[13] A. V. Zlobin, private communication.

HIGH FIELD NIOBIUM-TIN QUADRUPOLES

GianLuca Sabbi

LBNL, Berkeley, CA

Abstract

Insertion quadrupoles with large aperture and high gradient are required to achieve the luminosity upgrade goal of 10^{35} $cm^{-2}s^{-1}$ at the Large Hadron Collider (LHC). Nb_3Sn conductor is required in order to operate at high field and with sufficient temperature margin. We report here on the development of a "High-performance Quadrupole" (HQ) that will demonstrate the technology required for achieving the target luminosity. Conductor requirements, magnetic, mechanical and quench protection issues are presented and discussed. The HQ design is also suitable for an intermediate "Phase 1" upgrade, operating with large engineering margin.

INTRODUCTION

Superconducting accelerator magnets have supported advanced programs in experimental high-energy physics for the past 20 years. The ductile Niobium-Titanium alloy (NbTi) allows simple fabrication methods for cable and coils. However, NbTi performance is ultimately limited by its upper critical field Bc2=10.5 Tesla at 4.2K. A 3 Tesla increase of Bc2 can be obtained by lowering the temperature to 1.9K. This technique allows approaching a peak coil field of about 10 T in practical dipole and quadrupole magnets. However, several next-generation facilities demand significantly higher fields. In particular, a staged upgrade of the LHC and its injectors is under study to achieve a luminosity of 10^{35} $cm^{-2}s^{-1}$, a 10-fold increase with respect to the baseline design. Replacing the first-generation NbTi IR quadrupoles with higher performance magnets is one of the required steps in this direction. Although improved designs based on NbTi are being considered as an intermediate solution (Phase 1 upgrade), Nb_3Sn conductor is required to meet the ultimate performance goals for both operating field and temperature margin. Several design studies of Nb_3Sn IR quadrupoles for this application have been performed in the past (Fig. 1). Under typical upgrade scenarios, the new magnets will provide increased focusing power to double or triple the luminosity, and at the same time will be able to operate under radiation loads corresponding to the 10^{35} $cm^{-2}s^{-1}$ luminosity target.

Starting in 2004, the LHC Accelerator Research Program (LARP) has been coordinating the US effort to develop prototype magnets for the luminosity upgrade [1]. A series of 1-meter long "Technology Quadrupoles" (TQ) have been fabricated and tested, achieving a gradient well above 200 T/m in a 90 mm aperture. The TQ models are the basis for a series of 4-meter long quadrupoles (LQ) with same aperture and gradient, and for a series of 1 m long "High-gradient Quadrupoles" (HQ) which are the focus of the present paper.

MAGNETIC DESIGN

It is expected that the optimal coil aperture for the "Phase 2" upgrade quadrupoles will be in the range of

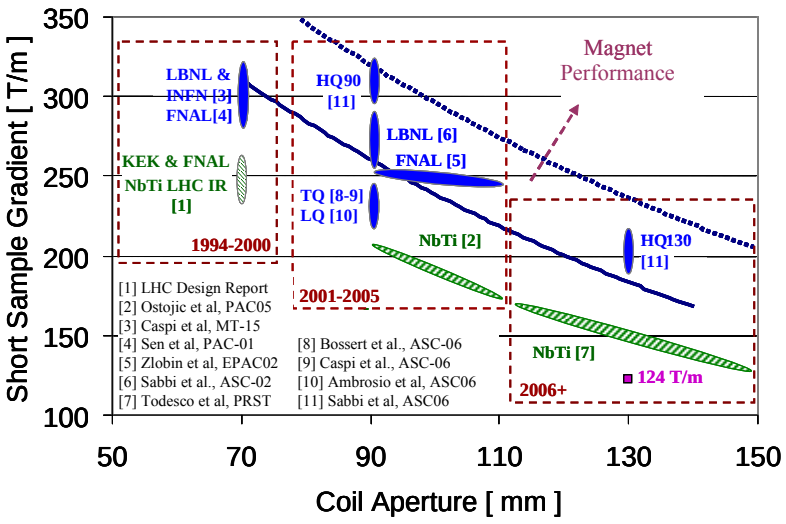

TABLE I
PERFORMANCE PARAMETERS

Parameter	Symbol	Unit	HQa	HQb
Short sample gradient*	G_{ss}	T/m	205	204
Short sample current*	I_{ss}	kA	17.0	16.5
Coil peak field	B_{pk} (I_{ss})	T	15.4	15.6
Inductance	L (I_{ss})	mH/m	11.4	12.0
Stored energy	U (I_{ss})	MJ/m	1.6	1.6
Lorentz force/octant (x)	F_x (I_{ss})	MN/m	3.9	3.6
Lorentz force/octant (y)	F_y (I_{ss})	MN/m	-5.1	-4.8
Cable width		mm	15.1	15.1
Aperture		mm	130	130

(*) Assuming J_c(12 T, 4.2 K) = 3.0 kA/mm^2; operating temperature T_{op}=1.9K

100-130 mm [2]. Recent studies show that quadrupoles with 130 mm aperture are suitable for the "Phase 1" upgrade [3]. Therefore, the development of Nb_3Sn quadrupoles with a 130 mm aperture addresses both near-term and long-term needs. From an R&D standpoint, the 130 mm aperture is also suitable for exploring the technological limits related to very high fields (15 T) and stresses (200 MPa). In addition, a 130 mm aperture coil can be combined with a 90 mm aperture TQ coil to produce a 4-layer configuration. The test of models with both 90 mm and 130 mm aperture allows covering the entire range of apertures being considered for the upgrade (Fig. 1).

Although minimizing the superconductor volume is not a critical design consideration for the IR quadrupoles, efficient field generation is essential in order to achieve high focusing power. A cos2θ geometry was selected for optimal magnetic efficiency in large round apertures. A 2-layer design has been the smallest number of parts and assembly steps, and was successfully used in several Nb_3Sn dipoles and quadrupoles. In order to limit the coil stresses and quench temperatures, a cable with large aspect ratio needs to be developed for this application. The HQ conductor needs to provide high critical current density at high field, with consistent properties and reliable delivery over a series of model magnets. Heat treatment optimization of recent OST 54/61 billets [4] resulted in Jc above 3 kA/mm2 at 12 T, 4.2 K for un-cabled strands. These properties justify assuming a design critical current density of 3 kA/mm2 (12 T, 4.2 K), taking into account some degradation due to cabling.

The HQ cross-section optimization targets are maximum design gradient and minimum coil stress. Conductor degradation due to high stress represents a major factor potentially limiting the HQ performance. Therefore, stress considerations need to be taken into account in selecting the coil cross-section. Comparison of different designs shows differences in the accumulated Lorentz forces that may be exploited to minimize the peak coil stress. Several fabrication constraints and cost-performance trade-offs also need to be taken into account, such as limits on cable compaction and winding radii, incorporation of wedges and conductor grading. A consistent set of assumptions (conductor parameters, iron properties, etc.) were defined for comparing different options. Table I lists the short sample performance parameters for two candidate designs.

MECHANICAL DESIGN

The HQ mechanical structure needs to provide an average azimuthal pre-load at the 150 MPa level over a 4 cm coil radial width, and support the coils against radial Lorentz forces of 3-4 MN/quadrant. Due to the increased force and stress levels for the HQ case, the coil support will be mainly provided by an outer shell or welded skin through the iron yoke. The use of a TQS-type approach for increasing the pre-load at cool-down is particularly attractive in view of the very high coil stress. A thin collar will facilitate coil pre-assembly and alignment.

The use of axial pre-load to support the coils against axial forces generated at the coil ends is also being investigated as part of the TQS and SQ model magnet series. The total axial Lorentz force is at the level of 1 MN/m in HQ, a factor of 2-3 larger with respect to the TQ and SQ. Therefore, it is expected that axial pre-load will be required to obtain satisfactory performance.

CONCLUSIONS

Progress in the conceptual design of the LARP HQ model quadrupole series was presented. Peak stresses of 150-200 MPa are expected. The preliminary magnetic, mechanical and quench protection analysis confirms that the proposed HQ models are feasible and consistent with the upgrade objectives. Future studies will include a detailed analysis and selection of the mechanical support structure, taking into account feedback from the ongoing model magnet and supporting R&D.

REFERENCES

[1] S.A. Gourlay, et al., "Magnet R&D for the US LHC Accelerator Research Program", IEEE Trans. on Appl. Superconduct., vol. 16, no. 2, June 2006, pp. 324-327.
[2] J.P. Koutchouk, "Investigations of the Parameter Space for the LHC Luminosity Upgrade", EPAC'06, Edinburgh, UK, June 26-30, 2006.
[3] E. Todesco, these proceedings
[4] S. Hong, et al., "Latest Improvement of Current Carrying Capability of Nb3Sn", Presented at the 19th International Conference on Magnet Technology, Genoa, Italy, September 2004.

LARP LONG Nb_3Sn QUADRUPOLE*

G. Ambrosio#, Fermilab, Batavia, IL 60510, U.S.A.

Abstract

A major milestone for the LHC Accelerator Research Program (LARP) is the test, by the end of 2009, of two 4m-long quadrupole magnets (LQ) wound with Nb_3Sn conductor. The goal of these magnets is to be a proof of principle that Nb_3Sn is a viable technology for a possible LHC luminosity upgrade.

INTRODUCTION

The LARP Long Quadrupole (LQ) is going to be the first 4m long Nb_3Sn quadrupole magnet ever built. With an aperture of 90 mm, and a gradient of 200 T/m, the LQ is a "Proof of Principle" magnet aiming at demonstrating that Nb_3Sn technology is mature for use in high energy particle accelerators. The LQ is thus a fundamental step toward the LARP goal of developing Nb_3Sn quadrupole prototypes for the LHC (Large Hadron Collider) [1] interaction regions for a possible luminosity upgrade.

The Long Quadrupole R&D builds upon other LARP tasks (such as the Technological Quadrupoles (TQ) [2,3], and the Long Racetrack [4]), and upon tasks performed by other programs (such as the Long Mirror under development at Fermilab [5]). A preliminary description of coil design and fabrication process was presented in [6]. The quench protection was presented in [7]. The present plan includes the fabrication of three LQ models by early 2010

MAGNETIC DESIGN

Two support structures (collar-based and shell-based) are under consideration using the same coils. The magnet parameters are presented in Table 1 for both structures at critical current values of 2400 and 2800 A/mm^2 (at 4.2 K, 12 T). The shell-based structure has slightly higher gradients (+4%) than the collar-based structure because the iron is closer to the coils.

The cable has 27 strands with 0.7 mm diameter. Cable width and mid-thickness are 10.08 mm and 1.26 mm respectively. The strand is RRP (Restack-Rod-Process) by OST (Oxford Superconducting Technology). A design with 54 Nb_3Sn sub-elements (54/61) will be used for the first set of coils. Use of RRP strands with larger number of sub-elements is under consideration for the third LQ.

Table 1: LQ Magnet Parameters

Parameter	**Unit**	**Collar-based LQ**		**Shell-based LQ**	
Critical current density at 4.2 K, 12 T	A/mm^2	2400	2800	2400	2800
N of layers		2			
N of turns		136			
Coil area (Cu + nonCu)	cm^2	29.3			
4.2 K temperature					
Quench gradient	T/m	221	231	233	243
Quench current	kA	13.3	14	13.4	14
Peak field in the body at quench	T	11.5	13	11.9	12.4
Peak field in the end at quench	T	12	12.5	11.4	12.4
Inductance at quench	mH/m	4.6	4.6	4.9	4.9
Stored energy at quench	kJ/m	406	443	439	479
1.9 K temperature					
Quench gradient	T/m	238	249	251	262
Quench current	kA	14.4	15.1	14.5	15.2
Peak field in the body at quench	T	12.4	13	12.9	13.4
Peak field in the end at quench	T	12.9	13.5	12.4	13.4
Stored energy at quench	kJ/m	472	516	512	559

*Work supported by the US Department of Energy
#giorgioa@fnal.gov

MECHANICAL DESIGN

Three mechanical designs (referred to also as support structures) have been developed for the Long Quadrupole. Two of them are based on the LARP TQ magnets. The collar-based LQ (Fig. 1) is a straightforward scale-up of the TQC magnet. The only new features are: (i) the skin will be welded (the latest TQC model used a bolted skin); (ii) possible introduction of coil alignment features.

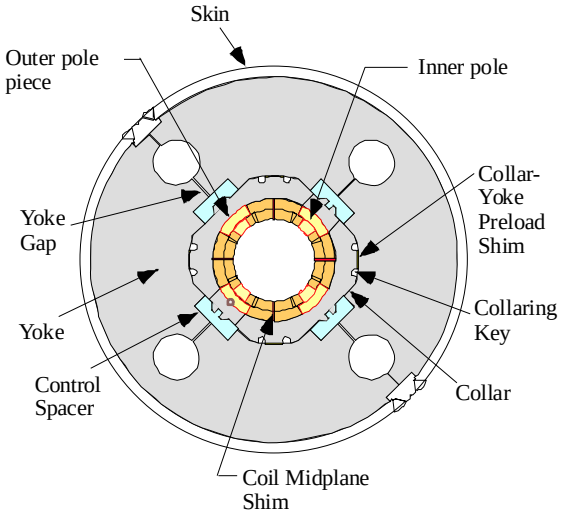

Figure 1: Collar-based LQ

The shell-based LQ (Fig. 2) is based on the TQS with some improvements: (i) optimized pads in order to reduce peak stress in the outer layer; (ii) slightly thinner aluminum shell, (iii) stainless steel rods for end pre-stress; (iv) new features for pre-assembly of the 4m structure before coil insertion (use of "masters", segmented pads and shell).

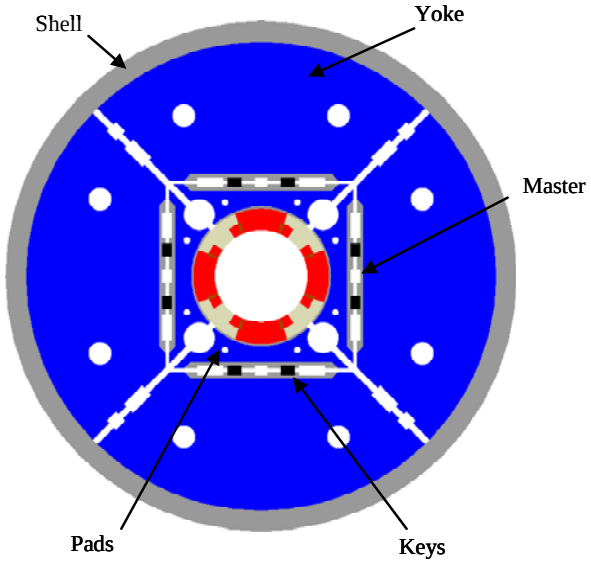

Figure 2: Shell-based LQ

The third design ("Hybrid design") combines some of the best features of the TQ designs (collars for coil assembly and alignment, and use of bladders for controlled application of pre-stress). Time and budget constrains didn't allow the development of short models using this design. Therefore it cannot be considered for the Long Quadrupole.

Further details about these designs can be found in [7].

PLANS

The fabrication and test plan is based on the unique advantages of each structure developed during the TQ R&D. The shell-based structure reached with TQS02 a gradient 10% higher than the LQ target (200 T/m) and has a very short magnet assembly and disassembly time. These features are very attractive for the first LQ model (LQ01), which aims exclusively at the target gradient and where LQ coils will be tested for the first time (possibly requiring to change some of them after the first test).

The collar-based structure provides more accelerator magnet features (such as coil alignment), which are very attractive for subsequent LQ models.

The TQ R&D has also shown that coils previously tested in a shell-based structure can be successfully retested in a collar-based structure.

The main steps of the plan are:

- First model (LQ01) with shell-based structure. Goal: to achieve LQ target gradient with a structure allowing quick exchange of coils.
- Second model (LQ02) with collar-based structure, reusing LQ01 coils. Goal: to demonstrate more accelerator magnet features with long Nb_3Sn coils, allowing significant savings by reusing LQ01 coils.
- Third model (LQ03) with structure depending on previous results. Goal: to demonstrate reproducibility of best performing LQ model, and to allow improvements by possible use of improved conductor.

By developing both structures (shell- and collar-based) this plan provides the highest probability of success within the short timeframe. It also allows building a large and unique set of expertise and experimental data for the design of prototypes for the LHC IR upgrade.

REFERENCES

[1] L. Rossi, "The Large Hadron Collider and the Role of Superconductivity in one of the Largest Scientific Enterprises", IEEE Trans. on App. Supercond., vol. 17, no. 2, pp. 1005-1014, June 2007.

[2] Bossert, et al., "Development and Test of TQCs, LARP Technological Quadrupole Magnets", to be published in IEEE Trans. on App. Supercond.

[3] Caspi, et al., "Test Results of TQS02 – a Second Nb3Sn Quadrupole Magnet Model for LARP" to be published in IEEE Trans. on App. Supercond.

[4] P. Wanderer, et al., "Construction and Test of 3.6 m Nb3Sn Racetrack Coils for LARP" to be published in IEEE Trans. on App. Supercond.
[5] F. Nobrega, et al., "Nb3Sn Accelerator Magnet Technology Scale-up using Cos-theta Dipole Coils" to be published in IEEE Trans. on App. Supercond.
[6] G. Ambrosio, et al., "Design of Nb3Sn coils for LARP long magnets", IEEE Trans. on App. Supercond., vol. 17, no. 2, pp. 1035-1038, June 2007.
[7] G. Ambrosio, et al., "LARP Long Nb3Sn Quadrupole Design" to be published in IEEE Trans. on App. Supercond.

LARP JOINT IR STUDIES

A.V. Zlobin, Fermilab, Batavia, IL 60510, U.S.A.

Abstract

LARP initiated Joint IR Studies (JIRS) in October 2007 (FY2008) to coordinate efforts related to the LHC Phase I and II upgrades previously situated either in Accelerator Systems or in Magnet Systems. This note outlines JIRS goals, main directions and milestones.

INTRODUCTION

After a number of years of operation at nominal parameters, the LHC will be upgraded for higher luminosity. The Interaction Region (IR) upgrade is currently planned at CERN in two phases with a target luminosity for Phase I of ~$2.5 \cdot 10^{34}$ $cm^{-2}s^{-1}$ and for Phase II of ~10^{35} $cm^{-2}s^{-1}$. In Phase I the baseline 70-mm NbTi low-beta quadrupoles will be replaced with larger aperture NbTi magnets and in Phase II with higher performance Nb_3Sn magnets.

US-LHC Accelerator Research Program (LARP) is working on the development of large-aperture high-performance Nb_3Sn magnets for the LHC Phase II luminosity upgrade. Significant progress in Nb_3Sn accelerator magnet R&D was made during recent years in the framework of LARP and core magnet programs. This included development and optimization of Nb_3Sn strands and cables, coil fabrication technologies based on the W&R approach, mechanical support structures and magnet assembly techniques for high-field magnets. Nb_3Sn magnet performance (quenches and field quality) was demonstrated by series of short dipole and quadrupole models [1-4]. A Nb_3Sn accelerator magnet technology scale up was also started with quite encouraging results [4-5].

Recent progress in the Nb_3Sn accelerator magnet technology suggests the possibility of using a limited number of Nb_3Sn quadrupoles in the Phase I upgrade to improve the IR performance at higher luminosity and provide an early demonstration of Nb_3Sn magnet technology in a real accelerator environment. To coordinate efforts related to the LHC Phase I and II upgrades, LARP has started Joint IR Studies (JIRS) in October 2007 (FY2008). These studies will extend and integrate connected tasks that were previously performed by LARP either within Accelerator Systems or in Magnet Systems and also help to improve efficiency in communication with CERN. This note outlines JIRS goals, main directions and milestones for the next two years.

JIRS MISSION AND TASKS

During the next two years (FY08-09) LARP Magnet R&D will focus on two major goals. The first goal is the continuation of the Nb_3Sn technology scale up using technological quadrupoles of the LQ series to demonstrate the viability of long (up to 4-m) Nb_3Sn quadrupoles [6]. The second goal is to study and extend the parameter space of Nb_3Sn IR quadrupoles to higher fields and apertures using 1-m long models of HQ series [7].

Next LARP will work on the development of Nb_3Sn *accelerator* magnets suitable for the LHC luminosity upgrades. The main goal of Joint IR Studies (JIRS) is to provide input parameters and guidance for this work. The general framework of JIRS is determined by the Mission Statement of LARP "Joint Interaction Region Studies". Based on this document JIRS are mostly concerned with the post-LQ and HQ magnet series:

- QA quadrupole – accelerator quality magnet.
- QB quadrupole – main Phase II upgrade magnet.
- "Slim" magnets in front of Inner Triplets.

The QA quadrupoles are defined above as the accelerator quality magnets designed to demonstrate the possibilities and limitations of Nb_3Sn accelerator magnet technology. Assuming the possibility of using a limited number of Nb_3Sn quadrupoles in the Phase I upgrade this magnet series could also be considered as a prototype of Nb_3Sn Phase I quadrupoles. Thus the work on QA quadrupole has highest priority. This effort will include definition and evaluation of a list of potential QA locations in LHC in communication with CERN including Q1-Q3 in a potential Phase I "hybrid" IR layouts. We will develop specifications for the accelerator-quality parameters of QA quadrupoles including magnet aperture and length, maximum and nominal gradients, alignment and field quality requirements, persistent current and snap-back effects, power supply and quench protection requirements, etc. We will examine the possibility of using LQ or HQ designs and tooling to build QA magnets. JIRS will also identify and propose bench tests on QA (or LQ or HQ) magnets that would help to explore and demonstrate Nb_3Sn accelerator magnet performance and operation lifetime (except radiation).

The QB quadrupoles are defined as prototypes for the Phase II upgrade. We will perform preliminary studies to generate a self-consistent set of target parameters for Phase II quadrupoles, including all the necessary accelerator quality parameters, consistent with possible upgrade scenarios. These studies will provide guidance for LARP magnet R&D, well before CERN defines the final design and operation parameters of Phase II IR quadrupoles. The preliminary QB design and accelerator-quality parameters will be also used to estimate and simulate correction system parameters and possible issues related to a QB implementation in the Phase II upgrade.

Some proposed IR concepts consider using the so called "slim" magnets (dipoles or quadrupoles) inside ATLAS and/or CMS detectors. In support of these studies JIRS will produce a list of preliminary parameters (aperture, length, outer diameter, nominal field/gradient, field quality, alignment, etc.) and operation conditions

(radiation deposition, forces and fields from detector magnet, dynamic and static heat load, etc.) for these magnets. The possibility of conventional NbTi technology or alternative magnet technologies (Nb_3Sn, Nb_3Al or HTS) needs to be evaluated and compared in terms of operational margin, magnet life-time, etc.

In FY08-09 JIRS are organized in two directions (Simulations and Studies) and include four tasks. The present JIRS structure is shown in Table I. The working plan for each task includes associated aspects related to QA, QB and "Slim" magnets. The highest priority (~80-90% of resources) will be given to QA general magnet studies and use of QA quadrupoles in the Phase I upgrade. Internal task interaction, exchange of information, discussions and feedback, and coordination with CERN will lead to the integrated results expected from JIRS.

Table I. JIRS structure.

WBS	Task	Coordinator
3.3	Joint IR Studies	A. Zlobin (Fermilab)
3.3.1	*Simulation*	
3.3.1.1	Operating Margins	N. Mokhov (Fermilab)
3.3.1.2	Accelerator Quality & Tracking	G. Robert-Demolaize (BNL)
3.3.2	*Studies*	
3.3.2.1.	Optics & Layout	J. Johnstone (Fermilab)
3.3.2.2.	Magnet Feasibility Studies	P. Wanderer (BNL)

PHASE I LUMINOSITY UPGRADE

CERN has adopted a staged LHC IR upgrade plan. Phase I upgrade, scheduled nominally for 2012, will increase the luminosity in two IRs used by ATLAS and CMS experiments to the level of ~$2.5*10^{34}$ $cm^{-2}s^{-1}$. It will be achieved mainly by reducing the beta-star in the interaction points by a factor of two from 50 to 25 cm and using larger-aperture NbTi quadrupoles. Phase II upgrade will increase the luminosity up to 10^{35} $cm^{-2}s^{-1}$ using higher performance Nb_3Sn magnets.

It is likely that the Phase II upgrade will be delayed with respect to the originally planned date (2015) providing more time for the development of Nb_3Sn quadrupoles with ultimate parameters. The progress in Nb_3Sn accelerator magnets achieved in the U.S., the magnet parameters and operation conditions as well as the upgrade schedule allows seriously considering the possibilities of U.S. participation in the Phase I IR upgrade. The U.S. could provide a limited number (4 or 8 out of the 16 required) of Nb_3Sn quadrupoles with more relaxed parameters for the new Inner Triplets.

The idea of hybrid triplets was originally proposed by CERN [8] to share the cost of the Phase I upgrade. The primary goals from the LARP standpoint are the improvement of the IR performance at higher luminosity (due to the higher nominal gradient and temperature margin of Nb_3Sn quadrupoles) and an earlier demonstration of Nb_3Sn accelerator magnet technology in the LHC before using it in the Phase II.

The hybrid proposal is an exciting challenge for LARP. Besides resolving various technical issues, the development and production of Nb_3Sn magnets for the Phase I upgrade would require launching a construction project similar to that produced the present baseline NbTi LHC IR quadrupoles. It will also involve some LARP R&D re-programming and a modest funding increase beyond current LARP budget.

The JIRS working group started technical analysis and evaluation of the Phase I hybrid concept and Nb_3Sn magnet requirements. This involves analysis of compatibility of Nb_3Sn quadrupoles with the Phase I IR optics, cryogenics, power and quench protection systems, etc. JIRS will establish and maintain broad and unrestricted communications with the LHC Insertions Upgrade Working Group (LIUWG) at CERN, but will work independently.

The cost and schedule analyses of the hybrid proposal will be also performed and presented to the DOE review in June 2008, at the same time as the LIUWG technical report on the Phase I upgrade conceptual design. A final commitment to U.S. deliverables in a hybrid Phase I upgrade will occur after a technical review including the magnet cost and schedule.

CONCLUSIONS

LARP Joint IR Studies will guide LARP magnet R&D towards its ultimate goal – LHC Phase II upgrade based on high-performance Nb_3Sn accelerator magnets. In FY08 JIRS primary focus is on evaluation of the possibilities of LARP contribution to the LHC Phase I upgrade. The goal is to pursue Nb_3Sn magnet R&D and suggest consistent IR optics and magnet parameters, without favoring any upgrade proposal. JIRS work will proceed in close communication with the AB and AT divisions at CERN.

REFERENCES

[1] R.C. Bossert et al., "Development and Test of LARP Technological Quadrupole Models of TQC Series", MT-20, Philadelphia, August 2007.

[2] S. Caspi et al, "Test Results of TQS02, a Second Nb_3Sn Quadrupole Magnet Model for LARP", MT-20, Philadelphia, August 2007.

[3] G. Velev et al., "Field Quality Measurements and Analysis of the LARP Technology Quadrupole Models", MT-20, Philadelphia, August 2007.

[4] A.V. Zlobin et al., "Development of Nb_3Sn accelerator magnet technology at Fermilab", Proc. of PAC'2007, Albuquerque, NM, June 2007.

[5] P. Wanderer, IR'07 mini-workshop, CARE-HHH-AMT, Frascati (Italy), 7-9 November 2007.

[6] G. Ambrosio et al., "LARP Long Nb3Sn Quadrupole Design Study", MT-20, Philadelphia, August 2007.

[7] H. Felice et al., "Magnetic and Mechanical Analysis of the HQ Model Quadrupole Designs for LARP", MT-20, Philadelphia, August 2007.

[8] L. Rossi, LARP collaboration meeting, October 2007.

PHASED APPROACH TO THE LHC INSERTION UPGRADE AND MAGNET CHALLENGES

R. Ostojic, CERN, Geneva, Switzerland

Abstract

The LHC is on its way for operation with beam in 2008. The first goal of CERN and the LHC community is to ensure that the collider is operated efficiently, gradually reaching its maximal performance. In parallel, discussions have started and there is already a wealth of ideas on the possible directions for upgrading the LHC insertions. In this talk, we illustrate some of the constraints limiting the upgrade scenarios, and argue that a phased approach with several intermediate targets is necessary. In the first phase, the known bottleneck in the low-β triplets needs to be removed in the perspective of the physics run of 2013. This phase relies on the mature Nb-Ti superconducting magnet technology, where improvements for a small scale production are still possible.

PHASING OF THE UPGRADE

The LHC, the largest and most complex endeavour in the history of high-energy physics, is almost complete. By the end of 2007, the collider will be fully installed and individual system tests completed. The machine sectors are being progressively cooled down and commissioned.

The LHC construction effort has been enormous and has taken up all of CERN's material and human resources and has required considerable international participation. In parallel, the HEP and accelerator communities have been investigating possible routes towards increasing the reach of this unique scientific instrument. There is a wealth of ideas how to upgrade the LHC systems, mostly in the high-luminosity (ATLAS and CMS) insertions. The strategy, as given in the strategy statement of the CERN Council [1], is clear: to maximize the physics return, any upgrade of the LHC insertions in the first period of running has to comply with the operations schedule and existing infrastructure. On the other hand, LHC relies on the injector chain and its reliability. These accelerators, in particular the venerable PS, must have priority in maintenance and upgrade. These boundary conditions lead to a phased approach to the upgrade of the LHC luminosity.

Within the long list of LHC systems, there are certain major constraints which have to be taken into account when discussing the scope and timing of the luminosity upgrade. One of the major ones concerns the available cooling power of the cryogenic system in the two interaction points. As discussed by L. Tavian in LUMI-06 [2], the cooling capacity of the refrigerators was defined on the basis of extensive evaluation of the heat loads, and made to match the "ultimate" beam parameters [3]. It is clear that any increase of cooling requirements, in particular those related to the increase of luminosity beyond 2 10^{34} $cm^{-2}s^{-1}$ will need dedicated cryogenic plants serving the inner triplets around CMS and ATLAS. Their installation will in turn most likely require some level of civil engineering in the underground areas. This type of insertion upgrade is best done at the time when the two experiments will also require longer shutdowns to perform their own extensive modifications.

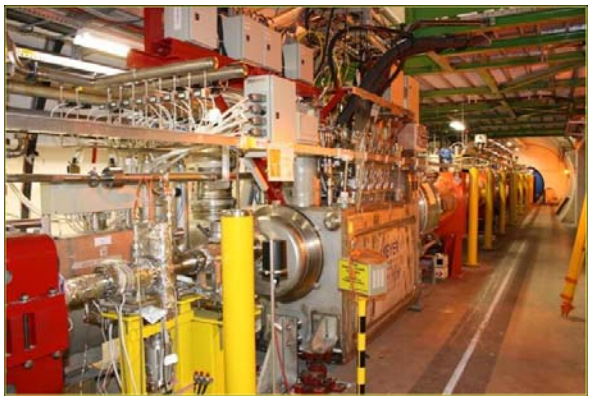

Figure 1: The low-β triplet in the ATLAS insertion.

Figure 2: A view from the low-β triplet towards CMS.

Another example of the general constraints is related to the LHC tunnel. The general access and transport of magnets to and from Points 1 (ATLAS) and 5 (CMS), illustrated in Figs.1-3, are such that long hauls over several kilometres alongside the chain of magnets and other equipment are unavoidable. Although care had been taken during tunnel studies to enable transport of magnets at any time, the LHC tunnel is a tight place and transport of equipment is a delicate affair that requires careful planning, even more so since some parts of the arcs may

have to be warmed up for exchanging magnets. The replacement of the triplets in the high luminosity insertions may therefore require more time than just a typical annual shutdown of the machine.

Figure 3: Transport of magnets in the LHC tunnel.

These examples, as well as the urgency in renovating the LHC injector chain, lead to a situation where for technical and cost reasons the upgrade of equipment in the LHC insertions will be naturally phased over a longer period of time and will contain intermediate targets. The first to be handled are several bottlenecks that are known to limit the luminosity reach (collimation system, triplet aperture). They should be removed as soon as practically possible.

In this context CERN has started work recently on the "Phase I" upgrade, which concerns ATLAS and CMS experimental insertions. The goal of the upgrade is to enable focusing of the beams to a $\beta^*=0.25$ m and reliable operation of the LHC at 2 10^{34} $cm^{-2}s^{-1}$ on the horizon of the physics run in 2013. The upgrade concerns mainly the low-β triplets, but does not foresee any modifications of the interfaces with the two experiments, which remain at their present location (19 m from the IP). The low-β quadrupoles will feature a wider aperture than the present ones, and will continue to use the technology of Nb-Ti Rutherford cables cooled at 1.9 K developed for the LHC dipoles. The D1 separation dipole, as well as any other element in the beam line will be adapted to the triplet aperture. However, the present cooling capacity of the cryogenic system and other infrastructure elements remain unchanged.

MAGNET CHALLENGES

Although the Nb-Ti technology has reached full maturity with the magnet developments for the LHC, the envisaged "Phase I" upgrade is not without concerns, related in particular to the relatively aggressive planning which requires a string test of the full inner triplet by 2012. An important aspect of this effort is the need to finalize the choice of the main parameters of the low-β quadrupoles on the basis of current knowledge of optics, while having a very limited feedback from the LHC operation. On the magnet side, a number of design features of Nb-Ti magnets could still be improved for a small scale production, in particular the cable insulation, allowing improved operational margins at ultimate LHC luminosity. In the same spirit, the thermal optimization of the coil and of the collaring and yoking structures, as well as the coupling to the heat exchanger, could be improved to allow more efficient use of the available cooling power at 1.9 K. Similarly, the shielding of the triplets, both within and outside the magnets, should be revised and improved if possible, such that the thermal loads at higher temperature levels are proportionally increased to alleviate the power extracted at the 1.9 K level.

The main effort of the intermediate upgrade will focus on the low-β quadrupoles themselves. Nevertheless, the performance targets are such that modifications in auxiliary equipment servicing the triplets, as well as in other sections of the insertions, will be necessary. For all the equipment, cost-effective solutions need to be found and external collaborations developed.

CONCLUSIONS

Due to the imperative of efficiently running the LHC, and also for a number of technical and cost reasons, the upgrade of equipment in the LHC insertions will be phased over a longer period of time and will contain intermediate targets. The "Phase I" upgrade is focused on removing known bottlenecks and enabling reliable operation of the machine at its "ultimate" parameters on the horizon of the physics run in 2013. This intermediate upgrade must be compatible with the foreseen operations schedule and the existing infrastructure. The shortest route for providing new low-β quadrupoles in this time frame is to use the existing technology of Nb-Ti cables cooled at 1.9 K, where several improvements are still possible.

Achieving optimal operation of the LHC in medium-term requires extensive modifications in the injector chain. The "Phase II" upgrade needs to be synchronised with the completion of new injectors, and with substantial improvements in the cryogenic infrastructure in the ATLAS and CMS insertions.

REFERENCES

[1] The European strategy for particle physics, CERN/2685.
[2] L. Tavian, LUMI-06, Valencia, Oct 2006.
[3] LHC Design Report, CERN-2004-003.

NEW RESULTS ON THE EARLY SEPARATION SCHEME

J. P. Koutchouk, G. Sterbini, CERN, Geneva, Switzerland

Abstract

A new strategy of luminosity leveling using the early separation scheme is proposed. It increases rather than decreases the integrated luminosity to levels above those presently predicted for the LHC luminosity upgrade. The multiplicity is kept under control at about 100.

INTRODUCTION

The principle of the early separation scheme is to decouple the crossing angle at the IP from the required beam separation in the common part by means of small dipoles included deep inside the detectors (figure 1) [1]. To avoid an intrusion in the inner detector, this ideal scheme may only be considered for 50 ns bunch spacing. For the nominal spacing of 25 ns, a residual crossing angle must be maintained to weaken the few long range interactions occurring just before and after the separator dipoles (D0). A detailed description can be found in [1].

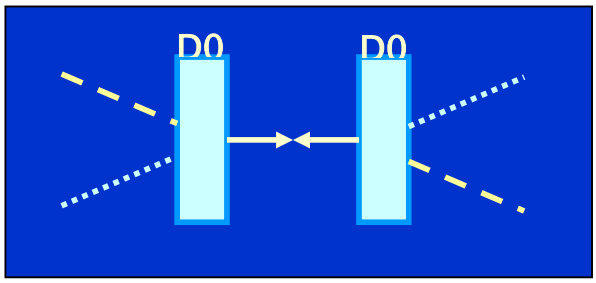

Figure 1: ideal full early separation

LAYOUT AND MAGNETIC FIELD

The required magnetic field integral depends on the D0 position chosen to be between two long range encounters. Table 1 gives possible positions for the dipole center of gravity versus bunch spacing and beam-beam tolerance. The 1.9 m position is inside the inner detector and impossible. The 18.8 m position is too close to the triplet and would require an unrealistic D0 field integral. The positions at 3.8 m and 5.6 m are favored, the first one allowing ideal early separation for a 50 ns spacing. For these positions, the required field integral is in the range 5 to 8 Tm, depending on the exact position and value of the β^* function.

Table 1: Possible dipole positions

	25 ns	**50 ns**
Full Early Separation (**0 LR @ 5σ**)	~~1.9 m~~	3.8 m
Partial Early Separation (**1 LR @ 5σ**)	5.6 m	11.25 m
Partial Early Separation (**2 LR @ 5σ**)	9.4 m	18.8 m

OUTCOME OF BEAM-BEAM STUDIES

Even though including this dipole inside the detectors does not appear impossible, there is a strong reluctance and fear that the calorimetry would be strongly disturbed. This was an incentive to investigate in simulation and experimentally the consequence of the long-range beam-beam interactions at a reduced distance that would occur with partial early separation if the D0 dipole would be relocated farther away from the IP. Experiments were conducted at RHIC and in the SPS in 2007. Their results are discussed in [2], with the following outcome: Experiments have shown that a certain number of long-range encounters at a reduced distance (5σ) can be tolerated. However, their exact number is not yet clear (4 to 8?) and requires further dedicated experiments at RHIC.

It would be premature to draw firm conclusions. However it becomes possible to investigate positions that would be less stressing for the detectors.

PEAK LUMINOSITY

The machine performance is estimated for the ultimate bunch charge of 1.7 10^{11} protons and the nominal position of the triplet (l*=23 m). The results are given in Table 2 for various configurations and 25 ns or 50 ns bunch spacing.

Table 2: Peak luminosity in 10^{34} $cm^{-2}s^{-1}$ versus scenarios

Bunch spacing	25 ns	50 ns
No early separation β*=25 cm	3.1	1.7
Full early separation β*=14 cm	-	4.9
Partial early sep. β*=14 cm	5.8	3.1
Partial early sep. β*=14 cm + electron lens	~7	
Partial early sep. β*=14 cm + crab cavities	9.8	

It is assumed that the long-range compensation by the electron lens allows reducing the beam separation at the first parasitic crossing to 3 σ. Decreasing the IP to triplet distance to 13 m instead of 23 m increases all figures by about 20%.

LUMINOSITY WITH LEVELING

The luminosity lifetime is dominated by the proton burning. It is of the order of 3.5 hours at 10 10^{34} $cm^{-2}s^{-1}$, inversely proportional to the luminosity and proportional to the bunch charge. This apparently is an advantage when increasing performance by increasing the beam

current and a handicap when increasing the performance by stronger focusing. This deficiency may however be circumvented by luminosity leveling. The early separation scheme lends itself to a very simple leveling strategy by adjusting the crossing angle. The angle bump is produced by the D0 dipoles and closed by an orbit corrector in front of each triplet [3]. The beam trajectory is therefore unchanged except in the experimental straight section, suppressing any basic optical side-effect and making it operationally extremely simple. Two issues have nevertheless to be considered: i) the modulation of the longitudinal extent of the luminous region, initially decreased by about a factor of 2; ii) the consequence of a large Piwinski angle, up to 3.5. The latter is a common issue to both upgrade paths and requires dedicated studies. Depending on the leveling scenario chosen, the luminosity can be kept up to 8 hours at a moderate cost in integrated luminosity (~10%).

After this initial study of leveling [3], it was realized that the leveling by the crossing angle includes a special provision that may be used if the machine would accept a larger bunch charge: indeed, an initially larger crossing angle reduces both the luminosity and the head-on beam-beam tune shift, unlike leveling with the β* function. This opens the door to a new optimization where the bunch charge and hence the luminosity can be increased thanks to leveling.

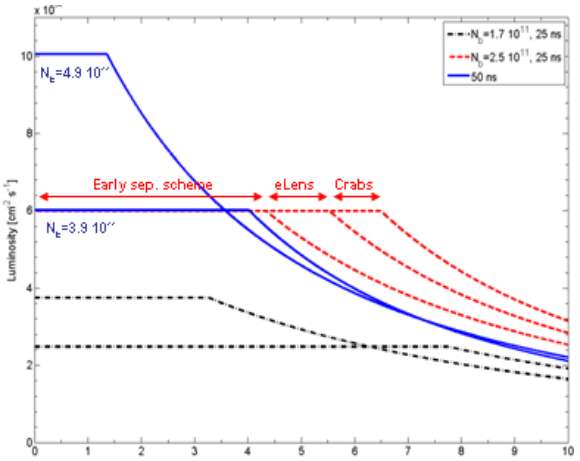

Figure 2: Luminosity [10^{34}] with leveling and HV crossings versus time [hour]: 1) Nb=1.7 10^{11} , p 2) Nb=2.5 10^{11} , p 3) 50 ns spacing and Nb= 4.9 10^{11}p

Examples are given on figure 2 where HV crossing is assumed. The two lower dotted curves show leveling without increase of the bunch charge beyond its ultimate value [3]. The dotted (red) intermediate curves show leveling with a bunch charge increased to 2.5 10^{11} proton, the assumed limit for 25 ns bunch spacing. The early separation scheme alone allows a constant luminosity of 6 10^{34} $cm^{-2}s^{-1}$ for 4 hours followed by the natural decay. The availability of weak crab crossing supplementing the early separation scheme extends the luminosity plateau by another 3 hours while the availability of electron lens compensation would allow an extension by 1 hour. Altogether, the performance in terms of integrated luminosity is increased by almost two with respect to the Valencia scenarios while the maximum pile-up and energy deposition are decreased by a factor of 3 to reach about 110. The plain (blue) curves show that similar results can be obtained with the same hardware and a bunch spacing of 50 ns if the bunch charge is increased to the level assumed in the LPA option [4].

RISETIME OF PERFORMANCE

As already mentioned, an upgrade based on stronger focusing rather than increased beam current suffers from faster luminosity decay. The general experience is that handling large currents is always more difficult and less efficient. It is however difficult to be quantitative. Using an approach by V. Shiltsev [5] based on a statistical analysis of accelerator performance, a scenario of performance increase in time was built for either increasing the beam current or decreasing the β* function, without taking into account the new leveling option described just above. Figure 3 shows that a strategy with lower beam current should yield about 20% more integrated luminosity with a much steeper rise. Given the many hypotheses, another cautious interpretation could be that 20% is the threshold of significance for integrated luminosity estimates.

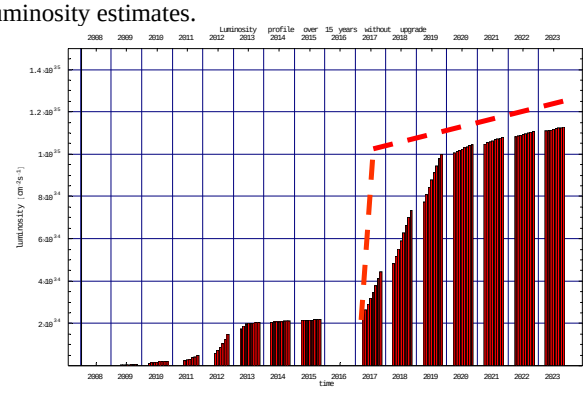

Figure 3: Luminosity [2 10^{34}/division] versus time [1 year/division]1) plain: beam current increase 2) dotted: increased focusing

CONCLUSION

The native luminosity leveling associated to the early separation scheme alleviates a serious defect of the LHC upgrade phase 2 related to a too fast decay of the luminosity with time. Indeed the leveling applies not only to the luminosity but as well to the beam-beam tune shift. The initially lower tune shift allows for more beam current. Hence leveling thru the collision angle opens the possibility of increasing significantly the integrated luminosity. It then becomes possible to propose a scenario with a constant luminosity of 6 10^{34} $cm^{-2}s^{-1}$ for 4.5 hours to 6.5 hours depending on the availability of "adds-on "

(electron lens, weak crab crossing). The multiplicity is significantly reduced to less than 120.

An issue for future study is the consequence of a large Piwinski angle. It should be noted that all advantages of the above solution can be provided by a local crab crossing scheme alone, would the presence of D0 inside the detectors be an overwhelming problem. This technically very challenging solution deserves as well feasibility investigations.

REFERENCES

[1] J.-P. Koutchouk, G. Sterbini, WEPCH094, *EPAC06*.
[2] Beam-beam session in the BEAM07 workshop of CARE-HHH-APD, Geneva, Sept. 2007, to be published.
[3] G. Sterbini, J.P. Koutchouk, A Luminosity Leveling Method for LHC Luminosity Upgrade using an Early Separation Scheme, LHC Porject Note 403, 2007.
[4] F. Zimmermann, in CARE-HHH BEAM07 workshop, 2007, to be published.
[5] V. Shiltsev, FNAL TD-1101 (2006).

INTEGRATING EARLY-SEPARATION DIPOLES IN CMS

Peter J. Limon, CERN, Geneva, Switzerland and Fermilab, Batavia, IL, USA

Abstract

Proposed methods of reducing the geometrical effects of the beam crossing angle include a dipole located close to the interaction point. In this note, I discuss the integration of the early separation dipole in the CMS detector. It appears that the forces and torques on the dipole are very great, and may prevent its use.

INTRODUCTION

A potential limitation to increasing the luminosity of the LHC by decreasing β□ at the interaction point is the geometrical effect of the finite beam crossing angle. The LHC crossing angle is relatively large, almost a half milliradian, in order to decrease the effects of the long-range beam-beam interactions. The crossing angle reduces the advantages of decreasing β□. For example, a reduction in β by a factor of two would result in a luminosity gain of a factor of two if the crossing angle were zero. With the present large crossing angle, reduction of β□ by a factor of two results in only a 30 percent gain in luminosity.[1]

THE EARLY-SEPARATION DIPOLE

Placement of the early separation dipole

For CMS, the closest reasonable placement of an early-separation dipole is about six meters from the IP, where the magnet can be supported from the massive and solid muon-detector steel, as shown in Fig. 1. In this location, there is one close encounter of the two beams if the bunch separation is the nominal 25 ns, but none if the separation is 50 ns or 75 ns. The integrated field strength of the dipole should be at least 8 T-m to separate the beams sufficiently before the next beam-beam encounter.[3]

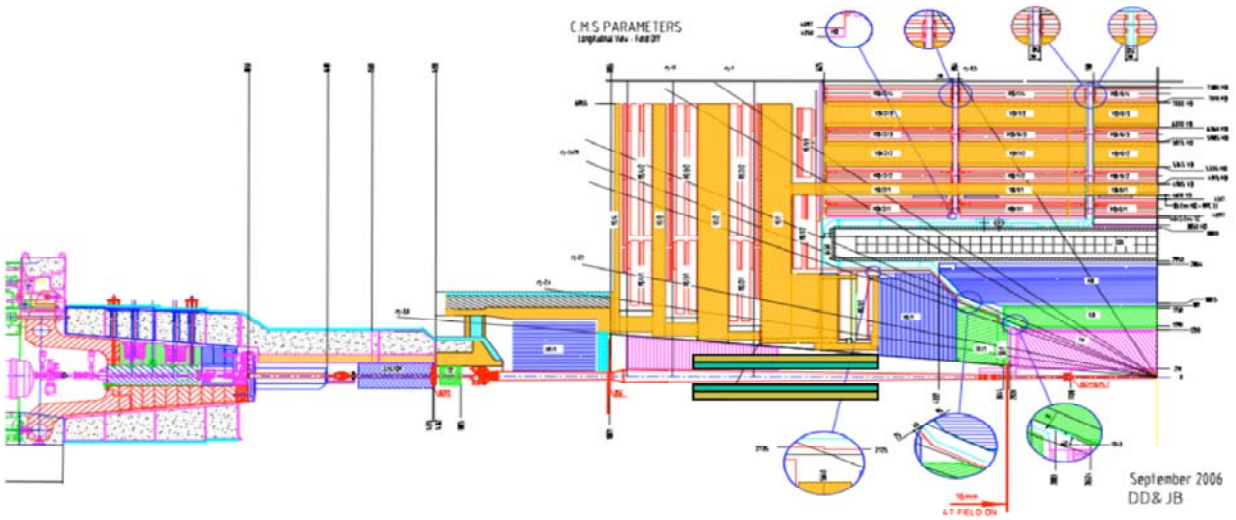

Fig. 1. An elevation view of CMS with an early-separation dipole located between 6 m and 8 m from the IP. The green shading are the magnet coils and collars. The yellow shading represents cooling channel filled with liquid helium

Aperture and size of the early separation dipole

The early-separation dipole is located in a region of fierce particle debris from the interaction point. These particles will shower and deposit much of their energy in the coils, increasing the temperature of the superconductor and stressing the cryogenic system. In order to decrease this effect, the early-separation dipole should have a large aperture. Since the dipole is close, and the particle flux and average energy from the interactions falls rapidly with angle, having a large aperture will significantly reduce the debris heating in the magnet. In this model, we take 0.3 m as the coil aperture. An additional advantage of having fewer particles hit the magnet is that the backscattering and albedo from the

magnet is also much reduced, making the detector backgrounds much less troublesome.

The early separation dipole is also restricted in its outer dimension, because of the tight space in which it must fit. If placed 6 m from the IP, the outer diameter of the cryostat cannot be more than about 1 m, probably significantly less when one takes into account the required services. For an aperture as large as 0.3 m, this permits very little space for a cold-iron yoke. Hence, this magnet is either without a steel return yoke, with a relatively thin warm iron yoke, or with a combination of thin cold and warm iron yokes. In any case, the fringe field of the magnet will be strong.

Field strength of the early separation dipole

For the purposes of this paper I have taken the central field in the dipole to be 4 T, easily reached by NbTi technology. Because of the significant particle debris heating, even for a large-aperture dipole, Nb3Sn may be required to gain greater temperature margin. Hence, the effective length of the dipole is about 2 m. A 0.3 m aperture dipole requires about 1500 kA-turns to generate a central field of 4 T.

Other advantages of the early separation dipole

There are additional advantages of a separation dipole besides decreasing the crossing angle. One is that it offers the possibility of leveling the luminosity by changing the crossing angle, thought to be a more robust and stable technique than varying the β at the IP. In addition, the smaller crossing angle makes crab cavities easier since the bunch rotation angle is smaller. Crab cavities, if they can be made to work, could reduce the effective crossing angle to zero.

THE FORCES ON THE EARLY SEPARATION DIPOLE

Parameters of the CMS solenoid

A significant feature of the CMS detector is the length, diameter and strength of the CMS solenoid magnet. Its coil is 12 m long and 4 m in diameter, and its central field is 4 T. A Its axial field along the beam line as a function of distance is shown in Fig. 2. Because it has a steel return yoke that is 13 m long, its field at 6 m from the IP, where the near end of the early-separation dipole is placed, is about 2.6 T. At the other end of the dipole, 8 m from the IP, the field is about 0.75 T. The early separation dipole feels a force due to the interaction of the current in its windings and the solenoid field.

Model and calculation of forces on the dipole

For the purposes of this paper, it is sufficient to idealize the solenoid field as uniform and everywhere parallel to the solenoid axis, and the dipole configuration to have ideal coils that are rectangular, with the sides parallel to the solenoid axis. I assume that the magnet bends in the horizontal plane. In this model, only the end turns of the dipole feel the forces caused by the solenoid field. The two ends feel forces in opposite directions, as shown in Fig. 3. The end closer to the IP then feels a force

F = Bsol x Idip = 3900 kN/m

For a coil 0.3 m wide this means a total force of about 1200 kN, or 120 tons in the vertical direction. The force on the other end of the magnet is about 35 tons, in the opposite direction. Hence, there is a net force of 85 tons, vertically, and a couple, that is, a torque around the center of the magnet of 1235 kN-m.

Of course, the model is not exactly accurate because the solenoid field is not exactly parallel to axis but is diverging. This results in components that are perpendicular to the coil along the long sides of the dipole. These forces may increase or decrease the net force and the torques, depending on details of the geometry. For the purposes of this paper, we are ignoring these higher-order effects.

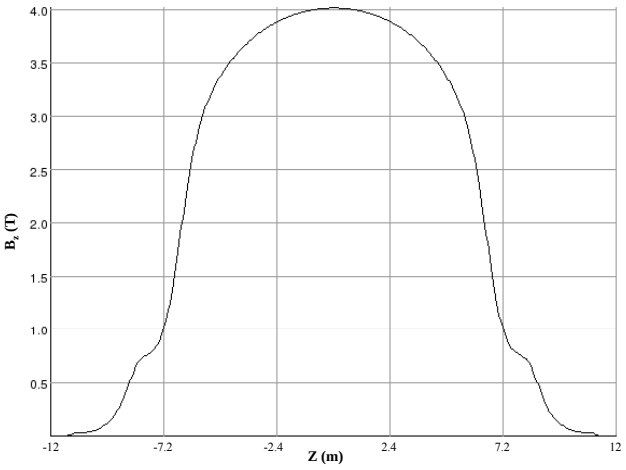

Fig. 2. The axial field of the CMS solenoid along the beam line as a function of distance along the beam line. (Courtesy of Vyacheslav Klyukhin, CMS & Moscow State University)

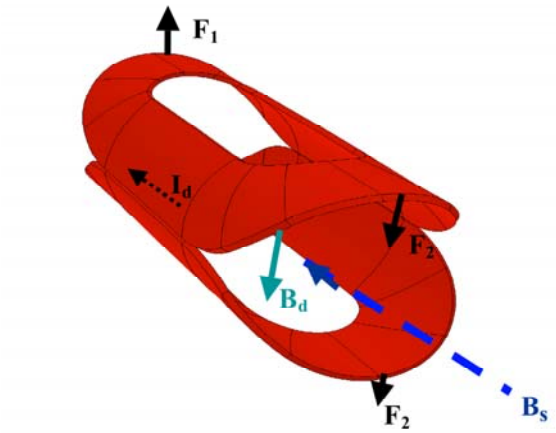

Fig. 3. A cartoon of an early-separation dipole showing the directions of the solenoid field Bs, the dipole current

Id, the dipole field Bd, and the forces on the ends of the magnet F1 and F2.

Effects of the forces on the dipole

The large forces and couple on the dipole make a massive support structure necessary. To get an idea of the scale of these forces, imagine a large airplane, a Boeing 757, for example, perched on one end of the dipole. This is one reason why the dipole cannot be cantilevered from the muon system to be closer to the IP. In fact, the support structure will be so massive that it will necessarily interfere with access to the detector and be the source of high backgrounds.

The forces on the upper and lower ends of the dipole coils are in the same direction, but because those forces must be reacted, the net effect is to crush the ends of the coil. The body of a cosine theta coil is robust under crushing forces because it is a Roman arch in compression, but the ends are not. Hence, the ends of the magnet must have some sort of strong inner support in direct contact with the insulated coils to prevent them from collapsing. This will decrease the effectiveness of the cooling just at the location of maximum debris heating, and increase the possibility of friction due to coil motion against this support. To my knowledge, no superconducting accelerator magnet has been made to work reliably with an internal coil support.

The forces on the coil ends are similar in magnitude to the self-generated forces of a high-field dipole, and will contribute stresses on the conductor of the order of 150 MP. This additional stress may make the use of Nb3Sn impossible. This would be unfortunate if the temperature margin of Nb3Sn is required for reliable operation.

POSSIBLE OTHER SOLUTIONS

There are at least two other possibilities that may solve some of the force problems. Neither of these solutions has been investigated to any great extent.

The CMS solenoid field could be locally cancelled near the dipole, at least approximately, by surrounding the dipole with a solenoid. This will cancel, or at least reduce the transverse forces on the dipole, substituting hoop stress and longitudinal forces on the small solenoid. These forces are large and will require support, but whether they are easier to deal with is not yet known. The increased size of the cryostat may require that the dipole have smaller aperture in order that the whole assembly can fit into the tight space allotted.

Another possibility is to have a complete iron yoke. Again, this may require a smaller aperture and consequently greater debris heating. It is not yet known whether this will decrease the forces on the dipole.

Neither of these solutions seems attractive due to the complexity and possible aperture decrease, but they will be investigated in the near future.

CONCLUSIONS

The forces on the coils of an early-separation dipole inside the field of a strong solenoid are very great, the order of 100 tons. They will require a massive support structure and internal support of the dipole coils at the coil ends. The additional stress on the conductor may make the use of Nb3Sn impossible. From this analysis alone, it appears that the use of an early-separation dipole will be very challenging. The results should inspire us to investigate other schemes to decrease the effects of finite crossing angle.

ACKNOWLEDGMENTS

The author would like to thank G. Sterbini, E. Laface, J.-P. Koutchouk and V. Kashikhin for useful discussions.

REFERENCES

[1] J.-P. Koutchouk, "Possible quadrupole-first options with $\beta^* \leq 0.25$ m", CARE-HHH-APD LUMI 2005 Workshop, Arcidosso, Italy, Aug. 2005

[2] J.-P. Koutchouk, "Insertion solutions from a parametric study", CARE-HHH-APD LUMI 2006 Workshop, Valencia, Spain, Oct. 2006

[3] G. Sterbini & J.-P. Koutchouk, "D0 and its integrability", CARE-HHH-APD LUMIN 2006 Workshop, Valencia, Spain, Oct. 2006

D0 design and beam-beam effect

G. Sterbini, J.-P. Koutchouk

HOW IS THE D0 EVOLVING SINCE IR06?

The Early Separation Scheme (ESS) layout (Figure 1) presented at the IR06 consisted of

- 1 dipole D0 inside the detector ($3-4$ m from the IP)
- 1 orbit corrector (OC) in front of the triplet, before the TAS, to restore the original beams'separation

It implies 4 LRs encounters at $\approx 5\sigma$ in the machine and a static crossing angle during the run.

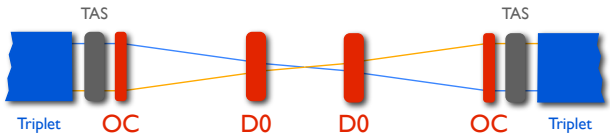

Figure 1: The Early Separation Scheme.

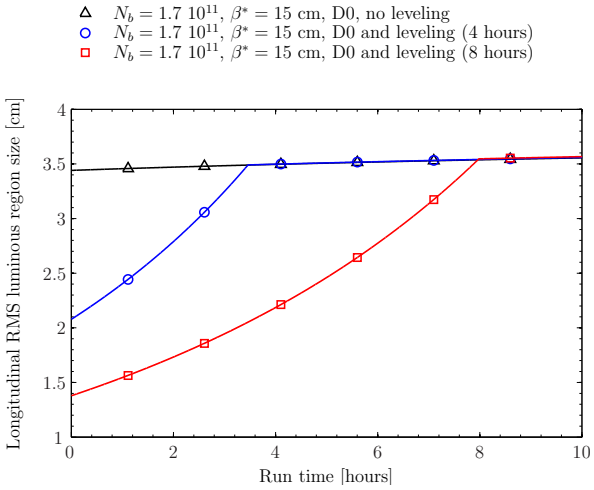

Figure 2: The luminous regions size during the run.

The impact of the leveling with the angle

A natural evolution of that scheme is the luminosity leveling with the angle: it is possible to control the luminosity with a proper feedback on the crossing angle. Apart from the luminosity, the leveling impacts on

- the luminous region length
- the HO tune shift
- the long range BB effect, since it modifies the beams'separation
- the D0 magnatic field: it has to change sign during the run.

The luminous region changes its length during the run (Figure 2): this can be an issue since the "events' density" per unit length of the luminous region varies during the leveling even if the the luminosity itself is kept constant.

The HO tune shift is reduced by the leveling (Figure 3, for H/V crossing): in principle, more beam current can be stored in the collider with an important gain in terms of integrated luminosity.

As shown in Figure 4 the beam separation varies: it is greater at the start and it is slowly reduced during the leveling. This is an advantage with respect to the beam-beam effect: the worst condition will occur when the beam current is already partially reduced.

In the case of a very long leveling time (8 hours) the D0 field has to change polarity (Figure 5): this possible difficulty is not yet addressed.

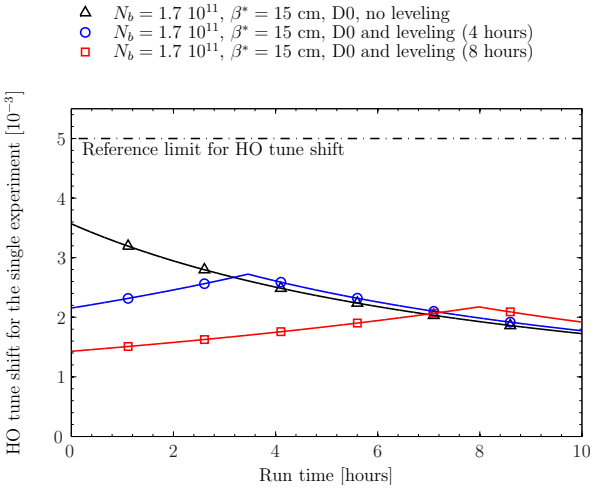

Figure 3: The head on tune shift during the run with ultimate bunch charge.

During the leveling the machine has to operate in a large Piwinski angle regime: the analysis of this issues goes beyond the scope of that work and is still to be addressed.

Can the D0 work at 50 ns?

We can use the Early Separation Scheme at 50ns with the following advantages:

- the constraint on the position of the D0 can be partially relaxed, it becomes possible to consider increasing the

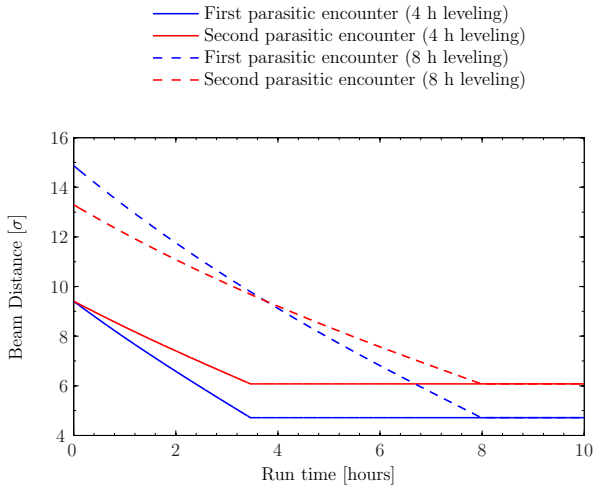

Figure 4: The beam separation during the run.

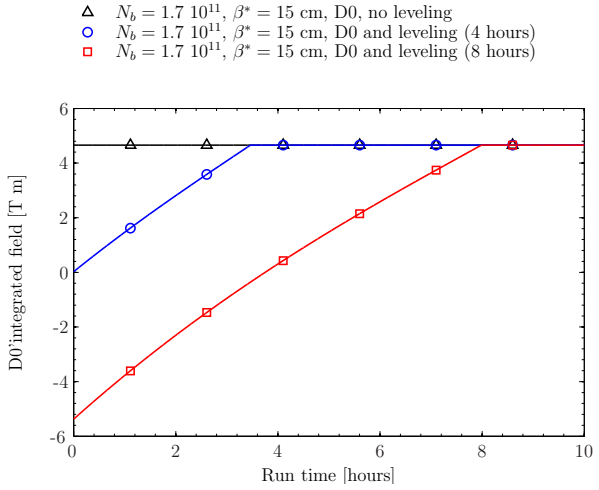

Figure 5: The D0 integrated field during the run.

IP-to-D0 distance

- the leveling with angle, apart from its intrisic advantage, provides a gain in the HO tune shift without the need of longitudinal flat bunch profile
- to decouple the crossing angle with respect to the beam separation in the triplets: we can increase it from the proposed 8.5 σ to 9.5 σ (or more).

The problems connected to the integration of the Early Separation Scheme in the detectors can still be a show stopper.

D0 AND BEAM-BEAM EFFECT

The requested integrated field of the D0 is a function of the D0 and OC positions and of the crossing angle. In Figures 6 we show the D0 integrated field requested with the OC at 19 m and $\beta^* = 0.15$ m. There are two curves: these represents two very different conditions during the leveling. At the start of the run the crossing angle is very large (16 σ), while at the end the crossing angle is likely reduced at 5 σ. In Figure 7 is shown the orbit corrector integrated field versus the D0 position. In Figures 8 and 9,

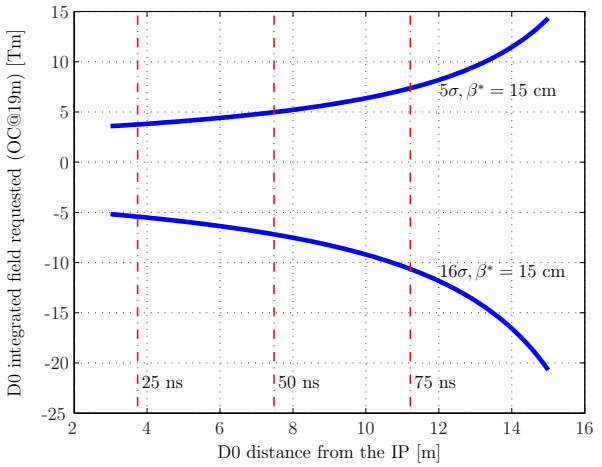

Figure 6: The D0 integrated field as function of the D0 position with the OC at 19 m from the IP. The two blue curves represent the strength needed at the beginning of a run (16σ)) and at the end (5σ).

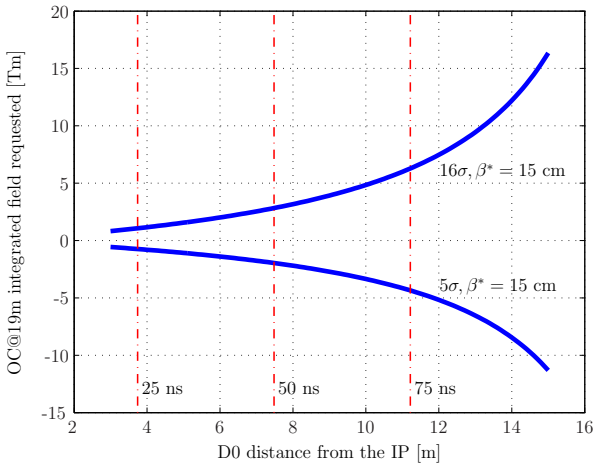

Figure 7: The OC integrated field as function of the D0 position with the OC at 19 m from the IP. The two blue curves represent the strength needed at the beginning of a run (16σ)) and at the end (5σ).

similarly, we showed the magnetic strength requested with $\beta^* = 15$ cm and the orbit corrector positioned at 15 m from the IP. The solution with the OC at 19 m and the D0 at $\approx$ 7 m seems to be the most promising for the technological feasibily of the scheme.

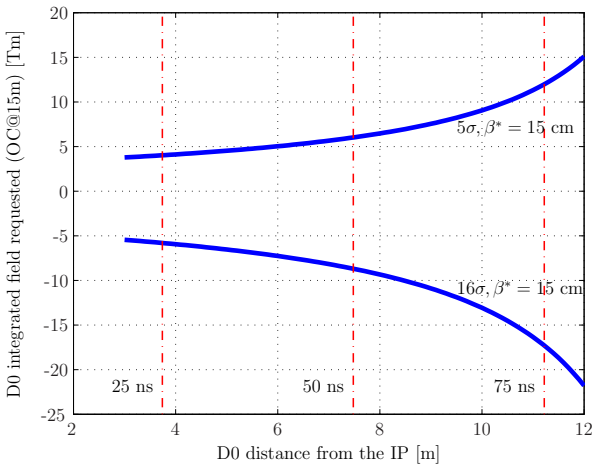

Figure 8: The D0 integrated field as function of the D0 position with the OC at 15 m from the IP. The two blue curves represent the strength needed at the beginning of a run (16σ)) and at the end (5σ).

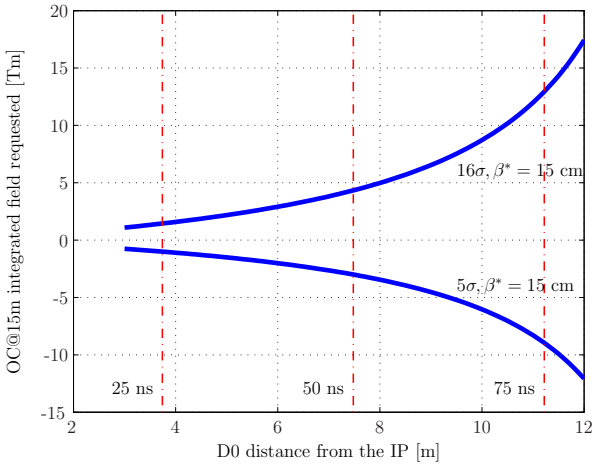

Figure 9: The OC integrated field as function of the D0 position with the OC at 15 m from the IP. The two blue curves represent the strength needed at the beginning of a run (16σ)) and at the end (5σ).

A first NbTi solution as been investigated [1] (1 m long magnet, with an integrated field of 3 Tm, Figure 10). Aperture is chosen very large (15 cm in diameter) to minimize the heat deposition. Some preliminary energy deposition studies have been performed ($L = 10^{35}$ cm^{-2} s^{-1}), and some shielding blocks has been proposed (Figure 11) [1].

An other fundamental aspect to be taken into account is the detectors' solenoidal field (Figure 12).

The location at 50ns ($7 - 9$ m) from the IP appears to present some advantages:

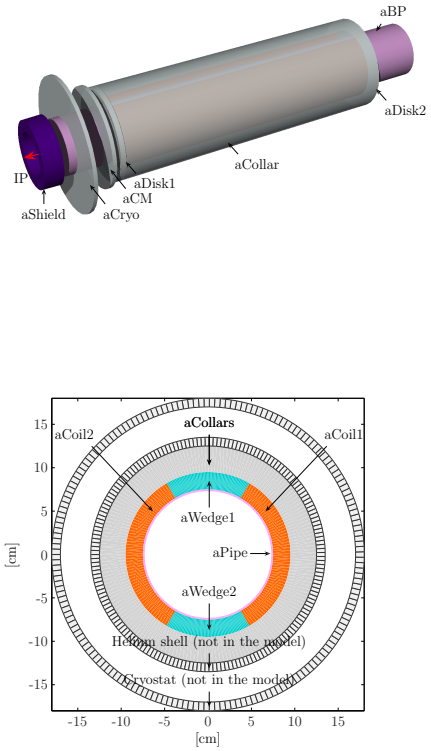

Figure 10: A possible implementation of the D0.

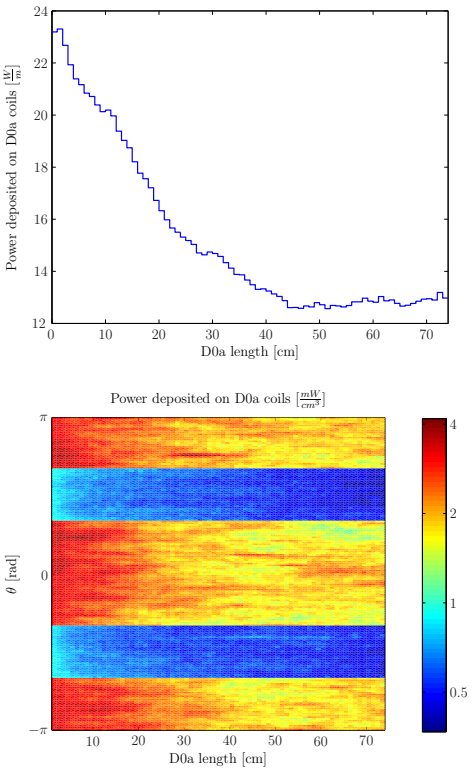

Figure 11: Preliminary results on the energy deposition of the D0.

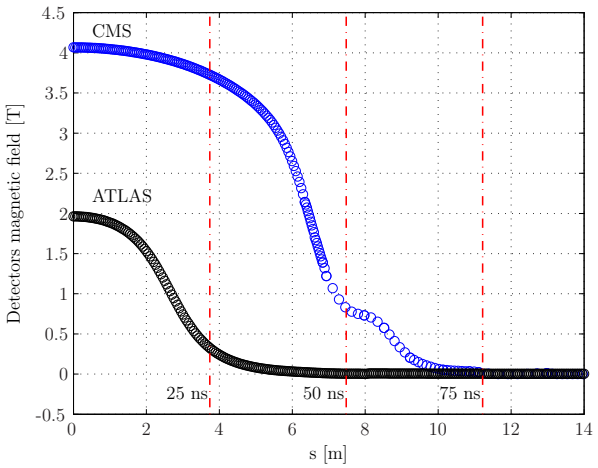

Figure 12: The detectors's solenoidal field.

- good trade-off between position and integrated field
- CMS solenoidals field is significantly lower ($\approx$ 1 T, negligible in ATLAS)
- connections, cryolines, maintainability should be less critical

We have still to answer the following questions:

- Does D0 blind the detectors? (see detectors talks)
- Are 8 LRs at 5σ acceptable for the beam lifetime ($N_b = 1.7\ 10^{11}$ ppb, $\epsilon_n = 3.75$ mm mrad)?

Results and limitations of RHIC and SPS's experiments

Only LHC can give a complete answer to the questions connected to the reduced beam separation. The machines that can be used for this kind of experiment are RHIC (with the wire), SPS (with the wire) and Tevatron (collider with similar bunch current but very different collision scheme with respect to the LHC). All these machines have circumferences from 4 to 6 times shorter than LHC: what is the impact of that is an issue to discuss. Some experiments have been done in the following approximations

- we do not consider coupling with HO collisions, other LRs, other lattice non linearities
- we approximate the beam field at 5σ with the wire field at 5σ
- we approximate the interaction in the weak-strong regime.

In Figure 13 we present some results on the RHIC experiment of the 20 June 2007 [2] (yellow ring). Five bunches were in the ring (bunches 1, 121, 181, 241, 301): the measured vertical emittance was very different between the bunches (respectively $44, 25, 28, 16, 25$ mm mrad).The separation beam-wire was vertical, so the normalized distance between beam and wire and the number of equivalent beam-beam long range (BBLR) vary from bunch to bunch [3].

From Figure 13 (plot on the top) we can observe that the Bunch 1 is the only one significantly affected by the wire. For that reason, in Figure 13 (plot on the bottom) we show the quantity scaled with respect to its vertical emittance: hence around 8 encounters at $\approx 5\sigma$ with $N_b = 1.7\ 10^{11}$ seems not to perturb significantly the beam lifetime. Reducing the separation between the beam and the wire to $\approx 3.5\sigma$, keeping a maximum current in the wire of 50 A, produced an observable beam loss. From the behaviour of bunch 121, 181, 301 (in the time interval 3000 s $< t <$ 4000 s), rescaling the separation and the number of long range [3], we can conclude that even $\approx$ 14 LRBBs (with the ultimate bunch current) at 5σ can be tolerated.

In the SPS beam–beam esperiment [4], among other results, it was observed that the effect of 1 wire (1.2 m long, at $\beta \approx 50$ m) at 30 A with a distance of 4.3σ ($= 6$ mm) from the SPS 37 GeV/c beam has not an observable effect (during the low beamlife of the SPS beam!). This is equivalent to 9 parasitic encounters at 4.3σ for the LHC ultimate current with LHC nominal normalized emittance in the SPS circunference.

CONCLUSIONS

The Early Separation scheme is compatible with leveling, 25ns and 50ns. If 8 LRs at $N_b = 1.7\ 10^{11}$ can be tolerated, the position between $7 - 8$ m from IP seems very promising for the engineering point of view. It is not yet clear if the detectors can efficiently operate in this scenario. For the beam–beam problems there are efforts to look for further MD time: even if partial, the experimental results are rather encouraging and consistent. At this stage it seems wise to preserve the avaibility of the slot $4 - 6$ m until clearer results are obtained: RHIC's long beam lifetime would be ideal for that purpose.

REFERENCES

[1] G. Sterbini, D. Tommasini, J.-P. Koutchouk, Layout VERSION 1 for the Early separation scheme in ATLAS, June 2007, CERN-AT Internal Note, Geneva.

[2] N. Abreu, G. Robert-Demolaize, U. Dorda, W. Fischer, J.-P. Koutchouk, G. Sterbini and F. Zimmermann, RHIC beam-beam experiment, 20 June 2007, to be published.

[3] Y. Papaphilippou, F. Zimmermann, "Estimates of Diffusion due to Long-Range Beam-Beam Collisions", Phys. Rev. ST Accel. Beams 5, 074001 (2002).

[4] **G. Burtin**, R. Calaga, **U. Dorda**, J.-P. Koutchouk, G. Sterbini, R. Tomás, **J. Wenninger**, F. Zimmermann, SPS beam-beam experiment, 24 July 2007, to be published.

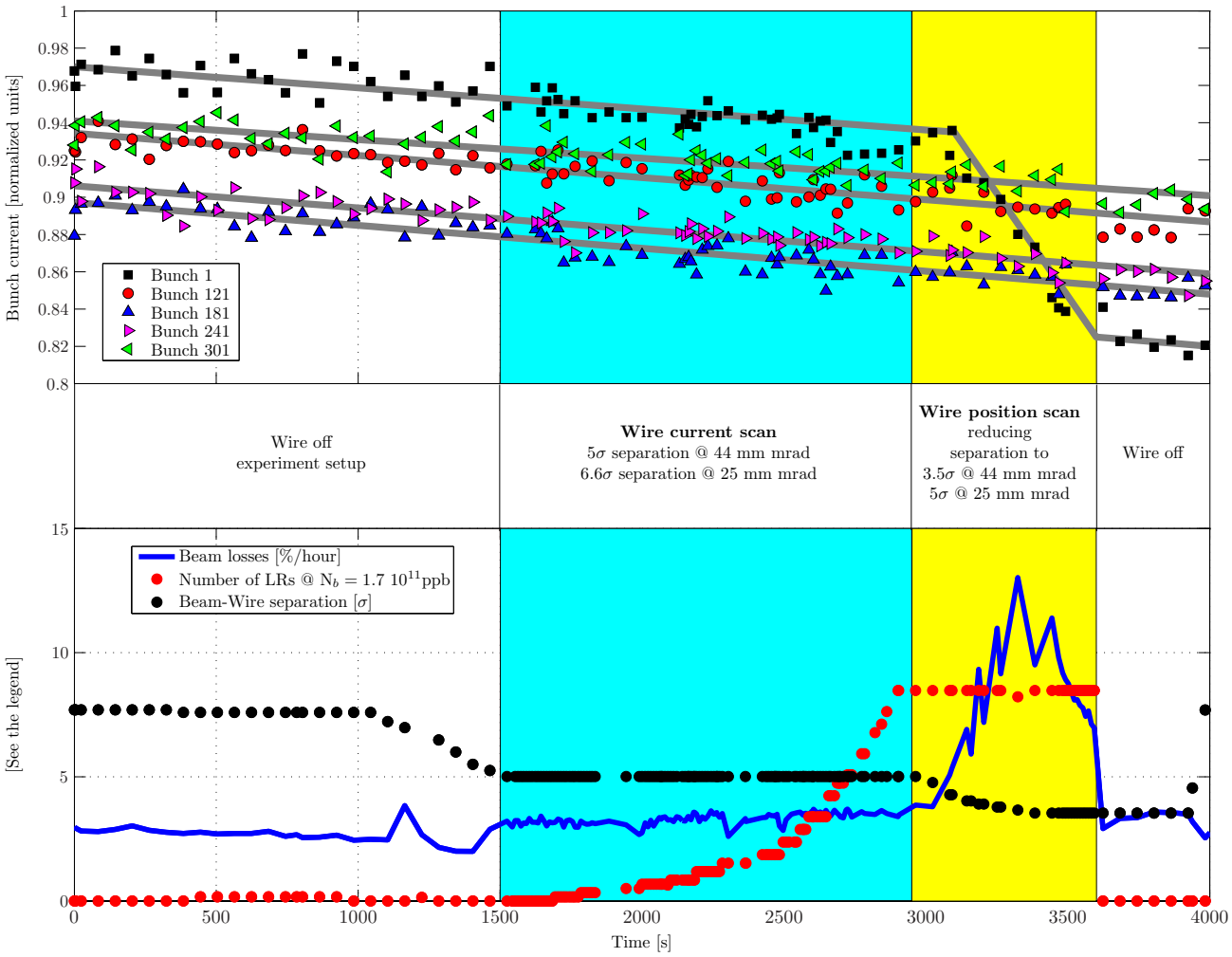

Figure 13: Yellow beam results of the 20 June 2007 RHIC experiment. In the plot on the top the evolution in time of the five bunches' current is shown. In the plot on the bottom the number of equivalent BBLRs and the beam-wire separation is computed for the Bunch 1 vertical emittance (44 mm mrad). During the wire current scan phase, the beam-wire separation was 5σ (with $\epsilon_v = 44$ mm mrad) and 6.6σ (with $\epsilon_v = 25$ mm mrad). At the maximum current (50 A on the 2.5 m wire) the equivalent number of BBLRs (at LHC ultimate bunch current, $N_b = 1.7\ 10^{11}$) was about 8 BBLRs (with $\epsilon_v = 44$ mm mrad) and about 14 BBLRs (with $\epsilon_v = 25$ mm mrad). No effect was observed. During the wire position scan phase (keeping the maximum current in the wire) the separation was reduced to about 3.5σ (with $\epsilon_v = 44$ mm mrad) and 5σ (with $\epsilon_v = 25$ mm mrad). For the 8 BBLRs at 3.5σ (bunch 1) the beam was clearly perturbed, on the other hand no significant effect was observed for 14 BBLRs at 5σ (bunches 121, 181, 301).

OPTICS ISSUES FOR PHASE 1 AND PHASE 2 UPGRADES

M. Giovannozzi, CERN, Geneva, Switzerland

Abstract

A review of the main issues of the upgrade scenarios of the LHC performance is presented. According to recent proposals, the upgrade of the LHC insertions is staged in two parts, which will be considered and discussed in some detail in this report.

INTRODUCTION

A recent result in the studies for the upgrade of the LHC performance is the definition of a staged approach (see Refs. [1-4] and references therein). It is now customary to distinguish between a Phase 1 and a Phase 2 upgrade, where:

- The Phase 1 upgrade aims at a consolidation of the LHC performance with ultimate beam parameters, corresponding to a bunch intensity of 1.7×10^{11} p and luminosity larger than 10^{34} cm^{-2} s^{-1}. The path to this is via a reduction of β^* down to 0.25 m, which requires the design of new large-aperture triplet quadrupoles based on NbTi superconducting cables. The cable is the spare cable used for the production of the LHC main dipole magnets. The overall impact of this upgrade on the long straight section (LSS) should be rather limited, in particular with no modifications to the experimental detectors as well as to the cryogenic system.
- The Phase 2 upgrade aims at an ambitious increase of the LHC luminosity by about a factor of ten, corresponding to 10^{35} cm^{-2} s^{-1}. By no means can such an upgrade be carried out without a deep revision of the insertions, including new triplet quadrupoles based on Nb_3Sn superconducting cables, special protections, and absorber elements. The new magnet technology is needed to improve the resistance of the devices to beam-induced losses: under routine operation the triplets will have to work at 35 MGy/year, which corresponds to less than one year lifetime for the nominal triplet layout. Last but not least, the detectors will have to be upgraded to exploit fully the new potential reach of the LHC ring.

THE PATH TO PHASE 1 INSERTION LAYOUT

The complete layout of the new insertion for the Phase 1 upgrade will require tackling a number of issues in various domains. The main items are discussed in the following.

Magnet technology

The choice of magnet technology imposes a number of constraints on the aperture, length, and operational gradient (see Ref. [5, 6] for a detailed account on these aspects). All these have a direct impact on the optics. As an example, the typical behaviour of the gradient as a function of magnet aperture is shown in Fig. 1 (from Ref. [6]).

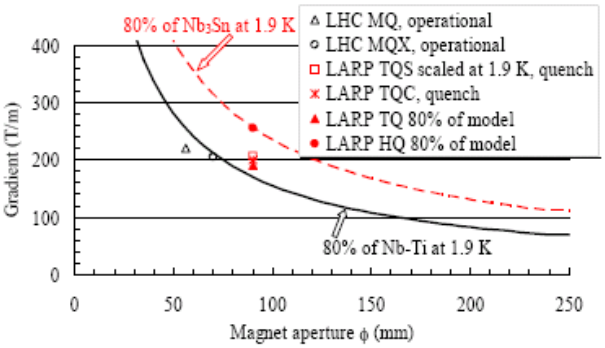

Figure 1: Dependence of the gradient (80% of the maximal critical gradient) as a function of magnet aperture for NbTi and Nb_3Sn quadrupoles at 1.9 K (from Ref. [6]).

Optics design of the low-beta triplet

The first challenge in the design of a low-beta triplet is the huge parameter space to be considered whenever a full optimization is required. In Refs. [7, 8] a full analytical treatment is presented. However, to reduce the complexity of the equations involved a simplification in the model used for the quadrupoles, which are represented as thin lenses, is introduced. Furthermore, a symmetry condition on the triplet layout was also imposed. Recently, two different approaches were proposed to tackle this problem. In the first one [9], a realistic layout is considered, but the parametric dependence of the optical parameters is expressed via fit functions (see Fig. 2 for an example).

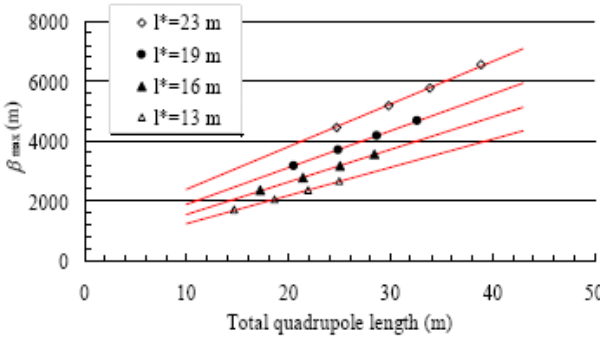

Figure 2: Dependence of β_{max} on the overall triplet length based on the fit approach (from Ref. [9]).

In the second one [10], a constant gradient point-to-parallel final focus is considered constructing a set of functions of one parameter representing the key quantities of the focusing system. These functions are the solutions of a system of equations that can be solved

numerically and can be used as a design tool. As an example of this approach the value of β_{max} as a function of the triplet quadrupoles gradient is shown in Fig. 3.

Figure 3: Boundaries of the region in the (β_{max}, gradient) space where a solution for a triplet or a quadruplet

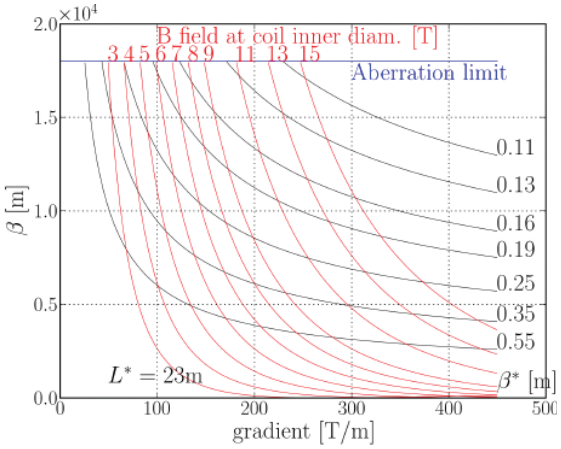

insertion for the LHC exists. The regions are limited by the quadrupole pole field and the value of β^* (from Ref. [10]).

The newly proposed approaches can be used to find the best solution to the problem, but still one has to define the correct constraints to be fulfilled by the optimal layout. The most relevant are summarized in the following:

- Aperture: this is the first merit function to be considered. The mechanical aperture should allow accommodating the beam envelop plus additional margin for, e.g., mechanical tolerances, closed orbit tolerances, beta-beating errors (see [11] for a review of the parameter set considered for the design of the nominal LHC ring). In the current design of the Phase 1 insertion upgrade the overall aperture budget is assumed to be 33 σ (for the beams) plus 22 mm (for the other sources) [2]. On top of this rough estimate, one should still consider some extra aperture for mitigation of energy deposition issues [12] and also impedance-related issues with the LHC collimators [13]. Indeed, increasing the triplet aperture would enable increasing the collimators' gap thus alleviating the impedance issue. Nevertheless it is important to emphasize that the impedance reduction due to a larger gap will have to be balanced against a reduced cleaning efficiency. The global solution of the performance limitation of the collimation system will be the matter of the Phase II collimation project.
- Maximum beta-function in the triplet: the driving criterion consists in minimizing it. Not only because of the aperture-related issues, but also because of the direct impact on chromaticity and its correction, off-momentum beta-beating, and single-particle dynamic aperture. A too large chromaticity generated by the low-beta triplets will not be correctable by the arc sextupoles [14]. The off-momentum beta-beating is already rather large for the nominal LHC, between 10 % and 30 % for a momentum offset between 3×10^{-4} and 8×10^{-4}, respectively (the latter takes into account the momentum off-set required for dispersion measurements). This is a potential source of problems for the performance of the collimation system [15] as the correction of the off-momentum beta-beating cannot be performed globally, but only in half of the machine circumference. This might have the effect of a secondary collimator becoming a primary one, thus spoiling completely the hierarchy of the various collimator devices. The choice of the half circumference with corrected off-momentum beta-beating is based exactly on these considerations. The current correction strategy foresees the use of the phase advance between the collision point 1 (ATLAS) and 5 (CMS) together with 32 families of sextupole magnets [14]. Single-particle dynamic aperture is intrinsically related with the field quality of the triplet quadrupoles. A larger value of β_{max} can enhance the harmful effects of magnetic field errors, thus imposing nonlinear corrector magnets to improve the overall field quality of the triplet system (as it is done for the nominal layout of the LHC insertions). An interesting result was obtained by analysing how the magnetic field errors depend on the magnet aperture [16] and by proposing a scaling law for the field quality, whose beneficial impact on the dynamic aperture was tested with numerical simulations [17].

These considerations led to the proposal of four different layouts [2, 3], which are under study to rank them and select the ones with the best performance [18, 19]. In Fig. 4 the four layouts are represented in the (β_{max}, gradient) space. The limitations imposed by the choice of the magnet technology, as well as those imposed by the correctability of the chromaticity are shown.

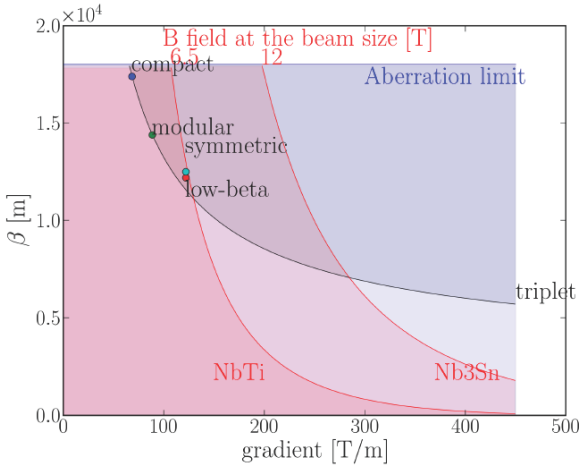

Figure 4: Summary plot in the (β_{max}, gradient) space of the various constraints including also the working points corresponding to the four optical layouts [2, 3] under consideration (from Ref. [19]).

It is worth mentioning that in addition to the study of the various layouts to find the optimum configuration each of them is also considered with flat beam optics [20]: this option is gaining more and more interest for the nice feature of allowing a better use of the available mechanical aperture with an interesting side effect of improving the situation with the beam-beam.

Optics design of the long straight section

Usually, the focus of the studies for the Phase 1 upgrade is on the triplet layout. However, the impact of this change on the performance of the remaining part of the LSS should not be neglected.

In Ref. [21] a complete account of the aperture situation for the current layout of the LSS assuming a Phase 1-like triplet is given. The problematic region is the one between the warm D1 separation dipole and the cold Q5 quadrupole. An attractive solution for overcoming the aperture bottleneck in the warm D1 is presented in [22] even so the option of a cold magnet to replace the nominal configuration is not excluded.

As far as the cold D2 separation magnet and the cold Q4 and Q5 are concerned, their aperture is a bottleneck, but not as severe as the D1. A different orientation of the beam screen might provide enough mechanical aperture. Nevertheless the situation of the LSS requires still some studies before drawing any conclusion about hardware changes.

THE PHASE 2 UPGRADE

As already mentioned, the Phase 2 upgrade aims at a ten-fold increase of the luminosity and hence requires deep revisions of the insertion regions, the detectors, and infrastructure, such as the cryogenic plants for IR1 and 5. Furthermore, while the Phase 1 upgrade was essentially based on the luminosity increase generated by the reduction of β^*, the Phase 2 will require a radical change also at the level of the beam parameters, which has a deep impact on the injectors' chain. Two options emerged [23], namely:

- Early Separation (ES) scheme: such a scheme is based on 25 ns bunch spacing and relies on strong focusing from the low-beta triplet ensuring a β^* value in the range 11 cm – 14 cm combined with ultimate beam parameters. The use of a so-called D0 dipole inside the detector requires deep modifications to the layout of the experimental region.
- Large Piwinski Angle (LPA) scheme: such a scheme is based on 50 ns bunch spacing, larger than ultimate beam parameters, and flat bunch profile in the longitudinal plane. The value of β^* is in the same range as the one foreseen for the Phase 1 upgrade.

A possible optical layout for Phase 2 was presented in Ref. [24]. The smaller value of β^* imposes even deeper modifications of the separation dipoles D1 and D2. In particular the option of a warm D1 might not be feasible anymore due to the too large gap required.

A common feature of the various scenarios for the Phase 2 upgrade is the need of highly-challenging ancillary systems to exploit fully the potential luminosity reach. These devices are essentially needed to mitigate the effect of the crossing angle either in the direction of enabling its reduction or to mitigate the luminosity reduction. In the first group one can list: slim dipoles, wire compensators, electron lenses; in the latter essentially crab cavities.

In all cases, both R&D efforts are required to develop the hardware as well as simulation studies to clarify the beam dynamics issues and machine experiments to probe the actual beam behaviour. This is particularly important in the case of beam-beam effects for which the complexity of the problem makes it necessary an experimental cross-check of the simulation results. This consideration leads to the conclusion that a vigorous R&D programme should be launched even before the implementation of the Phase 1 upgrade. In particular, according to the results shown in Fig. 5, where the average luminosity for the two Phase 2 upgrade scenarios as a function of β^* are shown including some sub-options, it seems clear that the feasibility of a crab cavity for a proton machine is a crucial issue for choosing between ES and LPA schemes. Hence, this piece of hardware could be the first item to be studied in the near future.

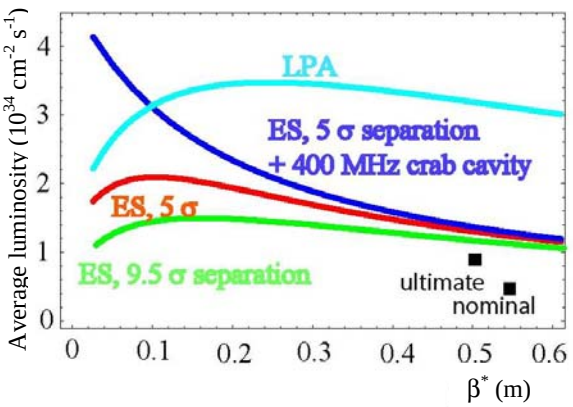

Figure 5: Average luminosity as a function of β^* for the two scenarios for the Phase 2 luminosity upgrade. For the sake of comparison, the luminosity for the nominal and ultimate performance is also shown (from Ref. [23]).

It is also important to mention that the Phase 2 upgrade opens up crucial operational issues. Indeed, the short luminosity lifetime imposes mitigation measures to be put in place as the huge luminosity variation will force the detectors to work in a highly non-optimal mode. Luminosity levelling could be performed by varying either the crossing angle or β^* [25]. None of these approaches was ever tried so far [26, 27]: experimental studies should be envisaged to have a non-controversial statement on the feasibility of luminosity levelling methods.

CONCLUSIONS AND OUTLOOK

The path towards a Phase 1 upgrade of the LHC insertions is essentially based on the development of new triplet quadrupoles with proven technology, i.e. NbTi magnets. In this respect, the strategy is unique and no alternative scenario is under development. The set of parameters for the required triplet quadrupoles is still to be finalized, but the main criteria were reviewed and presented in this report. The four proposed layouts were studied in details and two were selected for further optimization. The next steps will consist in providing a layout compatible with all hardware constraints; study the tenability of the optics, the injection optics and the squeeze sequence; perform detailed beam-beam simulations; evaluate the performance of the collimation system.

The situation of the Phase 2 upgrade is somewhat different. Two scenarios with different beam and optics parameters are being considered. Hence, in this case the efforts will focus not only on the development of new magnets based on new technology, i.e. Nb_3Sn superconductor, but also on a number of ancillary systems required to overcome the many beam dynamic issues related with the extreme beam parameters under consideration. Such systems are, e.g., crab cavities, wires and electron lenses to compensate the long-range beam-beam effects as well as additional magnets located next to or inside the experimental detectors. These devices are already challenging per se, and given their crucial role in achieving the goals of the Phase 2 upgrade their actual performance should be assessed well-before any final choice of the scenario is taken. In this respect, it seems advisable to launch the necessary R&D programmes quickly and, whenever possible, tests of some of these devices in the early stages of the LHC operation might be envisaged.

ACKNOWLEDGEMENTS

The results presented in this paper were worked out by many people. In particular, fruitful discussions with R. Assmann, C. Bracco, O. Brüning, U. Dorda, R. De Maria, S. Fartoukh, W. Herr, M. Meddahi, E. Todesco, R. Tomás, and F. Zimmermann are warmly acknowledged.

REFERENCES

[1] O. Brüning, "The CERN View on Accelerator Physics R&D", presentation given at the US LARP meeting, April 2007.

[2] J.-P. Koutchouk, L. Rossi, E. Todesco, "A Solution for Phase-one Upgrade of the LHC Low-beta Quadrupoles Based on Nb-Ti", LHC Project Report 1000.

[3] O. Brüning, R. De Maria, R. Ostojic, "Low Gradient, Large Aperture IR Upgrade Options for the LHC compatible with Nb-Ti Magnet Technology", LHC Project Report 1008, 2007.

[4] O. Brüning, "LHC Accelerator Physics Issues", presentation given at the US LARP meeting, October 2007.

[5] L. Rossi, E. Todesco, "Electromagnetic Design of Superconducting Quadrupoles", Phys. Rev. ST Accel. Beams 9, 102401, 2006.

[6] E. Todesco, these proceedings.

[7] T. E. D'Amico, G. Guignard, "Analysis of generic insertions made of two symmetric triplets", CERN-SL-98-014-AP, 1998.

[8] T. E. D'Amico, G. Guignard, "Experimental insertions made of two symmetric triplets", CERN-SL-98-020-AP, 1998.

[9] E. Todesco, J.-P. Koutchouk, "Scaling Laws for Beta* in the LHC Interaction Regions", LHC-LUMI-06 Conference Proceedings, CERN-2007-002, p. 61, 2007.

[10] R. De Maria, "Layout design for final focus systems and applications for the LHC interaction region upgrade", LHC Project Report 1051, 2007.

[11] O. Brüning, P. Collier, Ph. Lebrun, S. Myers, R. Ostojic, J. Poole, P. Proudlock, "LHC design report, Vol. I", CERN-2004-003, 2004.

[12] E. Wildner, these proceedings.

[13] R. W. Assmann, "Triplet aperture and collimation issues", presentation given at the LHC Insertion Upgrade Working Group, November 2007.

[14] S. Fartoukh, "Second order chromaticity correction of LHC V 6.0 at collision", LHC Project Report 308, 1999.

[15] R. W. Assmann, C. Bracco, "Chromatic phase space cuts from collimation", presentation given at the LHC commissioning and Upgrade section, November 2007.

[16] E. Todesco, B. Bellesia, J.-P. Koutchouk, "Field Quality in Low-Beta Superconducting Quadrupoles and Impact on the Beam Dynamics for the Large Hadron Collider Upgrade", Phys. Rev. ST Accel. Beams 10, 062401, 2007.

[17] R. Tomás, R. De Maria, M. Giovannozzi, these proceedings.

[18] R. De Maria, "Optics solutions for Phase I", presentation given at the LHC Insertion Upgrade Working Group, October 2007.

[19] R. De Maria, these proceedings.

[20] S. Fartoukh, "Flat beam optics", presentation given at the LHC Machine Advisory Committee, June 2006.

[21] S. Fartoukh, "LSS magnet aperture requirements", presentation given at the LHC Insertion Upgrade Working Group, September 2007.

[22] J.-P. Koutchouk, D. Tommasini, "A significant potential saving on the D1 for the LHC luminosity upgrade Phase 1". AT-MCS Internal Note 2007-08, EDMS 875274.

[23] F. Zimmermann, "Scenarios for the LHC Upgrade", presentation given at the CARE-HHH-APD Beam07 Workshop, CERN, October 2007.

[24] J.-P. Koutchouk, R. Assmann, R. De Maria, E. Métral, G. Sterbini, E. Todesco, F. Zimmermann, "A Concept for the LHC Luminosity Upgrade Based on Strong Beta* Reduction Combined with a Minimized Geometrical Luminosity Loss Factor", Proceedings of the PAC07 Conference, Albuquerque – NM (USA), p. 3387, 2007.
[25] J.-P. Koutchouk, G. Sterbini, these proceedings.
[26] V. Lebedev, "Levelling with β^*", presentation given at the CARE-HHH-APD Beam07 Workshop, CERN, October 2007.
[27] V. Shiltsev, "Summary of the luminosity performance session", presentation given at the CARE-HHH-APD Beam07 Workshop, CERN, October 2007.

Phase 1 Optics: Merits and Challenges *

Riccardo de Maria, CERN, Geneva, Switzerland

Abstract

Low gradient optics have been proposed for an upgrade of the LHC interaction region. Using lower gradient, larger aperture and longer NbTi quadrupoles with respect to the nominal layout, it is possible to achieve $\beta = 25\,\mathrm{cm}$ with additional aperture margins and better dynamic aperture. The main drawbacks are an increase of the number of the long range interactions and limitations in the downstream matching section. Four layouts and optics, which span the parameter space and modularity for NbTi technology, are proposed and studied extensively in order identify and quantify the merits and challenges.

INTRODUCTION

Phase I upgrade aims at reducing β^* from $55\,\mathrm{cm}$ to $25\,\mathrm{cm}$ while keeping as small as possible changes in the LHC interaction region layout. The new layout should also:

- limit the beam size in the focusing system for reducing chromatic aberrations and errors sensitivities,
- maximize the aperture margins in the focusing system for reducing the heat load, radiation damage and increasing operational margins
- make the final focusing system as short as possible for reducing the number of long range beam beam interaction, reducing the field of D1/D2 and reducing overall the cost.

The nominal LHC layout cannot fulfill the Phase 1 targets because the triplet magnets have aperture limitations.

A study has been performed to identify the possibilities for a replacement of the nominal triplet (see [1]). Four different layouts has been proposed (see [2] and [3]) in order to explore the parameter space and identify the benefits and limitations of several design criteria.

TRIPLET OPTIMIZATION

A simplified model has been used to study the parameter space of final focus system.

The model consists piecewise constant gradient point to parallel focusing systems (see Fig. 1). Using this model it is possible to reduce the parameter space to three quantities: the normalized gradient k, the distance of the first quadrupole from the IP (L^*) and the beta function at the IP (β^*). Using the fact that the phase advance in the triplet is negligible, it is possible to find the parameters of all possible piecewise constant gradient point to parallel focusing systems with the help of a set of univariate numerical functions (see Fig. 2). For more details refer to [1].

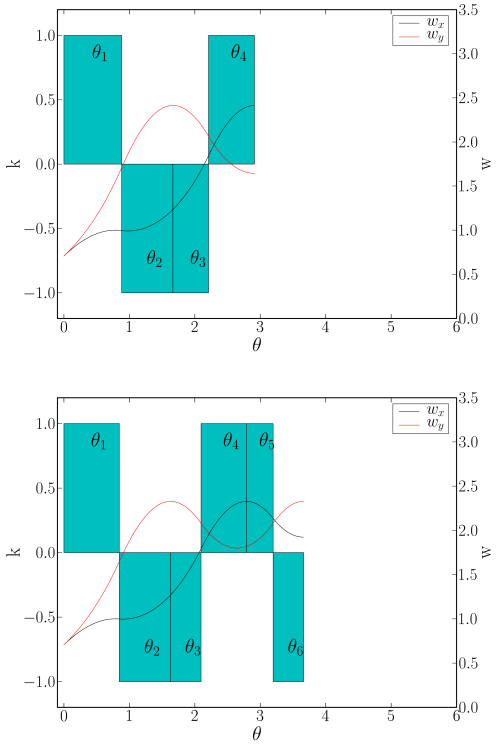

Figure 1: Point to parallel triplet and quadruplet focusing system.

Using these functions, it is possible to plot the maximum beam size of the beam in the triplet as a function of the gradient using the simplified models. This function divides the plane in a region where the focusing systems that have a negative focal length (above the black line in Fig. 3) and the one having positive focal length.

In the same plot it is possible to draw the region of the parameters of the quadrupoles compatible with NbTi (red region) using the peak field of $8\,\mathrm{T}$ and the edge of the beam region diameter a defined by $a = 33\sigma + 22\,\mathrm{mm}$.

Figure 3 shows that, when the gradient decrease, the aperture required by the beam increase slower than the aperture compatible with a given peak field. It implies that smaller is the gradient, larger will be the aperture margins. The clear advantage of low gradient quadrupole magnets is limited by the fact that the quadrupoles needs to be longer, the beta functions become larger and the chromatic aberrations increase. Another disadvantage is that the number of long range interaction increases as well.

* Work supported by CERN and EPFL

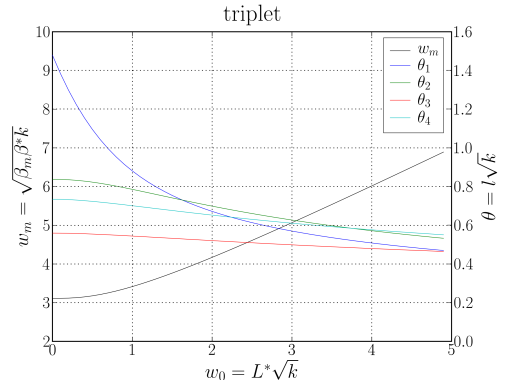

Figure 2: Parameters for all constant gradient point to parallel triplet focusing system.

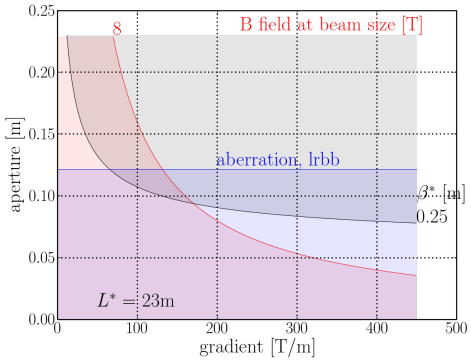

Figure 3: Triplet parameters space for the LHC upgrade.

The simplified model gives an indication of the parameters of possible focusing systems, however a realistic implementation is necessary to test the hypothesis and identify further limitations.

REALISTIC IMPLEMENTATIONS

In order to design a realistic focusing system, once the gradient is fixed, is necessary to introduce gaps between the quadrupoles in order to make room for coil ends that do not contribute to the field and interconnections. Additional room can be reserved for corrector packages.

The optimal quadrupole lengths are in general different for the every unit, one has to trade the aperture margins and the overall lengths with the possibility of using equal sized modules that reduce the cost of the equipment in terms of R&D and spare policy. It is worth noting that the first quadrupole unit requires always a smaller aperture, therefore it is possible to use a stronger quadrupole with the same peak field of the other units which translates in a gain in overall length and beta peak. Also in this case it is possible to trade this optimization with the cost of the equipment. In addition the larger aperture margins of the first unit can be used to install thick shielding tubes for protecting the coil from the debris coming from the IP that presumably will be higher for the first elements.

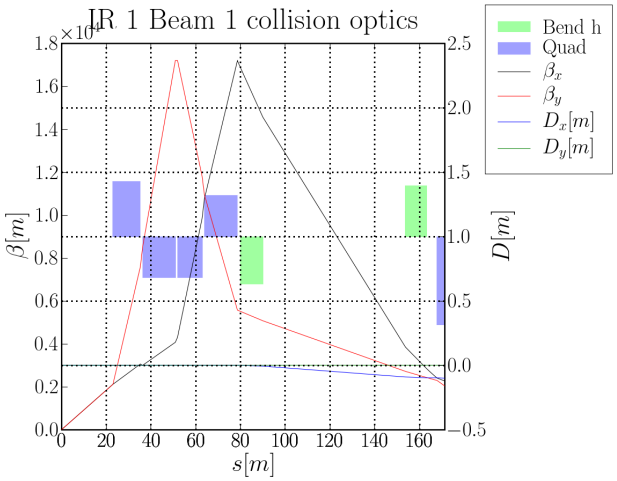

Figure 4: Upgraded IR layout: "Compact" (see [3]) .

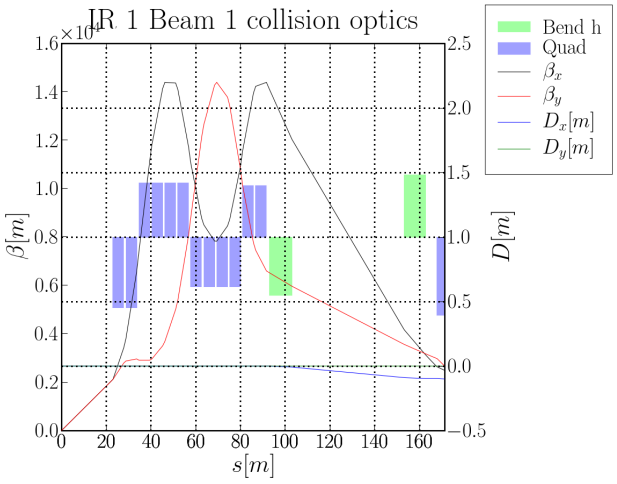

Figure 5: Upgraded IR layout: "Modular" (see [3]) .

Four different layouts (see Fig. 4, 5, 6, 7) were designed and studied using different gradients and modularity.

These options were extensivily studied and further infomartion will be available in [4].

Compact

This option (see Fig. 4,) uses a triplet layout and the lowest possible gradient compatible with tolerable aberrations. The overall length is minimized (the name comes from there) using an optimized gradient for Q1 and optimized lengths for Q1, Q2 and Q3. The gap between the quadrupoles is 1 m for the interconnection (a recent study REF established that the minimum distance between quadrupoles in two different cryostats is 1.3 m but smaller in case they are in the same cryostats). In order to find a

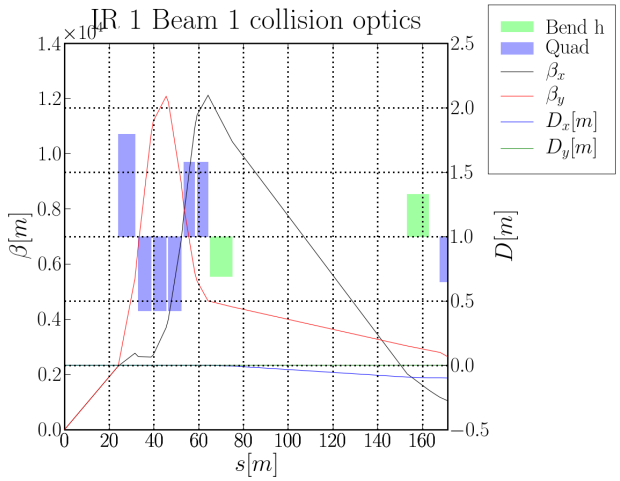

Figure 6: Upgraded IR layout: "Lowbetamax" (see [3]) .

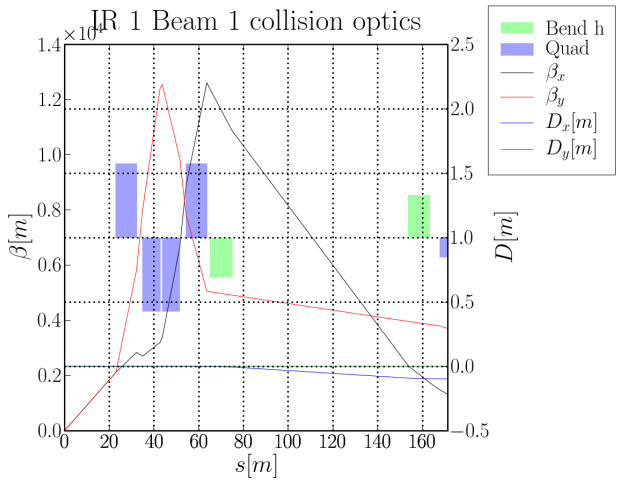

Figure 7: Upgraded IR layout: "Symmetric" (see [2]) .

suitable collision optics an additional Q6 module has been installed. This layout has been proposed in [3].

Modular

This option (see Fig. 5,) uses a quadruplet design with an intermediate gradient. All the modules have the same length (the name comes from there) but the first two have a larger gradient implying or a reduced aperture for the first two modules or reduced aperture margins in the other modules. The gap between the quadrupoles is 1 m. An advantage of this option is the large set of gaps that can be used for mask absorbers or corrector magnets. In order to find a suitable collision optics an additional Q6 module has been installed. This layout has been proposed in [3].

Lowbetamax

This option (see Fig. 6,) uses a triplet layout and the highest gradient compatible with some additional aperture margin in the triplet. The first element uses a reduced aperture and modules of three different lengths. These choices limits the peak of the beta function in the triplet (the name comes from there). No additional quadrupole modules are installed. This layout has been proposed in [3].

Symmetric

This option (see Fig. 6,) uses a triplet layout and the highest gradient compatible with some additional aperture margin in the triplet. This option uses only two different modules of different length but same aperture and gradient. The modules are arranged almost symmetrically with respect to the center of the triplet assembly (the name comes from there). The gaps are the same w.r.t the nominal layout. The triplet layout first presented in [2].

All these options do not cover all the possibilities and should be considered working hypothesis for identifying merits and limitations for the several options in terms of gradient and modularity.

Layout parameter

The layout data can be summarized in Table 1:

For these layouts collision optics with crossing schemes for the entire LHC has been developed.

APERTURE BOTTLENECKS

The quantity n_1 (see [7]) has been used for evaluating the aperture margins in the interaction region. The aperture model is indicated for the new elements in Table 1. For the rest of the elements the aperture model is the same as the one of the official LHC optics V6.501 with few exceptions for D2 Q4 and Q5. The aperture of these elements has been optimized for the injection optics with a particular orientation of the beam screen. In case of the upgraded optics the beta functions and as a consequence the crossing scheme pose tighter constraints at collision. The beam screens are consequently rotated in the locations where it is possible to increase aperture margins.

The apertures are computed using closed orbit tolerances of 3 mm, energy spread of $\delta = 0.00086$ and nominal aperture tolerances. Additional informations are given in [6].

The results are summarized in Tab. 2.

CHROMATIC EFFECTS

The upgrade optics present stronger chromatic effects due the reduction of β^* which implies a stronger impact of quadrupole errors in the final focusing system.

Table 3 shows the values for the required strengths of the arc sextupoles for compensating the first order chromaticity and the off momentum beta beating for two different energy error.

	Compact	Modular	Lowbetamax	Symmetric
L* [m]	23	23	24	23
Gradient [T/m]	91,68	115,88,82,84	168,122	122
Module L [m]	12.2,14.6,11	4.8	7.4,5.7,4.9	9.2,7.8
Total L [m]	55	68	40	41
LRBB	23	26	19	19
Aper. MQX [mm]	170,220	130,170	90,130	130
B.S. MQX [mm]	74,79;99,104	54,59;99,104	34,39;54,59	54,59
B.S. D1 [mm]	50,64;45,64	50,64;45,64	50,64;45,64	50,64;45,64

Table 1: Layout parameters for different LHC interaction region layouts. The beam screen apertures are given in term of half gap and radius and for the MQX the two couple refers to the twos aperture. The quadrupole apertures were proposed in [5]. The D1 apertures were proposed in [6].

	Compact	Modular	Lowbetamax	Symmetric	LHC
MQX, ap 1	20.026	14.141	7.821	15.466	7.215
MQX, ap 2	16.953	12.633	8.830	8.438	6.845
D1	5.303	6.379	7.607	7.323	7.431
D2	5.372	4.271	7.959	6.518	15.152
Q4	7.387	6.432	8.685	7.184	15.615
Q5	4.701	3.859	10.425	7.028	16.871

Table 2: Aperture bottlenecks for the upgrade optics and the nominal LHC in terms of n_1

The results show that while the natural chromaticity is still correctable by the arc sextupoles, the off momentum beta beat increases by a factor of 3 to 5 with respect to the nominal values. It is not clear whether the rest of the LHC subsystems can cope with such a large beating or if this effect can be corrected while keeping acceptable flexibility in the machine.

Dynamic aperture

In collision the dynamics aperture (DA) is dominated by the non linear fields in the interaction region. The larger contribution to the reduction of DA is the "other" beam which should reduce the DA to 6σ. For additional informations refer to [8].

Another important contribution comes from the field imperfections in large beta area (i.e. triplets, D1, D2 and the first elements of the matching section). For the LHC it has been estimated that for preserving the DA to 6σ with beam beam, the minimum DA over 60 seeds without beam beam effect should be larger than 12σ (see [7]).

In case of the upgrade is important to design magnets with a field quality that preserves a DA of 12σ. Estimates for the field quality of new magnets can be found using the scaling laws presented in [2] and the present production.

Table 4 shows the results for the four upgrade optics and the LHC. Designs with larger aperture margins present larger DA when only triplets error are included. In case of aperture bottlenecks in the matching section, the field quality of those elements starts to be dominant. These two facts explain the large differences between the Compact and Modular design with respect to the Lowbetamax and Symmetric. The differences between the Symmetric and Lowbetamax, very similar in terms of field quality, could be explained by the averaging effect of a different number of modules and the uncertainty of the method (for additional information refer to [9]).

TRANSITION TO INJECTION

An optics with $\beta^* > 5\,\mathrm{m}$ is required at injection where the transverse beam size is a four time larger. A set of transition optics should be found in order change the IR configuration from injection to collision. The quadrupole settings should smoothly change and the transition optics should keep the phase advance in order ease the procedure and accommodate the restriction in the power supply.

For the LHC the set of transition optics is hard to find because of the limitations in the maximum current of the magnets and limitations of mechanical aperture in the LSS. Without one these two limitations is very straightforward to find a solution because the number of parameters are larger than the number of constraints. In case of limitations of aperture, which translates in limitations of the maximum beta in some location, and limitations of quadrupole strengths, which translate in limitations of tunability (roughly proportional to the product βk), the parameters are not truly independent and the solution may or may not exist.

A preliminary study show that is possible to keep the phase advance of the insertion for a large range of β^* only for Lowbetamax and Symmetric.

	Compact	Modular	Lowbetamax	Symmetric	LHC
Sextupoles [%]	88,56	87,58	74,46	75,46	48,28
Beat. $\delta = 3 \cdot \cdot 10^{-4}$ [%]	40	40	30	30	10
Beat. $\delta = 8 \cdot \cdot 10^{-4}$ [%]	150	150	100	105	30

Table 3: Chromatic aberrations for the upgrade optics and the nominal LHC. The first row show the required strength of the arc sextupoles for compensating the first order chromaticity, while the last two rows present the off momentum beta beating for two different energy error.

	Compact	Modular	Lowbetamax	Symmetric	LHC
Full	16	11	14	12	12
Triplet only	22	17	14	12	
Triplet excluded	16	11	20	16	

Table 4: Minimum DA over 60 seeds without beam beam effect and field imperfections of D1 and D2. The second row and the third row show the DA excluding in addition all field imperfections but the triplet and the triplet respectively. The field quality for the triplets is estimated using the results showed in [2].

CROSSING SCHEME AND ANTISYMMETRY

The LHC optics present a certain degree of left-right symmetry with respect to the IP in the quadrupole polarity (opposite) and position. Nevertheless the quadrupole strengths don't follow the antisymmetry because the dispersion boundary conditions don't follow it. Anyway the nominal layout tries to force the antisymmetry, because it seems beneficial for finding smooth transitions (see [10]). In addition for the TOTEM experiment (see [11]) it is useful to have antisymmetric optics function up to Q6. In developing the optics for the upgrade, this strategy additional constraint, restrict the flexibility and the ability of finding optimized optics. It is not excluded that further optimization can recover the symmetry.

CONCLUSION

The development of four different optics showed he actual limitations and challenges for Phase 1 upgrade.

At this stage of the studies there are outstanding issues that need to be further investigated.

There are aperture bottleneck in D1, D2, Q4, Q5. The limitation in D1 is an avoidable and require a new design for the dipole. The limitations for D2, Q4, Q5 depends on the triplet layout. A further optimization can reduce the problem but on one hand the triplets have a limited number of free parameters to use and on the other hand the LSS is not flexible enough to accept all possible optics function that merely fulfill the aperture requirements. This limitation is more severe for the Compact and Modular options, while is presumably fixable for the symmetric option and barely acceptable for the Lowbetamax option.

The impact of the larger off momentum beta beat and the third order chromaticity need to studied. It is a global quantity and it may affect other LHC subsystem (e.g the collimation system).

The solution presented even though were designed to be as realistic as possible, represents an effort to study the possibilities and implication of several design criteria: gradient and aperture of the quadrupoles, number of modules, triplet or quadruplet design.

The analysis presented is not exhaustive. For a realistic design many refinements are need. In particular it is important to check whether the heat load and radiation damage levels are compatible with the new elements and redesign the final focus system for increasing the aperture margins and reserving the right locations for correctors and diagnostics (orbit corrector and BPM).

The results presented so far show that the Lowbetamax option show the best overall performance closely followed by the Symmetric option which offers a simpler tough less flexible design. Both options can be further optimized to gain aperture margins and represent an good starting point for the final design.

REFERENCES

[1] R. de Maria. Layout design for final focus systems and applications for the LHC interaction region upgrade. LHC-Report 1051, CERN, sep 2007.

[2] J. P. Koutchouk, L. Rossi, and E. Todesco. A Solution for Phase-one Upgrade of the LHC Low-beta Quadrupoles Based on Nb-Ti. lhc-project-report 1000, CERN, April 2007.

[3] O. Bruening, R. de Maria, and R. Ostojic. Low Gradient, Large Aperture IR Upgrade Options for the LHC compatible with Nb-Ti Magnet Technology. LHC-Report 1008, CERN, jun 2007.

[4] R. Assmann, F. Borgnolutti, C. Bracco, O. Brüning, U. Dorda, R. De Maria, S. Fartoukh, M. Giovannozzi, W. Herr, M. Meddahi, E. Todesco, R. Tomás, and F. Zimmermann. Comparative analysis of four optical layouts for the Phase 1 upgrade of the Large Hadron

Collider insertion regions. Technical report, CERN, Geneva.

[5] F. Borgnolutti and E. Todesco. Design issues in a 130mm aperture triplet. In *CARE-HHH IR07 Proceedings, Frascati*, oct 2007.

[6] S. Fartoukh. LSS magnet aperture requirements for the LHC insertion upgrade, a first estimate. Technical Report LHC-PROJECT-Report-1050, CERN, oct 2007.

[7] O. Bruening, P. Collier, P. Lebrun, S. Myers, R. Ostojic, J. Poole, and P. Proudlock. LHC Design Report. Technical Report CERN-2004-003, CERN, 2004.

[8] U. Dorda and F. Zimmermann. Beam-beam issues for 'phase 1' and 'phase 2'. In *CARE-HHH IR07 Proceedings, Frascati*, oct 2007.

[9] R. Tomas, M. Giovannozzi, and R. de Maria. Correction of mulitpolae field errors in insertion regions for the phase-1 LHC upgrade and dynamic aperture. In *CARE-HHH IR07 Proceedings, Frascati*, oct 2007.

[10] Oliver Sim Bruening. Optics Solutions in IR1 and IR5 for Ring-1 and Ring-2 of the LHC Version 6.0. Technical Report CERN-LHC-Project-Note-187, CERN, April 1999.

[11] K. Eggert. Total cross-section, elastic scattering and diffraction dissociation at the Large Hadron Collider at CERN: TOTEM Design Report. Cern-lhcc-2004-002, CERN, January 2004.

CORRECTION OF MULTIPOLAR FIELD ERRORS IN INSERTION REGIONS FOR THE PHASE 1 LHC UPGRADE AND DYNAMIC APERTURE

R. Tomás, M. Giovannozzi and R. de Maria, CERN, Geneva, Switzerland

Abstract

The Phase 1 upgrade of the LHC interaction regions aims at increasing the machine luminosity by reducing the beam size at the interaction point. This requires an in-depth review of the full insertion region layout and a large set of options have been proposed with conceptually different designs. This paper reports on a general approach for the compensation of the non-linear field errors of the insertion region magnets by means of dedicated correctors. The goal is to use the same correction approach for all the different layouts. The correction algorithm is based on the computation of the high orders of the polynomial transfer map using MAD-X and Polymorphic Tracking Code, while the actual performance of the method is estimated by computing the dynamic aperture of the layouts under study.

INTRODUCTION

The design of the interaction region (IR) of a circular collider is one the most critical issues for the machine performance. Many constraints should be satisfied at the same time and the parameter space to be studied is huge (see Refs. [1, 2] and references therein for an overview of the problem). The strong focusing required to increase the luminosity generates large values of the beta-function at the triplet quadrupoles. This in turns enhance the harmful effects of the magnets field quality on the beam dynamics. It is therefore, customary to foresee a system of non-linear corrector magnets to perform a quasi-local compensation of the non-linear aberrations. This is the case of the nominal LHC ring, for which corrector magnets are located in the Q_1, Q_2, and Q_3 quadrupoles, the latter including non-linear corrector elements.

The strategy for determining the strength of correctors was presented in Ref. [3] and is based on the compensation of those first-order resonance driving terms that were verified to be dangerous for the nominal LHC machine. In general, the proposed approach is based on a number of assumptions that are in general valid for the nominal LHC machine, but not necessarily true for the proposed upgrade scenarios [4,5], such as perfect antisymmetry of the IR optics between the two beams circulating in opposite directions. Indeed, some LHC upgrade options may not respect the antisymmetry of the IR optics between the two beams and the set of dangerous resonances might not be the same as for the nominal LHC or even be different among the LHC upgrade options. Furthermore, it might be advisable to use a method that should take into account all possible sources of non-linearities within the IR, such as the field quality of the separation dipoles and also collective beam effects like the long-range beam-beam interactions.

For these reasons a more general correction algorithm should be envisaged, thus allowing a direct and straightforward application to any of the upgrade options or, more generally, to any section of an accelerator. The propose method is based in the analysis of the non-linear transfer map a given section of a particle accelerator. The essential details about the non-linear effects of the elements comprised in the section of the machine under consideration are retained in the polynomial transfer map. For this reason the one-turn transfer map was proposed as an early indicator of single-particle instability with a reasonable correlation with the dynamic aperture [6–8].

In the next sections the proposed method is described and some applications to Phase 1 LHC upgrade layouts given.

MATHEMATICAL BACKGROUND

The transfer map between two locations of a beam line is expressed in the form

$$\vec{x}_f = \sum_{jklmn} \vec{X}_{jklmn}\, x_0^j\, p_{x0}^k\, y_0^l\, p_{y0}^m\, \delta_0^n, \qquad (1)$$

where $\vec{x}_f$ represents the vector of final coordinates $(x_f, p_{xf}, y_f, p_{yf}, \delta_f)$, the initial coordinates being represented with the zero subindex, and $\vec{X}_{jklmn}$ is the vector containing the map coefficients for the four phase-space coordinates and the momentum deviation δ, considered as a parameter. The MAD-X [9] program together with the Polymorphic Tracking Code (PTC) [10] provide the computation of the quantities $\vec{X}_{jklmn}$ up to any desired order.

To assess how much two maps, X and X' deviate from each other, the following quantity is defined:

$$\chi^2 = \sum_{jklmn} ||\vec{X}_{jklmn} - \vec{X}'_{jklmn}|| \qquad (2)$$

where $||\cdot||$ stands for the quadratic norm of the vector. To disentangle the contribution of the various orders to the global quantity χ^2, the partial sum χ_q^2 over the map coefficients of order q is defined, namely

$$\chi_q^2 = \sum_{j+k+l+m+n=q} ||\vec{X}_{jklmn} - \vec{X}'_{jklmn}|| \qquad (3)$$

so that

$$\chi^2 = \sum_q \chi_q^2. \qquad (4)$$

In principle, this definition could be used to introduce a weighting of the various orders, using a well-defined amplitude in phase space. This option is not considered in the applications described in this paper.

Furthermore, χ_q^2 is split into a chromatic $\chi_{q,c}^2$ and achromatic $\chi_{q,a}^2$ contribution, corresponding to

$$\chi_{q,a}^2 = \sum_{j+k+l+m=q} ||\vec{X}_{jklm0} - \vec{X}'_{jklm0}||. \qquad (5)$$

It is immediate to verify that $\chi_q^2 = \chi_{q,c}^2 + \chi_{q,a}^2$.

CORRECTION OF MULTIPOLAR ERRORS

Algorithm

The basic assumption is that the multipolar field errors of the IR magnets are available as the results of magnetic measurements. The ideal IR map X without errors is computed using MAD-X and PTC to the desired order and stored for later computations. Including the magnetic errors to the IR elements perturbs the ideal map. To cancel or compensate this perturbation, distributed multipolar correctors need to be located in the IR. The map including both the errors and the effect of the correctors will be indicated with X'. The corrector strength is determined by simply minimising χ_q^2 for these two maps. For efficiency, the minimisation is accomplished order-by-order (see, e.g., Ref. [11] for a description of the dependence of the various orders of the non-linear transfer map on the non-linear multipoles). In such an approach the sextupolar correctors are used to act on χ_2^2, the octupolar ones on χ_3^2, and so on.

The code MAPCLASS [12] already used in [13] has been extended to compute χ_q^2 from MAD-X output. The correction is achieved by the numerical minimisation of χ_q^2 using any of the existing algorithms in MAD-X for this purpose.

Performance evaluation

The evaluation of the performance of the method previously described is carried out using two of the three layouts proposed for the upgrade of the LHC insertions (see, e.g., Refs. [2, 4, 5, 14] for the details on the various configurations under consideration).

The field quality of the low-beta triplets is considered to follow the assumption reported in Ref. [15]. This implies that the various multiple components b_n, a_n given by

$$B_y + i\,B_x = 10^{-4}\,B_2 \sum_{n=2}^{\infty} (b_n + i\,a_n) \left(\frac{x + i\,y}{R_{ref}}\right)^{n-1}, \qquad (6)$$

where B_x, B_y represents the transverse components of the magnetic field, and R_{ref} the reference radius, scale down linearly with the reference radius, taken at a given fraction of the magnet aperture ϕ, according to [15]

$$\sigma(b_n, a_n; \alpha\,\phi, \alpha\,R_{ref}) = \frac{1}{\alpha}\sigma(b_n, a_n; \phi,\ R_{ref}). \qquad (7)$$

As a natural consequence, large-bore quadrupoles will feature a better field quality than smaller aperture ones. The multipolar components used for the simulations discussed in this paper are listed in Table 1.

An example of the order-by-order correction is shown in Fig. 1 for the so-called low $\beta_{\max}$ configuration [2, 5]. A total of sixty realisations of the LHC lattice are used in the computations. It is worthwhile stressing that even though the random errors are Gaussian-distributed with zero mean and sigma given by the values in Table 1 re-scaled to the appropriate value of the magnet aperture, the limited statistics used to draw the values for a single realisation (corresponding to 16 magnets) implies that in reality non-zero systematic errors are included in the simulations.

Table 1: Random part of the relative magnetic errors of the low-beta quadrupoles at 17 mm radius [16]. The components b_n and a_n stand for normal and skew multipolar errors, respectively.

Order	b_n $[10^{-4}]$	a_n $[10^{-4}]$
2	0.349431	0.477730
3	0.100570	0.309803
4	0.067294	0.062218
5	0.135565	0.057960
6	0.012633	0.016546
7	0.003812	0.014816
8	0.006825	0.003813
9	0.008446	0.003973

One corrector per IR side and per type (normal or skew component) are used. Different locations of the non-linear correctors can be used for the minimisation of χ_q^2. The configuration having the lowest χ_q^2 after correction is selected for additional studies (see next section). The difference between a non-optimised positioning and the best possible one is illustrated in Fig. 2. There, the results of the proposed correction scheme in the case of a symmetric configuration (see Refs. [2, 4, 14]) are shown. The configuration corresponding to the grey dots achieves slightly better corrections over the ensemble of realisations and therefore is selected for further studies.

DYNAMIC APERTURE COMPUTATION

Assessment of the non-linear correction algorithm

The main goal of the error compensation is to increase the domain in phase space where the motion is quasi-linear, thus improving the single-particle stability. It is customary to quantify the stability of single-particle motion using the concept of dynamic aperture (DA). The DA is defined as the minimum initial transverse amplitude becoming unstable beyond a given number N of turns. The standard protocol used to compute the DA for the LHC machine is

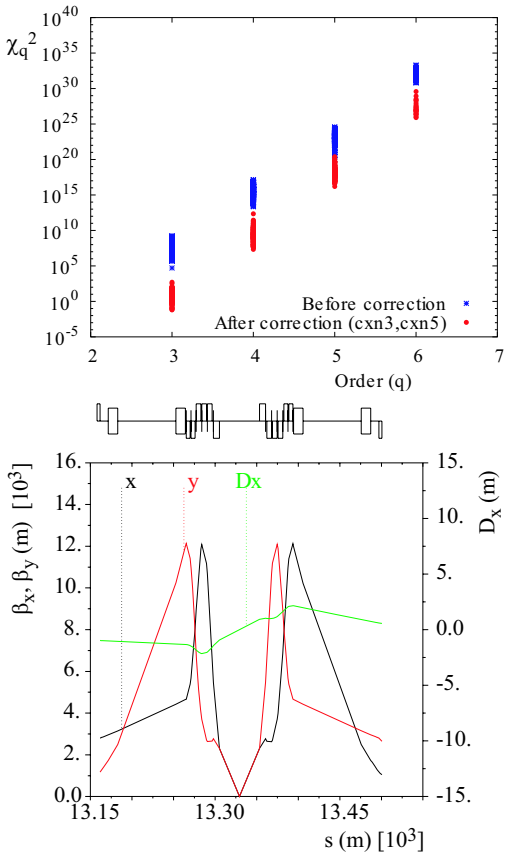

Figure 1: Evaluation of the various orders of χ_q^2 (upper plot) before (blue markers) and after (red markers) correction. Sixty realisations of the random magnetic errors are used. The layout is the low $\beta_{\max}$, whose optics is also reported (lower plot).

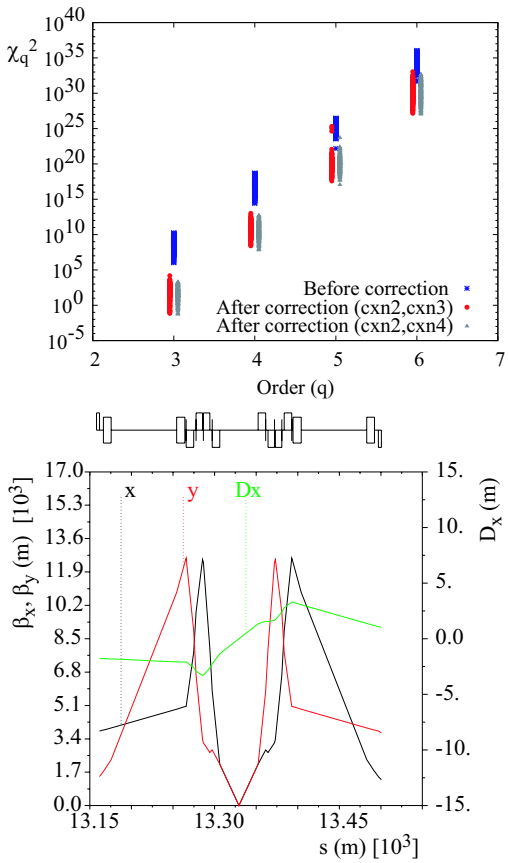

Figure 2: Evaluation of the various orders of χ_q^2 (upper plot) before (blue markers) and after (grey markers) correction. The red markers represent a non-optimised (in terms of correctors location) compensation scheme. Sixty realisations of the random magnetic errors are used. The layout is the symmetric one, whose optics is also reported (lower plot).

based on $N = 10^5$ and a sampling of the transverse phase space (x, y) via a polar grid of initial conditions of type $(\rho\cos\theta, 0, \rho\sin\theta, 0)$ with $\theta \in [0, \pi/2]$. In practise, five values for θ are used. The scan in ρ is such that a $2\,\sigma$ interval is covered with 30 initial conditions. The momentum offset is set to $3/4$ of the bucket height.

As far as the magnetic field errors used in the numerical simulations are concerned, the as-built configuration of the LHC is used. The information concerning the measured errors, as well as the actual slot allocation of the various magnets is taken into account in the numerical simulations. The errors on the results of the magnetic measurements are included in the numerical simulations by adding random errors to the various realisations of the LHC ring. On the other hand, the field quality of the low-beta triplets from Table 1 and the scaling law from Ref. [15] are used. It is worth mentioning that the layouts under studies are not finalised, yet. In particular, the details for the implementation of the separation dipoles D1 and D2 are not fixed. As a consequence, no estimate concerning their field quality was taken into account in the modelling of the LHC ring. As for the evaluation of the correction schemes, sixty realisations of the random multipolar errors in the triplets are used and the value of DA represents the minimum over the realisations. The accuracy of the numerical computation of the minimum DA is considered to be at the level of $\pm 0.5\sigma$.

In Fig. 3 the DA for the two LHC upgrade options, low β_{max} and symmetric, as a function of phase space angle is plotted with and without non-linear corrections schemes.

The correction algorithm proved to be particularly successful in the case of the symmetric layout. Indeed, for this configuration about $2.5\ \sigma$ are recovered thanks to the correction of the non-linear b_3 and b_6 errors.

The compensation in the case of the low β_{max} layout is less dramatic, allowing to recover $2.5\ \sigma$ for small angles, only. It is also important to stress that the baseline DA is not the same for the two layouts, as the low β_{max} is already well above $14.5\ \sigma$ without any correction. Furthermore, not only the optics is different for the options, but also the triplets' aperture. The first implies a different enhancement of the harmful effects of the triplets field

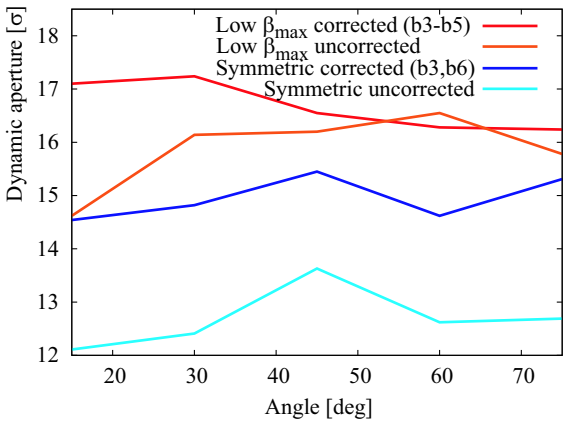

Figure 3: Comparison of the dynamic aperture for the so-called LHC upgrade layouts low β_{max} and symmetric with and without correction of the non-linear magnetic errors in the low-beta quadrupoles.

quality, while the latter has a direct impact on the actual field quality because of the scaling law [15]. It is clear that the DA for the low β_{max} is already well beyond the targets used for the design of the nominal LHC even without non-linear correctors. The situation for the symmetric option is slightly worse and a correction scheme might be envisaged.

Digression: Dynamic aperture vs. low-beta triplet aperture

A third layout proposed as a candidate for the LHC IR upgrade is the so-called compact [2, 5]. It features very large aperture triplet quadrupoles (150 mm diameter for Q_1 and 220 mm for Q_2 and Q_3). Thanks to the proposed scaling law, the field quality is excellent and the results DA is beyond 16 σ and hence does not require any correction scheme.

Nevertheless, a detailed study of the dependence of the dynamic aperture on the magnets aperture is carried out. The overall LHC model is the same as the one described in the previous sections, the main difference being the scan over the aperture of Q_1 and simultaneously over the apertures of Q_2 and Q_3. The optics is assumed to be constant, which implies that the configurations corresponding to larger magnets apertures than the nominal ones cannot be realised in practise.

The results are shown in Fig. 4. The minimum, average, and maximum (over the realisations) DA are shown for the two type of scans. The horizontal lines represent the asymptotic value of the DA and are obtained by using a huge (and unrealistic) value for the triplets aperture.

The dependence on the aperture of Q_1 is rather mild, because of the not too high value of the beta-function, and there exists a rather wide range of apertures for which the DA is almost constant. In particular for $\phi > 110$ mm the asymptotic value of the DA is reached. A constant drop of DA is observed for $\phi < 100$ mm and, in general, the three

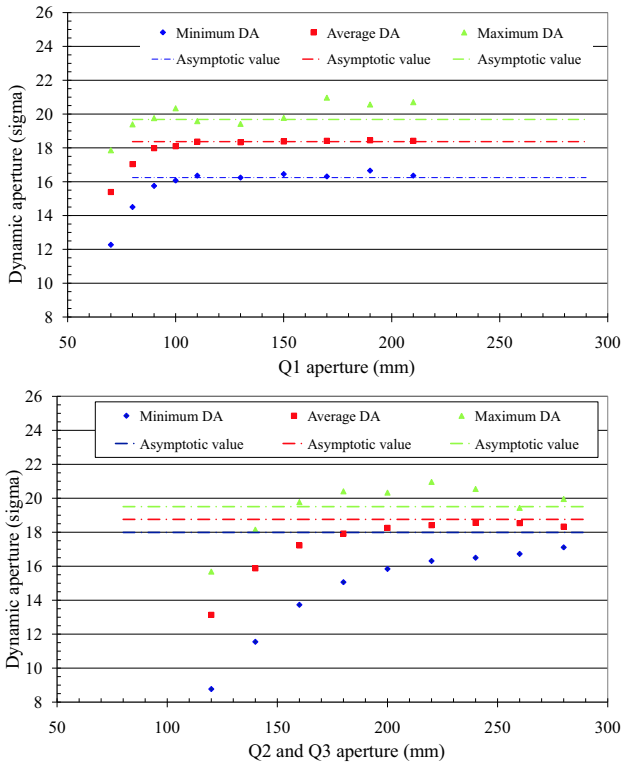

Figure 4: DA as a function of the low-beta quadrupoles aperture. The scan over the aperture of Q_1 is shown in the upper plot (nominal aperture 150 mm), while Q_2 and Q_3 are considered in the lower plot (nominal aperture 220 mm). The layout is the so-called compact one.

curves behave the same.

The dependence of DA on the Q_2 and Q_3 aperture is somewhat different. The asymptotic value is hardly reached for apertures larger than 250 mm and the DA drop with aperture is monotonic and smooth. The spread between the asymptotic values for minimum, average, and maximum DA is smaller than for the case of the scan over the aperture of Q_1.

As an example, the behaviour of the DA as a function of aperture is fit with two functions (exponential and power law) and the results are shown in Fig. 5. The difference between the asymptotic and the actual DA value is plotted as a function of the Q_2 and Q_3 aperture. The agreement between the fit functions and the simulation results is excellent, even though, for the time being no theoretical argument explains these results.

CONCLUSIONS

A general algorithm for the correction of multipolar errors in a given section of a circular accelerator has been developed. It is based on the computation and comparison of map coefficients obtained from standard accelerator codes such as MAD-X and PTC. The algorithm aims at minimising the difference between a target transfer map and the

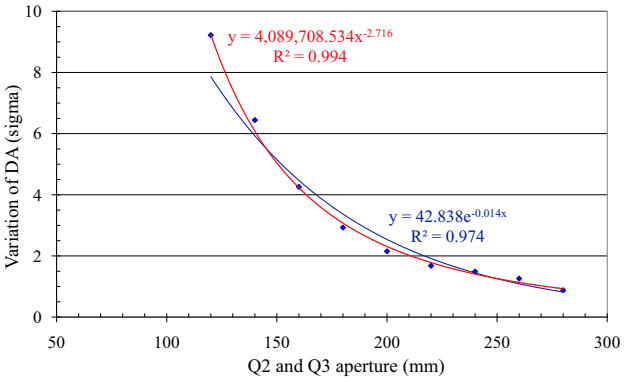

Figure 5: Behaviour of the minimum DA as a function of Q_2 and Q_3 aperture. Two types of fit functions are also shown.

actual one. Both order-by-order and global optimisation strategies are possible. Of course, the algorithm can be used also to optimise the location of the corrector elements. In its present form the non-linear magnetic field errors are the only source of non-linearities included in the transfer map. Nevertheless, other sources of non-linear effects in the transfer map could also be included in the correction algorithm, such as beam-beam kicks from long-range encounters. The efficiency of such an approach should be tested in practise with dedicated studies.

The correction algorithm was successfully tested on two layouts for the proposed IR upgrade of the LHC machine. The quality of the correction was also verified by means of numerical simulations aimed at computing the dynamic aperture. In the two cases under consideration a sizable increase of the dynamic aperture due to the correction scheme is observed.

In the numerical simulations used to evaluate the dynamic aperture a new scaling law for the magnetic field errors as a function of the low-beta quadrupoles aperture was used. The impact of such an assumption on the value of the dynamic aperture was assessed in details with a series of dedicated studies, where the triplets aperture is scanned. Smooth dependency of the dynamic aperture with respect to the magnets aperture is found, and exponential or power laws are fitted to the numerical data with very good agreement. These results could be used as an additional criterion for the definition of the required aperture of triplet quadrupoles. Indeed, one could derive the minimum aperture for which the dynamic aperture does not require any correction. Such a condition should then be taken into account together with the ones related to the needed beam aperture and energy deposition issues.

ACKNOWLEDGMENTS

Fruitful discussions with O. Brüning, S. Fartoukh, W. Herr, and E. Todesco are warmly acknowledged.

REFERENCES

[1] M. Giovannozzi, these proceedings.

[2] R. de Maria, these proceedings.

[3] O. Brüning, S. Fartouk, M. Giovannozzi, T. Risselada, "Dynamic aperture studies for the LHC separation dipoles', LHC project note 349, 2004.

[4] J.-P. Koutchouk, L. Rossi, E. Todesco, "A Solution for Phase-one Upgrade of the LHC Low-beta Quadrupoles Based on Nb-Ti", LHC Project Report 1000, 2007.

[5] O. Brüning, R. de Maria, R. Ostojic, "Low Gradient, Large Aperture IR Upgrade Options for the LHC compatible with Nb-Ti Magnet Technology", LHC Project Report 1008, 2007.

[6] M. Giovannozzi, W. Scandale, E. Todesco, "Prediction of long-term stability in large hadron colliders", Part. Accel. 56 195, 1996.

[7] M. Giovannozzi, E. Todesco, A. Bazzani and R. Bartolini, "PLATO: a program library for the analysis of nonlinear betatronic motion", Nucl. Instrum. and Methods A 388 1, 1997.

[8] M. Giovannozzi, W. Scandale and E. Todesco, "Dynamic aperture extrapolation in presence of tune modulation", Phys. Rev. E57 3432, 1998.

[9] H. Grote and F. Schmidt, "MAD-X - An Upgrade from MAD8", CERN-AB-2003-024, ABP.

[10] E. Forest, F. Schmidt and E. McIntosh, "Introduction to the Polymorphic Tracking Code", KEK Report 2002-3.

[11] A. Bazzani, G. Servizi, E. Todesco, G. Turchetti, "A normal form approach to the theory of nonlinear betatronic motion", CERN 94-02, 1994.

[12] R. Tomás, "MAPCLASS: A code to optimize high order aberrations", CERN-AB-Note-017 ABP, 2006.

[13] R. Tomás, "Nonlinear optimization of beam lines", Phys. Rev. ST Accel. Beams **9**, 081001 (2006).

[14] R. Assmann, F. Borgnolutti, C. Bracco, O. Brüning, U. Dorda, R. de Maria, S. Fartoukh, M. Giovannozzi, W. Herr, M. Meddahi, E. Todesco, R. Tomás, F. Zimmermann, "Comparative analysis of four optical layouts for the Phase 1 upgrade of the Large Hadron Collider insertion regions", LHC Project Report, in preparation.

[15] B. Bellesia, J.-P. Koutchouk, and E. Todesco, "Field quality in low-β superconducting quadrupoles and impact on the beam dynamics for the Large Hadron Collider upgrade", Phys. Rev. ST Accel. Beams **10**, 062401 (2007).

[16] E. Todesco, private communication.

Q0 Status *

E. Laface†, W. Scandale, CERN, Geneva, Switzerland,
C. Santoni, Université Blaise-Pascal, Clermont-Ferrand, France

Abstract

The Q0 scheme of the LHC insertion region is based on the introduction of a doublet of quadrupoles at 13 meters from IP. In this scenario the value of β^* can be reduced to 0.25 m with a moderate increase of the β function inside the inner triplet. We present here an optical layout, with the required magnets parameters such as gradients, lengths, positions and apertures. We also discuss in some details the tolerance on alignment and the energy deposition.

INTRODUCTION

One possible option for the LHC IR upgrade [1] is based on the introduction of two new quadrupoles inside the experimental devices, at 13 meters from IP.

The potential of this scenario, discussed in [2], is to reduce the quadratic growth of the β function, since the two new quadrupoles should introduce an oscillation of β between the IR triplet and the IP. Ideally, the modified shape of the β function should allow to interconnect the optics with $\beta^* = 0.25$ m in the IP-side to the optics with $\beta^* = 0.55$ m in the inner triplet side, as shown in Fig. 1.

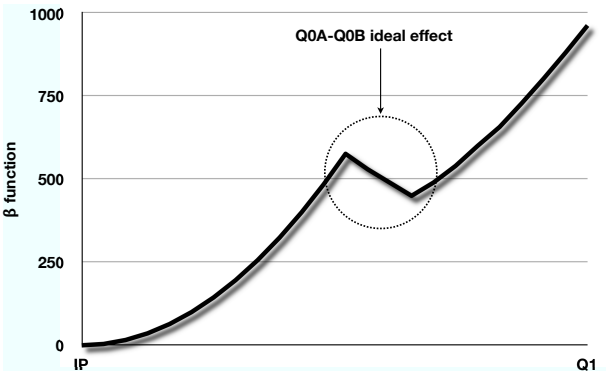

Figure 1: β shift with Q0.

This ideal behavior is the starting point for a new optimization of the interaction region based on five magnets, in which the two Q0s should reduce the quadratic increase of the β function and the inner triplet should provide the final focusing at the interaction point.

In this paper we present an IR layout compatible with LHC optics, in which $\beta^* = 0.25$ m, while the maximum β value is limited to 5820 m (Fig. 3).

* Work supported by the European Community-Research Infrasctructure Activity under the FP6 "Structuring the European Research Area" programme (CARE, contract RII3-CT-2003-506395).

† Emanuele.Laface@cern.ch

OPTICS LAYOUT

Geometry

The proposed configuration of the interaction region is represented in Fig. 2 and summarized in Table 1. The optical functions are shown in Fig. 3 for the first 70 meters from IP and in Fig. 4 for the whole interaction region.

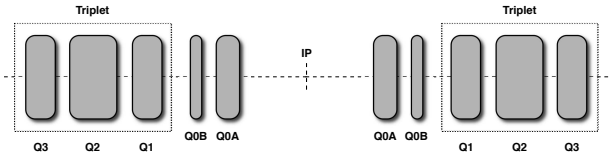

Figure 2: Q0 Layout.

Table 1: IR Layout.

Magnet	**L*** [m]	**Length** [m]	**Gradient** [T/m]
Q0A	13.0	7.2	240
Q0B	20.8	3.6	196
Q1	25.8	8.6	200
Q2	37.1	11.5	172
Q3	52.0	6.0	160

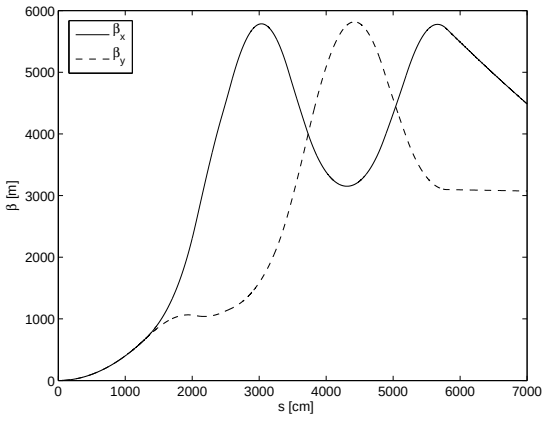

Figure 3: β function in the Q0-Triplet region when $\beta^* = 0.25$ m.

With the nominal LHC IR layout and with $\beta^* = 0.25$ m, the maximum value of β is of about 9700 m (Fig. 5 and Fig. 6).

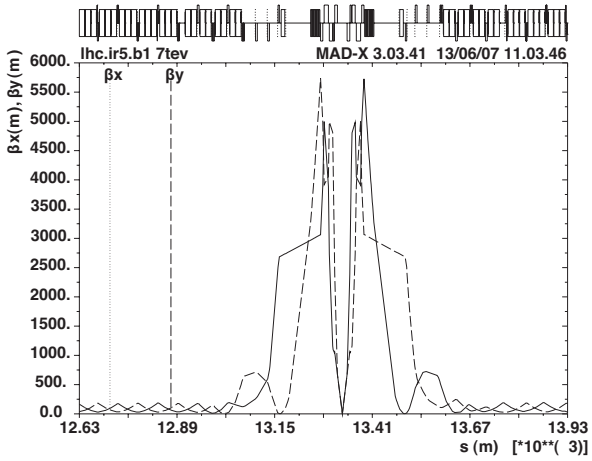

Figure 4: β function with Q0 layout and $\beta^* = 0.25$ m.

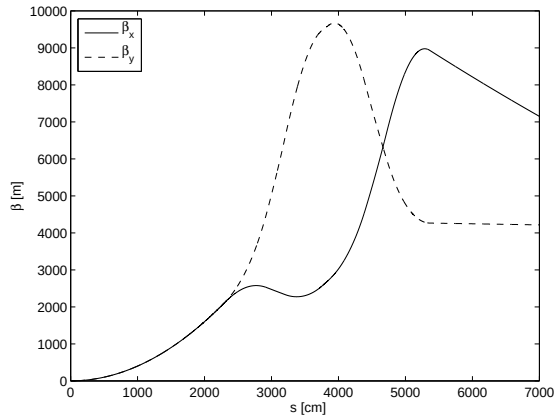

Figure 5: β function in the nominal layout when $\beta^* = 0.25$ m.

By using the Q0 doublet, the maximum value of β decreases to 5820 m. The increase of the initial luminosity is of a factor 2 with respect to the LHC optic at $\beta^* = 0.50$ either in a zero-crossing angle scheme [3] or when compensating the far beam-beam effect. Otherwise it is mandatory to increase the crossing angle according to [4] and [5]:

$$\theta_{\rm c} = \theta_{\rm c0}\sqrt{\frac{{\beta_0}^*}{\beta^*}}(6.5 + 3\sqrt{\frac{{\rm N_b n_b n_{LR}}}{{\rm N_{b0} n_{b0} n_{LR0}}}}) \qquad (1)$$

where $\rm n_b$ is the number of bunches, $\rm N_b$ is the number of protons for each bunch, $\rm n_{LR}$ is the number of long-range beam-beam collisions and the 0 index represents the nominal values. The crossing angle affects the luminosity, through the geometric factor, expressed by:

$$F \approx \frac{1}{\sqrt{1 + (\frac{\theta_{\rm c}\sigma_{\rm z}}{2\sigma^*})^2}} \qquad (2)$$

(where $\sigma_{\rm z}$ is the rms bunch length and σ^* is the transverse

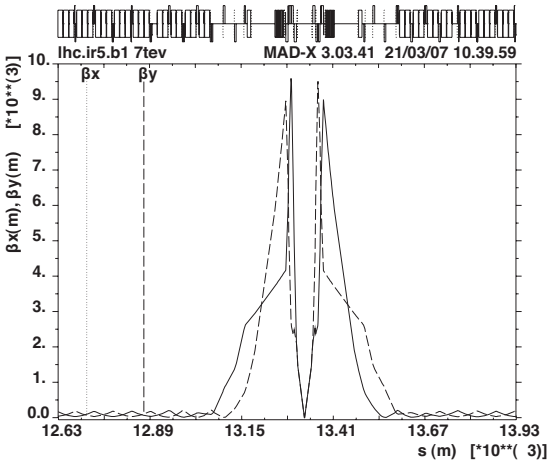

Figure 6: Nominal layout at $\beta^* = 0.25$ m.

rms beam size). The luminosity is given by:

$$L = F\frac{n_{\rm b}{\rm N_b}^2 {\rm f_{rev}}}{4\pi{\sigma^*}^2} \qquad (3)$$

where $\rm f_{rev}$ is the revolution frequency of the bunch. If the crossing angle is of 403 μrad, then the gain of the initial luminosity is of 1.75.

Aperture

The minimum value of the quadrupole aperture $\rm D_{min}$ is estimated by means of the formula [6]:

$${\rm D_{min}} > 1.1\cdot(10+2\cdot 9)\sigma + 2\cdot({\rm d} + 3\,{\rm mm} + 1.6\,{\rm mm}) \quad (4)$$

with a beam envelope of 9 σ, a beam separation of 10 σ, a β-beating of 20%, a peak orbit excursion of 3 mm, and a mechanical tolerance of 1.6 mm. The parameters depending on β are the rms beam radius σ and the spurious dispersion orbit $\rm d$. The values for beta function, the apertures and the peak field are summarized in Table 2.

Table 2: Magnet apertures and peak field.

Magnet	β Max [m]	$\rm D_{min}$ [mm]	Peak field [T]
Q0A	2300	60	7.2
Q0B	4300	72	7.1
Q1	5780	80	8.0
Q2	5820	80	6.9
Q3	5770	80	6.4

The required integrated gradients may be reached using $\rm NbTi$ superconductor technology or with $\rm Nb_3Sn$ but with an higher margin for the energy deposition. In an further optimized solution should be possible to decrease the gradient of Q1 increasing the Q3 with minor changes into the β function. It should also be possible to have the same gradients for the five magnets (Q0A-Q3) saving the number of power supply.

Detuning

The injection optics corresponds to a β^* of 5 m. The corresponding β function along the IR is shown in Fig. 7.

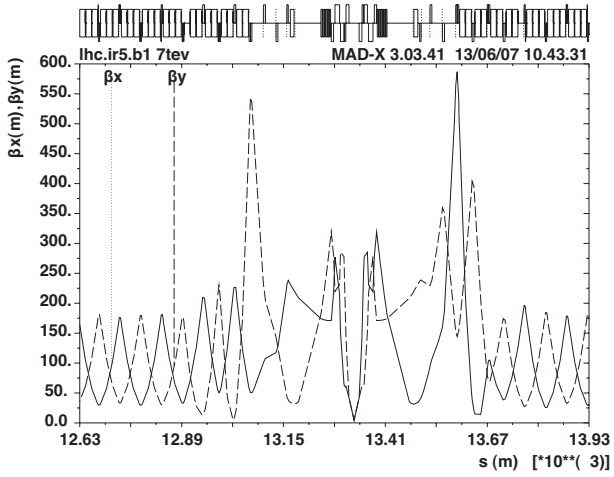

Figure 7: β function at injection.

The transition between injection and collision is performed by varying the gradients of Q4-Q11 as shown in Fig. 8. In a more careful optimization, polarity changes should be prevented. Note that, during the detuning, the gradients of Q0-Q3 remain unchanged.

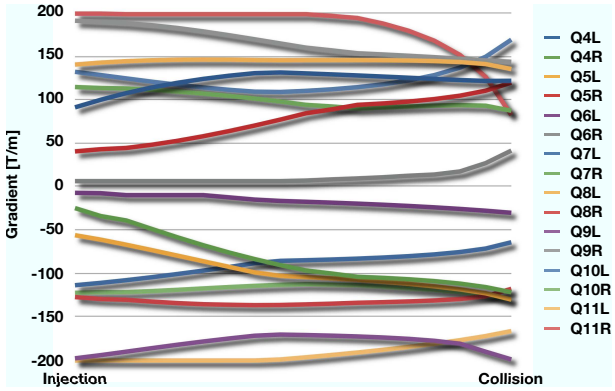

Figure 8: Q4-Q11 gradients from injection to collision.

MISALIGNMENTS

Following the arguments in [7] and [8] it is possible to estimate the misalignment tolerance of Q0A and Q0B. We have to consider two cases, one in which there is a relative misalignment in between Q0A and Q0B, the other in which Q0A-Q0B are in a rigid structure and misaligned with respect to the inner triplet.

In thin lens approximation, the shift $\delta_x(s)$ of the closed orbit, resulting from quadrupole displacements ΔX_{Q_i}, is given by:

$$\delta_x(s) = \xi \left[\sum_i \left(\theta \sqrt{\beta_x} \right)_i \cos\left(\pi Q_x - |\Delta\mu_i|\right) \right] \qquad (5)$$

where $\theta_i = K_i l_i \Delta X_{Q_i}$ is the deflection angle of the dipolar component of the misaligned magnet Q_i, $\Delta\mu_i = \mu_x(s) - \mu_x(s_i)$, Q_x is the tune, and the ξ parameter is $\frac{\sqrt{\beta_x(s)}}{2\sin(\pi Q_x)}$.

Note that the sign of $\delta_x(s)$ depends on two factor: the beam and the quadrupole. A positive dipolar component for beam 1 corresponds to a negative one for beam 2. An alignment error in the shared region creates a different effect respect to a misalignment in the not-shared sequence. On the other hand, if the Q0A and Q0B magnets move in phase, the kicks of the quadrupoles tend to be compensate since the positive dipolar component for the focusing magnet corresponds to a negative dipolar component for the defocusing magnet. This is why, quadrupoles with opposite gradients in a rigid structure, tend to compensate the misalignment error of the structure itself.

A numerical estimation of $\delta_x(s)$ induced by Q0A misalignment can be performed using $Q_x = 64.31$, $K = 0.01027\ \mathrm{m}^{-2}$, $l = 7.2$ m, $\beta_x = 2300$ m and $|\mu_x(s) - \mu_x(s_i)| = \frac{\pi}{2}$. In this case $\delta_x(s) \approx 0.825\sqrt{\beta_x(s)}\Delta X_{Q_x}$ that means a closed orbit error of 1.5 mm for a displacement of 50μm.

For Q0B one should use $K = -0.0084\ \mathrm{m}^{-2}$, $l = 3.6$ m, $\beta_x = 4300$ m, $Q_x = 64.31$ and $|\mu_x(s) - \mu_x(s_i)| = \frac{\pi}{2}$. Then one has $\delta_x(s) \approx -0.459\sqrt{\beta_x(s)}\Delta X_{Q_x}$ and a closed orbit error of 0.8 mm for a misalignment of 50μm.

This displacements of the orbits is disruptive for the luminosity: a 7.5μm of counter-phase misalignment decrease the luminosity of 10%. It's evident that a system of correctors is mandatory to compensate this kind of effects.

If the Q0 doublet is mounted in a rigid structure, the closed orbit error induced by a misalignment of the structure itself is compensated to a large extent and the alignment tolerance becomes of some hundreds of μm.

ENERGY DEPOSITION

A preliminary evaluation of the energy deposition in Q0A and Q0B magnet is performed using the design of Fig. 9

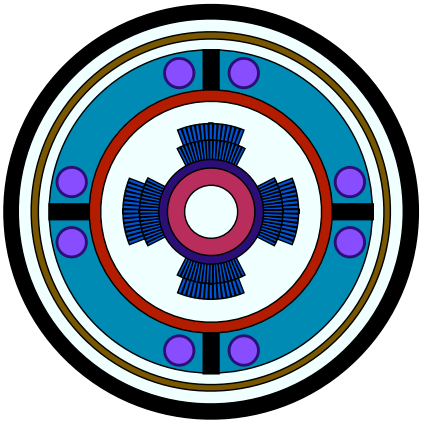

Figure 9: Q0 design.

and the regions inside the magnet are schematized as illus-

trated in Fig. 10.

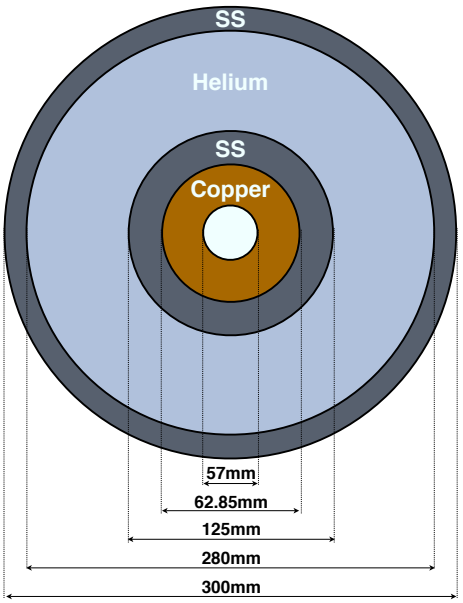

Figure 10: Q0 structure for the FLUKA model.

Here the aperture of the magnet is 57mm because is based on a preliminary model of Q0A magnet. The magnetic field map is obtained from a 2D ROXIE model and the total energy absorbed by this geometry is evaluated in a simulation with the FLUKA code. The results of the simulation is in Fig. 11 for the Q0A and in Fig. 12 for the Q0B.

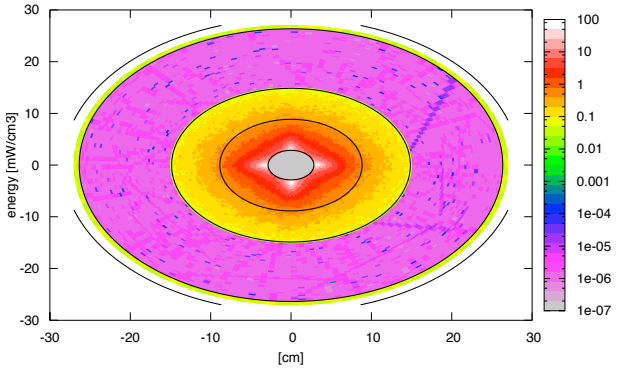

Figure 11: Total energy absorbed by Q0A.

For this simulation was used a luminosity of 10^{35} events per second per cm^2 and a 1 meter long TAS in front of Q0A.

The power on the magnets is 106 W (14.7 W/m) for Q0A and 42.5 W (11 W/m) for Q0B. These powers exceeds the capabilities of the cryogenic system that can extract at most ~ 10 W/m in ideal conditions. Some solutions can be evaluated to reduce the energy deposition as proposed in [9].

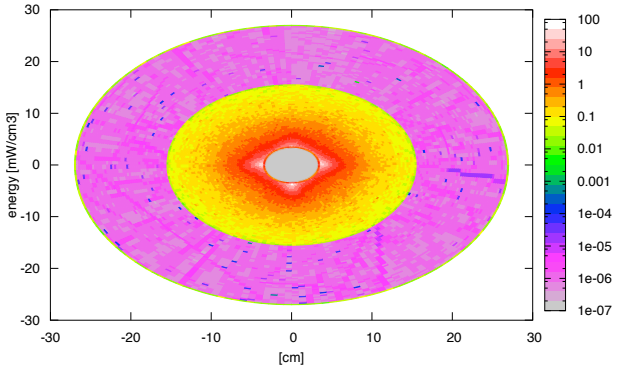

Figure 12: Total energy absorbed by Q0B.

CONCLUSIONS

The Q0 layout is rapidly evolving from the original idea proposed in [2] towards a full integration into the LHC nominal optic (v6.5). The optics proposed in this paper requires a Q0A quadrupole with a gradient of 240 T/m, just compatible with NbTi technology.

Misalignment tolerances for Q0A and Q0B are similar to those required for the inner triplet; it's reasonable to think that the same system of correctors used in the triplet can be applied for Q0A-Q0B.

The energy deposition is an issue that must be fully explore to propose reasonable solutions compatibles with a system of energy extraction in a limited volume such as inside the detector.

REFERENCES

[1] F. Zimmermann, "LHC Upgrade Scenarios", Proceedings of PAC 2007, Albuquerque, New Mexico, USA.

[2] E. Laface et al., "Interaction region with slim quadrupoles", Proceedings of EPAC 2006, Edinburgh, United Kingdom.

[3] J.-P. Koutchouk and G. Sterbini, "An early beam separation scheme for the LHC", Proceedings of EPAC 2006, Edinburgh, United Kingdom.

[4] Y. Papaphilippou and F. Zimmermann, "Weak-strong beam-beam simulations for the LHC", Proceedings of LHC99, Workshop on beam-beam effects, CERN-SL-99-039 AP p. 103,1999.

[5] Y. Papaphilippou and F. Zimmermann, "Estimates of Diffusion due to Longe-range Beam-beam Interactions", Phys. Rev. Special Topics Accel. Beams 5:074001, 2002.

[6] F. Ruggiero et al., "Performance limits and IR design of a possible LHC luminosity upgrade based on *NbTi* SC magnet technology", Proceedings of EPAC 2004, Lucerne, Switzerland, p. 608.

[7] S.Weisz, "Alignment of the low-β quadrupoles", LHC Project Note 59, CERN, Switzerland.

[8] T.Sen, "Alignment Tolerances of IR Quadrupoles in the LHC", FERMILAB-Conf-99/304, Batavia, Illinois, USA.

[9] E. Wildner "Are large aperture NbTi magnets compatible with 1e35?", Proceedings of LUMI 2007 Workshop, Frascati, Italy.

ENERGY DEPOSITION IN THE TRIPLET AND TAS ISSUES *

F. Broggi#, INFN-LASA, Milan, Italy

Abstract

Energy and power deposition in the low-beta insertion magnets may be the limiting factor in the choiche and/or performance for luminosity upgrade configuration for LHC. In this paper, after a general review of the problem about the type and properties of the secondary particles, the effect of the Target Secondary Absorber (TAS), for different distance l* of the insertion from the Interaction Point (I.P.) in various configurations is reported. Then the effect of the magnetic sequence of the quadrupoles for the two crossing plane, horizontal and vertical (H,V) is evaluated. Moreover the effect of the magnetic field of the solenoid is computed. All theese parametric studies tend to have a scaling law of the energy deposition in the insertion magnets vs. all the parametrs involved.

INTRODUCTION

The evaluation of the energy and power deposition in the triplet magnet is a key point in the performance of an LHC luminosity upgrade scenario. As a matter of fact the power deposed scales with the luminosity and the beam dynamics of the secondary particles may differ significantly from one configuration to another. The effect of the various elements and parameters involved must be carefully evaluated, in order to have a feeling of the relative importance of the parameters and try to obtain a scaling law of the power deposition as a function of all the parameters. The energy deposition in the insertion is computed with the FLUKA [1][2] montecarlo code.

This paper is extracted from a talk given at the workshop CARE-HHH-APD IR'07, hold in Frascati, November 2007, (see [3] for more and larger plots), and summarize many studies performed in the last year, after the analogous workshop hold in Valencia in October 2006; here only the main results are reported, corresponding reference are indicated for detailed results plots and discussion.

It is worth noting that the values of power deposition and their location must not be considered as real and referred as an actual power deposition in the tripled once the upgrade configuration is adopted.

The values have only a relative meaning, just to qualitatively evaluate the effects of the parameters involved in the problem.

In order to have an actual situation with reliable values, all the parameters must be taken into account, for example the beam pipe thickness and shape (in the actual situation it is designed and optimized in order to avoid backscattering to the detector), the presence of valves and vacuum pumps, whose effect may be locally important.

To this aim the study of the actual LHC layout (version 6.5) has been separately performed [4].

SECONDARIES

1300 p-p 7 TeV events, as from DTUJET[5] event generator, are used as source events, the particles realized (secondaries) are then tracked along the insertion magnetic structure and treated by FLUKA as soon as they interact with the line elements. The 7 TeV p-p interaction type are the inelastic scattering, the single diffractive and the elastic scattering, the corresponding cross sections are 60 mb, 12 mb and 40 mb respectively. For this study only the inelastic scattering and single diffractive events are important, giving a cross section of 72 mb. In order to have a safety factor, 80 mb will be considered. The most numerous (75%) particles produced are pions (27% of the total particles are π^0), about 82% of the energy is carried by pions and protons and neutrons, while protons and neutrons carry the highest specific energy (about 980 GeV/part for protons and about 600 GeV/part for the neutrons).

The pseudorapidity distribution of the secondary particles versus the energy, (Fig.1) shows many particles

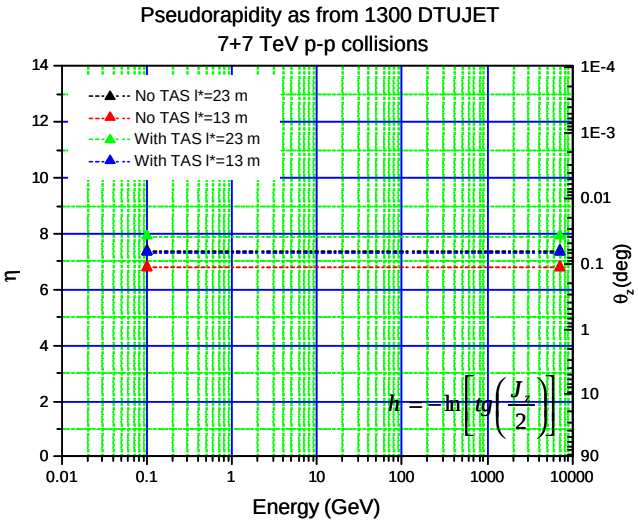

Figure 1: Pseudorapidity of the secondary particles, the marked lines show the pseudorapidity cuts correponding to different angular acceptance with or without the TAS.

with low energy and high transverse momentum (that will be absorbed by the detector and absorbed or degraded by the beam pipe). The particles inside the angular acceptance of the beam pipe/TAS (the ones lying above the marked lines) are the most energetic and can depose their energy in the quadrupoles.

Because of this pseudorapidity distribution the total energy impinging on a triplet element decrease as the element approach the IP. As a matter of fact the contribution to the energy deposition can be splitted into

Work performed in the frame of the the FLUKA collaboration with some CARE support
francesco.broggi@mi.infn.it : francesco.broggi@cern.ch

two terms, the energy impinging on the internal surface and the energy impinging on the front one. Approaching the IP, the energy impinging on the front surface decreases, while the one on the internal surface increases, leading to a decrease of the total energy hitting the element as shown in Fig. 2.

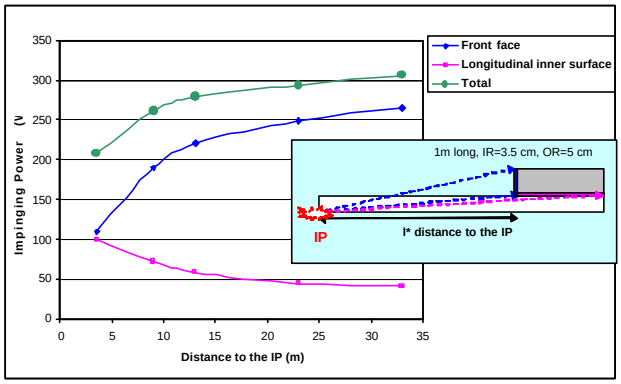

Figure 2: Energy impinging vs the distance from IP.

The decreasing/increasing of the energy depends on the aspect ratio of the element; for typical magnet geometry the above results can be applied.

The power carried by one 7 TeV beam is about 7760 W (with a luminosity $L=8.64 \times 10^{34}$ cm^{2} s^{-1}) of which about 60% is carried by charged particles, the energy deposition mechanism is mainly due to electromagnetic showers (about 73%) (see the high amount of π^{0}, as told in the previous section) and ionisation by heavy charged particles (about 15%).

TAS AND ITS EFFECTS

The main functions of the TAS are the reduction of the angular acceptance toward the insertion magnets, and to shield the first quadrupole.

Previous parametric studies about the energy deposition in the triplet vs. l* [6] showed that

- The highest peak power deposition occurs in Q2a (the second quadrupole),
- This peak power deposition is almost constant for l* variations between 13 to 23 m,
- The power deposed into the TAS is almost constant for the l* variations considered.
- The TAS affects only the total power deposed into Q1, having negligible effect on the peak power in it.

This facts and other studies [7] demostrate that the TAS must not be considered as a passive tool but an actual part of the insertion whose effect must be carefully evaluated.

Here the studies performed to evaluate the TAS effect were done for l*=23 m, $L=8.64 \times 10^{34}$ cm^{2} s^{-1} and quadrupole aperture of 100 mm. The cases studied were:

- NO TAS at all
- Adaped TAS (aperture of 20 mm).
- External front shielding of Q1 without interfering with the beam pipe

The results were compared with the "nominal" configurations of TAS opening of 17 mm.

The results showed that the TAS does not affect the maximum peak power in the front part of Q1 (as shown in slide n°11 of the presentation related to this talk) [3], the main effect is in a more azimuthally spreaded power distribution in the front part of Q1(slide 12 [3]).

In this slide the last case is not reported because the external shield only affects the total power deposition in Q1 and only in it.

The shielding effect of the front absorber on the peak power in the front part of Q1 can be seen in slide 12 [3].

The absolute maximum of the peak power, occuring at the front of the second quadrupole, is unaffected by the TAS, while the maximum peak power in Q1, occuring at its end is affected by the TAS (slide 13 [3]).

QUADRUPOLE FIELD SEQUENCE

The quadrupole field of the triplet, according to the usual convention for LHC is FDDF, but some upgrading scenarios can forsee a DFFD sequence. This fact together with the considerations that the crossing planes for IP1 (ATLAS experiment) is vertical (V) while for IP5 (CMS experiment) is horizontal (H), induced to investigate possible correlations between the quad sequence and crossing plane.

The results (as from slides 18 and 19 for [3]) show a symmetry between DFFD_H with FDDF_V and DFFD_V with FDDF_H. If the peak power is considered (slide 19[3]) the maximum of the deposition does not occur at the same longitudinal position, and the value of the maximum differs for the different configuration. The case FDDF_H (CMS) is less critic showing a lower peak power deposition, almost half than in FDDF_V).

DETECTOR SOLENOID FIELD EFFECT

The two high luminosity experiment (ATLAS and CMS) have different detector solenoid field and dimension, CMS has a peak value of 4 T while ATLAS have 2 T (see slide 20 [3] for the geometric charateristics).

The effect of this field on the power deposition in the triplet has been evaluated, (as shown in slide 20,21 and 22[3]) the power deposition in the triplet does not depend on magnetic field of the solenoid.

CONCLUSIONS AND PERSPECTIVES

Many parameters affecting the power deposition in the triplet have been investigated. The TAS is effective in shielding the first quadrupole, but has negligible effect on the others and on the peak power levels. The crossing plane influence the actual FDDF layout, being more critical for the ATLAS experiment (V plane).

The detector solenoid field has no effect on the triplet.

Further studies are necessary in order to get a scaling law of the power deposition, by varying the various parameters involved, i.e. the aperture of the quadrupoles,

their material composition and technology (NbTi or Nb_3Sn), the quadrupole gradient, the crossing angle.

The next step in the study will be the investigation of the quadrupole aperture effect.

All the studies reported have a continuous feedback and comparison with similar studies performed at FERMILAB performed with the MARS code, in particular a comparison of the two codes has been carried out using the same simplified IP5 model (considering only the first quadrupole) and parameters, with good agreement [8].

REFERENCES

[1] A.Fasso`, A.Ferrari, J.Ranft, and P.R.Sala, "FLUKA: a multi-particle transport code", CERN-2005-10 (2005), INFN/TC_05/11, SLAC-R-773.

[2] A.Fasso`, A.Ferrari, S.Roesler, P.R.Sala, G.Battistoni, F.Cerutti, E.Gadioli, M.V.Garzelli, F.Ballarini, A.Ottolenghi, A..Empl and J.Ranft, "The physics models of FLUKA: status and recent developments", Computing in High Energy and Nuclear Physics 2003 Conference (CHEP2003), La Jolla, CA, USA, March 24-28, 2003, (paper MOMT005), eConf C0303241 (2003), arXiv:hep-ph/0306267.

[3] F.Broggi, http://indico.cern.ch/getFile.py/access?contribId=21&sessionId=4&resId=0&materialId=slides&confId=19477.

[4] C. Hoa, F. Broggi, J-P. Koutchouck, G. Sterbini, F. Cerutti, E. Wildner, "Parametric Study of Heat Deposition from Collision Debris into the Insertion Superconducting Magnet for the LHC Luminosity Upgrade", PAC 2007 Conference, June 25-29, Albuquerque, New Mexico, USA.

[5] P.Aurenche et al. "DTUJET-93", Computer Physics Comm., 83, 107,(1994).

[6] F.Broggi, "Energy Deposition in the LHC Triplet Versus Distance to the Interaction Point", "3rd CARE-HHH-APD Workshop LHC-LUMI-06 Towards a Roadmap for the Upgrade of the CERN & GSI Accelerator Complex', 16-20 October 2006, Valencia, Spain.available at http://indico.cern.ch/contributionDisplay.py?contribId=67&sessionId=6&confId=4777

[7] E.Wildner, AT-MCS Note 2007-0.

[8] C.Hoa, http://indico.cern.ch/getFile.py/access?contribId=21&sessionId=4&resId=3&materialId=slides&confId=19477

ARE LARGE-APERTURE NbTi MAGNETS COMPATIBLE WITH 1E35?

E.Wildner, C.Hoa, E.Laface, G.Sterbini, CERN, Geneva, Switzerland

Abstract

To protect magnets in the insertion region, we have some degrees of freedom to use for optimal performance. Aperture, distance from the IP, the length of the magnets and the design of absorption systems are important parameters for the optimization. We look exclusively here at the effects of the collision debris, which give the major contribution to the heat deposition in the insertion magnets. To answer the challenging question in the title of this contribution, the approach was to use the baseline upgrade scenario for phase 1 and simply imagine higher particle fluxes from the higher luminosity (no change in optics). From this, a simple approach of magnet shielding using a liner in the cold bore tube gave us the answer: NbTi technology may be compatible with a luminosity of 10^{35}. This gives also the interesting possibility to extract heat from this liner at a higher cryogenic temperature. However the final demonstration needs a detailed model.

We have also made some parameter variations (crossing angle, TAS aperture) and checked the Q0 upgrade scenario concerning deposited heat. The effect of a D0 magnet on heat deposition in the IR has also been evaluated.

THE PHASE I UPGRADE SCENARIO

Two scenarios for the upgrade phase I have been studied, the first is the "symmetric, large aperture layout" [1] and one of the proposals in [2], the "compact, low gradient final focus system". The reason for taking this latter solution from [2] is to see the effect of the very large apertures. For the latter we have calculated two cases, the one proposed in the report and a second option where the length of the available LHC cable has been taken into account for the cross section design. The layout dimensions are shown in figures 1 and 2 and the magnets are described in table Table 1.

Figure 1: The Symmetric layout. The magnets have two cable layers. The cylinder to the left represents the TAS.

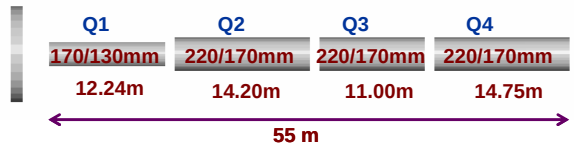

Figure 2: The Compact1 and Compact2 layouts. The Compact2 one has the largest aperture and only one cable layer.

Table 1: Magnet data

Magnet	MQCX	IRQB	IRQA	IRQF	IRQE
Layaout	Symm	Comp1	Comp1	Comp2	Comp2
Position	All	Q1	Q2-Q4	Q1	Q2-Q4
Gradient [T/m]	120	91.5	68.3	91.5	68.3
Aperture [mm]	130	170	220	130	170
Peak Field [T]	8.7	8.6	8.4	6.8	6.8
Layers	2	2	2	1	1

The quadrupole field maps have been calculated over 27 cm radius of the cold mass (value coming from the wanted grid of the field-map combined with the output data volume possibilities from field calculation software, for the time being) , which has been taken as the outer radius of the cold-mass. This means that we have to take into consideration that the total deposited heat in the structure may be larger for a larger volume of the cold mass. For comparisons and at this stage of the study this is good enough.

The collars have been modelled as aluminium with the idea to deposit energy far from the coils. For the energy in the coils this has minor impact and in future simulations we will replace aluminium with stainless steel in the collars for mechanical reasons.

The models contain cable insulation and cold bore insulation and this will be of importance in particular when the effects of irradiation will be simulated.

The parameters for the optics are, for all layouts, a betastar of 0.25 m and a vertical crossing angle of 220 micro radians. The collision points are simply modelled using Gaussian smearing of the collision points corresponding to the beam size and the bunch length.

6000 particles have been used for the Compact1 and Compact 2 models and 10000 for the Symmetric. This choice was only made from time constraints to finish the studies timely. For this preliminary study, analysis shows that the choice of a relatively small number of particles gives a good idea of the situation and refined studies will use sufficient number of particles to ensure less than 5 % statistical errors.

The TAS (Target Absorber for Secondaries) opening has been calculated using the formula

$$D_{\min} = 1.1 \cdot (9 + 2 \cdot 10)\sigma + 2(d + 3mm) + 2 \cdot 1.6mm$$

where the beam size is 1 σ, the beam separation 10 σ, d is the spurious dispersion orbit. The orbit excursion is 3 mm and mechanical tolerances have been taken as 1.6 mm. The factor 1.1 is the contingency for the beta-beating. For our case we used the value of 41 mm.

The opening of the TAS should be small to protect the magnet but sufficiently large not to intercept the beam. The efficiency of the TAS depends on the distance to the IP and of the free space available. Simulations of several insertion layouts show the TAS essentially protects the first 20 cm of the first quadrupole behind the TAS.

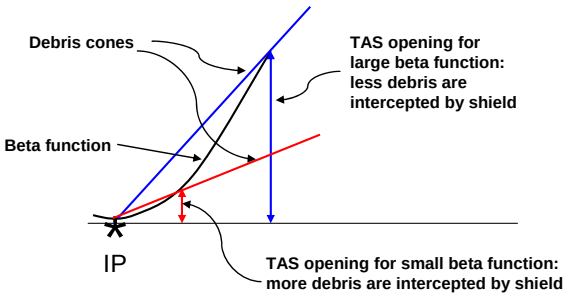

Figure 3: Illustration of important parameters for the TAS: For the case above: If he TAS is placed close to the IP where the beta-function is smaller (smaller beam size) then the opening of the TAS can be smaller.

RESULTS FROM THE CASE STUDIES

It is important to score the results from the simulations to correspond to the use of the information. We distinguish 3 different important quantities to be evaluated:

- Energy deposited in the cable (peak heat deposition)
  We make the binning for the scoring so that it corresponds to a maximum volume of equilibrium for the heat transport (cable transverse size, with a length of, in our case, 10 cm, which should correspond to the twist pitch of the cable). This is important to evaluate to see if there is a risk for quench.
- Total power deposited in the magnet
  It is important to know the volume of the magnet (the model has to be realistic) to be able to evaluate how much power has to be evacuated from the magnet structure.
- The power deposited per meter of magnet (a general overall estimate)

The results, calculated with FLUKA ([3],[4]), for the luminosity value of 2 10^{34} (corresponding to phase I) can be seen in Figure 4, the peak heat deposition along the magnets. First we can see that the 3 scenarios are similar, the largest aperture solution has the lowest heat deposition. We also see that there is an evident build-up in the first quadrupole. This build-up, including the part of the debris cone in between the two first quadrupoles seems to cause an important deposition peak on the front face of the second quadrupole. We can also see, that our present recommended limit of 4.3 mW/cm^3 (the quench limit/ 3) is exceeded.

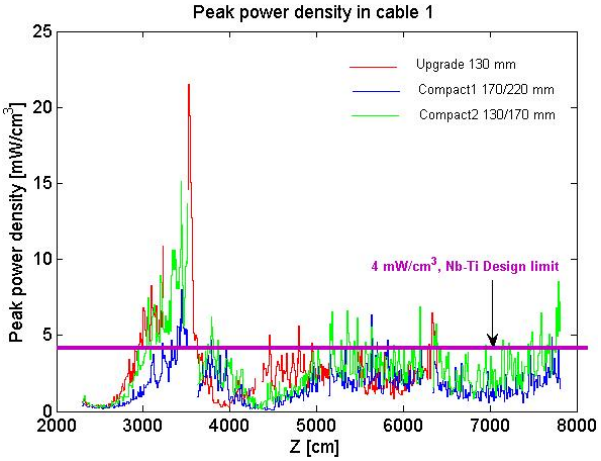

Figure 4: The peak heat deposition along the magnets in the inner triplet. The peak limit 4.3 mW/cm^3 is exceeded. The largest aperture solution is the best ("Compact 2").

In Figure 5 we see the total energy deposited in the triplet magnets. The "symmetric" solution has two times higher energy deposition than the other calculated upgrade scenarios, for magnets Q2a and Q3.

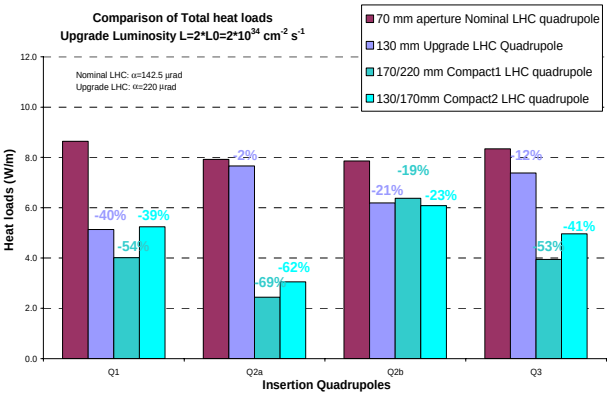

Figure 5: Total energy deposited in the triplet magnets. The 130 mm aperture solution ("Symmetric") has two times higher energy deposition than the other calculated upgrade scenarios for magnets Q2a and Q3.

Q0 OPTION

The Q0 option is described in [5]. The basic idea is to break the beta-function in a way that, in the triplet, we will have smaller beam-size which means smaller apertures. The layout is shown in Figure 6 and the magnet and optics parameters in Table 1 and in Table 2. The Q0 is close to the interaction point. This means less deposited

heat in the first magnets due to the fact that debris from the collision that contribute less to the deposited energy are intercepted at larger angles with respect to the magnet axes [6]. The energy deposition in the Q0 magnets and in the following triplet has been evaluated.

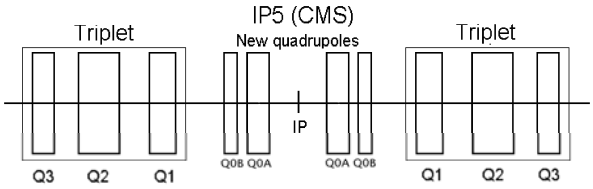

Figure 6: Q0 layout basic layout.

TABLE 1
MAGNET DATA FOR THE Q0 LAYOUT.

Magnet	L*[m]	Length [m]	Gradient [T/m]
Q0A	13.0	7.2	240
Q0B	20.8	3.6	196
Q1	25.8	8.6	200
Q2	37.1	11.5	172
Q3	52.0	6.0	160

TABLE 2
MAXIMUM BETA FUNCTION AND APERTURE IN MAGNETS FOR THE Q0 LAYOUT.

Magnet	β_{max}[m]	D_{min} [mm]
Q0A	2300	57.0
Q0B	4300	68.5
Q1	5780	75.2
Q2	5820	75.4
Q3	5770	75.1

The result for the deposited peak power distribution is shown in Figure 7. The peaks are more pronounced than for the Symmetric and the Compact cases. The apertures are smaller and this may be the reason for the higher deposition in spite the fact that the magnets are positioned close to the IP, which normally gives a reduction in the deposition [6]. This case has to be run with larger apertures to be comparable. The present Q0 layout gives peaks largely above the recommended limits. The overall deposited power is shown in Figure 8. Except at some local positions, the deposited power is below 10 W/m.

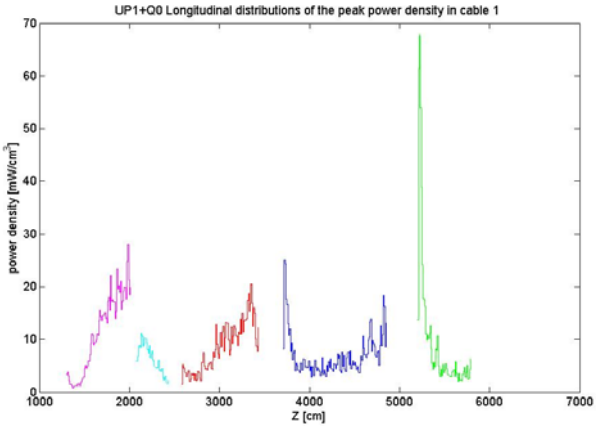

Figure 7: The longitudinal distribution of the peaks in the Q0 option scenario. The peaks are higher than for the Symmetric and Compact cases. The recommended limit is 4.3 mW/cm^3.

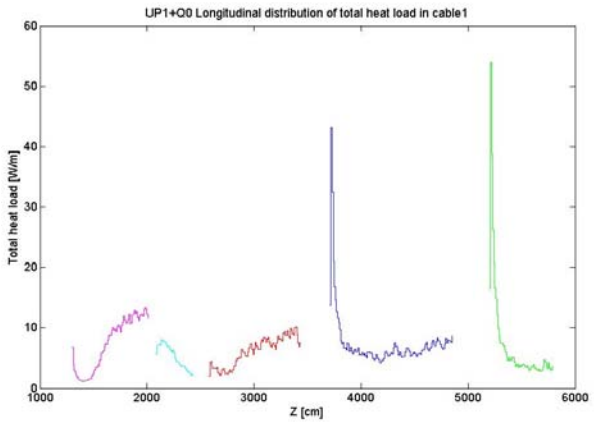

Figure 8: The total heat load along the Q0 doublet and the triplet, integrated over the azimuth.

In Figure 9 we see a 3D plot of the innermost cable of the first magnet Q0A, a smooth build-up along the magnet where the influence of the magnetic field can be distinguished

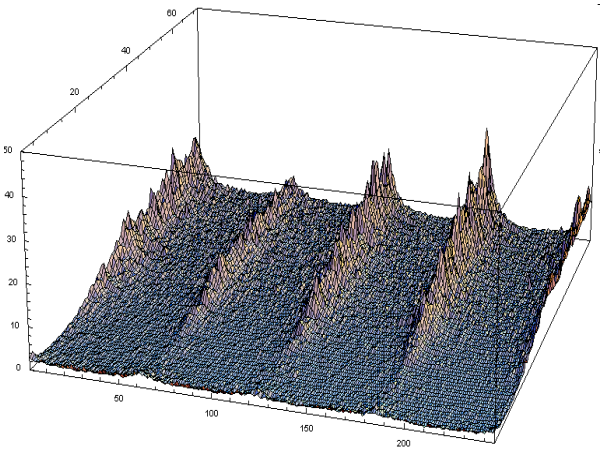

Figure 9: Energy deposition in the inner cable of Q0A

. The same plot for the second magnet in the triplet (Figure 10) shows a smoothed out energy deposition.

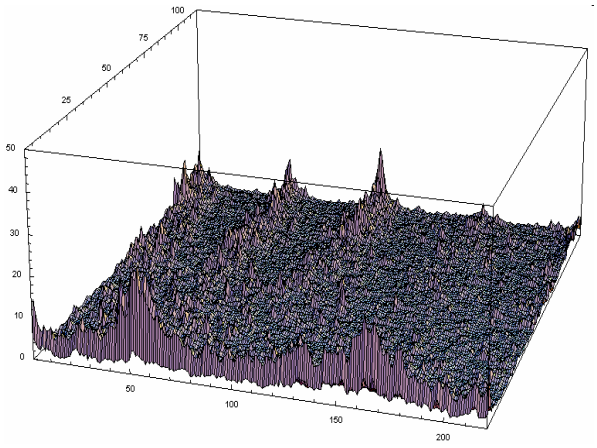

Figure 10: Energy deposition in the inner cable of the second triplet magnet.

Approximate values for the total power deposited in the Q0 magnets, assuming a design like described in [7] we get for Q0A a value of 106 W (14.7 W/m) and for Q0B a value of 42.5 W (11 W/m). The triplet magnet design has to be improved to give a reasonable indication of the total power. However, the power deposited in the triplet magnet cables gives a good first indication of the peak power deposited.

The apertures of these magnets are not comparable to the magnets used in the other scenarios. The present layout has high energy deposition that can possibly be reduced by opening the apertures as in the other cases. This remains to be checked.

PROTECTING THE IR MAGNETS

As described in [8] the deposited energy can be absorbed by a sufficiently thick liner. Figure 11 shows the effect of a thick liner: the peaks are absorbed in the liner and the coil is protected. The thickness of the liner has been estimated simply from the extension of the high energy deposition region in Figure 11 adding some small margin for the closeness to the beam axis where particle energies are higher. The aperture has, in a final design, to be large enough for the beam requirements (optimization).

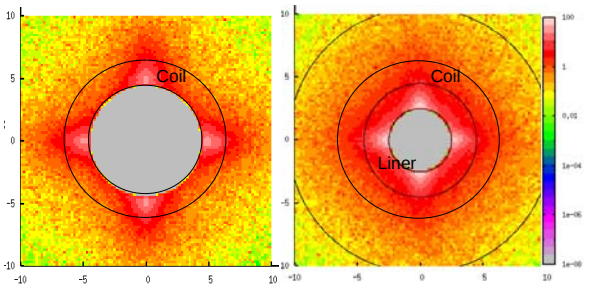

Figure 11: Absorbing the peaks of the energy deposited in the quadrupoles: To the left without liner and to the right a thick liner is inserted inside the aperture to protect the coil from the deposition peaks.

In addition we have checked the effect of a mask. See Figure 12. The idea of this mask is to collect the particles accumulating between the magnets and impinging on the surface of the downstream magnet.

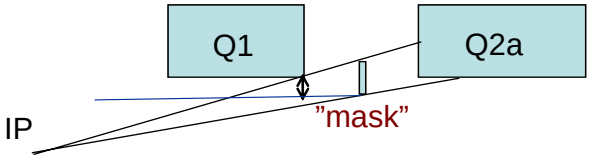

Figure 12: The idea of the mask is to absorb the energy built up between the magnets.

The configuration that was implemented is shown in Figure 13. One case with a small tungsten mask of 1 cm thickness, 10 cm long and one case with a liner of 2 cm stainless steel have been tested. The implementation has to be optimized.

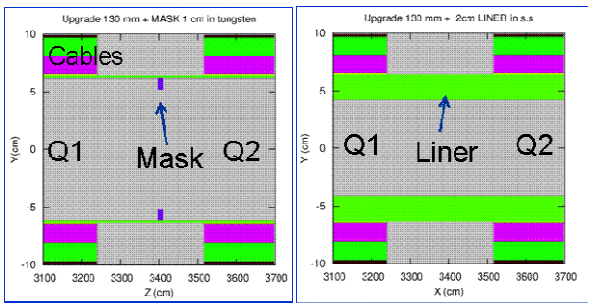

Figure 13: Left, a small mask inserted inside the beampipe, right a thick liner inside the beampipe.

The result of the calculations is displayed in Figure 14. The peaks are considerably reduced. For the thick liner the reduction is 95% and for the small mask inserted in

from of the second quadrupole the reduction is 36%. This is a good indication that with correctly dimensioned apertures and liners we should be able to protect the coils from the collision debris.

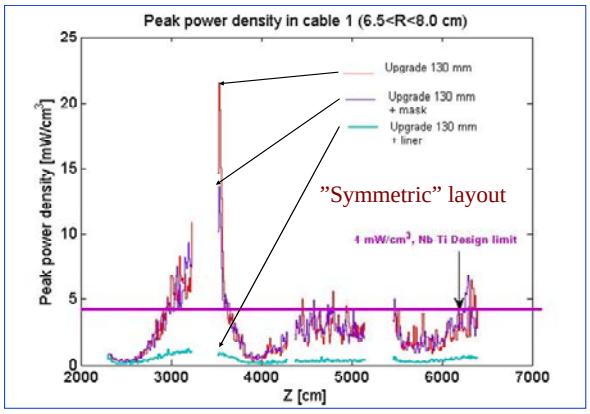

Figure 14: Implementing absorbers reduces the pek power deposition. The mask reduces the peak in the second quadrupole by 36% and the thick liner reduces the peaks by 95% in this case.

The total energy deposition in the magnets decrease around 30% if a liner is introduced. A small mask is inefficient for the total heat load.

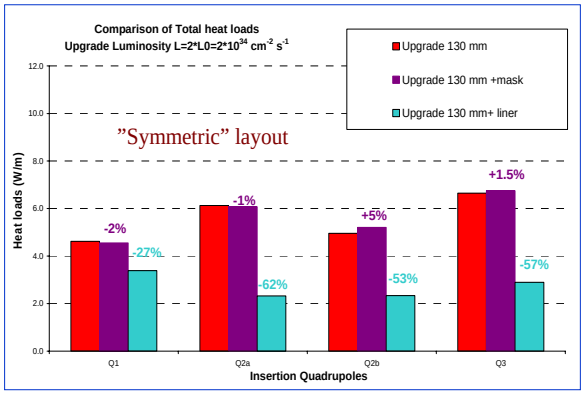

Figure 15: The total heat load for the "symmetric" layout, original layout and layout with mask and with liner.

EXTRAPOLATION TO PHASE II

From the results discussed in the previous paragraph we can answer the question in the title: there is no indication that we cannot with some optimization (future work) of the magnets and using realistic liner thicknesses and material to have sufficient apertures it seems possible to stay below the limits for the deposited peak energy deposition in the NbTi coils (4.3 mW/cm^3). We have to scale the results above to 5 times higher energy deposition values, since the upgrade phase II luminosity is 5 times higher and energy deposition scales linearly. We have assumed, for this exploratory study, that the layout and optics are similar for phase one and for phase. However, the optics is not yet defined: betastar may be lower than in our study and magnet apertures and lengths may change. This may also alter the collision conditions and needs a refined study on the proton distributions in the collision points. The crossing angle impact has to be checked and taken into account, the crossing angle changes for different Luminosity options. Some magnetic arrangements may also help; for example the D0 option has been checked to see if a chicane has an effect on the collision debris impact on the triplet magnets.

CROSSING ANGLE

The effect of the crossing angle for the "symmetric" proposal of the triplet upgrade has been investigated and is displayed in Figure 16. There is a 20% increase in the peak at the entrance of Q2a and some additional peak build-up in Q1 and Q3 if the crossing angle is increased from 142.5 µrad to 220.0 µrad. The crossing angle is vertical in our calculations and analysis has to be done also for the effect of the horizontal crossing angle and the effect of the D0 deflecting in the same plane as the crossing scheme.

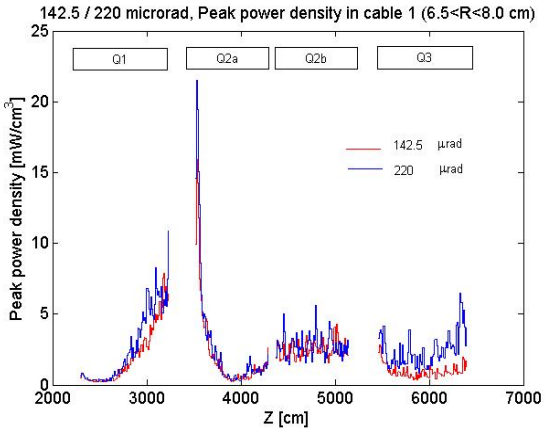

Figure 16: Peak energy deposition for 142.5 µrad and 200.0 µrad vertical crossing angle.

The total deposited energy is changed only marginally, see Table 3, "Symmetric" upgrade case, vertical crossing angles. For For Q2b the energy deposition decreases for the others there is a small increase. The total in the quadrupoles increases by 7 % when the crossing angle increases from 142.5 µrad to 220.0 µrad.

TABLE 3
POWER DEPOSITED [W] IN THE INSERTION ELEMENTS FOR TWO DIFFERENT CROSSING ANGLES IN THER VERTICAL PLANE.

Element	142.5 [µrad]	220.0 [µrad]
TAS	321.2	315.6
BP	15.4	16.8
Q1	46.5	48.2
Q2a	54.9	59.7
Q2b	50.0	48.3
Q3	60.4	69.4
Total Quads	211.9	225.7

TAS OPENING

The effect of the TAS has been evaluated. We can see in Figure 17 the effect of the TAS, the effect is only detectable for the first quadrupole, the Q1. The TAS absorbs essentially particles impinging head on the magnet entrance. The magnets downstream of the TAS absorb essentially particles coming from inside the beam-pipe.

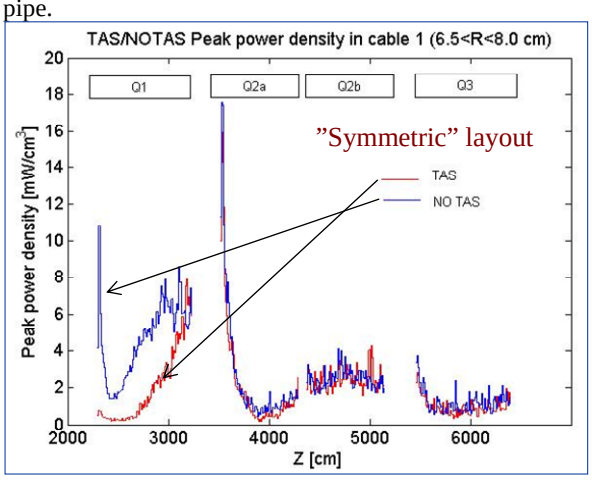

Figure 17: The effect of the TAS can be observed only for the first quadrupole.

Different apertures of the TAS, from 36 mm to 42 mm in steps of 2 mm, have also been calculated. As expected a larger TAS opening affects the Q1 quadrupole; a larger aperture TAS means a somewhat higher energy deposition on the fist magnet (approximately 10% per every 2 mm). However for the other triplet magnets the effect is marginal, see Figure 18.

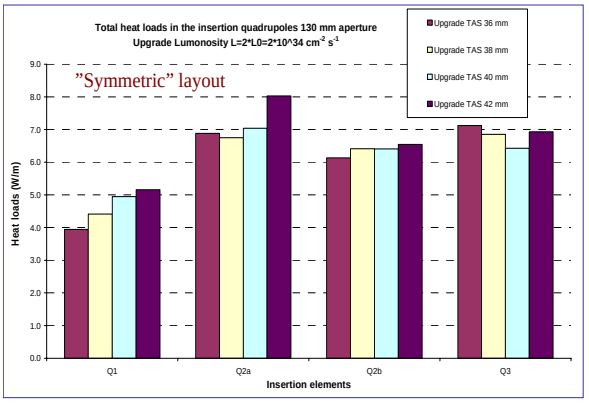

Figure 18: The TAS aperture has been varied and on the first quadrupole the effect is larger with increasing TAS aperture. For the following quadrupoles the effect is less evident.

EFFECTS OF THE D0 SCHEME

The fact that the debris products have different magnetic rigidities than the beam may be used in a chicane to filter the unwanted particles. The effect of D0, see [8] for this proposal, can be good in this respect to protect the magnets. In Figure 19 we see the D0 magnet, placed only 3m from the IP. The field is 3 T and the length of the magnet is 2 m.

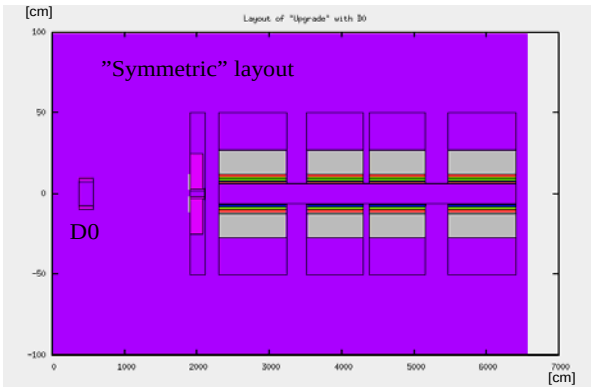

Figure 19: The D0 magnet is placed 3m from the IP, its field is 3T, the length is 2 m and the aperture is 15cm. D0 is deflecting horizontally in this example.

The total deposited energy is spread over the TAS and is less penetrating into the triplet. See Figure 20 where the TAS can be seen inside the aperture of the magnet and absorbing more energy when the D0 field is present (right) than in the case with no D0 effect (left).

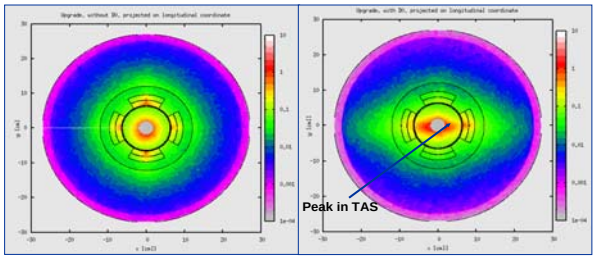

Figure 20: Effect of the vertical field D0 (transverse projection).

The peaks are changed azimuthally between a case with vertical crossing and a horizontal field of the D0 (This combination is just for demonstration of the effect), see Figure 21We see an impact of the D0 also on the peak energy deposited in the inner cable of the quadrupoles, see effect in Q2a in Figure 21.

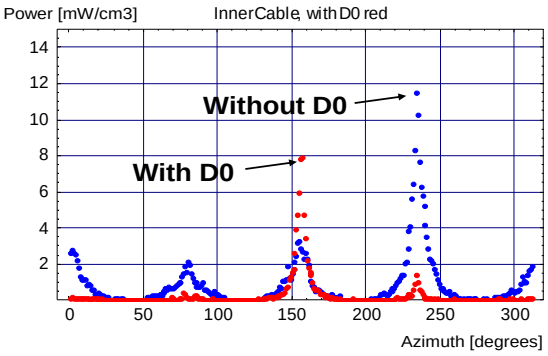

Figure 21: D0 redistributes the energy deposition, here is shown the azimuthal distribution of the peak energy deposited in the inner cable for the longitudinal scoring bin (slice) with the highest peak.

CONCLUSION

We have indications that the energy deposited in the triplet magnets for the upgrade scenarios chosen in this study (the "symmetric" 130 mm aperture and the very large aperture "compact" layouts) could be handled by optimized absorbing systems even for luminosities up to 10^{35}. However, the study is made using a scaling of the Phase I solution and further studies have to be made for a real phase II case.

The aperture of the TAS is influencing essentially the first quadrupole in the triplet. The D0 scheme has an important impact on the energy deposition and has to be carefully studied for all crossing angles; the crossing angle has also an impact on the deposited energy.

REFERENCES

[1] J. P. Koutchouk, L. Rossi, E. Todesco, "A Solution for Phase-one Upgrade of the LHC Low-beta Quadrupoles Based on Nb-Ti", LHC Project Report 1000.

[2] O. Brüning, R. De Maria, R. Ostojic, "Low Gradient, Large Aperture IR Upgrade Options for the LHC compatible with Nb-Ti Magnet Technology", LHC Project Report 1008.

[3] 'FLUKA: a multi-particle transport code', A. Fasso`, A. Ferrari, J. Ranft, and P.R. Sala, CERN-2005-10 (2005), INFN/TC_05/11, SLAC-R-773

[4] 'The physics models of FLUKA: status and recent developments', A. Fasso`, A. Ferrari, S. Roesler, P.R. Sala, G. Battistoni, F. Cerutti, E. Gadioli, M.V. Garzelli, F. Ballarini, A. Ottolenghi, A. Empl and J. Ranft, Computing in High Energy and Nuclear Physics 2003 Conference (CHEP2003), La Jolla, CA, USA, March 24-28, 2003, (paper MOMT005), eConf C0303241 (2003), arXiv:hep-ph/0306267.

[5] E. Laface et al., "Interaction Region with Slim Quadrupoles", CERN-LHC-Project-Report-970, Geneva 2006

[6] Christine Hoa: "Procedures and first investigation of the power radiated by proton-proton collisions into an early separation dipole for the LHC Luminosity Upgrade",LHC Project Note 395.

[7] Elena Wildner: "Heat deposition and backscattering for one of the configurations of the IR for LHC upgrade", Internal Note CERN/AT/MCS/ Mars 2007

[8] J.-P. Koutchouk, G. Sterbini, "An Early Beam Separation Scheme for the LHC Luminosity Upgrade", CERN-LHC-Project-Report-972, Geneva, 2006

SLHC AND ATLAS, INITIAL PLANS

M.Nessi, CERN, Geneva, Switzerland

Abstract

The recent developments in the plans and scenarios proposed by the LHC machine experts towards the SLHC, have triggered various concerns and reserves in the ATLAS community. In particular the eventual need to insert dipoles, quadrupoles and protection elements inside the detector creates major concerns, because of its complex logistics and the risk of reducing the effectiveness of the ATLAS internal radiation shielding. Justifications and constraints on how to best use this space are given.

CONCERNS AND STRATEGY

It took almost a decade to design and optimize, from the point of view of radiation and activation protection, the inside of the ATLAS detector. The main concerns are low- and high-energy neutral and charged particles, produced at the interaction point (IP) and capable of breaking down in a cascade of lower-energy particles, when interacting with the various detector elements. This in particular along the beam pipe region, where small angle and diffractive energy is copiously produced in the hadron interactions. The second source of concern comes from secondary particles produced in the various collimation and optical elements of the LHC beam line, particles that start showering when entering the experimental region.

The ATLAS muon spectrometer, which consists of thousands of gaseous detectors (~15000m^2) is particularly sensitive to such energy depositions, because they will generate a background that will obscure the detector readout, impacting directly on the physics performance of ATLAS.

Based on this strategy, various regions have been created inside the detector as pockets of energy absorption, in between active detection regions. The goal has always been to keep the active detector readout occupancy below a level where combinatorial effects can fake physics. All this took years of optimization, and all possible space was used to tune the detector for the LHC maximum design luminosity (ATLAS Note: ATL-GEN-2005-001)

ATLAS AND SLHC PLANS

ATLAS is starting to be prepared for the physics potential of the SLHC, knowing that some of its present detector components will suffer in performance when exposed to beam intensities beyond the LHC design luminosity as foreseen at SLHC. Some of the detector components are known to suffer from aging due to radiation, in such a way that they will need to be fully replaced and upgraded after about 300-400 fb^{-1} of integrated and delivered beam Luminosity. In particular, the inner detector, which is sitting inside the central 2T field solenoid, will need to be fully rebuilt with a new layout and technology, capable of coping with the new energy density and with a substantially better granularity in the readout geometry. This substantial high-technology part of the detector will need a vigorous R&D and design plan, before being ready for mass production and later integration inside ATLAS. The Collaboration has already started this new phase of the project very actively, with the goal of preparing for real construction around 2010-2011, when the physics potential of the LHC will be known and the SLHC project will be in its construction phase.

Other parts of ATLAS will need partial upgrades, in particular in their front-end electronics readout. Some of the very forward detection elements in the calorimeters and muon spectrometer will need a new fresh approach as well. The overall radiation protection strategy will also require to be fully reviewed and optimized.

To this complication we have now to add the possibility of inserting active beam elements inside the detector, which might directly impact on the overall performance and on the logistics of the various services and mechanical structures.

In general, ATLAS, when planning for SLHC, is interested in collecting as much as possible integrated luminosity on tape, while keeping the peak luminosity as low as possible to avoid excessively high densities of particles in the detector (detector pileup). Therefore it will welcome every attempt to increase the lifetime of the beams, the duty cycle of the overall machine and any new idea to effectively level the peak luminosity in favour of an increased integrated luminosity.

Where to place active beam elements in ATLAS?

Over the last 2 years we have explored various possible scenarios on how to effectively increase luminosity by a factor 10. Among this, is the idea of an early full or partial separation scheme, which adds dipoles and eventual quadrupoles in the detector region. Some of these plans have evolved with time with more and more realism on both sides. The bunch separation is kept at 25 or 50 ns in this phase of the project, the idea of inserting directly dipoles inside the inner detector (ID) cavity has been abandoned, new interesting techniques like wire compensation and crab cavities are discussed and are part of the future strategies.

Four regions have been identified in the detector capable in principle to host beam optics elements, as it is visible in figure 1 and table 1:

- The JF region: placed inside the bore of the endcap calorimeter cryostat. This region hosts today beam pipe elements (ion pumps, bellows, ..) and a neutron moderator. The region will need to be kept as transparent as possible to particles, in order to avoid adding substantial background to the inner detector and to the electromagnetic end cap calorimeter. Recently this region is becoming interesting as a possible solution to a potential problem related to the boiling of liquid Argon inside the forward calorimeter at SLHC beam intensity. At this stage of the project the uncertainties are such that we prefer to withdraw this location from the list of potential dipoles position. Bringing there the necessary cryogenics and power services, seems also to be a very difficult challenge

- The JD region: it hosts a SS-cylinder which today contains copper shielding elements. There, a small dipole could be hosted. The problem in this case is to avoid diluting the level of shielding protection to the muon spectrometer region just nearby. The typical distance to the IP is of about 7000-8000 mm. This region moves with the detector elements during the ATLAS access periods.

- The JTT region: inside the bore of the end cap toroid magnets, in a field-free region, placed at about 10000 mm in z. This region is more stable mechanically, but will move during access periods

- The JF region: the most far way solution (Z ~ 14000 mm), completely surrounded by a massive Fe shielding element. This region is the preferred one by the experiment and might be fully redesigned for SLHC, taking into account the shielding needs and the various mechanical and logistics constraints.

Optimizing for beam elements and for shielding protection at SLHC will in any case require a vigorous design and simulation effort over the next few years.

Table 1: possible available space for beam elements

Position	**Maximal radius**	**Zmin, Zmax position**
JF region	180 mm	3490 mm, 4580 mm
JD region	430 mm	6800 mm, 8660 mm
JTT region	870 mm	8690 mm, 12870 mm
JF region	1500 mm	12950 mm, 18600 mm

Today the JF region, among the four, is the preferred one by ATLAS. It will be the one offering most space, less services constraints and a bigger potential for shielding upgrades from the detector side. The only problem is that it will need to be full dismounted during shutdown periods, when the detector will have to be in its open configuration.

At this stage of the project, to pursue more realistic simulations we will need some detailed scenario. A full evaluation of such a layout is a major effort and involves several detector specialists.

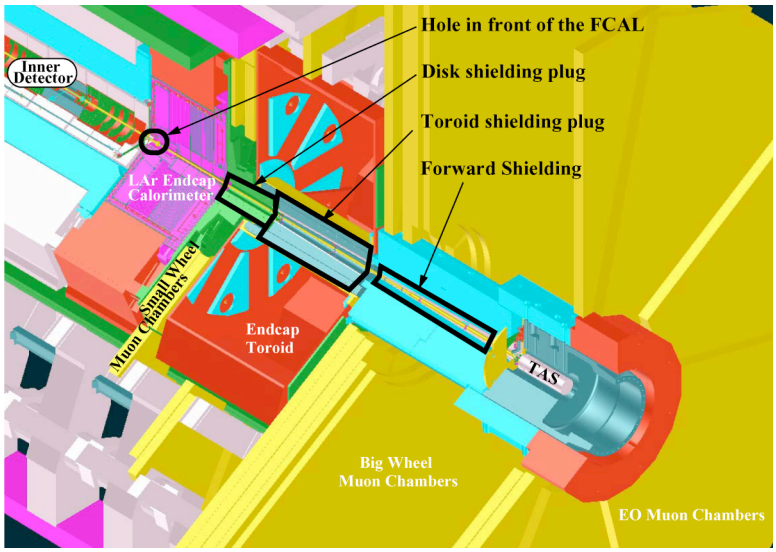

Figure 1: ATLAS longitudinal layout, showing possible position where additional beam elements can be hosted

LHC INTERACTION REGION UPGRADES AND THE MACHINE-EXPERIMENT INTERFACE

E. Tsesmelis, CERN, Geneva, Switzerland

Abstract

Schemes for increasing the luminosity delivered to the ATLAS and CMS experiments at the LHC, based on the implementation of modified or additional inner triplet quadrupoles and/or dipoles close to the interaction points, are being developed and result in the need to upgrade the interaction regions around Point 1 and Point 5. This paper presents some of the challenges for the experiments and for the LHC Collider resulting from such schemes and provides some suggestions for further studies.

INTRODUCTION

Discussions on upgrades to the LHC interaction regions required to follow the increase in LHC luminosity have been taking place in regular working group meetings between the machine and experiment groups during 2007 [1,2]. The interaction region upgrade options considered in the working groups consist of:

- Assuming the baseline LHC optics with stronger and/or larger aperture inner triplets.
- Moving the existing/modified inner triplets closer to the interaction point (IP).
- Incorporating additional `thin' quadrupoles (Q0) between the existing or modified inner triplets and the IP.
- Including a dipole (D0) in close proximity to the IP.

Several issues resulting from modifications to the interaction regions have been highlighted in these working groups. For the experiments, this includes the displacement, mechanical interference and/or removal of components of the particle detectors, particularly in the forward region; the effect of the magnetic fields of the machine magnets on the spectrometer magnets; and the scattering and albedo of particles into the particle detectors, especially in the Muon Systems, from the inclusion of additional machine elements inside the particle detectors. On the machine side, issues related to the R&D and production of magnets with the required material (NbTi and Nb_3Sn) and performance will need to be carried out and the minimisation and removal of the heat deposited in the magnets from the products from the high-energy collisions at the IP would need to be addressed. Issues at the machine-experiment interface include an overall design that will enable the particle detectors to open for maintenance and modifications and the implementation of stable mechanical supports and technical services (cryogenics, power and cooling) for the machine magnets within the particle detectors.

INTEGRATION OF MACHINE ELEMENTS IN ATLAS AND CMS

In the case of ATLAS, the Forward Calorimeter is relatively close to the IP and thus machine magnets can be installed on the non-IP side. Servicing the calorimeter would require that the experimental beam pipe be of constant diameter which would, however, result in an increase of the background in ATLAS. The ATLAS spectrometer solenoid is short and relatively weak (2T) and so is expected to have a correspondingly small effect on the machine Q0 and D0 magnets. After careful optimisation, the dense shielding around the ATLAS experimental beam pipe could become an integrated machine magnet and radiation shielding structure but care must be taken not to decrease the radiation shielding by the insertion of machine magnets. Figure 1 shows an example of integrating the Q0 quadrupole magnets in ATLAS.

Issues of integration in CMS differ considerably from those in ATLAS. The CMS Forward Calorimeter is relatively far away from the IP at 10 m. and machine elements cannot be installed in front. Therefore, integrating the Q0 and D0 magnets will require major modifications to the CMS detector because of the need to move the Forward Calorimeter closer to the IP. Moreover, as the CMS solenoid is relatively long (6 m.) and strong (4T), the fringe field close to D0 is expected to be important.

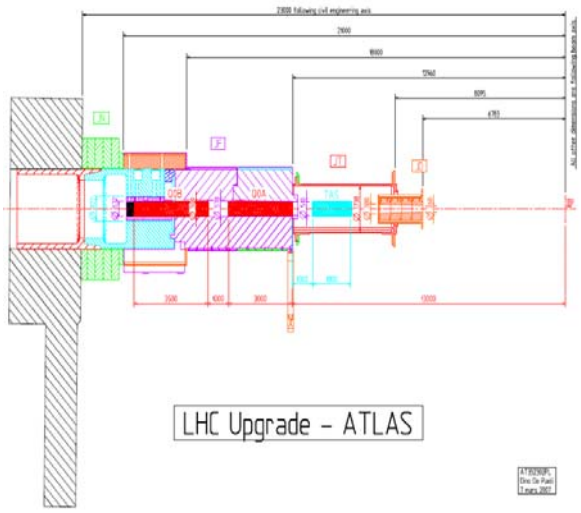

Figure 1: Integration of Q0 quadrupoles in ATLAS.

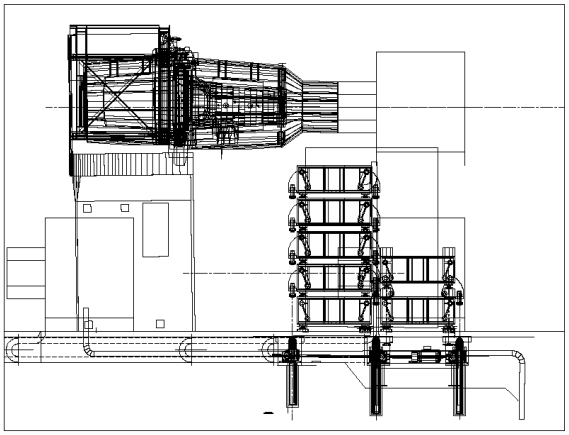

Figure 2: Supplementary structure for the CMS Forward Shielding.

EXPERIMENTAL BEAM PIPES

The experimental beam pipe is one of the major sources of background in ATLAS. In order to mitigate the effect, together with reducing the material activation, an aluminium beam pipe replacing the stainless steel structure has been proposed for installation prior to running at nominal luminosity. An ATLAS experimental beam pipe composed entirely of beryllium should also be considered for higher luminosities as the activation of the beam pipe then becomes negligible and the decrease of the background rate in the ATLAS Muon System is significant.

As the CMS experimental beam pipe is tapered, the background to the detector is reduced and since the solenoid magnet return yoke shields most of the Muon System, there is less need for an extensive shielding around the experimental beam pipe. CMS does not expect any modification to their experimental beam pipe. Together with the forward beam pipe on the non-IP side of the Forward Calorimeter having a diameter of 400 mm and being in the shadow of the Forward Calorimeter, the present beryllium beam pipe around the IP and the stainless steel beam pipe elsewhere are expected to serve the needs of the LHC upgrade.

MACHINE MAGNET CHALLENGES

The total heat load and the peak power deposition in the machine magnet coils from debris from high-energy collisions at the IP are potentially issues of concern. Methods to remove this heat must be implemented. The development of Nb_3Sn magnets will be required for any significant luminosity increase. Such magnets have higher temperature margins but further R&D is needed.

Moreover, the interaction of unshielded magnets with the solenoidal fields of the spectrometer magnets and the neighbouring iron, particularly in the case of CMS, is an issue as is the integration of the dense radiation shielding with the services of the machine magnets. Issues related to forces, torques, field disturbance and quench forces should be studied.

Mechanical support structures need to be designed to support the new machine magnets in the forward positions of ATLAS and CMS. The integration of the technical services (cryogenics, power and cooling) of the machine magnets in the particle detectors need to be studied further.

RADIATION SHIELDING

The CMS Forward Shielding, located at the two ends of the UXC55 underground cavern, is designed to reduce the background radiation in the experimental area and in the CMS detector. The Forward Shielding is near the limits of mechanical strength and a new concept or supplementary system is needed. In the case of the latter option, insertions for a second set of jacks at each end are already built in to the UXC55 floor and would thus form the basis for supporting a supplementary structure closing around the existing shielding (see Figure 2).

TAS absorbers have been designed to reduce the heating of machine magnet coils by absorbing the energy of the beam debris from the IP and to shadow the coils by reducing the number of particles hitting them. However, the neutron production in the TAS absorbers will fill the cavern like a gas and will be a major source of background in the Muon Systems of the experiments, thus requiring much care in the design of new TAS absorbers. Studies on the energy deposition and conceptual design of new TAS absorbers is underway [3].

MACHINE-INDUCED BACKGROUND

The impact of the machine-induced background to the experiments, resulting from beam-gas and beam halo, will be studied as of the initial LHC running period. The determination of the background's spectrum will be used to benchmark the extensive simulation studies which in turn can be used with more confidence to make predictions of the machine-induced background at the upgraded LHC. This will provide a good judgement on whether an increase of this background at an upgraded LHC is tolerable.

EXPERIMENT INSTALLATION, COMMISSIONING AND EXPLOITATION

Installation and commissioning of new particle detectors, machine elements (magnets and their supports /services) and other equipment (experimental beam pipes, vacuum equipment and radiation shielding) would need to be carefully planned in order to least disrupt LHC operation as all activities will be carried out inside the experimental areas. Fitting all work inside one standard machine shutdown period should be analysed.

The increased activation of material in the experimental areas is expected to seriously affect the maintenance of the particle detectors given the restrictions arising for access scenarios. Remote handling might become

mandatory in the design of new particle detectors and probably should be developed for existing ones.

CONCLUSIONS

The present studies show that the integration of new machine elements inside the experimental areas and particle detectors is feasible but challenging. The work on developing modified interaction regions at Point 1 and Point 5 should continue and in particular should concentrate on studies regarding the energy deposition in the TAS absorbers, integration of magnet systems and their associated services (cryogenics, power and cooling), the experimental beam pipe and the radiation shielding. The backscattering to the particle detectors from additional machine elements needs also to be studied.

ACKNOWLEDGEMENTS

We would like to thank the organisers of the workshop for the invitation to make this contribution and for the excellent organisation of this very interesting and useful event.

REFERENCES

[1]http://indico.cern.ch/categoryDisplay.py?categId=1450
[2]http://indico.cern.ch/categoryDisplay.py?categId=1462
[3]E. Wilner, CARE-HHH-APD Mini-Workshop IR'07 (Interaction Regions for the LHC Upgrade, DAFNE and SuperB), Frascati, November 2007

Beam-beam issues for LHC upgrade phases 1 and 2

U. Dorda, F. Zimmermann, CERN, Geneva, Switzerland

Abstract

While long-range beam-beam interaction will not be the limiting effect in the first years after LHC start-up, it will definitely become one in the upgrade scenarios. Upgrade phase 1 will include an exchange of the triplet magnets allowing for a $\beta^* = 25$ cm optics. Phase 2 is an even more ambitious upgrade that will include a modification of the detectors. Currently two phase-2 upgrade scenarios are proposed: the "Dipole Zero" (D0) and the "Large Piwinski Angle" (LPA) option.

After some general notes and a brief description of the applied simulation model, the upgrade phase 1 issues and optics will be discussed with regard to beam-beam performance. The following two sections will deal with upgrade phase 2.

GENERAL

BBTrack [5], a weak-strong 6D tracking code, was used to track (linear transfer matrices between nonlinear elements, interaction points (IPs) 1 & 5 only) particle distributions (initial energy offset $\delta p/p = 2.7 \times 10^{-4}$) for 300,000 turns in LHC at top energy (7 TeV) and determine the particle stability with help of the Lyapunov exponent. The dynamical aperture (DA) is defined as the amplitude at which 40% of the particles in a radial range of width $\delta r = 0.2\sigma$ are chaotic.

For comparison, the main beam-beam parameters of the nominal LHC are: 15 LR collisions at each side of the IP ($\beta^* = 0.55$) with a full crossing angle $\theta = 284\mu$rad (average separation $\bar{d} \approx 9.5\sigma$) at 1.15 p/bunch. This crossing angle was chosen to obtain an acceptatble long-range beam-beam effect [4]. Namely with this crossing angle a dynamic aperture (DA) of 5.4σ is expected that could be improved to $DA = 7.2\sigma$ by a wire compensation [6].

LHC UPGRADE PHASE 1

By 2013 the whole triplet will need to be exchanged and a new interaction region (IR) scheme with $\beta^* = 25$ cm will be implemented in order to boost the luminosity. In the following, 3 different optics - "low β max", "modular" and "compact" - as proposed by R. de Maria et al in [7] - are briefly discussed. A forth option, similar to the low β max one, called "symmetric" was proposed by J.P Koutchouk, E Todesco et al in [2]. In order to keep an average beam-beam separation of $\bar{d} \approx 9.5\sigma$ the crossing angle in all three options is increased with respect to the nominal LHC (from $\theta = 284\mu rad$ to 450μrad). Given the same magnet technology, the stronger focussing requires a longer triplet and hence it introduces more long-range beam-beam encounters (LRBBIs). The number of long range beam beam encounters (LRBBIs) and other important parameters are summarized in Table 1 and Fig. 1. In order to cope with these additional LRBB encounters and potentially also with a higher beam current or simply to improve the nominal beam-beam performance a wire compensator (BBLR) is foreseen. A wire compensation does not interfere with the IR design as it only requires a) that the wire be placed at a position with equal β-function in both transverse planes, b) a reasonably large β to allow accommodating a wire compensator with a practical wire diameter and c) a small phase advance between the wire and the LRBBIs. Suitable positions can be found in all scenarios. Simulations showed that the simple criterion

variable	nominal	low β max	Compact	modular
β^* [m]	0.55	0.25	0.25	0.25
#LRBBIs	16	19	22	23
wire @ [m]	104	136	170	160
β_{wire} [m]	1780	3299	2272	3000
σ_{dsep}	1.6	3.6	2.2	X

Table 1: Comparison of three proposed phase 1 upgrade optics with respect to their long-range beam-beam (LRBB) performance.

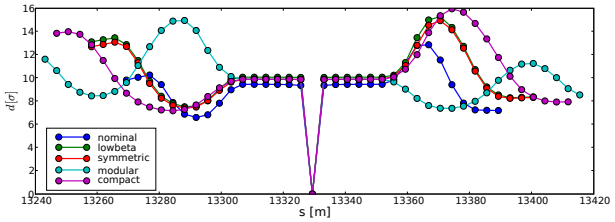

Figure 1: Comparison of the normalized beam-beam separation at IP5 for the nominal LHC and four upgrade scenarios.

of minimizing the number of LRBBI is a reasonable guide for optimisation, and that accordingly the low β-max optics performs best. Its DA for 1.15×10^{11} p/bunch is 5.1σ. For 1.7×10^{11}p/bunch the DA shrinks to 3.8σ. Figure 3 a) shows the stability diagram of the low β max optics. Subfigure b) shows that a wire compensation can reduce the tune footprint to the head-on one. Figure 4 demonstrates the enhanced DA due to the wire compensator.

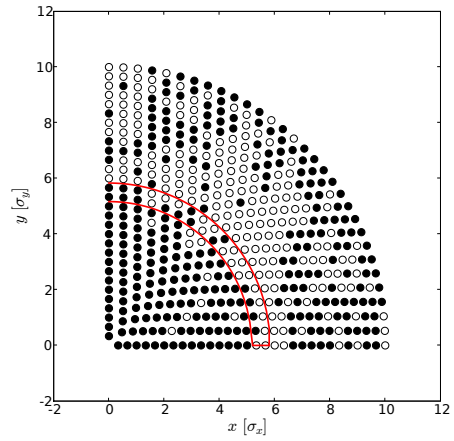

(a) Stability. black=stable, white=chaotic

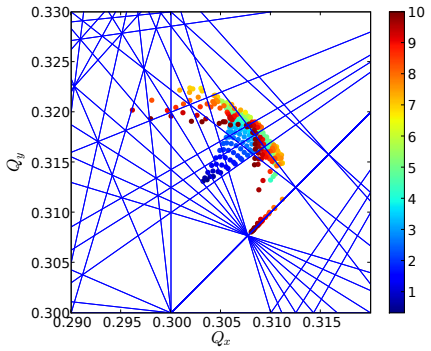

(b) Tune footprint

Figure 2: Low β max optics for $1.15 \cdot 10^{11}$ p/bunch

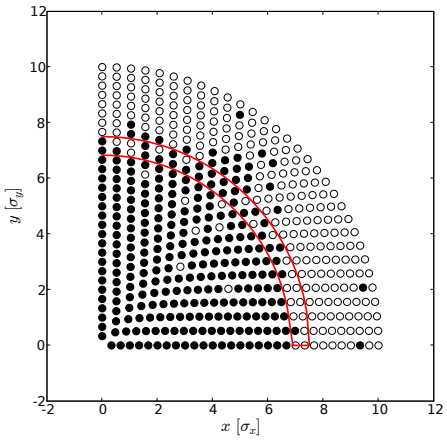

(a) Stability

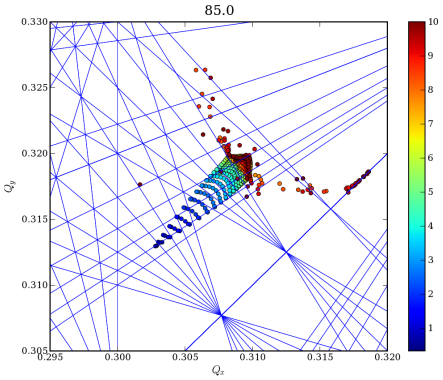

(b) Tune footprint

Figure 3: The low β^* max optics: A wire compensator could eliminate the long-range beam-beam tune spread and increase the DA to 7σ.

LHC UPGRADE PHASE 2 - 'DIPOLE ZERO' (D0)

General notes

One scenario for the phase-2 upgrade foresees the installation of an "early separation" dipole "D0" about 6m from the collision point and a reduced crossing angle [3]. This scheme implies two long range encounters at a reduced separation of about 5σ on each side of the two high-luminosity IPs. Unfortunately no consistent optics was made available for this scheme, so we have added a D0 to the low β max optics. While this allows to study beam-beam issues realted to close encounters, it may not properly model two essential components of the whole picture: 1) Although the HO collision is scale invariant, the reduced spot size ($\beta^* \approx 8cm$) at the IP causes a large increase of the sensitivity to noise created within the focussing system. As the D0 is part of the latter and its adequate mounting is challenging this issue could be important. 2) As mentioned above, also a decrease in β^* causes an increase of triplet length and it requires a larger crossing angle in order to keep the same normalized beam-beam separation. For those two reasons it is not possible to reduce the problem to the simple question "can we stand two close encounters?"

Studies

Figure 5 a) shows the beam-beam separation of our model and b) compares the footprint with and without the D0 activated. Though the footprint appears to be smaller with D0, the stability is worse: While the tunes of high and low amplitude particles are shifted equally, intermediate amplitude particles behave differently: With D0 present the footprint folds at lower amplitudes. This tune footprint folding (which unfortunately could not be reproduced in the SPS or RHIC machine studies so far due to the lack of a head on collisions) proved to be one of the main instability-contributions in simulations. Fig. 6 demonstrates that this folding at lower amplitueds indeed reduces the DA already for nominal beam current. Going to the ultimate intensity of $1.7 \cdot 10^{11}$ p/bunch - as foreseen for this optics - leaves an unbearably small stable region. In this case no wire compensation can be used, since the wire has a finite diameter, only functions in hte 1/r regime of the beam-

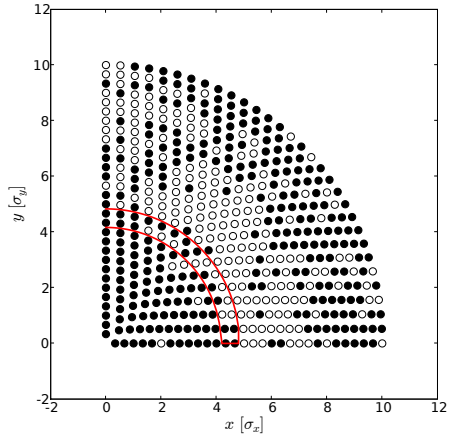

(a) The DA of the compact optics is $\approx 4.2\sigma$

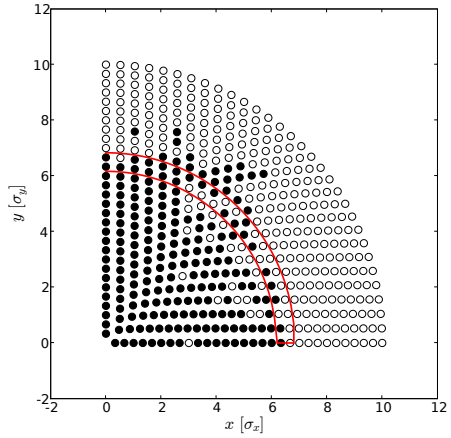

(b) A wire compensation could increase the DA of the compact optics to $\approx 6.2\sigma$

Figure 4: Stability diagrams for the "compact" optics with and without wire compensator.

beam force and must be placed in the shadow of the collimators at amplitudes above 7σ. Only an electron lens used "as wire" would be an option. Figure 8 shows a stability study considering only the head-on interaction and two long-range encounters per side of each IP at a variable distance. The minimal acceptable beam-beam separation seems to be around 6.5σ.

RHIC

Experiments at RHIC and at the CERN SPS have been performed in order to study the effect of close encounters [8]. While the results of these experiments help to understand the loss mechanisms and to benchmark simulations, they must be treated with caution when extrapolating to the LHC due to the lack of head-on collisions. For example the phase-1 upgrade optics "low β max" produces in simulations a DA of 3.8σ for 1.7×10^{11}p/bunch including HO

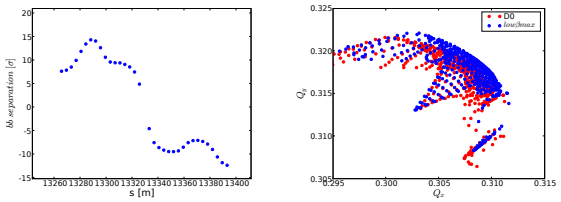

(a) Normalized beam-beam separation in the D0 considered optics

(b) Tune footprint of the low β max optics with and without D0 model

Figure 5: Beam-beam separation and tune footprint for our model D0 option.

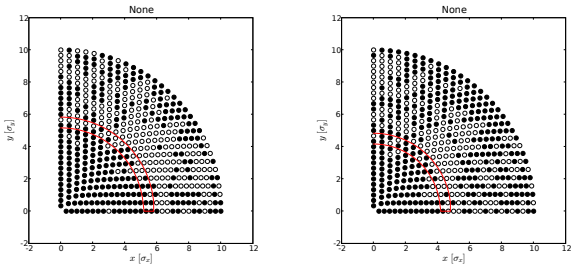

(a) Stability in the base line low β max optic

(b) Stability with the D0 activated

Figure 6: Stability diagram for the DO option with the nominal bunch charge of 1.15×10^{11} p/bunch

while without HO at 2.5×10^{11} a DA of 5σ!

Figure 9 shows two typical results of the RHIC beam-beam experiments with a single long-range encounter at varying beam-beam distance. First losses are observed at about 7σ separation. Results of parameter scans obtained with the RHIC wire compensator (Fig. 10) show an onset of beam loss at 6σ for a wire strength euqivalent to 2 LR encounters.

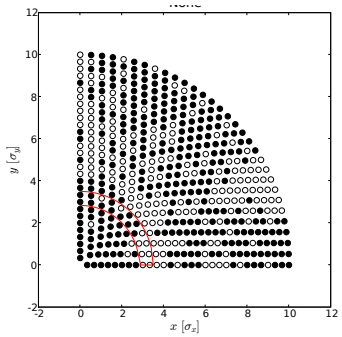

Figure 7: Stability diagram for the D0 upgrade scenario with $1.7 \cdot 10^{11}$p/bunch

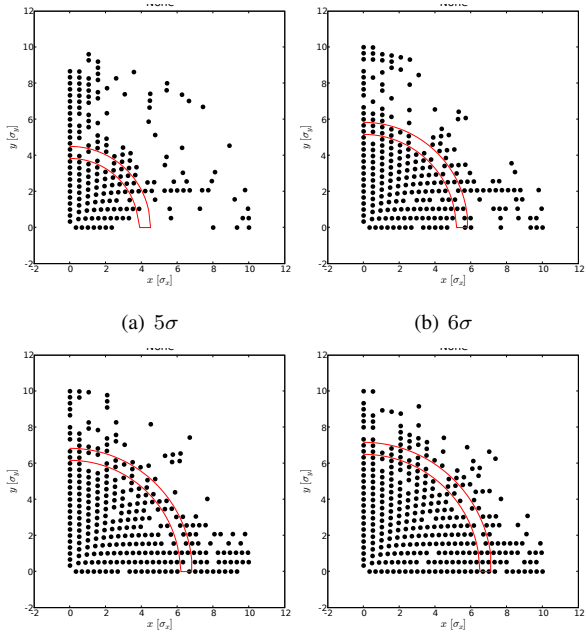

(a) 5σ (b) 6σ

(c) 7σ (d) 8σ

Figure 8: Stability diagram for the D0 model with HO and 2 LR encounter per side per IP at 1.7×10^{11} p/bunch and varying separation(crossing angle)

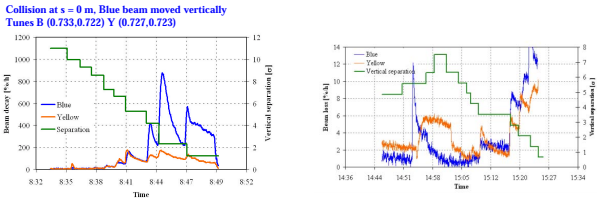

(a) Injection energy. (b) Top energy

Figure 9: RHIC Beam-Beam experiments with a single long-rang ebeam-beam encounter and a bunch population of 1.5×10^{11}p/bunch. shown are the loss reates for both beams and the normalized distance as a function of time.

D0 - CONCLUSION

While the idea of separating the two beams as early as possible seems to be an obvious aproach to take, it faces potentially severe long-range beam-beam issues in addition to detector integration issues. With few exceptions the - due to the lack of HO - optimistic experiments at RHIC and the CERN SPS indicate a drastically perturbed beam-stability already with a single long-range encounter at 6-7 σ separation. In addition numerous issues such as the crab cavity, likely required in this scheme, and the electron lens for compensation must be addressed. To study these questions in detail, it is of great importance to develop a realistic optics as soon as possible.

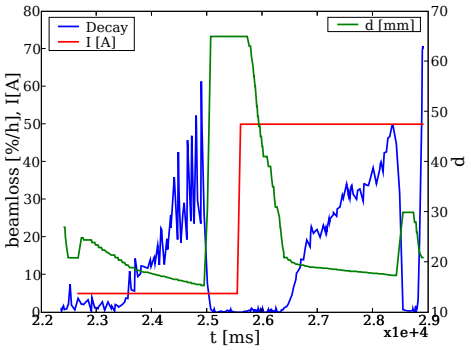

Figure 10: Distance scan with RHIC BBLR at top energy (100 GeV Ions) with transverse beam size $\sigma = 4mm$. Shown are the beam loss and the absolute beam-wire distance as a fucntion of time.

LHC UPGRADE PHASE 2 - LARGE PIWINSKI ANGLE (LPA)

The second proposed upgrade scenario is the LPA [1] comprising $4.9{\cdot}10^{11}$ p/bunch with flat beams at 50 ns bunch spacing corresponding to an LR effect enhanced by a factor of 2.5 compared to nominal LHC. Figure 11 shows the stability region and the tune footprint of this option. Only a wire compensation can make the LPA viable (Fig. 12)

LPA - conclusions

The LPA option has the advantage of being predictable. As its optics layout will be very similar to that one of upgrade phase 1 and not too different from nominal LHC, experimental tests can be performed at the original LHC. The wire compensation can be installed without any risk at any time and its effectiveness can be proven already in the nominal LHC. In case crab cavities become indeed operational they can be installed as a complement. The impact of the synchro-betatron resonances, more strongly excited at a large Piwinski angle, must be studied in more detail but it is not expected to be a severe issue for the low synchrotron tune of the LHC.

CONCLUSION

The preferred optics for phase 1 is the low β max optics as it features the lowest number of long-range beam-beam encounters. Seen from the LRBB point of view the LPA option appears more robust and more predictable for the LHC upgrade phase two.

Thanks

The authors want to thank R. de Maria for his continuous support with the upgrade optics, R. Calaga, R. Tomas, J.P Koutchouk and G. Sterbini for the fruitfull co-operation and the RHIC BBLR team for helpfull input.

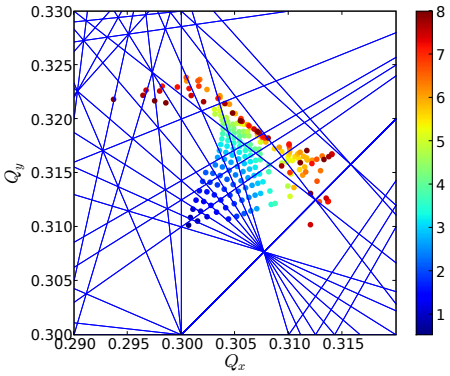

(a) Tune footprint

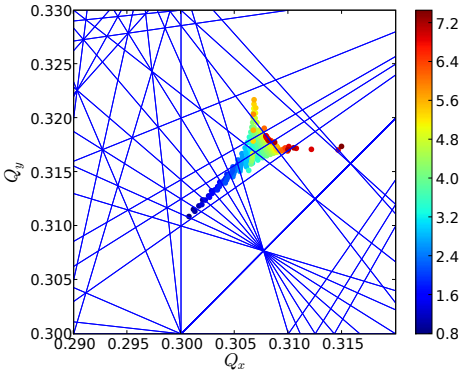

(a) Tunefootprint

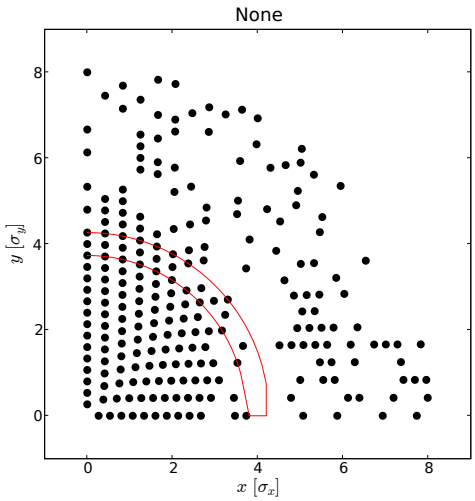

(b) Stability diagram

Figure 11: Tune footprint and stability diagram for LPA

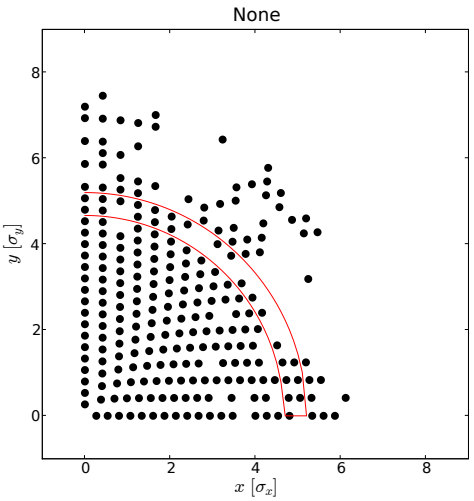

(b) Stability diagram

Figure 12: Tune footprint and stability diagram for LPA for LPA with wire compensation

REFERENCES

[1] F. Zimmermann, "LHC Upgrade Scenarios", CERN-LHC-PROJECT-Report-1018, 2007

[2] J.P. Koutchouk et al., "A Solution for Phase-one Upgrade of the LHC Low-beta Quadrupoles Based on Nb-Ti.", LHC-PROJECT-Report-1000, April 2007

[3] J.P. Koutchouk and G. Sterbini, "An Early Beam Separation Scheme for the LHC Luminosity", LHC-PROJECT-Report-972, Aug 2006

[4] W. Chou and D. Ritson, "Dynamic aperture studies during collisions in the LHC.", LHC-Project-Report-123, June 1997

[5] U. Dorda, "'BBTrack - a tracking program for studying long-range beam-beam interaction"', http://ab-abp-bbtrack.web.cern.ch/ab-abp-bbtrack/

[6] U. Dorda et al. "LHC beam-beam compensation using wires and electron lenses."', "LHC-PROJECT-Report-1023", "2007"

[7] R. de Maria, "Layout design for final focus systems and applications for the LHC interaction region upgrade", LHC-PROJECT-Report-1051, 2007.

[8] W. Fischer, "Experiments with a DC wire in RHIC", PAC 07.

DAΦNE LIFETIME OPTIMIZATION WITH COMPENSATING WIRES AND OCTUPOLES

C. Milardi, D. Alesini, M.A. Preger, P. Raimondi, M. Zobov, LNF-INFN, Frascati, Italy
D. Shatilov, BINP, Novosibirsk, Russia.

Abstract

Long-range beam-beam interactions (parasitic crossings) were one of the main luminosity performance limitations for the lepton Φ-factory DAΦNE in its original configuration. In particular, the parasitic crossings led to a substantial lifetime reduction of both beams in collision. This puts a limit on the maximum storable current and, as a consequence, on the achievable peak and integrated luminosity. In order to mitigate the problem, numerical and experimental studies of the parasitic crossings compensation by current-carrying wires have been done. During the operation for the KLOE experiment two such wires have been installed at both ends of the interaction region. They produced a relevant improvement in the lifetime of the *weak* beam (positrons) at the maximum current of the *strong* one (electrons) without luminosity loss, in agreement with the numerical predictions. The same compensating mechanism has been adopted during the run for the FINUDA experiment as well, with less evident benefits than in the previous case.

The interplay between nonlinearities originating from the beam-beam interaction and the ring lattice has been studied by theoretical simulation and experimental measurements. Compensation procedures have been set up relying on the electromagnetic octupoles installed on both rings and used in addition to wire compensation.

In this paper the parasitic crossings effects in the DAΦNE interaction regions and their compensation by wires and octupoles are described. A detailed theoretical analysis of the interplay about different non-linearities is presented; eventually experimental measurements and observations are discussed.

INTRODUCTION

The Frascati Φ-factory DAΦNE is an e^+e^- collider operating at the energy of Φ-resonance (1.02 GeV c.m.) [1]. Its best peak luminosity reached so far is 1.6×10^{32} $cm^{-2}s^{-1}$ with a maximum daily integrated luminosity of about 10 pb^{-1} [2]. Recently the accelerator complex has undergone a major upgrade with drastic change in its interaction regions (IRs) layout [3].

In order to obtain such a high luminosity at low energy high current bunched beams were stored in two colliding rings sharing two IRs, whose only one at a time hosted an experimental detector (see the original layout in Fig. 1).

Usually, the number of adjacent filled buckets is in the range 109÷111 out of 120 available. A short gap is needed for ion clearing in the electron ring. It's worth reminding that in DAΦNE the bunch separation of 2.7 ns is the shortest among all existing colliders and particle factories.

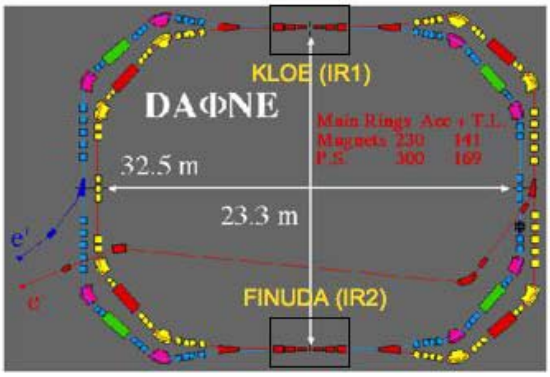

Figure 1: DAΦNE layout before the upgrade.

In order to minimize the effect of parasitic crossings (PC) between the colliding bunch trains the beams collided under a crossing angle in the range 20÷30 mrad. However, despite the crossing angle, the long-range beam-beam interactions (LRBB) remained one of the most severe limitations to the DAΦNE performance in terms of luminosity. In fact LRBB interaction led to a substantial lifetime reduction of both beams, limiting the maximum storable currents and, as a consequence, the maximum achievable peak and integrated luminosity. The latter was strongly influenced by the beam lifetime because in the topping up regime a fraction of the integrated luminosity is lost during the time required to switch the injection system from one beam to the other.

Looking for a compensation scheme to reduce the impact of LRBB interactions, it has been decided to install two windings (wires) at both ends of the IRs. This approach revised an idea originally proposed by J. P. Koutchouk [4] for LHC, and recently tested during single beam operation on SPS [5, 6]. Simulations using LHC compensation devices also predicted a relevant dynamic aperture enlargement for the Tevatron collider [7].

An improvement in the beam lifetime has been also obtained by understanding the interplay between nonlinearities coming from beam-beam interaction and magnetic lattice; the effect has been cured by using the octupole magnets installed on both rings.

The DAΦNE experimental studies about LRBB compensation, using built for the purpose wires and octupoles, yielded quite encouraging results and gave the opportunity, for the very first time, to test the wire compensation scheme in collision.

PARASITIC CROSSINGS IN IR1

In its original configuration DAΦNE consisted of two independent rings sharing two interaction regions: IR1 and IR2. Bunches experienced 24 PCs in each IR, 12 before and 12 after the main interaction point (IP), until splitter magnets drove them into two different rings.

The KLOE detector was installed in IR1. While delivering luminosity to KLOE [8] bunches collided with a horizontal crossing angle of 29.0 mrad, and were vertically separated in IR2 by a distance larger than 200 σ_y. For this reason, in the following considerations only LRBB interactions in IR1 are taken into account.

Table 1: Parameters for the Pcs, one every four, in IR1.

PC order	Z-Z_{IP} [m]	β_x [m]	β_y [m]	μ_x-μ_{IP}	X [σ_x]	Y [σ_y]
BB12L	-4.884	8.599	1.210	0.167230	26.9050	26.238
BB8L	-3.256	10.177	6.710	0.140340	22.8540	159.05
BB4L	-1.628	9.819	19.416	0.115570	19.9720	63.176
BB1L	-0.407	1.639	9.426	0.038993	7.5209	3.5649
IP1	0.000	1.709	0.018	0.000000	0.0000	0.0000
BB1S	0.407	1.966	9.381	0.035538	-6.8666	3.5734
BB4S	1.628	14.447	19.404	0.092140	-16.4650	63.196
BB8S	3.256	15.194	6.823	0.108810	-18.7050	157.74
BB12S	4.884	12.647	1.281	0.126920	-22.1880	25.505

Table 1 summarizes the main parameters for some PCs in the IR1: relative position, beta functions, phase advances with respect to the IP1 and transverse separation in terms of $\sigma_{x,y}$.

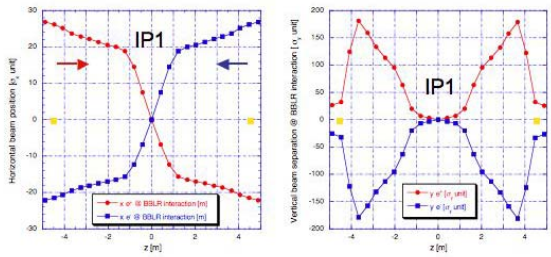

Figure 2: PCs horizontal (left) and vertical (right) beam-beam separation in the IR1 expressed in terms of $\sigma_{x,y}$ and computed for the KLOE optics. Arrows indicate the incoming direction of the positron (red) and electron (blue) beams, yellow dots show the place where the wires are installed.

The more evident effect of the LRBB interactions on the beam dynamics was provided by orbit deflection. In fact, the PCs induce orbit distortion that can be satisfactory reproduced by the machine model, based on the MAD [9] code, when the PCs are taken into account. MAD predictions agree with the orbit distortion obtained from the beam-beam simulation code Lifetrack [10] as well (see Fig. 3).

Moreover, the lifetime of each beam started decreasing during injection of the opposite beam and remained low soon after injection.

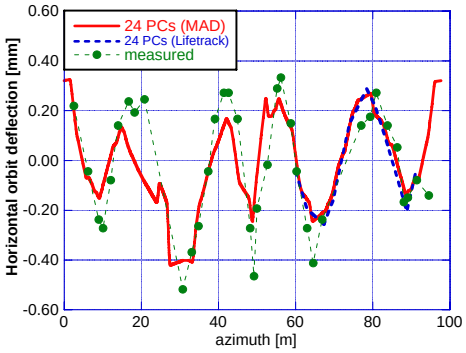

Figure 3: computed orbit deflection due to 24 BBLR interactions for a positron bunch colliding with an electron beam of 10 mA/bunch.

Typically, in collision, the electron beam current reached 1.8÷2.2 A, while the maximum positron beams is 1.3÷1.4 A. Exceeding these values the lifetime of the beams dropped down to 700÷800 sec.

This behaviour has been recognized as one of the main limitations of the collider performance.

NUMERICAL SIMULATIONS

The "weak-strong" tracking code LIFETRAC was used to simulate the equilibrium distribution of the positron ('weak') beam. The main sources of long beam tails were the 2 PCs nearest to the Main IP, but the other PCs also gave some contribution, so we accounted for all them. The wires were simulated as additional PCs with variable current ("wire-PC"), so that no special tracking algorithm for wires was used.

This approach was justified by the rather large values of the $\beta_{x,y}$ functions at the wire locations (16.5 and 4 m respectively), much larger than both the bunch and wire length. This allowed simulating the interaction with the wire as a single kick, neglecting the effect of displacements of the "strong" bunch: due to synchrotron oscillations the longitudinal coordinate of collision points for the real PC depends on the particle's longitudinal coordinate, while the wire are fixed, but due to the large beta values a shift of few millimetres gives actually no effect. On the other hand, the betas are small enough to produce a large separation in units of the transverse beam size (≈20), so that the actual "shape of wire" (i.e. density distribution inside the wire-PC) can be neglected: it works like a simple 1/r lens. Some simulation results are shown in Fig. 3.

The beam current was chosen to be large enough to yield long beam tails due to PCs (a), then the wires were switched on and the tails reduced (b). When the wires are powered with wrong polarity, the tails blow-up becomes even stronger (c).

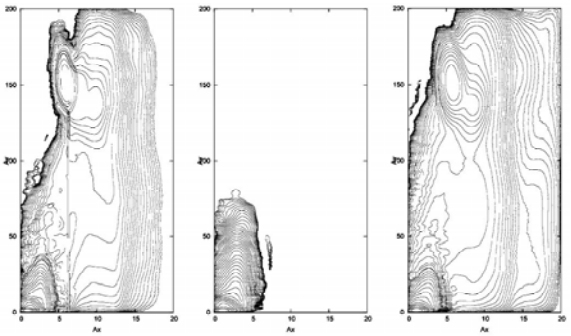

Figure 4: Particle equilibrium density in the normalized transverse phase space, starting from left: wires off (a), wires on (b) and wires powered with wrong polarity (c).

As a matter of fact, the PCs compensation with a single wire on each side of the interaction region was not perfect since distances between the beams at PC locations were different in terms of the horizontal sigma and phase advances between PCs and wires were not completely compensated (see Table 1). Indeed, the numerical simulations did not show improvements in luminosity. However, the positive effect of tails reduction and corresponding lifetime increase is very important, because it leads to a larger integrated luminosity.

WIRE DESIGN AND INSTALLATION

The wires have been built and installed in IR1 in November 2005. Each device was made by two windings of rectangular shape, 20 coils each, and installed symmetrically with respect to the horizontal plane, see Fig. 3.

Figure 5: The wires installed at one end of IR1.

Our device differs from the LHC one for several aspects: they were installed outside the vacuum chamber exploiting a short section in IR1, just before the splitters, where the vacuum pipes are separated to host Lambertson type correctors not essential for operation and therefore removed. The wires carried a tunable DC current, and produced a stationary magnetic field with a shape similar to the one created by the opposite beam.

EXPERIMENTAL RESULTS DURING THE KLOE RUN

A systematic study of the wires in collision has been undertaken during the machine shifts in March 2006.

The wires were powered at 3.6 A to compensate as much as possible the beam lifetime of the positron beam that, due to the limited maximum achievable current [11], can be considered as the 'weak' one.

It has been experimentally verified that the residual orbit distortions with maximum deviations of +0.4 -0.5 mm due to the PCs were very well corrected with wire currents of ≈1 A. This is a proof that the wires behaved as correctors "in phase" with the PCs. It has been also measured that the wires introduced some betatron tunes shifts.

The residual orbit distortion due to the wires at 3.6 A was corrected by the ordinary dipole correctors, while the tune shifts were compensated by means of the quadrupoles in a dispersion free straight section.

Several luminosity runs have been compared switching the wires on and off in order to study their impact on the collisions. In the following the two most relevant sets are presented taking into account 2 hours long runs. The results in Fig. 7 show some clear evidences. Switching on and off the wires we obtain the same luminosity while colliding the same beam currents. The positron lifetime is on average higher when wires are on, while the electron one is almost unaffected. The beam blow-up occurring from time to time at the end of beam injection, corresponding to a sharp increase in the beam lifetime, almost disappears.

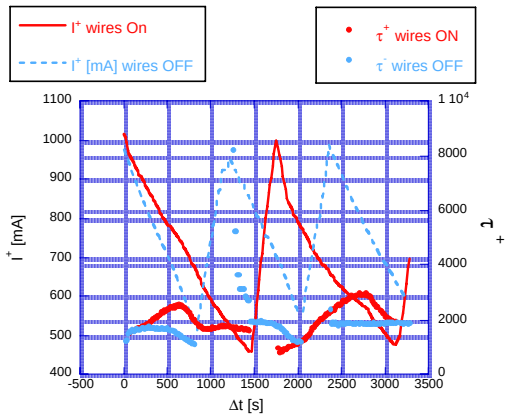

Figure 6: Positron current and lifetime as a function of time: wires on (red) and wires off (cyan).

A further aspect becomes evident when comparing, on the same plot, the positron current and lifetime with and without wires (see Fig. 6). The positron current starts

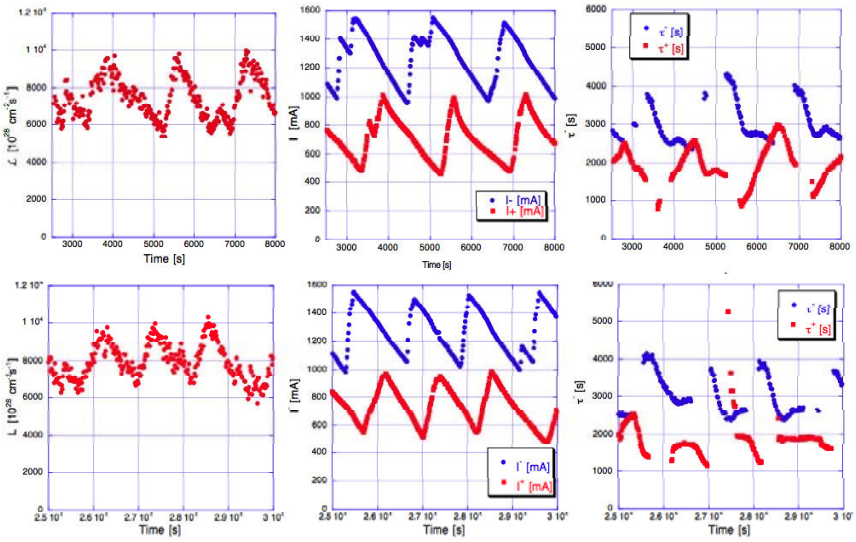

Figure 7: Luminosity, colliding currents and lifetime as a function of time: wires on (upper frames) and wires off (lower frames).

from the same value; then, in the case of wires off, the lifetime of the current is longer than in the case with wires on. In this way it is possible to keep the same integrated luminosity injecting the beam two times only instead of three in the same time interval, or to increase the integrated luminosity by the same factor keeping the same injection rate.

EXPERIMENTAL RESULTS DURING THE FINUDA RUN

During the upgrade [12] preceding the FINUDA run the KLOE detector has been removed and IR1 replaced with a straight section equipped with four electromagnetic quadrupoles. This was a much more flexible configuration in order to detune the optical functions in the unused IP, and to avoid further contributions to the betatron coupling.

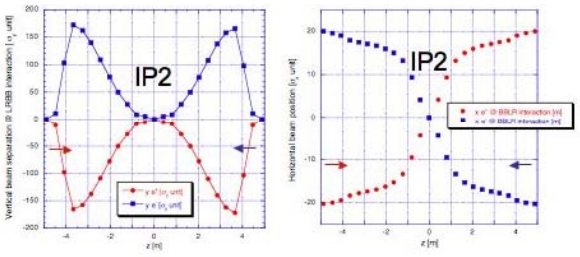

Figure 8: PCs vertical (left) and horizontal (right) beam-beam separation in IR2 expressed in terms of $\sigma_{x,y}$ and computed for the FINUDA optics. Arrows indicate the incoming direction of the positron (red) and electron (blue) beam.

The FINUDA IR was based on four permanent magnet quadrupoles placed inside the FINUDA 1.1 T solenoidal field and on four conventional quadrupoles installed outside it.

Despite the value of the betatron functions at IP2 were the same as during the KLOE run as well as the horizontal crossing angle, due to the different magnetic layout the PCs occurred at smaller beam separation (see Fig. 8) and were more harmful.

Using the wires for LRBB compensation at IR2 produced a few percent increase in the positron lifetime; however, the orbit deflection could not be corrected with a constant current in the wires.

A better compensation of the PCs occurring in IR1was obtained by halving β_y and increasing the beam vertical separation (~2 cm) at IP1, switching on at the same time the wires installed in IR1.

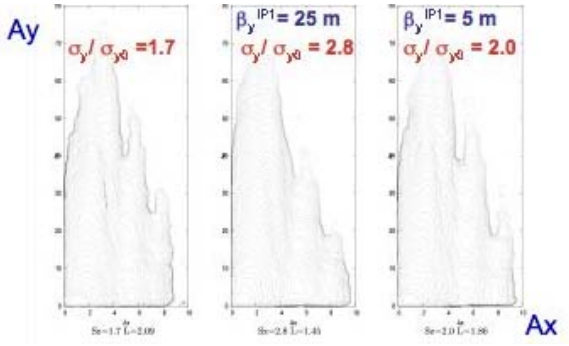

Figure 9: Particle equilibrium density in the normalized transverse phase space computed taking into account the main beam-beam interaction at IP2 (left), adding the contribution of the first PC at IP1, with 2cm vertical separation and a β^{IP1}_y = 25 m (center), and β^{IP1}_y = 5 m (right).

Beam-beam simulations, showing the transverse beam blow-up dependence on parasitic crossings, for a given beam-beam separation, have been useful in this optimization process as can be seen from Fig. 9.

NON-LINEARITY INTERPLAY

LRBB interaction originates nonlinear fields, which interfere and add up with the non-linear terms coming from the ring lattice.

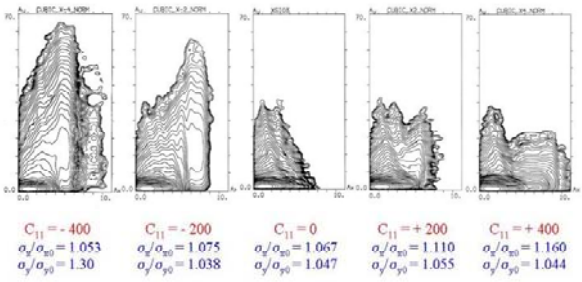

Figure 10: Particle equilibrium density in the normalized transverse phase space computed taking into account the main interaction point and different C_{11} (unit m^{-1}) values, for each case the relative variation of the transverse horizontal and vertical dimension are reported.

Such interplay has been studied combining experimental measurements and theoretical simulations [13]. The tune shift on amplitude (C_{11}) measurement provided an efficient and simple way to evaluate the lattice contribution to the nonlinear terms for each ring, independently from the influence of PCs.

Simulations have been used to understand the mutual interaction between the two contributions. Fig. 11 shows the growth of the transverse beam dimensions in the case when the main interaction point and the tune shift on amplitude are taken into account. An evident transverse beam blow-up appears when $|C_{11}| > 200\ m^{-1}$.

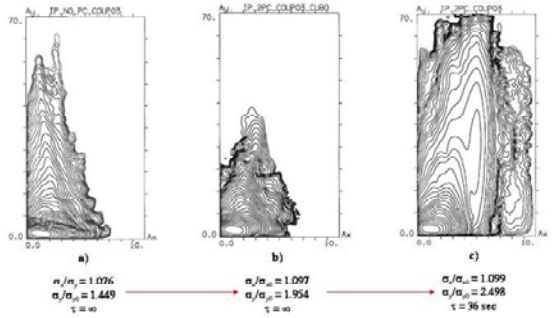

Figure 11: Particle equilibrium density in the normalized transverse phase space computed taking into account the main beam-beam interaction at IP2 (left), adding the contribution of the first PC at IP1, with 2cm vertical separation and a β^{IP1}_y = 25 m (center), and β^{IP1}_y = 5 m (right).

When also the first PC was considered the growth in the beam transverse dimensions became even more evident, see Fig. 11, especially for $C_{11} > 0$ affecting mainly the transverse vertical plane.

Unlike the strength of the nonlinear component coming from the lattice, which is fixed, the one due to the PCs depends on the current stored in the colliding bunches. As a result the overall nonlinear term affecting the beam dynamics can have a considerably excursion as the colliding currents decay. Such effect has been clearly observed especially during the last FINUDA run mostly for the positron beam, which at the maximum current, just after injection, had a very low lifetime, less than 500 s. By tuning the working point and the electromagnetic octupole, during the injection, it has been possible to double the positron beam lifetime at its maximum current. The working point was moved toward the integer and the octupole current increased consistently with nonlinearities compensation.

PARASITIC CROSSINGS IN THE UPGRADED DAΦNE RINGS

Relying on the experience gained about LRBB compensation during the KLOE and FINUDA runs the two DAΦNE IRs have been modified in view of the SIDDHARTA experiment run [14, 15], which will be also used to test a new collision scheme based on large Piwinski angle and *crab-waist* [17]. The vacuum pipe [16] in the unused IR2 provides now complete beam separation while the one in IR1 consists of straight pipes, different for each beam, merging in a *Y* shaped section just before the *low-beta* defocusing quadrupole. This new layout almost cancels the problems related to beam-beam long range interactions, because the two beams experience only one parasitic crossing inside the defocusing quadrupole where, due to the large horizontal crossing angle, they are very well separated ($\Delta x \sim 20\ \sigma_x$). It is worth reminding that in the old configuration the colliding beams had 24 parasitic crossing in the IRs and in the main one the separation at the first crossing was in the range $\Delta x \sim 4 \div 7\ \sigma_x$, as can be seen from Fig. 1 and Fig. 6.

CONCLUSIONS AND ACKNOWLEDGMENTS

Current-carrying wires and octupoles have been used in order to compensate LRBB interactions and crosstalk between beam-beam effects and lattice nonlinearities.

Weak strong simulations proved to be reliable and helpful in finding the proper approach to the compensation of nonlinearities coming from LRBB interaction and from the ring lattice as well.

The wires installed in the DAΦNE IRs proved to be effective in reducing the impact of BBLR interactions and improving the lifetime of the positron beam especially during the KLOE run.

Studying and understanding the impact of the parasitic crossing at DAΦNE had a relevant impact on the definition of the new criteria adopted in the design of the new IRs for the DAΦNE upgrade.

We are indebted to G. Sensolini, R. Zarlenga and F. Iungo for the technical realization of the wires.

REFERENCES

[1] G. Vignola et al., Frascati Phys.Ser.4:19-30,1996;
C. Milardi et al., Frascati Phys.Ser.16:75-84,1999.
[2] C. Milardi et al., PAC07, p. 1457.
[3] D. Alesini et al, LNF-06/033 (IR), 2006.
[4] J.P. Koutchouk, LHC Project Note 223 (2000)
[5] J.P. Koutchouk et al., EPAC2004, p. 1936.
[6] F. Zimmermann et al., PAC2005, p.686.
[7] T. Sen, PAC2005, p.2645.
[8] A. Gallo et al., EPAC2006, p.
[9] H. Grate et al., "The MAD Program".
[10] D. Shatilov, Particle Accelerator 52:65-93, 1996.
[11] C. Milardi et al., e-Print: physics/0607129.
[12] C. Milardi et al., PAC07.
[13] M. Zobov, Physics/0311129.
[14] M. Zobov for DAΦNE Team,ARXIV:0709,3696.
[15] C. Milardi et al., this Workshop
[16] P.Raimondi, D.Shatilov, M. Zobov, physics/0702033.
[17] S. Tomassini et al., PAC07, p. 1466.

Wire compensation: Performance, SPS MDs, pulsed system

U. Dorda, F. Zimmermann, CERN, Geneva, Switzerland

Abstract

A wire compensation (BBLR) scheme has been proposed in order to improve the long range beam-beam performance of the nominal LHC and its phase 1 and phase 2 upgrades[1]. In this paper we present experimental experience of the CERN SPS wires (BBLR) and report on progress with the RF BBLR.

SPS MDS

Two wire compensators are installed in the CERN SPS (Fig. 1). They are located at positions with about equal beta functions in the transverse planes ($\beta \approx 50$ m) and are separated by a betatron phase advance of $\Delta\Phi \approx 3°$. Each one can be powered with an integrated DC current of up to $I_{\max} \cdot l_{\mathrm{BBLR}} = 360 A\mathrm{m}$. While a single BBLR allows simulating long-range beam-beam interactions, as a pair they can be used to test the compensation. It must be noted that there is no-head on collision in the SPS and thus no head-on related tune spread. The situation therefore differs from the real LHC case. Still it allows us to gain experimental hints and to benchmark simulations. In the experiments, it was always attempted to correct for the linear orbit and tune changes due to the BBLR.

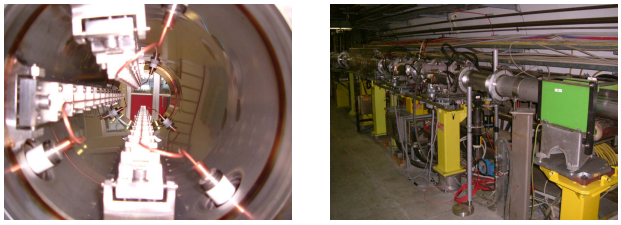

(a) BBLR 2 contains 3 wires (b) The BBLR in the SPS tunnel

Figure 1: The SPS BBLR

Figure 2 a) shows one of the first results obtained in 2002: A beam-wire separation scan of one BBLR with a current equivalent to the integrated effect of 60 LHC long-range beam-beam interactions. The result indicates that a beam-beam separation of 9.5σ may to be acceptable. Subfigure b) shows a tune scan of the wire compensation which proves that the unperturbed beam lifetime can be restored over a wide tune range. The loss of compensation efficiency at lower tune values is not yet understood.

Figure 3 shows the compensation for various parameters of the second BBLR. The best compensation is achieved at equal BBLR strength and an offset of 1mm with respect to the position of the first BBLR, due to a difference in the β function and a assumed 0.5mm relative alignment error.

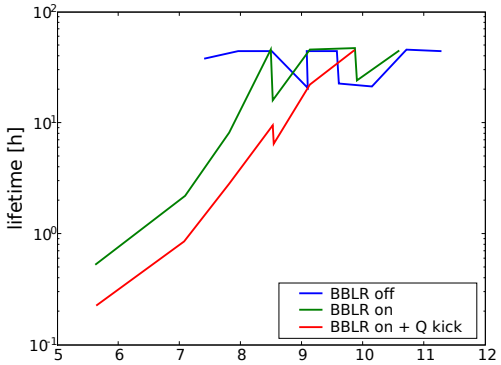

(a) Beam - wire distance scan with a wire current equivalent to the integrated effect of 60 LHC long-range beam-beam collisions.

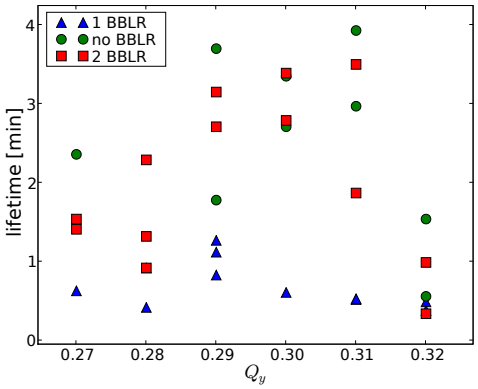

(b) Tune scan of the BBLR compensation

Figure 2: Compensation tests in the CERN SPS. Beam lifetime as a function of the beam wire distance (a) and as a function of the vertical betatron tune (b).

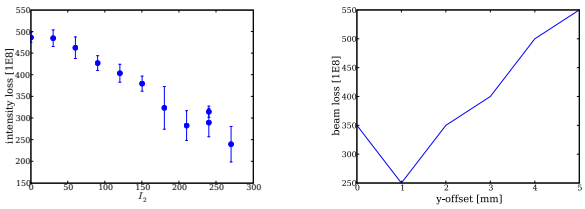

(a) Wire current scan of the compensating BBLR2 (b) Position scan of the second compensating BBLR

Figure 3: Beam loss as a function of the current and relative position of the second BBLR with respect to the first (19mm from the beam,250Am)

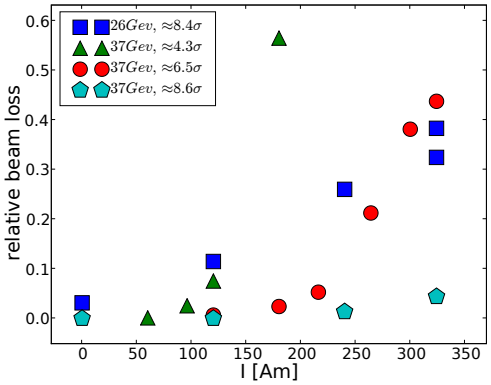

(a) Indication of a threshold effect.

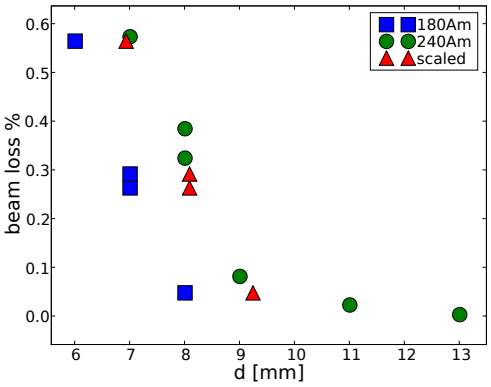

(b) A current scaling fits the expectation

Figure 4: Beam loss over s at various beam energies, normalized beam-wire distances and excitation currents

In 2007 we had the opportunity to perform experiments at various energies (26, 37 and 55 GeV). Figure 4 a) shows the relative beam loss as a function of the BBLR current for various beam-wire separations d at two energies. There are indications for a threshold effect at 37GeV, which might be attributed to the limited geometric aperture of the SPS (the beam is cut at 4σ) or/and to the limited measurement resolution. Subfigure b) shows experimental data of a d-scan at two wire currents as well as one dataset scaled in current according to [2], which is in good agreement with the 240Am data. The scaling law requires that for an identical DA the value of $I/(n^2\epsilon)$ (where n is the normalized beam-wire separation) must be the same.

RHIC observed first hints of a strong chromaticity dependence of the beam-loss in the RHIC BBLR studies of 2007. This was followed up and confirmed in the 2007 SPS MDs (Fig. 5)

PULSED BBLR

In the nominal LHC almost half of the bunches will be PACMAN bunches - bunches at one or the other end of the bunch train that experience a reduced number of long

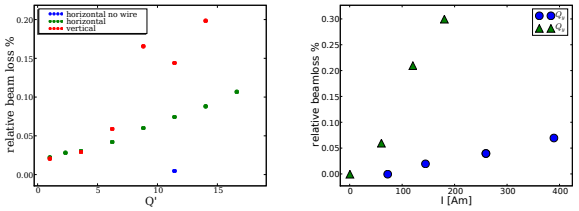

(a) (b)

Figure 5: Chromaticity dependence observed in the SPS for d=6.6σ at 55 GeV

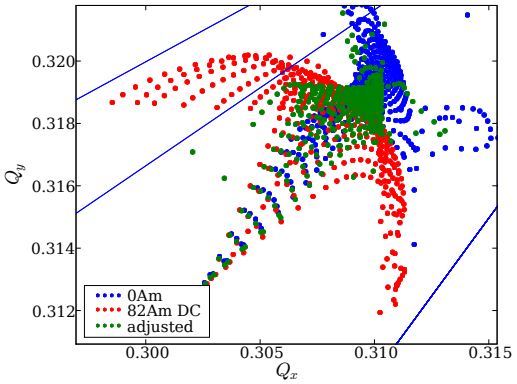

(a) Tune footprint for the extreme Pacman bunch without wire excitation, with a DC wire optimized for nominal bunches (82Am) and with a compensation adjusted to minimize the tune foot print of the extreme Pacman bunch

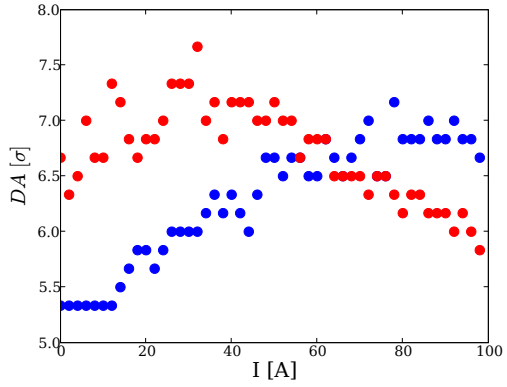

(b) The Dynamic Aperture (DA) for nominal bunches and the extreme Pacman bunch as a function of the compensation current

Figure 6: Motivations for adjusting the BBLR strength for PACMAN bunches

range interactions. While a constant intermediate wire current level could improve the stability of both, the nominal and the Pacman bunches, an individually adjusted wire current could enhance the performance even further. Figure 6 illustrates this for the case of the extreme Pacman bunch, which is the bunch at the very end of each bunch train and thus does not experience any LRBB on one side of IP1 and IP5.

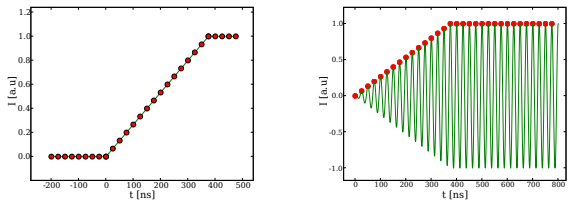

(a) Pulsed DC BBLR (b) RF-BBLR

Figure 7: Comparison of a ramped DC to a RF approach. The red dots indicate the moments when a specific current-value is required, the green line the actual current on the wire.

Until recently a ramped DC approach as indicated in Figure 7 a) was followed. But as this approach led to unfulfillable hardware requirements, an alternative approach - the RF-BBLR based on the idea of F. Caspers, shown in Figure 7 b) - is now pursued, where instead of creating a linear slope a pulsed RF signal is used.

The RF-BBLR is based on a $\lambda/4$ resonator as indicated in Figure 8 a). The advantages of a RF-BBLR are the following:

- Zero slope of the current at the moment of the LRBB encounters reduce the required timing precision.
- Required RF technology is available.
- RF fields are easier to shield
- As the waves are counterpropagating to the beam (Fig 8 b) the magnetic and electric effects add up and therefore the power requirements are reduced by a factor of 4.
- A resonating structure should very reliable and the power losses should be limited.
- The power generator can be placed on the surface with only a passive radiation hard transformer installed in the tunnel.

Any turn to turn current jitter causes emittance growth. While for a ramped DC BBLR the amplitude jitter is linearly proportional to the timing jitter, this is not the case for a RF-BBLR. Allowing a $\Delta\epsilon < 10\%$ over 20h for a linearly pulsed BBLR the amplitude noise must be kept lower than $\Delta I < 3\mathrm{mA}$ which corresponds to $\Delta t < 0.02\mathrm{ns}$. For a RF-BBLR this tolerance is increased to $\Delta t < 0.126\mathrm{ns}$. This value can be further relaxed if the orbit feedback works well or if a feedback is integrated into the power generator.

First experimental prototypes have been built and tested. In Figure 9a) it can be seen that the prototype behaves like a resonator with well defined resonances. Subfigure b) shows the experimental verification of the RF-BBLR principle at low power. The response on the BBLR to an excitation by a pulsed RF-voltage is an oscillating current whose amplitude linearly increases and then saturates at a constant level.

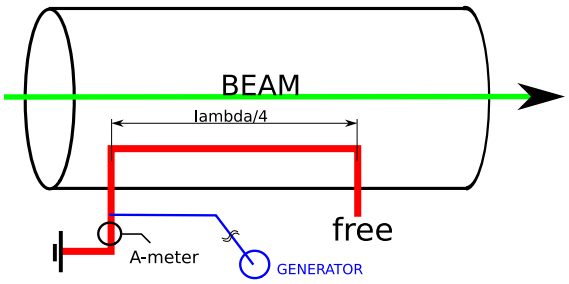

(a) The RF BBLR is based on a resonating structure

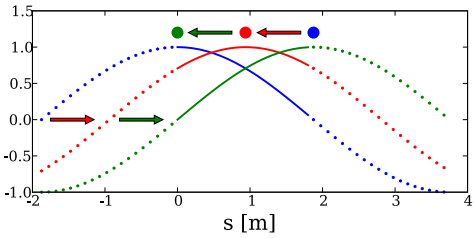

(b) The electromagnetic waves on the wire and the beam counter-propagate

Figure 8: Schematic layout and wave propagation for the RF-BBLR

Therefore the signal reproduces the target shape shown in Fig.7. In a parallel effort, the RF-properties of the existing BBLRs installed in the SPS were characterized in terms of their interaction with the beam and their resonant behavior. Figure 10 shows a beam induced signal that refelects the bunch pattern. This beam-induced current will need to be measured and be taken care of by a feedback system. Subfigure b) shows the result of resonance measurements, where the arrows indicate the contributions from the BBLR itself and those from the connecting coaxial cable, respectively. The next steps towards a usable RF BBLR will be:

- Building a phase-noise measurement setup especially adapted for one-turn sensitivity
- Field simulations of the RF-BBLR
- Building a high power version

For all these actions a dedicated budget is required.

CONCLUSIONS

The SPS BBLR MDs have proven to be a valuable source of data, helping to understand the long range beam-beam interaction and its compensation. The 2007 MDs have scanned a large parameter space and in particular explored the energy scaling, the possible thresh-

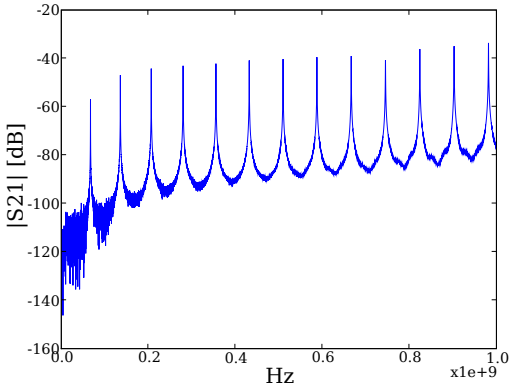

(a) Measuring the resonant structure: S11

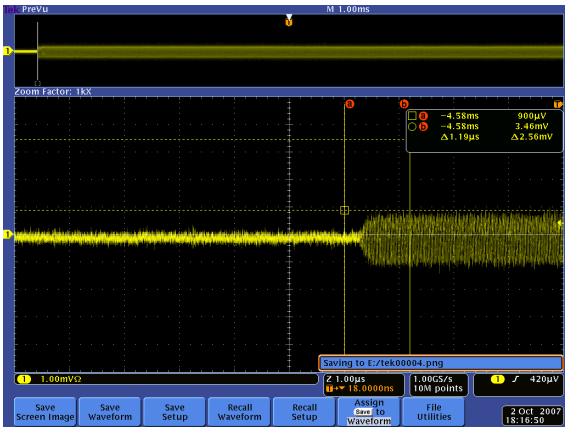

(b) Current on the BBLR as a function of time for a excitation by a pulsed RF-signal.

Figure 9: Results from the experimental RF-BBLR prototype.

old behavior and its chromaticity dependence. The RF-BBLRdevelopment is rapidly advancing.

Thanks

The authors want to thank F. Caspers, T. Kroyer for the fruitful co-operation on the RF-BBLR. The help of J. Wenninger, R. Calaga, R. Tomas, J.P Koutchouk and G. Sterbini in the SPS MDs is gratefully acknowledged. I acknowledge support by the European Community-Research Infrastructure Activity under the FP6 Structuring the European Research Area programme

REFERENCES

[1] U. Dorda & F. Zimmermann, "Beam-beam issues for LHC upgrade phase 1 and 2', these proceedings

[2] F. Zimmermann, "Scaling of Diffusive Aperture with Wire Current", unpublished [http://cern-ab-bblr.web.cern.ch/cern%2Dab%2Dbblr/documentation.htm], 2003

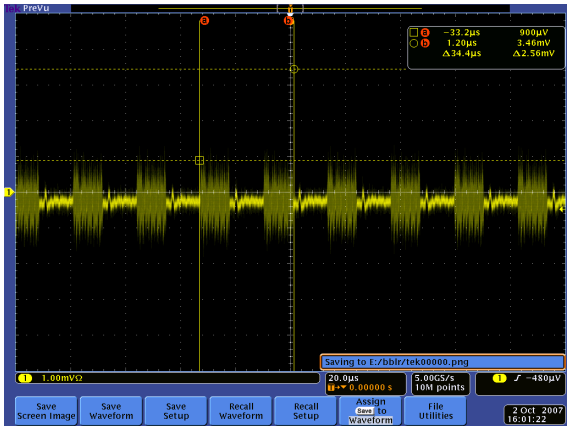

(a) Signal induced in the SPS BBLR by a bunch train.

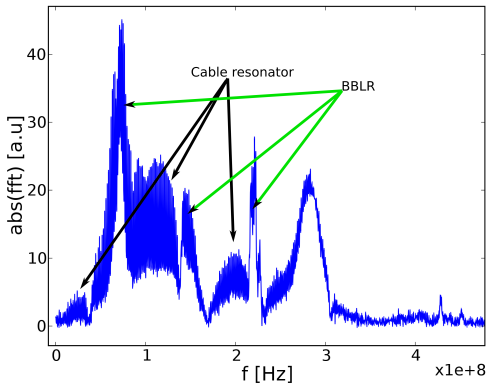

(b) Resonant structure. The contributions of the BBLR itself can be clearly separated from the effect due to the connecting cable.

Figure 10: The CERN SPS BBLRs

Small angle crab crossing for the LHC *

R. Calaga, BNL, Upton, NY 11973, USA
U. Dorda, R. Tomás, F. Zimmermann, CERN, Geneva, Switzerland

Abstract

A small angle crab compensation (∼0.5 mrad) is foreseen to improve the LHC luminosity independently of the IR upgrade paths to enhance the luminosity of the LHC by 15% for the nominal and factor of 2-3 for various upgrade scenarios. Crab cavities ensure head-on collisions and recover the geometric luminosity loss from the presence of a finite crossing angle at the interaction point (IP). An R&D program is underway to design and fabricate superconducting RF (SRF) prototype cavity at 800 MHz to test several SRF limits in the deflecting mode. If the prototype is installed in the LHC, it can be used for a first demonstration of crab crossing in hadron beams to understand potential emittance growth mechanisms due to crab cavities.

INTRODUCTION

The upgrade plans (phase I & II) of the LHC aim to increase the luminosity by a factor of 2-10. The luminosity gain is achieved mainly via an interaction region (IR) upgrade along with an increase of the bunch current. The IR upgrade involves reducing the collision point β-functions from a nominal β^* of 0.55 m to a β^* of 0.25 m or in some extreme cases to a value as small as 0.08 m. Some relevant parameters of the LHC for both nominal and upgrade options are listed in Table .

Regardless of the final choice of magnet technology and optics layout, most schemes will have a finite crossing angle with which the bunches collide at the IP. This crossing angle translates to a geometric luminosity reduction factor which increases steeply with decreasing β^* as

$$\frac{L}{L_\circ} \approx \left[1 + \left(\frac{\sigma_z}{\sigma_x^*}\tan\left(\theta_c/2\right)\right)^2\right]^{1/2}$$

An elegant mitigation using crab cavities, first proposed by Palmer in 1988 for linear colliders, and later extended to circular colliders by Oide and Yokoyo is expected to compensate the geometric luminosity loss due to the finite crossing angle. Crab crossing has been demostrated at KEK-B (e^-/e^+ storage ring) and is actually operational since April 2007. Fig 1 shows a plot of the luminosity gain as a function of reduced β^* for the LHC with and without crab crossing.

The effect of crab cavities become clearly evident when the curves with crab crossing is compared to the red curve resulting from an upgrade without crab crossing. The crossing angle has to be increased in proportion to the reduction of β^* to provide the required beam separation to combat long range beam-beam effects. Therefore, without crab cavities the effective gain in the luminosity is significantly less than the case with crabs as seen in Fig. 1. The finite RF wavelength in the crab cavities gives rise to an associated residual reduction factor which is included in the luminosity calculation. This reduction factor is small for small crossing angles (<1 mrad) but it may become significant for larger crossing angles at higher frequencies [1]. A large angle crab scheme (8 mrad) proposed in 2006 [1]

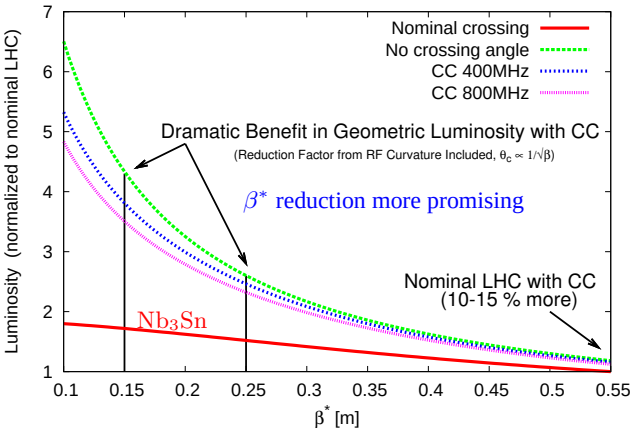

Figure 1: Luminosity scope showing the dramatic benefit of the crab compensation at smaller β^*. Note that the effect of RF curvature of the crab cavities is included.

was deemed risky since the feasibility of the upgrade would solely depend on the crab cavities which have never been tested in hadron machines. Therefore, a small or a moderately increased angle crab scheme is proposed to compensate the existing crossing angle. Two different crab schemes and and related technological issues will be discussed in the following sections.

LOCAL & GLOBAL SCHEME

For the upgrade, two crab schemes are under consideration that address different spatial and technological constraints posed by the LHC lattice. In a local scheme the conventional crab crossing layout is employed where two cavities are placed $\pi/2$ in phase advance on either side of the interaction point (IP). The first cavity tilts the incoming bunch with finite crossing angle to ensure a effective head-on collision and the second cavity tilts the head and the tail of the bunch back to its original closed orbit leaving the rest of the machine unperturbed. The transverse kick volt-

* We acknowledge the support of the European Community-Research Infrastructure Activity under the FP6 "Structuring the European Research Area" program (CARE, contract number RII3-CT-2003-506395). This work was partly performed under the auspices of the US Department of Energy

Table 1: Some relevant parameters for the LHC nominal and upgrade lattices.

Parameter	Unit	Nominal	Upgrade
Circumference	[km]	27	27
Beam Energy	[TeV]	7	7
Number of Bunches	n_b	2808	2808
Protons/Bunch	$[10^{11}]$	1.15	1.7
Average current	[Amps]	0.58	0.86
Bunch Spacing	[ns]	25	25
Norm Emmit: ϵ_n	[μm]	3.75	3.75
Bunch Length, σ_z (rms)	[cm]	7.55	7.55
$IP_{1,5}$ β^*	[m]	0.55	0.25
Betatron Tunes	-	{64.31, 59.32}	{64.31, 59.32}
Beam-Beam Parameter, ξ	per/ip	0.003	0.005
Effective Crossing Angle: θ_c	[μrad]	285	445
Piwinski Parameter	$\frac{\theta_c \sigma_z}{(2\sigma^*)}$	0.64	0.75
Main RF Frequency	[MHz]	400.79	400.79
Harmonic Number		35640	35640

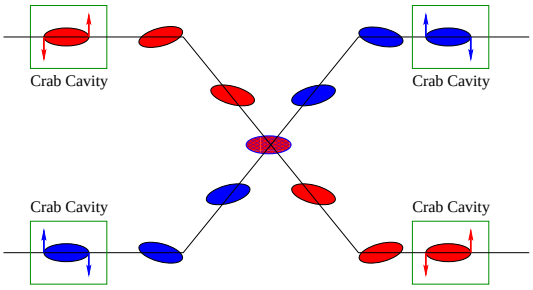

Figure 2: Local crab compensation scheme using transverse deflecting cavities near the IP to provide head-on collisions.

age required is

$$V_{crab} = \frac{cE_0 \tan(\theta_c/2)}{\omega_{RF}\sqrt{\beta_{crab}\beta^*}} \qquad (1)$$

where E_0 is the beam energy, ω_{RF} is the RF frequency of the cavity, β_{crab} and β^* are the beta-functions at the cavity and the IP respectively. The nominal beam-to-beam line separation is <20 cm in most of the LHC ring except for the region near IR4 where it is ∼40 cm [3]. Conventional elliptical cavities with frequencies < 1 GHz may become difficult to accommodate transversely. However, the effect of the finite RF curvature and long bunches prefer lower frequencies. Therefore, a compromise between the physical and RF constraints may require a frequency choice of 800 MHz with some IR beam line modifications unless a new compact design with a frequency of $<$ 800 MHz can be conceived.

An alternate version of the crab compensation where cavities located elsewhere in the ring satisfy certain phase advance conditions to the IP can alleviate some of the space constraints in the local scheme. This concept was successfully commissioned and now in operation at KEK-B [2].

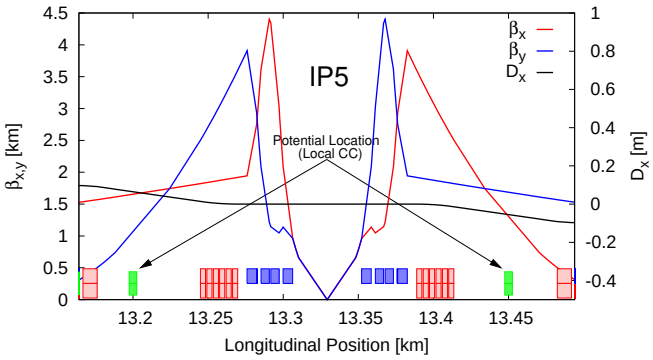

Figure 3: Optics function for the nominal LHC collision in IR5 region and potential locations for local crab cavities. The IR1 will have a similar configuration.

In this scenario, the head and the tail of the bunch oscillate around a reference closed orbit around the ring with a effective head-on collision at the IP. The transverse kick voltage required for one IP with a single cavity in the global case is given by

$$V_{crab} = \frac{2cE_0 \tan(\theta_c/2) \sin(\mu_x/2)}{\omega_{RF}\sqrt{\beta_{crab}\beta^*}\cos(\psi^x_{cc\to ip} - \mu_x/2)} \qquad (2)$$

where $\psi^x_{cc\to ip}$ is the phase advance from the cavity to the IP and μ_x is the betatron tune. For n IP's with m cavities, a system of linear equations can be solved to derive the respective voltages for the cavities, using an obvious generalization of Eq. 2.

It should be noted that constraints from dynamic aperture and collimation limit this scheme to small crossing angles ($<$ 1mrad) because of the additional z-dependent closed orbit introduced by the oscillating bunch [1].

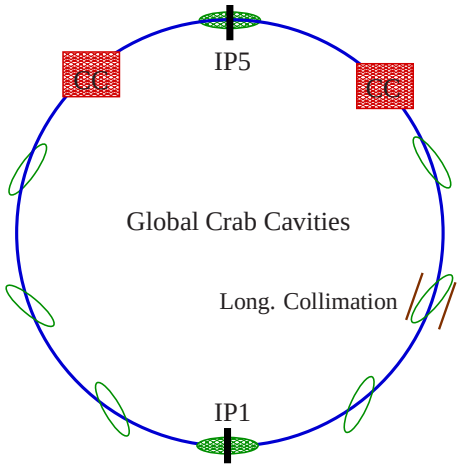

Figure 4: Schematic of a possible global crab crossing scheme to have head-on collisions at IP1 and IP5.

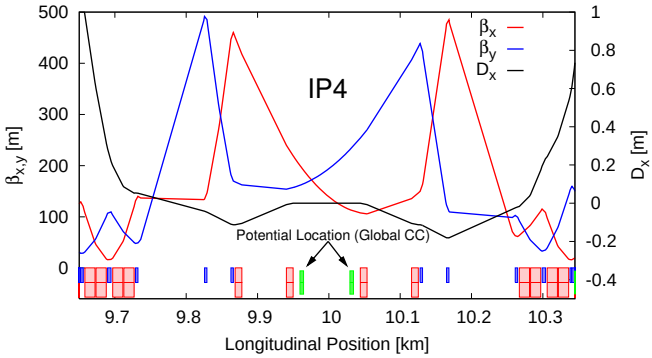

Figure 5: Optics function for the nominal LHC at 7 TeV and potential locations for a global crab cavity in the IR4 region.

CAVITY DESIGN

An LHC baseline design with superconducting RF elliptical cavities conceptually similar to KEK-B design is considered. In the view of the bunch length and RF curvature lower frequencies are more desirable. However, the cavity dimensions and space constraints prefer a higher frequency. An intial crab crossing proposal with large crossing angle (8 mrad) lead to a development of a 400 MHz design [1]. For small crossing angles (∼0.5 mrad) which is the current baseline, an 800 MHz cavity appears to be a good compromise. The corresponding geometric luminosity reduction is as seen in Fig **??**. A coupled two-cell cavity is being considered as a fundamental unit in the π mode to impart a total kick of ∼2.5-3.0 MV per module (∼2.5-3.0 MV/m including cryostat). For reference, the KEK-B cavities achieved a field gradient of approximately 2 MV/m or a bit higher, limited mainly by multipacting and/or field emission near the iris region consisting of co-axial coupler [4]. A schematic of the original semi-optimized two-cell LHC cavity at 400 MHz and a scaled 800 MHz prototype is shown in Fig. 6. The relevant geometrical parameters of the cavity structure are listed in Table 2.

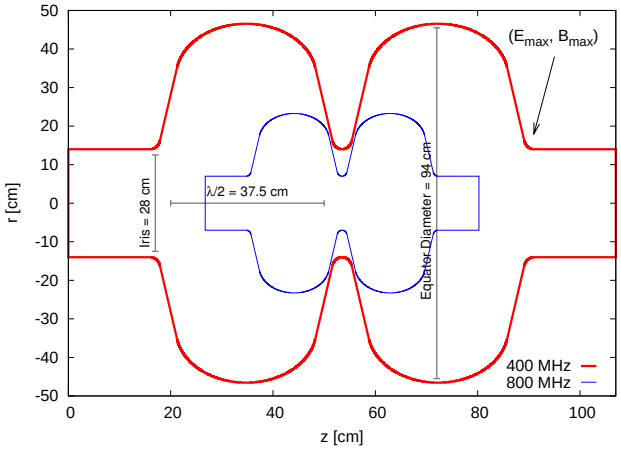

Figure 6: Graphic of the proposed two-cell 400 MHz cavity and a scaled 800 MHz cavity.

Table 2: Cavity geometrical parameters for inner and outer $\frac{1}{2}$ cells for 400 MHz. The 800 MHz cavity is a scaled model with same geometrical ratios.

Parameter	Crab Cavity	
	Middle Cell	End Cell
Frequency [MHz]	400	400
Iris Radius, R_{iris} [cm]	14	14
Wall Angle, α [deg]	10	10
Equatorial Ellipse, $R = \frac{B}{A}$	1.0	1.0
Iris Ellipse, $r = \frac{b}{a}$	1.5	1.5
Cav. wall to iris plane, d [cm]	1.5	1.5
$\frac{1}{2}$ Cell Length, $L = \frac{\lambda\beta}{4}[cm]$	18.75	18.75
Equator Height, D [cm]	50	50
Cavity Beta, $\beta = v/c$	1.0	1.0

An extensive scan of the cavity geometric parameters was performed to obtain the optimum RF characteristics for the inner and outer half-cell of the two-cell cavity. The relevant RF parameters for the superconducting cavities are plotted as a function of the respective geometrical parameters in Fig. 7.

For crab cavities, the ratio of the peak surface fields to total kick voltage is much larger than a typical accelerating cavity. It must be noted that the tabulated geometrical values are not final. A a first step the same geometric parameters are chosen for both middle and end cells. The final optimization will be based on higher order mode (HOM) damping, peak field specifications, and mechanical constraints. For example, the maximum achievable kick voltage for the two cell cavity will be limited by the peak surface magnetic field. An increase in wall angle (α), iris ellipse ratio (r), and cavity wall distance to the iris plane (d) can significantly reduce the magnetic field without compromising the other RF parameters. If a further decrease

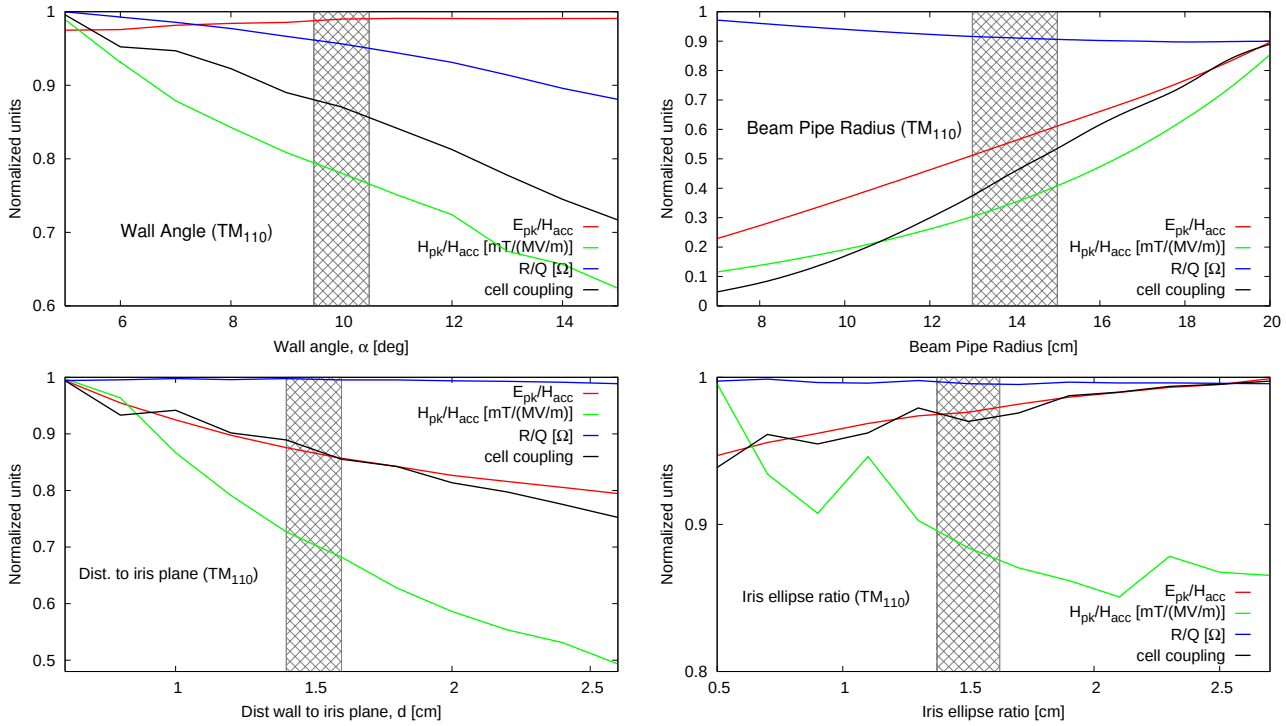

Figure 7: Cavity geometrical parameters as a function of relevant RF parameters leading to an input for optimization of the $\frac{1}{2}$ cell geometry.

in peak fields is needed, a reduction in the beam pipe is necessary. However, this might lead to the trapping some HOMs. A fine tuning of the cavity shape may increase the kick gradient providing for margins for optics as well as longitudinal space requirements.

Based on the semi-optimal choice of geometrical parameters listed in Table 2, some relevant RF characteristics of the final two-cell cavity design are listed below:

- Peak Fields (B_{kick}: 2.5 MV, 400-800 MHz):
  - E_{peak} $\sim$ 18-30 MV/m. The highest surface fields so far have been demonstrated in TESLA cavities which reached 70-90 MV/m. The limitation is believed to be due to field emission.
  - B_{peak} $\sim$ 93-125 mT. The highest surface fields have again been demonstrated in TESLA cavities which have reached upto 150-190 mT. The theoretical limit in type II superconductors like Nb is approximately 220mT which is caused due to breaking of cooper pairs.
  - The ratio $B_{peak}/B_{kick} \approx 12$ is large compared to typical accelerating cavities with a ratio of 4-5. Modifications to the cavity geometry suggested above can be used to reduce the peak magnetic field.
- The transverse shunt impedance is given by

$$\frac{R_\perp}{Q_0} = \frac{1}{(kr)^2 \omega U} \int_0^L E_{z(r=r_0)} e^{ikz} dz \quad (3)$$

$$\approx 120\ \Omega\ \{800\text{MHz}, 2\text{Cells}\} \quad (4)$$

- An orbit offset of the crab cavity can result in beam loading which is given by

$$V_b \approx Q_L I_b \frac{R_\perp}{Q}(\delta x) \quad (5)$$

$$\approx 0.1\ \frac{MV}{mm}\{Q_L = 10^6, I_b = 0.85A\} \quad (6)$$

  Local orbit correctors around the cavity can be envisioned to control the beam orbit at the sub-millimeter level. The input and HOM power from the cavity naturally provide a feedback signal to precisely center the beam in the magnetic center of the cavity.
- A Power of 2-20 kW may be required ($Q_L = [10^5 - 10^6]$) for beam loading, cavity conditioning, microphonics, Lorentz force detuning and other mechanical effects. Sources at these power levels for 800 MHz frequency are commercially available in the form of inductive output tubes (IOTs).

Since the mode of choice is a dipole mode, the parasitic mode with the orthogonal polarization needs to be well separated in frequency and damped to avoid creating a spurious crossing angle in the other transverse plane. A mode

separation of about 50 MHz for the 400 MHz design and of a similar magnitude for the 800 MHz can be achieved by squashing the cavity transversely by design to a ratio of 0.75 [1]. The beam harmonics are separated by 40 MHz (bunch spacing 25ns). Therefore, there is sufficient frequency space to adequately separate the orthogonal mode and avoid overlap with beam harmonics.

COUPLERS & TUNERS

A combination of couplers and beam pipe ferrites need to be employed to both supply the input power for the mode of operation and to extract lower order (LOM) and higher order modes (HOMs). Some possible options for the required couplers are:

- A co-axial coupler will be used to provide the input power for the deflecting operating mode. Dual couplers and contoured co-axial tips as shown in Fig. 8 can be used to minimize the coupler kicks and wakefield effects.

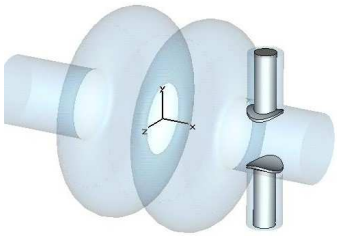

Figure 8: Dual coaxial couplers with optimized pringle shaped tips to reduce the effect of short range wakes and transverse coupler kicks.

- A beam Pipe co-axial line as depicted in Fig. 9 can be used to extract both the LOM and HOMs similar to the KEK-B damping scheme. A choke rejection filter can be tuned for the operating mode and all the other modes can be transmitted to a room temperature ferrite absorber. Damping of most modes to $Q_{ext} \sim 10^2$ has been demonstrated at KEK-B with such a scheme. However, the assembly of this coupler is fragile and poses significant technical challenges in addition to leading to potential multipacting near the high field region.

- A waveguide coupler can be substituted for the beam pipe coax (see Fig. **??**) but the damping is limited to $Q_{ext} \sim 10^3$ [5]. This setup is structurally robust and longitudinally compact, but it has yet to be determined if the damping provided by the waveguides is sufficient for high current operation in the LHC.

- New concepts (for example: radial beam-pipe coax) may need to be developed to provide the equivalent damping of the beam-pipe coaxial line while having the virtue of being compact and more robust like

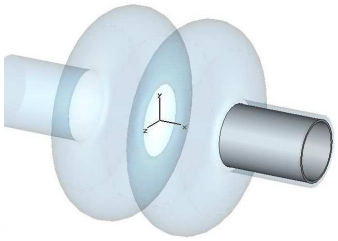

Figure 9: Beam pipe coax with a choke rejection filter to reject the kick mode (TM_{110}) and to couple to all other modes strongly.

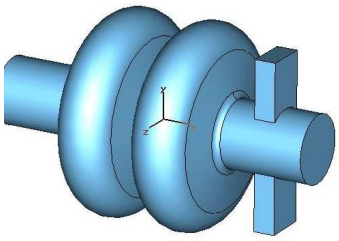

Figure 10: Waveguide couplers to extract LOM & HOM modes from the cavity.

waveguides. Simulations are underway to test the effectiveness of radial type couplers.

- TESLA type loop couplers can be used but perhaps limited by their inability of handing CW power. The cavity design along with the beam-pipe will be optimized to effectively propagate most HOMs through the beam pipe to a room temperature ferrite which can handle power levels of 10-20 kW.

Tuning of the operating mode, the LOM and the relevant HOMs may become necessary to minimize input power and to avoid the overlap of harmful resonances with beam harmonics. The two available tuning mechanism are:

- A beam-pipe coaxial coupler can also be used for tuning. This system is used in the KEK-B cavities where it has proven to be effective and simple during operation. This system also allows a large tuning range due the direct coupling to electro-magnetic fields.

- Conventional tuners (for example: mechanical push-pull) have been demonstrated extensively on accelerating cavities. In addition, the presence of both peak magnetic and electric fields at the iris of the cavity can be exploited by "iris based tuners" which deform only the irises of the cavity. The latter may provide a more efficient and larger tuning range compared to conventional cavity body tuners.

PHASE NOISE & EMITTANCE GROWTH

Several sources of emittance growth due to imperfections of crab compensation have been identified. The effect

of amplitude (or voltage) jitter is negligible and can be easily compensated with available low-level RF technology as shown in Table . However, phase jitter from the RF sources is of major concern. A phase error in the RF wave causes an offset of the bunch rotation axis translating into a transverse offset at the IP as shown in Fig. 11. The offset at the IP is given by

$$\Delta x_{IP} = \frac{c\theta_c}{\omega_{RF}}\delta\phi \qquad (7)$$

where θ_c is the full crossing angle and $\delta\phi$ is the phase error.

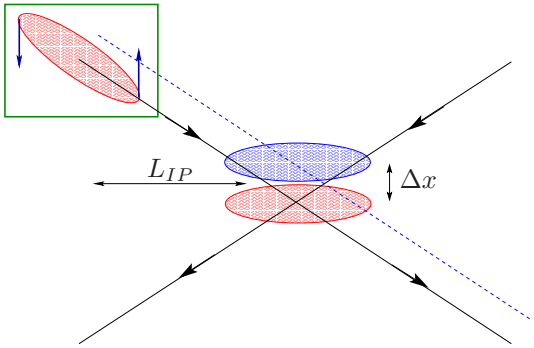

Figure 11: RF phase jitter of the crab compensation results in a transverse offset of the bunch at the IP.

This random offset at the IP is potentially severe due to beam-beam effects. In addition the phase jitter can lead to random dipole kicks on the beam which is expected to result in an even more severe emittance growth than the random IP offsets. For nominal LHC upgrade parameters, and for a maximum emittance growth of 1%/hr and a feedback gain of approximately 0.2, Table shows a list of tolerances derived from analytical estimates [1, 6, 7] using random uncorrelated phase noise (white noise) and some corresponding strong-strong simulations results which represent the most pessimistic scenario. Tolerances feasible by today's technology are also listed.

However, measurements of the phase jitter from the KEK-B crab cavities show that the noise modulation is not "white" but has a frequency spectrum as shown in Fig. 12 (courtesy K. Akai). Sidebands of -65 db below the main RF signal (509 MHz) are visible in a 200 Hz span (32Hz, 37Hz, 46Hz, 50Hz, 100Hz) and sidebands of almost -80db down are visible in a 200 kHz span (32 kHz, 64kHz). A wider span of 3MHz show no visible sidebands above the noise level.

Simulations were performed including beam-beam offset (weak-strong) with frequency dependent noise like the ones in Fig. 12. Fig. 13 shows the emittance growth as a function of the amplitude for three different sine like effects similar to the ones observed in the KEK cavities. A quadratic fit to the 32 KHz (one of the fastest frequencies observed in KEK-B) line suggests a maximum tolerance of $\sigma_{noise} \approx 6 \times 10^{-12}$ m corresponding to an emittance growth of 1% per hour. The measured amplitude of -80db

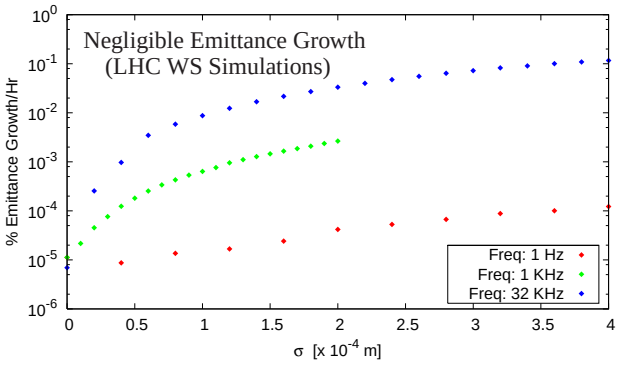

Figure 13: Simulated emittance growth for a beam-beam offset at two IPs modulation at different frequencies (1 Hz, 1KHz, and 32 KHz) at the IP ($\beta^* = 0.25m$) as a function of the modulation amplitude.

translates to an IP offset of 6×10^{-13} m which is an order of magnitude smaller than the maximum tolerance for 1% emittance growth per hour. Also, preliminary simulations in Ref. [8] suggests that the tolerances can be relaxed linearly with the correlation time of the noise source. Since the slow noise sources are the dominant ones, the phase tolerance should be much less stringent than the naive estimates based on white noise. In addition a transverse feedback alleviates some of the tightest requirements.

OPTICS & RF TOLERANCES

Orbit and lattice errors such as linear imperfections, nonlinear imperfections, and coupling can impact the effectiveness of the crab crossing scheme.

- An additional z-dependent horizontal orbit and beta-beating can impact the efficiency of the collimation system and reduce the available aperture. However, the bunch oscillation around the closed orbit can provide an extra degree of freedom to collimate in the longitudinal plane as depicted in Fig. . Tracking studies are underway to determine the additional losses and produce loss maps in order to address the pertinent collimation issues.

- Error in optics functions (β_{crab} & $\Delta\phi_{cc\rightarrow ip}$) are analogous to a voltage error (ΔV_{crab}) which results in residual crossing angle. For example, a betatron phase error ($\Delta\phi_{err} \sim 0.25°$) results in residual angle ($\theta_{res} < 1$ μrad) which is negligible. The $\Delta\phi_{cc\rightarrow ip}$ and/or voltage can be optimized with luminosity & lifetime measurements. An intentional voltage variation can be used for luminosity leveling via the crossing angle. A local β-function modification at cavity location is envisioned to provide an extra degree of freedom and some margin for cavity voltage.

- Betatron coupling in the lattice introduces a vertical crossing angle and offset at the IP. A preliminary estimate using a random tilt error of approximately 1

Table 3: For 1% Emittance Growth/Hr, gain=0.2 (Random turn-to-turn)

Jitter Estimate	Amp.	Phase	
		Beam-Beam	Dip. Kicks
Analytical	$\sim 0.04\%$	0.01° (0.006°)	0.006° (0.003°)
Simulation (WS)		0.002°	-
Simulation (SS, K. Ohmi)		$< 0.001^\circ$	
Feasible Today	0.01%	0.003°	

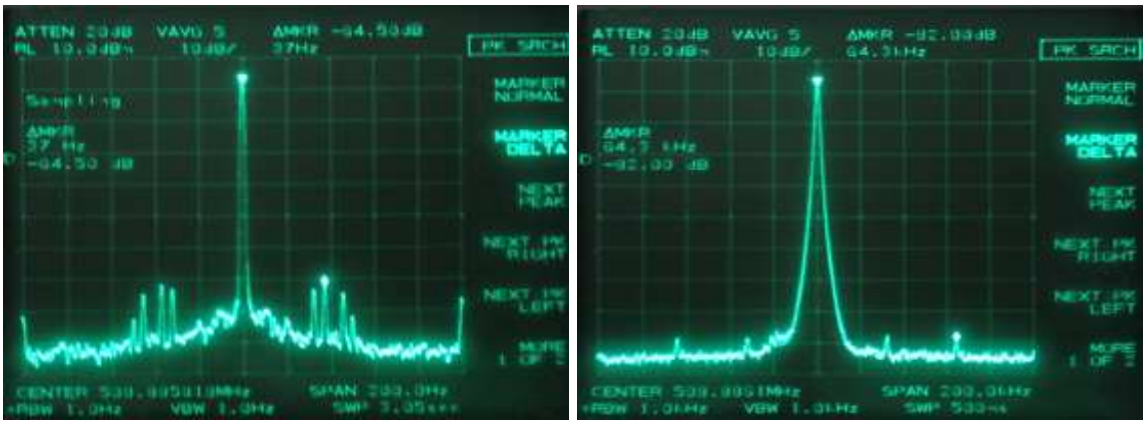

Figure 12: Spectrum of the KEK-B crab cavities during operation with a. frequency span of 200 Hz (left) and 200 kHz (right). The main frequency line is modulated by the side-bands which are approximately -60 dB and -80 db below the main line (Courtesy KEK crab cavity group).

mrad in the quadrupoles, resulting in a $\Delta Q_{min} = 1.5 \times 10^{-3}$, introduces a vertical crossing anlge of approximately 6 μrad which is negligible. Tracking studies are underway to determine the tolerances on coupling errors for operating at the nominal working point.

In addition the effects of synchro-betatron resonance, finite energy spread and chromaticity in the presence of beam-beam effects require extensive simulations which are also underway.

R&D OF CAVITY AND COMPONENTS

An international collaboration is being organized to establish a crab cavity team which will address the various beam dynamics and technical challenges associated with the development of the LHC crab cavities. As a first step towards this R&D, a prototype cavity at 800 MHz is being proposed in order to test several SRF limits with deflecting mode superconducting cavities like:

- Q_0 slope, Max kick gradient (B_{kick}), Multipacting
- RF stability and Tuning
- LOM/HOMs damping to specifications

In addition the prototype will allow a first test of crab crossing with hadron beams and an investigation of the effects of RF curvature, phase noise and other relevant studies.

A preliminary R&D chart outlines the various tasks related to the development of the prototype and the subsequent path towards crab structures for the LHC upgrade is shown in Fig. 14.

CONCLUSION

Extensive studies underway to investigate a small angle crab compensation (0.5 mrad) for the LHC upgrade. It foreseen to improve the LHC luminosity nominal LHC upto 15% and factor of 2-3 for the upgrade scenarios. Two different crab compensation schemes have been described in details along with the challenges associated with the integration of the cavities into the LHC. A preliminary cavity design and corresponding RF characteristics are presented. A prototype R&D program to design and fabricate superconducting RF cavities at 800 MHz both is seen as the first step of the R&D program which will subsequently lead to the crab compensation at the LHC.

ACKNOWLEDGMENTS

We would like to thanks J. Tuckmantel, K. Oide, K. Akai, K. Hosayama, K. Ohmi and the KEK-B crab cavity team for valuable discussions.

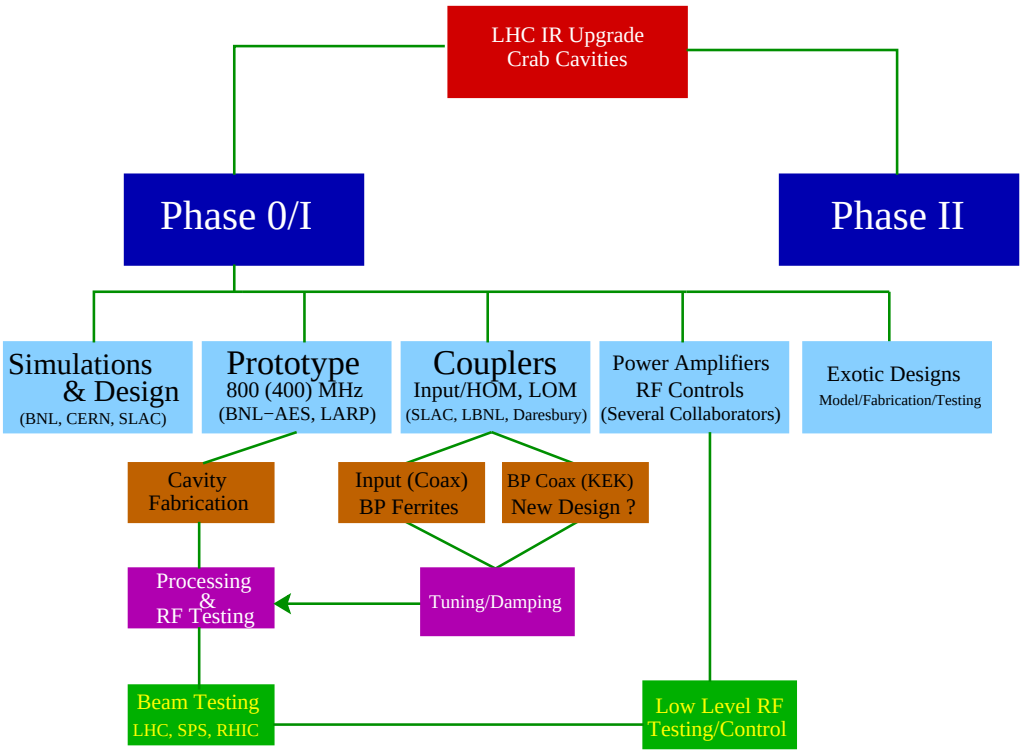

Figure 14: R&D chart for the LHC crab cavity prototype development and fabrication.

REFERENCES

[1] R. Calaga, R. Tomás, F. Zimmermann, Crab cavity option for LHC IR upgrade, in the proceedings of LHC-LUMI-06, Valencia, Spain, 2006.

[2] K. Oide et al., Compensation of the crossing angle with crab cavities at KEK-B, in the proceedings of the particle accelerator conference, Albuquerque, New Mexico, 2007.

[3] J. Tuckmantel, private communication.

[4] K. Hosayama, private communication.

[5] D. Li, Simulations from LBNL cavity ...

[6] F. Zimmermann, U. Dorda, Progress of beam-beam compensation schemes, in the proceedings of LHC-LUMI-05, Arcidosso, Italy, 2005.

[7] J. Tuckmantel,RF & feedback systems for bunch shortening in the proceedings of LHC-LUMI-05, Arcidosso, Italy, 2005.

[8] K. Ohmi, Beam-beam effect with an external noise in LHC, these proceedings.

CRAB WAIST COLLISION STUDIES FOR e+e- FACTORIES

M. Zobov, P. Raimondi, LNF-INFN, Frascati, Italy
D. Shatilov, BINP, Novosibirsk, Russia
K. Ohmi, KEK, Tsukuba, Japan

Abstract

Numerical simulations have shown that the recently proposed "crab waist" scheme of beam-beam collisions can substantially boost the luminosity of existing and future electron-positron colliders. In this paper we describe the crab waist concept and discuss potential advantages that such a scheme can provide. We also present the results of beam-beam simulations for the two currently proposed projects based on the crab waist scheme: the DAΦNE upgrade and the Super B-factory project.

INTRODUCTION

In high luminosity colliders with standard collision schemes the key requirements to increase the luminosity are: the very small vertical beta function β_y at the interaction point (IP); the high beam intensity I; the small vertical emittance ε_y and large horizontal beam size σ_x and horizontal emittance ε_x for minimization of beam-beam effects. However, β_y can not be much smaller than the bunch length σ_z without incurring in the "hour-glass" effect. It is, unfortunately, very difficult to shorten the bunch in a high current ring without exciting instabilities. In turn, the beam current increase may result in high beam power losses, beam instabilities and a remarkable enhancement of the wall-plug power. These problems can be overcome with the recently proposed Crab Waist (CW) scheme of beam-beam collisions [1] where a substantial luminosity increase can be achieved without bunch length reduction and with moderate beam currents.

These advantages have triggered several collider projects exploiting the CW collision potential. In particular, the upgrade of the Φ-factory DAΦNE is aimed at increasing the collider luminosity toward to 10^{33} $cm^{-2}s^{-1}$ [2] to be compared with $1.6x10^{32}$ $cm^{-2}s^{-1}$ obtained during the last DAΦNE run for the FINUDA experiment [3]. At present the upgraded DAΦNE is being commissioned and the first crab waist collisions are expected in the winter/spring 2008 [4]. Besides, the physics and the accelerator communities are discussing a new project of a Super B-factory with luminosity as high as 10^{36} $cm^{-2}s^{-1}$ [5], i.e. by about two orders of magnitude higher with respect to that achieved at the existing B-factories at SLAC [6] and KEK [7]. The decision on the Super B-factory construction will depend much on the results of the CW collision tests at DAΦNE.

In the following we briefly discuss the Crab Waist collision concept and present results of beam-beam simulations for the DAΦNE upgrade and for the Super B-factory project.

CRABBED WAIST CONCEPT

The Crab Waist scheme of beam-beam collisions can substantially increase collider luminosity since it combines several potentially advantageous ideas. Let us consider two bunches with the vertical σ_y, horizontal σ_x and longitudinal σ_z sizes colliding under a horizontal crossing angle θ (as shown in Fig. 1a). Then, the CW principle can be explained, somewhat artificially, in the three basic steps.

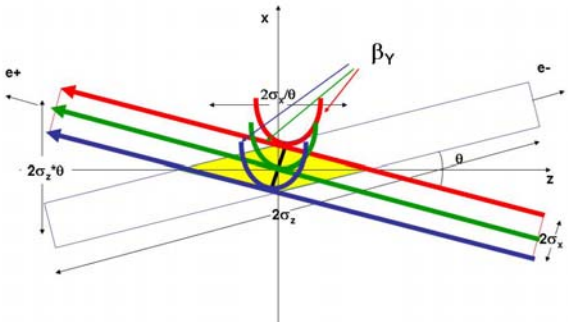

a)

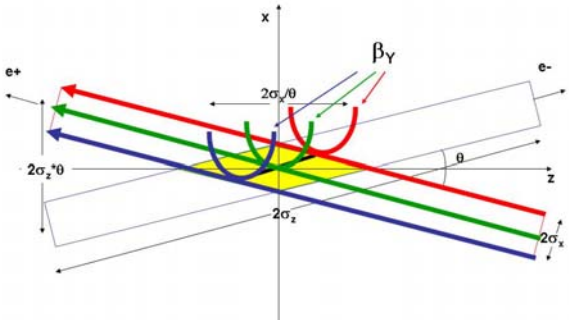

b)

Fig. 1 Crab Waist collision scheme
((a) – crab sextupoles off; (b) – crab sextupoles on)

The first one is large Piwinski angle. For collisions under a crossing angle θ the luminosity L and the horizontal ξ_x and vertical ξ_y tune shifts scale as (see, for example, [8]):

$$L \propto \frac{N\xi_y}{\beta_y^*} \propto \frac{1}{\sqrt{\beta_y^*}}; \quad \xi_y \propto \frac{N\sqrt{\beta_y^*}}{\sigma_z\theta}; \quad \xi_x \propto \frac{N}{(\sigma_z\theta)^2}$$

Here the Piwinski angle is defined as:

$$\phi = \frac{\sigma_z}{\sigma_x} tg\left(\frac{\theta}{2}\right) \approx \frac{\sigma_z}{\sigma_x}\frac{\theta}{2}$$

with N being the number of particles per bunch. Here we consider the case of flat beams, small horizontal crossing angle $\theta << 1$ and large Piwinski angle $\phi >> 1$.

The idea of colliding with a large Piwinski angle is not new (see, for example, [9]). It has been also proposed for hadron colliders [10, 11] to increase the bunch length and the crossing angle. In such a case, if it were possible to increase N proportionally to $\sigma_z\theta$, the vertical tune shift ξ_y would remain constant, while the luminosity would grow proportionally to $\sigma_z\theta$ (see the above formulae for the luminosity and tune shifts). Moreover, the horizontal tune shift ξ_x drops like $1/\sigma_z\theta$. However, differently from [10, 11], in the crab waist scheme described here the Piwinski angle is increased by decreasing the horizontal beam size and increasing the crossing angle. In this way we can gain in luminosity as well, and the horizontal tune shift decreases due the larger crossing angle. But the most important effect is that the overlap area of the colliding bunches is reduced, since it is proportional to σ_x/θ (see Fig. 1).

Then, as the second step, the vertical beta function β_y can be made comparable to the overlap area size (i.e. much smaller than the bunch length):

$$\beta_y^* \approx \frac{\sigma_x}{\theta} << \sigma_z$$

We get several advantages in this case:

- Small spot size at the IP, i.e. higher luminosity L.
- Reduction of the vertical tune shift ξ_y.
- Suppression of synchrobetatron resonances [12].
- Reduction of the vertical tune shift with the synchrotron oscillation amplitude [12].

Besides, there are additional advantages in such a collision scheme: there is no need to decrease the bunch length to increase the luminosity as proposed in standard upgrade plans for B- and Φ-factories [13, 14, and 15]. This will certainly helps solving the problems of HOM heating, coherent synchrotron radiation of short bunches, excessive power consumption etc. Moreover, parasitic collisions (PC) become negligible since with higher crossing angle and smaller horizontal beam size the beam separation at the PC is large in terms of σ_x.

However, large Piwinski angle itself introduces new beam-beam resonances which may strongly limit the maximum achievable tune shifts (see [16], for example). At this point the crab waist transformation enters the game boosting the luminosity. This is the third step. The transformation is described by the Hamiltonian

$$H = H_0 + \frac{1}{2\theta} x p_y^2$$

Here H_0 is the Hamiltonian describing particle's motion without CW; x the horizontal coordinate, p_y the vertical momentum. Such a transformation produces the vertical beta function rotation according to:

$$\beta_y = \beta_y^* + \frac{(s - x/\theta)^2}{\beta_y^*}$$

As it is seen in Fig. 1b, in this case the beta function waist of one beam is oriented along the central trajectory of the other one.

The crab waist transformation gives a small geometric luminosity gain due to the vertical beta function redistribution along the overlap area. It is estimated to be of the order of several percent [17]. However, the dominating effect comes from the suppression of betatron (and synchrobetatron) resonances arising (in collisions without CW) through the vertical motion modulation by the horizontal oscillations [18, 19]. In practice the CW vertical beta function rotation is provided by sextupole magnets placed on both sides of the IP in phase with the IP in the horizontal plane and at $\pi/2$ in the vertical one (as shown in Fig. 2).

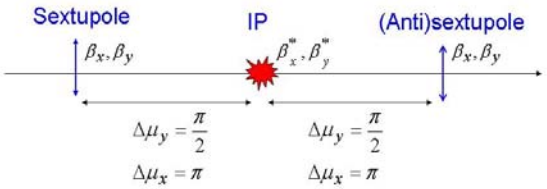

Fig. 2 Crab sextupole locations.

The crab sextupole strength should satisfy the following condition depending on the crossing angle and the beta functions at the IP and the sextupole locations:

$$K = \frac{1}{2\theta}\frac{1}{\beta_y^*\beta_y}\sqrt{\frac{\beta_x^*}{\beta_x}}$$

A numerical example of the resonance suppression is shown in Fig. 3 while beam-beam tails reduction with crab sextupoles is clearly demonstrated in Fig.7.

DAΦNE UPGRADE SIMULATIONS

In order to estimate the achievable luminosity in DAΦNE with the crab waist scheme and to investigate distribution tails arising from beam-beam collisions, which may affect the beam lifetime, simulations with the code LIFETRAC [20] have been performed. The beam parameters used for the simulations are summarized in Table 1. For comparison, the parameters used during the last DAΦNE run with the FINUDA detector (2006-2007) are also shown [3].

As discussed above, in order to realize the crab waist scheme in DAΦNE, the Piwinski angle $\phi = \theta\sigma_x/\sigma_z$ should be increased and the beam collision area reduced: this will be achieved by increasing the crossing angle θ by a factor 2 and reducing the horizontal beam size σ_x. In this scheme the horizontal emittance ε_x will be reduced by a factor of 1.7, and the horizontal beta function β_x lowered from 1.7 to 0.2 m. Since the beam collision length decreases proportionally to σ_x/θ, the vertical beta function β_y can be also reduced by about a factor 3, from 1.7 cm to 0.6 cm. All other parameters will be similar to those already achieved at DAΦNE.

Table 1.Comparison of beam parameters for FINUDA run (2006-2007) and for DAΦNE upgrade

	DAΦNE FINUDA	DAΦNE Upgrade	
$\theta_{cross}/2$ (mrad)	12.5	25	Larger Piwinski angle
ε_x (mm×mrad)	0.34	0.20	
β_x^* (cm)	170	20	
σ_x^* (mm)	0.76	0.20	
$\Phi_{Piwinski}$	0.36	2.5	
β_y^* (cm)	1.70	0.65	Lower vertical beta
σ_y^* (μm)	5.4 (low	2.6	
Coupling, %	0.5	0.5	Already achieved
I_{bunch} (mA)	13	13	
N_{bunch}	110	110	
σ_z (mm)	22	20	
L ($cm^{-2}s^{-1}$) x10^{32}	1.6	10	

Using the parameters of Table 1 and taking into account the finite crossing angle and the hourglass effect luminosity in excess of 1.0x10^{33} $cm^{-2}s^{-1}$ is predicted with the achieved beam currents during the KLOE run, about 6 times higher than the one obtained until now. The only parameter that seems to be critical for a low energy machine is the high vertical tune shift: ξ_y = 0.08, to be compared with the value of 0.03 so far obtained at DAΦNE. In order to check whether these tune shifts (and the luminosity) are achievable we have performed the luminosity tune scans. Figure 3 shows 2D luminosity contour plots in the tune plane for the crabbed waist collisions with the crabbing sextupoles on (left) and off (right), for comparison.

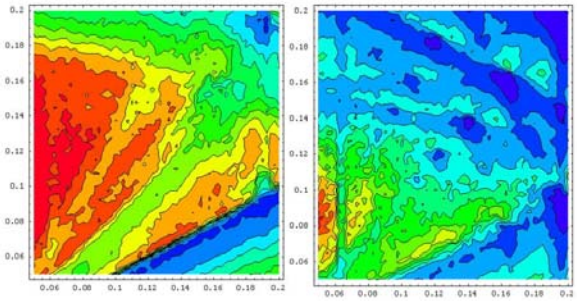

Fig.3 Luminosity tune scan (ν_x and ν_y from 0.05 to 0.20). CW sextupoles on (left), CW sextupoles off (right).

"Geographic map" colors are used to produce the plots: the brighter red colors correspond to higher luminosities (mountains), while the blue colors are used for the lowest ones (rivers and oceans). For each plot 10 contour lines between the maximum and minimum luminosities are drawn. Comparing the two plots in Fig. 3 one can see that the good luminosity region with crabbing sextupoles on is much wider than with sextupoles off since many more betatron resonances arise without CW. The absolute luminosity values are higher in the crabbed waist collisions: a peak luminosity of 2.97x10^{33} cm^{-2} s^{-1} is foreseen against L_{max} = 1.74x10^{33} $cm^{-2}s^{-1}$ in the case without CW. It should be noted that the worst luminosity value obtained with CW (2.5x10^{32} $cm^{-2}s^{-1}$) is still higher than the present luminosity record at DAΦNE. Without CW the lowest luminosity value drops by an order of magnitude, down to L_{min} = 2.78x10^{31} $cm^{-2}s^{-1}$.

Strong-strong beam-beam simulations for DAΦNE upgrade have been carried out with 3D code BBSS [16]. In Fig. 4 one can see the single bunch luminosity as a function of number of turns.

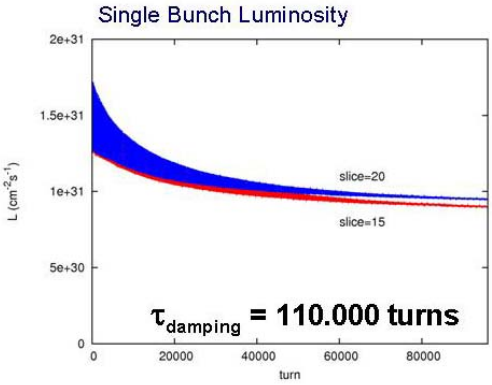

Fig. 4. Luminosity evolution in strong-strong simulations.

The simulations are very much CPU time consuming due to a large number of longitudinal slices required to simulate the crab waist conditions with the vertical beta function smaller than the bunch length. For this reason beam size and luminosity have been tracked over only one damping time. However, already from this picture one can conclude that theoretically the luminosity as high as 10^{33} $cm^{-2}s^{-1}$ (considering 110 bunches circulating in DAΦNE) is achievable and no harmful collective effects like flip-flop or coherent oscillations should be expected.

SUPERB BEAM-BEAM SIMULATIONS

Beam-beam studies for SuperB started with a beam parameters set similar to that of the ILC damping ring (see Table 2).

Table 2. Parameters for early ILC-like design and current SuperB design. For the SuperB, the first entry is for LER and the bracketed numbers are for HER

Parameters	ILC-like	SuperB
ε_x (nm-rad)	0.8	1.6
ε_y (pm-rad)	2	4
β_x (mm)	9	20
β_y (mm)	0.08	0.30
σ_x (μm)	2.67	5.66
σ_y (nm)	12.6	35
σ_z (mm)	6	6
σ_e (x10^{-4})	10	8.4 (9.0)
θ (mrad)	2x25	2x17
N_{part}/bunch (x10^{10})	2.5	6.2 (3.5)
N_{bunch}	6000	1733
Circumference (m)	3000	2250
Damping time τ_s (ms)	10	16
RF frequency (MHz)	600	476

Numerical simulations with LIFETRAC have shown that the design luminosity of 10^{36} $cm^{-2}s^{-1}$ is achieved already with 2-2.5x10^{10} particles per bunch. According to the simulations, for this bunch population the beam-beam tune shift is well below the maximum achievable value. Indeed, as one can see in Fig.5, the luminosity grows quadratically with the bunch intensity till about 7.5x10^{10} particles per bunch. We have used this safety margin to significantly relax and optimize many critical parameters, including damping time, crossing angle, number of bunches, bunch length, bunch currents, emittances, beta functions and coupling, while maintaining the design luminosity of 10^{36} $cm^{-2}s^{-1}$. The optimized set of beam parameters used in simulations is shown in the second column of Table 2. The most recent set of SuperB parameters can be found in [21].

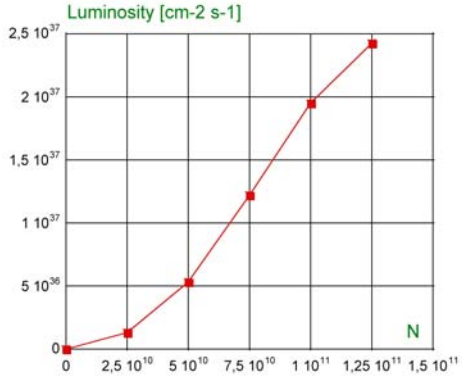

Fig. 5 SuperB luminosity versus bunch intensity

In order to define how large is the "safe" area with the design luminosity, a luminosity tune scan has been performed for tunes above the half integers, which is typical for the operating B-factories. The resulting 2D contour plot is shown in Fig.6. Individual contours differ by 10% in luminosity. The maximum luminosity found inside the scanned area is 1.21x10^{36} $cm^{-2}s^{-1}$, while the minimum one is as low as 2.25x10^{34} $cm^{-2}s^{-1}$. We can conclude that the design luminosity can be obtained over a wide tune area.

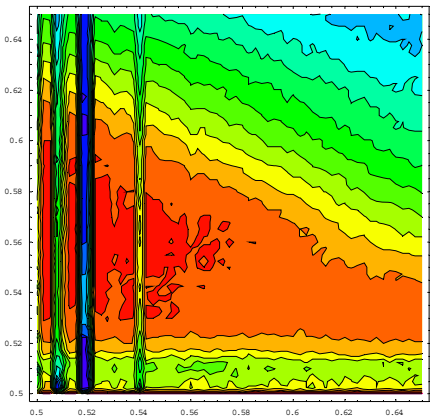

Fig. 6 SuperB luminosity tune scan (horizontal axis - ν_x from 0.5 to 0.65; vertical axis – ν_y from 0.5 to 0.65)

It has also been found numerically that for the best working points the distribution tails growth is negligible. In particular, in Fig. 7 we show distribution tails induced by the beam-beam interaction in the space of normalised betatron amplitudes as a functions of the bunch current. The unit current corresponds to the nominal bunch current, while the numbers under the pictures indicate the vertical size blow up factor – σ_y/σ_{y0}. As it is clearly seen comparing the last two pictures in Fig. 7, the crab sextupoles strongly suppress both the distribution tails and the vertical size blow up.

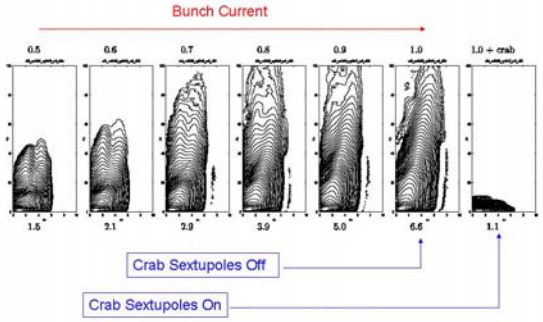

Fig. 7. Beam-beam induced tail growth as a function of bunch current.

CONCLUSIONS

Our studies indicate that by exploiting the crab waist scheme of beam-beam collisions the luminosity of the Φ-factory DAΦNE can be pushed beyond 10^{33} $cm^{-2}s^{-1}$ level, while the luminosity of the low emittance Super B-factory can be as high as 10^{36} $cm^{-2}s^{-1}$.

REFERENCES

[1] P. Raimondi, 2nd SuperB Workshop, Frascati, 2006.
[2] D. Alesini et al., LNF-06/33 (IR), 2006.
M. Zobov et al., e-print Arxiv:0709.3696.
[3] C. Milardi et al., PAC07, p.1457.
[4] M. Biagini et al., PAC07, p.66.
[5] SuperB CDR, e-print Arxiv:0709.3696.
[6] J. Seeman et al., EPAC06, p. 643.
[7] Y. Funakoshi et al., PAC05, p.1045.
[8] D. Shatilov and M. Zobov, ICFA BDN 37, 99 (2005).
[9] K. Hirata, Phys.Rev.Lett.74:2228-2231,1995.
[10] K.Takayama et al., Phys.Rev.Lett.88:144801,2002.
[11] F. Zimmermann, F. Ruggiero, PRSTAB5 :061001.
[12] D. Pestrikov, Nucl.Instrum.Meth. A336, 427 (1993).
[13] J. Seeman, PAC05, p. 2333.
[14] H. Koiso, PAC05, p. 64.
[15] DANAE Letter of Intent, see http://www.lnf.infn.it.
[16] K. Ohmi et al., PRSTAB 7, 104401 (2004).
[17] I. Koop, private communications.
[18] P. Raimondi et al., e-Print:physics/0702033, 2007.
[19] K. Ohmi et al., PAC07, p.1493.
[20] D. Shatilov, Particle Accelerators 52, 65 (1996).
[21] M. Biagini, this Workshop.

DYNAMIC APERTURE STUDIES IN e^+e^- FACTORIES WITH CRAB WAIST

S.Glukhov, E.Levichev, P.Piminov, D.Shatilov, BINP, Novosibirsk, Russia

Abstract

Crab Waist collision scheme being applied to the electron-positron collider may limit a dynamic aperture essentially. In the paper we discuss some aspects of such limitation including low emittance lattice, strong crab sextupoles, crosstalk between beam-beam nonlinear force and lattice nonlinearities, and small multipole errors in the final focus quadrupoles.

INTRODUCTION

Crab Waist (CW) collision approach was proposed recently [1-3] to obtain extremely high luminosity in e^+e^- colliders. This approach exploits two main potentially advantageous ideas.

According to the first idea, the Piwinski angle is increased by decreasing the horizontal beam size (low emittance lattice) and increasing the crossing angle. The most important effect here relates to the reduction of the overlap length of colliding bunches (much smaller than the bunch length) allowing us to obtain an ultra-low β_y at IP (fraction of mm).

However, a large Piwinski angle introduces new beam-beam resonances and may limit the maximum achievable tune shifts. This is where the second advantageous idea – the CW innovation – is required. The CW transformation boosts the luminosity, mainly by suppression of betatron and synchrobetatron resonances.

The CW correction scheme is realized in practice by two sextupole magnets in phase with the IP in the *x* plane and at π/2 in the *y* plane, on both sides of the IP.

The CW scheme features can reduce collider dynamic aperture through the following mechanisms:

- A low-emittance strong-focusing lattice requires a set of powerful sextupole magnets for chromaticity correction.
- The crab sextupoles phased as described above cancel each other exactly in a kick approximation limit. In reality the finite sextupole length and inevitable lattice errors break the cancellation condition.
- An extremely low beta-star at IP provides very large betatron amplitudes in the final focus quadrupoles making them sensitive to the magnetic multipole errors.
- The increased particles density at the interaction point (beam-beam effects) together with the reduced dynamic aperture emphasizes the importance of joint study of these two effects more realistically than before.

Below we consider these sources of the dynamic aperture limitation in the Crab Waist machines in details.

LOW EMITTANCE LATTICE

Some general features of the DA in the low emittance lattice can be found by simple analytic estimation using a well-known sextupole Hamiltonian in harmonic form

$$H = \nu_x J_x + \nu_y J_y + (2J_x)^{3/2}\sum_n [3A_{1n}\cos(\varphi_x - n\theta) + A_{3n}\cos(3\varphi_x - n\theta)] - 3(2J_x)^{1/2}(2J_y)\sum_n [2B_{1n}\cos(\varphi_x - n\theta) + B_{+n}\cos(\varphi_+ - n\theta) + B_{-n}\cos(\varphi_- - n\theta)],$$

where $\theta = s/R$ is the azimuthal angle (an independent variable), R is the average orbit radius and the five types of harmonics ($j = 1,3$)

$$A_{jn} = \frac{1}{48\pi}\sum_m \beta_{xm}^{3/2}(k_2 l)_m \cos(j\psi_x - \nu\theta + n\theta)_m,$$

$$B_{1n} = \frac{1}{48\pi}\sum_m \beta_{xm}^{1/2}\beta_{ym}(k_2 l)_m \cos(\psi_x - \nu\theta + n\theta)_m,$$

$$B_{\pm n} = \frac{1}{48\pi}\sum_m \beta_{xm}^{1/2}\beta_{ym}(k_2 l)_m \cos(\psi_\pm - \nu_\pm\theta + n\theta)_m$$

represent the main structural resonances. Sextupoles are considered as kicks with the normalized integrated strength $(k_2 l)_m$, and the values subscribed by "±" have the form $\psi_\pm = \psi_x \pm 2\psi_y$, etc.

After some manipulation [4, 5] the following simple estimation of the DA size can be found

$$A_x = k_x(\nu_x,\nu_y)\cdot\frac{\sigma_{x0}}{\xi_x}, \quad A_y = k_y(\nu_x,\nu_y)\cdot\frac{\sigma_{y0}}{\xi_y}, \qquad (1)$$

where σ is the beam size at the DA observation point and ξ is the natural chromaticity. Coefficient k depends weakly on the tune point and the lattice details.

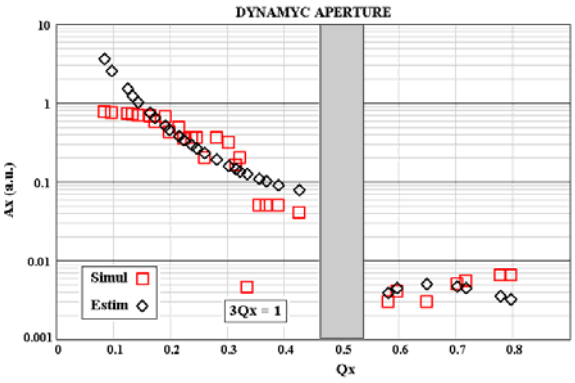

Fig. 1 Horizontal DA size obtained analytically (red) and numerically (black). Grey strip shows the optically unstable area near the half integer resonance.

To verify the above expressions we performed a computer simulation of the DA size as a function of the horizontal tune that unambiguously represents the lattice focusing strength (emittance). The results as they are

shown in Fig.1 demonstrate good correspondence between analytic and numeric calculation.

CRAB WAIST SEXTUPOLES

Betatron phase advance between two (point-like) crabbing sextupoles (see Fig.2) provides an exact cancellation of its influence on DA.

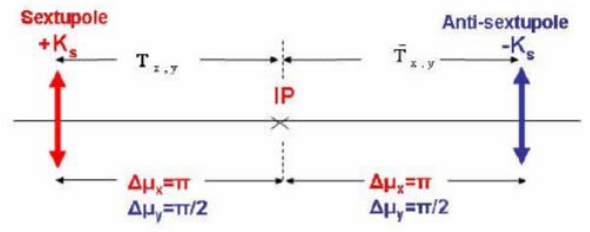

Fig.2 Crabbing sextupoles arrangement

However, due to different reasons (lattice errors, finite length of the sextupoles, chromatic effects, beam-beam effects, etc.) the exact phase tuning breaks and the residue aberration (small but applied for strong sextupoles) influence the dynamic aperture.

We studied these effects numerically for a simple collider model which includes a set of nonlinear beam-beam kicks, two CW sextupoles, two "other" sextupoles, which imitate chromatic sextupoles and a set of matrices providing the betatron phase tuning between the nonlinear elements. The results of the simulation are presented below.

Fig.3 shows a scan of the horizontal DA ratio with and without the linear phase mismatch between the crab sextupoles.

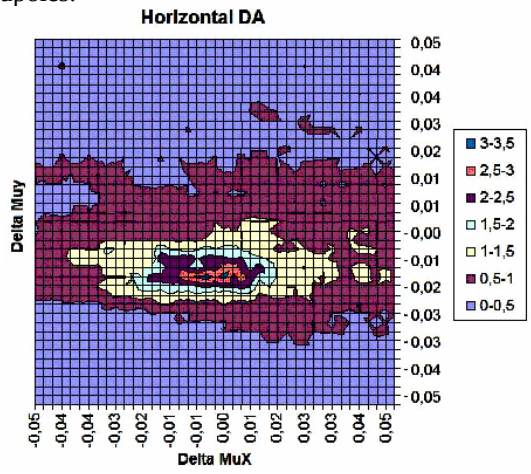

Fig.3 A horizontal DA changes as a function of the betatron phase error between crab sextupoles

The color in the Fig.3 indicates the ratio DA_{error}/DA_{ideal} as a function of the betatron phase error between the crab sextupoles: $\Delta\mu_x = 2\pi n - \mu_x(S_1 - S_2)$, $\Delta\mu_y = \pi n - \mu_y(S_1 - S_2)$. One can see that the residue perturbation of the mismatched crabbing sextupoles interferes with the perturbation from all other (chromatic) sextupoles and can either increase (twice for $\Delta\mu_y = -0.01$) or decrease (twice for $\Delta\mu_y = +0.01$) the dynamic aperture.

The fact that the real sextupole is not a kick-like object but has finite length yields another effect on the DA. Fig.4 shows how the DA reduction depends on the crab sextupole length: for L = 0.2 m the vertical DA shrinks by factor of 3 and the horizontal one twice.

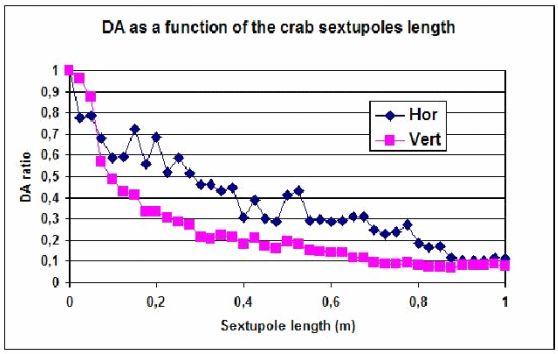

Fig.4 DA reduction vs. the crab sextupole length

BEAM-BEAM AND SEXTUPOLES

Strong sextupole effect (both chromatic and crab) can interfere with the intensive beam-beam interaction and produce a crosstalk in a self-consistent manner: beam-beam interaction reduces a DA initially limited by the sextupoles and the reduced DA gives the beam lifetime degradation through the beam tail growing.

To investigate these phenomena we have combined a beam-beam computer code LIFETRACK [6] with the general tracking code ACCELERATICUM [7] and applied new software to the DAΦNE e^+e^- collider in the Siddharta Crab Waist operation mode [8].

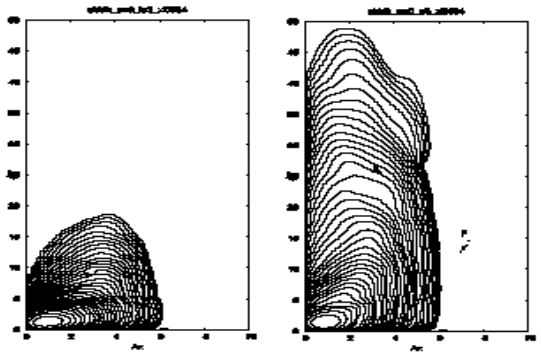

Sextupole off *Sextupole on*

Fig.5 Vertical tail grows due to the joint effect of the BB and chromatic sextupole nonlinearities

The results are given in Figs. 5 and 6. The plots in Figures demonstrate the contour lines for the particle density distribution in the betatron amplitude space. In Fig.5 the beam-beam effects are studied with the chromatic sextupoles on and off. One can see that the sextupoles induce the vertical tail growth, which, in case

of DA deficiency, would degrade the beam lifetime. In Fig.6 the crab sextupoles are added to the chromatic ones and again the chromatic sextupoles are on (right plot) and off (left plot).

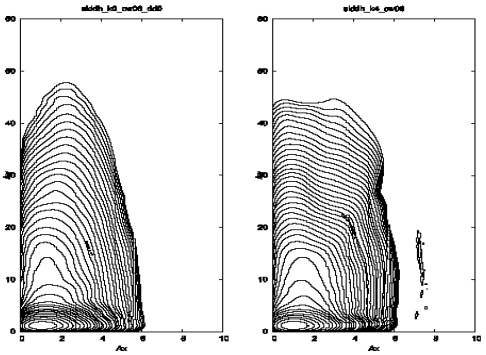

Sextupole off *Sextupole on*

Fig.6 Vertical tail growth due to the joint effect of the BB and chromatic sextupoles is cured by the crab sextupole switched on for both plots

But this time there is no vertical amplitude growth because the crab sextupoles improve the situation for the beam-beam effects in the case of the Crab Waist collision scheme.

MULTIPOLE ERRORS IN THE FF QUADS

High beta values in the final focus quadrupoles and possible offset of the beam orbit in the first quad (due to the large crossing angle) can emphasize the influence of the high multipoles content in the FF quads to the beam dynamics.

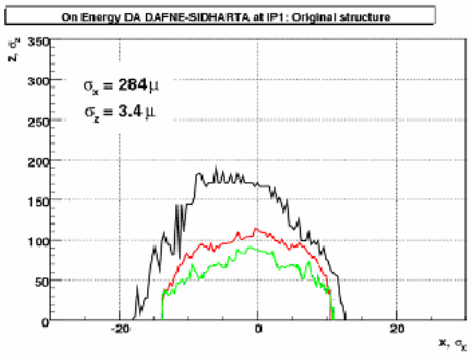

Fig.7 The ideal DA (black) vs. the DA with errors in the FF quadrupoles for the electron (red) and positron (grin) beams

For the Siddharta experiment at DAΦNE new permanent magnet FF quadrupoles were produced by Aster Enterprises Inc. and the magnetic field components were carefully measured by rotating coils. We introduced the harmonic coefficients in the machine lattice and provided particles tracking by the ACCELERATICUM code. As the beams orbit is shifted in the FF quadrupoles by x_0 = ±11 mm, the field expansion coefficients have to be transformed to the shifted coordinate frame according to

$$\left(B_n' + iA_n'\right) = \sum_{k=n}^{\infty}\left(B_n + iA_n\right)\left[\frac{(k-1)!}{(n-1)!(k-n)!}\right]\left(\frac{x_0}{R_0}\right)^{k-n},$$

where R_0 is the coil measuring radius.

The results of the DA calculation with the field errors in the FF quadrupoles are depicted in Fig.7 and one can see that when the multipole errors are taken into account, the vertical DA reduces almost twice as compared to the ideal case.

CONCLUSIONS AND OUTLOOK

Several sources of the DA limitations in the Crab Waist collider have been considered. The conclusions are:

- A low emittance lattice provides general DA reduction according to $A \sim \sigma/\xi$ where σ and ξ are the beam size and natural chromaticity, respectively.
- In spite of the fact that crab sextupoles are properly phased to cancel combined aberrations but lattice errors, finite length, etc. can detune the phasing and cause the DA deterioration.
- Common influence of the BB and lattice nonlinearities should be studied carefully by the special codes, which consider all above effects realistically.
- Crab Waist scheme provides tough constrains to the FF quadrupole multipole errors tolerance.

REFERENCES

[1] P. Raimondi, "Status of the SuperB Effort" presentation at the 2nd Workshop on Super B Factory, LNF-INFN, Frascati, March 2006

[2] P. Raimondi and M. Zobov, DAΦNE Technical Note G-58, April 2003; D. Shatilov and M. Zobov, ICFA Beam Dyn. Newslett. 37, 99 (2005)

[3] P. Raimondi, D. Shatilov, M. Zobov, LNF-07/003 (IR), 2007

[4] E.Levichev and V.Sajaev, Nonlinear phase space study in a low-emittance light source using harmonic approximation, PA, 1997, Vol.56, pp.161-180

[5] V.A. Kvardakov, E. Levichev, Proc of the EPAC'06, Edinburgh, UK (26-30 June 2006). WEPCH038 2002

[6] D.Shatilov, Part. Acc. 52, 65 (1996)

[7] P.Piminov. Master's thesis, BINP, Novosibirsk, 2000 (in Russian)

[8] D.Alesini et al. DAΦNE Note G-68, Frascati, November 28, 2006

SUMMARY OF CARE-HHH IR'07

W. Scandale and F. Zimmermann, CERN Geneva, Switzerland

Abstract

We summarize the highlights and main conclusions of the CARE-HHH-APD mini-workshop on the LHC Interaction Region (IR) upgrade "IR'07" held in Frascati from the 7th to the 9th of November 2007.

OVERVIEW

The IR'07 CARE-HHH-APD mini-workshop was organized at INFN Frascati from the 7th to the 9th of November 2007. The workshop was attended by 39 experts (Fig. 1), about half of whom came from CERN. The workshop scope covered the upgrade of the LHC interaction region (IR), the DAFNE IR upgrade, and plans for SuperB. More specifically, the key topics included the performance and limitations of the LHC-IR upgrade optics, the optimization of new LHC IR triplet magnets, the US-LARP magnet strategy (response to Lucio Rossi's "challenge"), heat deposition, early-separation dipoles, detector-integrated quadrupoles, crab cavities wire compensators and crab-waist collisions. The goals of IR'07 were threefold: (1) to narrow down the possible IR optics options and to converge on magnet parameters, (2) to identify the ingredients of the two LHC upgrade phases, and (3) to strengthen the collaboration with DAFNE/SuperB studies as well as to explore the applicability of advanced IR concepts to the LHC. The workshop web site *http://care-hhh.web.cern.ch/CARE-HHH/IR07* comprises a link to the agenda and talks posted on INDICO.

Figure 1: The IR'07 participants on the workshop site (photo courtesy A. Mostacci and C. Bosteels).

The workshop was structured in 9 sessions:

- **Session 1: introduction**, convener Walter Scandale, with presentations by M. Calvetti, C. Milardi, M. Biagini, W. Scandale, S. Peggs, E. Todesco and D. Tommasini;
- **Session 2: IR triplet magnets**, convener James Strait, with presentations by P. Wanderer, G.L. Sabbi, G. Ambrosio, A. Zlobin and R. Ostojic;
- **Session 3: early separation**, convener Catia Milardi, with presentations by J.-P. Koutchouk, P. Limon, G. Sterbini, W. Scandale and F. Zimmermann;
- **Session 4: optics**, convener Steve Peggs, with presentations by M. Giovannozzi, R. De Maria, R. Tomas, E. Laface and G. Robert-Demolaize;
- **Session 5: energy deposition**, convener Jean-Pierre Koutchouk, with presentations by F. Broggi and E. Wildner;
- **Session 6: D0 and Q0 detector interference**, convener Peter Limon, with presentations by M. Nessi, J. Nash, E. Tsesmelis and S. Peggs;
- **Session 7: beam-beam compensation and crab cavities**, convener Frank Zimmermann, with presentations by U. Dorda, C. Milardi, again U. Dorda, R. Calaga and F. Zimmermann;
- **Session 8: crab waists and flat beams**, convener Marica Biagini, with presentations by M. Zobov, E. Levitchev and P. Raimondi;
- **Session 9: final round table and conclusions**, conveners Walter Scandale and Frank Zimmermann.

A total of 42 talks were delivered in 3 days. They were complemented by four round-table discussions. All presentations were of highest quality and to the point.

HIGHLIGHTS

Unfortunately, due to space and time limitations, we can only present a few selected highlights, somewhat subjectively extracted from the various presentations, as well as from the four round-table discussions.

News from LARP

S. Peggs and A. Zlobin described recent changes in the organization of the US-LARP [1, 2]. T. Markiewicz now is in charge of the accelerator systems, and P. Wanderer

responsible for magnet systems, including HQ model magnets managed by G.L. Sabbi and LQ magnets organized by G. Ambrosio.

Most importantly a new working group was created, called "Joint IR studies" (JIRS), which is the US equivalent of R. Ostojic's LHC IR Upgrade Working Group (LIUWG) at CERN. Both LIUWG and JIRS bring together magnet experts and beam dynamicists. However, JIRS also, and in particular, looks at Nb_3Sn magnets and it investigates other Nb_3Sn magnet applications for an LHC upgrade such as early separation dipoles, Q6, dispersion suppressor dipoles etc., all of which LIUWG does not.

A recent DOE review encouraged LARP to engage in crab-cavity R&D and to participate in a broad crab-cavity collaboration [1]. A Small Business (SBIR) proposal by the Long-Island company Advanced Energy Systems (AES) aims at fabricating an 800-MHz prototype LHC crab cavity. Also a merger of light-source and LHC deflecting-cavity efforts is foreseen.

L. Rossi had "challenged" the US LARP to provide 4–8 Nb_3Sn quadrupoles for the phase-1 upgrade, with the NbTi complement made by CERN. This challenge has formally been expressed in a memo of S. Peggs, who stressed that the single strategic goal of LARP is to make Nb_3Sn magnet technology fully mature for phase 2. The delivery of several cold masses is no longer R&D but would require a "construction project" separate from LARP. Lastly, any Nb_3Sn magnet for phase 1 would need to perform at least as well as the NbTi magnets built at CERN [1].

A. Zlobin presented details of the JIRS organization, which includes two "simulations" task forces, one on operating margins headed by N. Mokhov, the other on accelerator quality and tracking, supervised by G. Robert-Demolaize, and two "studies" task forces, one on optics& layout guided b J. Johnstone, and the second on magnet feasibility led by P. Wanderer [2].

Phase-1 Triplet Magnets

E. Todesco discussed a 130-mm aperture triplet [3]. Quadrupoles based on NbTi could provide $\beta^* = 0.25$ m with 3σ margin for collimation. A conceptual design of such NbTi magnet was presented, including issues related to field quality, stresses and protection. This same triplet could be replaced by one made of Nb_3Sn, which would give more than a factor 2 higher temperature margin.

Magnet R&D

G.L. Sabbi stressed that the LARP HQ130 prototype magnet already meets the specifications on field gradient and aperture for an LHC upgrade [4].

D. Tommasini described a novel procedure of ceramic wet winding for producing high-performance Nb_3Sn dipole coils, developed at CERN. With this production technique a 12-T field was reached at 4.2 K with zero training quenches [5].

Early Separation

J.-P. Koutchouk presented an update on the early-separation upgrade scenario [6]. Full early separation at 25-ns spacing requires the D0 dipole to be at 1.9-m distance from the IP, which can be discarded due to an incompatibility with the detector. J.-P. Koutchouk retained the options of a full early separation scheme with 50-ns spacing, needing a first magnet at 3.8 m from the IP, and of a partial early separation scheme with 1 or 2 long-range encounters at 5σ separation, that would allow moving the D0 dipole further away from the IP towards a distance of 5.6–9.4 m.

To boost the luminosity performance, a partial early separation scheme can be enhanced by an electron lens at a separation of 3σ or by a crab cavity. The latter would yield a 50–70% increase in luminosity. J.-P. Koutchouk also illustrated the benefits from luminosity leveling. The performance which was estimated for the improved early-separation scenario was almost doubled compared with that shown at LUMI'06 [7], while the projected pile up was reduced by a factor 3 or 4.

Quoting the experience at the ISR, where a β^* decrease was implemented within a few weeks, and applying a statistical law ("CPT theorem") for the performance improvement of accelerators that had earlier been proposed by V. Shiltsev [9], J.-P. Koutchouk concluded that 3–4 years are required for an LHC upgrade based on beam-current increase, compared with no more than 1 year for an upgrade aiming at smaller β^* values.

P. Limon studied the integration of D0 or Q0 magnets with the CMS detector [8]. He concluded that the magnets themselves can be built, but that the consequences for the experiment are potentially severe. He sketched a possible organizational path towards a solution.

Round Table Discussion after 3 Sessions

The discussion focused on L. Rossi's challenge. A primary question was whether the magnet development for phase-1 and phase-2 would represent a complementing synergy or divergent goals, and if there actually was a need for Nb_3Sn magnets in the upgrade phase 1. Nb_3Sn promises to be better suited for increased beam losses, and to provide a larger temperature margin, since the available cooling capacity is improved (D. Tommasini, A. Zlobin). There is some evidence to support these positive statements, but not yet a full experimental verification. P. Limon stressed that building phase-1 Nb_3Sn magnets in the US would not be a good return on investment.

It seems unlikely that one can build fully functional phase-2 quadrupoles in time for phase 1. Radiation survival is a concern for intermediate magnets. J. Strait emphasized that one should be sure these magnets do not become a failure point.

Which β^* value might one hope for in phase-1? Reducing β^* to 0.25 m alone gives a marginal return (about 20% increase in the average luminosity). J.-P. Koutchouk explained that the main idea of phase 1 is "to provide margins

in case". The phase-1 IR upgrade must be complemented by other improvements, e.g. crab cavities, collimator upgrade, and linac4, in order to yield a large benefit, as was pointed out by both R. Ostojic and W. Scandale.

Concerning the new technique for fabricating Nb_3Sn coils developed at CERN, how fast could this new procedure become beneficial (if)? Should it be explored in parallel to other magnet development activities? D. Tommasini elaborated that no epoxy is employed in this scheme. However, the mechanical, electrical & thermal properties of the coils still need to be confirmed. Perhaps the question was still premature at this workshop.

How can the effort on the D0 & Q0 detector-embedded magnets be streamlined? P. Limon emhasized that background studies by the experiments are urgently needed. J. Nash qualified that such studies are very expensive, and that a reasonable starting point must be found first. The detector studies involve an intricate shielding optimization for each new set of parameters. S. Peggs stressed that the LARP involvement in this area is limited. Machine experiments in RHIC on the acceptable number of long-range collisions are underway, but given the multidimensional parameter space and the inherent difficulties of beam-beam experiments and their interpretation, no clear final answer should be expected soon, though we might get some hints. J.-P. Koutchouk and J. Nash recommended to proceed in steps and to converge, together with the experiments, towards an optimal solution. P. Limon added that the detector solenoids, the support structures, and the expected heat load all require that the first accelerator magnets be placed more than 6 m away from the IP.

Is the production of a mixed quadrupole triplet in a competitive bid an efficient idea? S. Peggs remarked that the bid was not competitive, and that "perception is not reality". He recommended that the mandate of the CERN LIUWG be adjusted to include Nb_3Sn options and magnetic elements other than the triplets, and that it be aligned with the JIRS mandate. E. Todesco summarized that the reactions to the challenge of L. Rossi were controversial. P. Limon emphasized that the LARP goal consists of only design, papers and one prototype. D. Tommasini commented that a hybrid solution minimizes the risk. He added that spare NbTi quadrupoles will be available as a backup. Field quality in a mixed triplet is another possible matter of concern.

Concerning the crab-cavity experience at KEKB, S. Peggs observed that KEKB is running with crab cavities. R. Calaga and F. Zimmermann pointed out that the KEKB crab cavities restore the geometric luminosity and even increase the beam-beam tune shift, while the KEKB beam current is presently limited by an unrelated problem. The question "would CERN be ready to install crab cavities in the LHC?" was posed by S. Peggs. The effect of crab-cavity noise could in principle be checked in any hadron storage ring.

What are the possible experimental tests of various types of leveling? At BEAM'07 the talks by V. Lebedev and V. Shiltsev reported on the experience at the Tevatron [10]. The interpretation of this experience was controversial. Experimental tests e.g. at RHIC (and at LHC) would be useful.

Should the LHC luminosity be increased via higher current and/or lower beta*? Both approaches may be needed. F. Zimmermann recalled that the Tevatron and the SPS had increased their luminosity primarily with a higher beam current. At the ISR reducing beta* was successful, but the ISR beam currents were extremely high.

What is the minimum acceptable luminosity lifetime? Representatives of the experiments responded that 5 hours would be acceptable. Another statement from the experiments – how fast they can turn on after establishing collisions – was requested and not readily available.

It was speculated whether a large off-momentum beta beating might be acceptable for the "less-critical momentum cleaning" (J.-P. Koutchouk). Answering this question requires a study of the collimation performance with such type of beta beating.

It was already shown that larger-aperture magnets can be produced without increasing the outer magnet diameter. As part of the phase-1 upgrade, the only modification to the LHC IR cryoplants that may be necessary is one for the rf in point 4 (R. Ostojic).

Upgrade Optics

M. Giovannozzi reviewed the optics constraints for the upgrade [12]. He highlighted that aperture and off-momentum beta beating can make a big impact on the collimation performance. He argued that the beta beating is more readily accepted in the momentum cleaning insertion than on the other half of the ring. The available aperture may be optimally used by colliding "flat beams", e.g. beams with unequal IP beta functions [13]. The optimum trade off between beam screen and beam aspect ratio needs to be found.

R. De Maria discussed the choice of the quadrupole gradient for the new triplet magnets [14]. He compared three upgrade optics solutions — the so-called "modular" [15], "low β max" [15] and "symmetric" solution [16] —, and he examined aperture bottlenecks at other IR magnets. He concluded that the long straight sections are pushed to their limits, that optimization at the percent level gives rather large performance differences, and that flat beams will probably be the preferred scheme for pushing the performance at the edge.

R. Tomas presented a correction scheme for nonlinear triplet field errors which is based on minimizing the norm of a Taylor map characterizing the optical transport, using the Python code "MAPCLASS" [17]. The minimization with a set of higher-order correctors reduces the value of the norm by at least 5 orders of magnitude. As a result of this correction, the dynamic aperture increases by 1–2σ, in tracking simulations. R. Tomas also found that the presently chosen quadrupole aperture is about the smallest acceptable value with regard to dynamic aperture: For even

slightly smaller quadrupole diameter the dynamic aperture quickly collapses. Standard scaling laws for the field errors were assumed in his study.

Energy Deposition

E. Wildner described simulations of heat deposition in the triplet quadrupoles for the so-called "symmetric" and "compact" upgrade optics [18]. For the same luminosity, the total heat load per magnet is reduced by up to 50–60% for the larger aperture quadrupoles of the upgrade. As a further mitigation the introduction of a tungsten mask between quadrupoles Q1 and Q2 was studied, as was a 2 cm stainless steel liner covering the inside of the quadrupoles. In particular the liner was very efficient in reducing the peak power density by a factor 20, from 21.5 mW/cm^{-3} to 1.1 mW/cm^{-3}. The latter value is more than a factor 3 below the acceptable design limit of NbTi magnets. E. Wildner also simulated the effect of an early-separation dipole D0 on the peak energy deposition, and she found that the D0 magnet does not increase local heat loads, rather the opposite. Summarizing, the largest aperture quadrupoles are most favorable in view of the heat load from collision debris, and a 2-cm thick liner leads to a dramatic improvement, making a luminosity of 10^{35} cm^{-2}s^{-1} look like a realistic possibility.

Detector Interference

M. Nessi discussed the view of ATLAS. He identified several regions where D0 or Q0 magnets might be embedded in the ATLAS detector [19]. The least problematic region is at the border of the forward shield (JF) and the nose shield (JN), which would also offer a convenient retractable support.

J. Nash, representing CMS, first reminded the audience that the SLHC's priority is the particle physics programme [20]. The performance will be characterized not only by the peak luminosity and not alone by the integrated luminosity, but backgrounds, acceptance and detector pile up also matter. Different physics channels require different conditions. Depending on the channel luminosity, leveling or forward acceptance could prove important. The scenario chosen by nature will not be known until the first data from LHC are available. J. Nash stressed that therefore it is important not to exclude any option at the present stage. On its own, CMS has no need for any changes to the forward region and shielding of its detector. Pile-up studies have been launched, but no definite statement can yet be made on how much pile up CMS will be able to withstand. Any IR modification can lead to rather costly changes of the CMS infrastructure.

Beam-Beam Compensation and Crab Cavities

U. Dorda presented results of long-range beam-beam simulations for the LHC upgrade [21]. He found that at the nominal bunch intensity the dynamic aperture for the "low β max" upgrade optics is about 5.5σ, which decreases to 4.5σ if a D0 magnet is added. The value of the dynamic aperture was determined using the Lyapunov criterion for the detection of an extended region of chaotic trajectories. At the ultimate intensity of 1.7×10^{11} protons per bunch the dynamic aperture with D0 shrinks to about 3σ, suggesting that an electron lens compensator may become indispensible for this upgrade path. For the alternative "large Piwinski angle" (LPA) upgrade scheme, the dynamic aperture, with wire compensator, is about 5σ.

R. Calaga compared the global and local crab cavity schemes for the LHC [22]. He showed a schematic drawing and parameters for a prototype LHC crab cavity operating at 400 or 800 MHz. The global crab scheme leads to a peak orbit change of about 2.5 mm for head and tail particles and to a tune shift on the order of 10^{-4}. RF noise measurements are available from the 500-MHz KEKB crab cavities. Introducing the measured KEKB noise spectrum in LHC simulations, the resulting transverse emittance growth is found to be negligible. R. Calaga outlined an R&D programme which will first lead to a prototype and which should ultimately pave the way towards full crab crossing in the LHC. In addition to the prototype fabrication, other important items in the sketched programme are the cavity design optimization, couplers, amplifiers, rf controls, tuning, low level rf , processing, rf testing and beam testing. Crab cavities will be helpful already for the nominal LHC, and even more so for the upgrade phases 1 and 2.

U. Dorda reported progress on wire compensation and, in particular, on the development of a novel "RF wire", a pulsed compensator [23]. Instead of using fast switches the "RF BBLR" is based on an rf resonator circuit. Its advantages are feasibility and much reduced timing-jitter tolerances. F. Caspers had first proposed this type of device. An early prototype was assembled and its characteristic rise time measured and adjusted in the laboratory. In parallel the rf properties of the conventional wire compensators installed in the SPS were measured, as well as the beam-induced signals on these wires. The ongoing studies prepare the ground for an ultimate implementation of pulsed wire compensators in the LHC.

Round Table on Long-Range Collisions, Wire Compensators, and Crab Cavities

The round-table discussion after this session reached the following conclusions. With the upgrade, the long-range beam-beam effects become more important, but they are no showstopper. The wire compensator is essential for upgrade phase 2 and even before. It typically gains 2σ in aperture for the various upgrade schemes. A controversial question was the maximum number of "low-distance" ($\sim 5\sigma$) long-range encounters that can be accepted. The answer may depend on many other parameters, such as beam energy, lattice, chromaticity and tunes. The interpretation of the experience at Tevatron, RHIC and SPS appears ambiguous. Reliable simulations tools are needed to answer the

question for a specific case. The interplay of the long-range collisions with the head-on beam-beam interaction is also important and must be taken into account.

Another critical question raised at the round table is whether, with the large triplet qudrupoles, we can open the collimators to 9σ if the dynamic aperture is at a lower amplitude of 5–7σ. This question should be addressed by the collimation team.

A wire compensator was successful at DAFNE, where it yielded a higher average luminosity. There is a good understanding of its beneficial effect. Also a partial compensation with octupoles had a positive influence in DAFNE.

The SPS wire machine experiments of 2007 at 37 and 5 GeV indicate the existence of a current "threshold" for the long-range beam-beam effect. Below the threshold the beam lifetime is not affected by the long-range collisions. If confirmed, this threshold would drive the parameters of the early-separation upgrade scheme.

In LHC simulations, a dc wire can have a beneficial effect, but a pulsed wire would further improve the dynamic aperture of all bunches and, hence, the overall beam lifetime.

The impact of crab cavities on the collimation system will also need to be studied by the collimation team, in particular for the global crab scheme.

The funding of the auxiliary upgrade devices is an unresolved issue. An SBIR proposal was submitted by a Long Island company (AES) to the US DOE for building an LHC crab-cavity prototype. Funding for LHC wire compensators and especially for pulsed wire compensators must still be found.

Crab Waist

M. Zobov explained the ideas underlying the "crab waist" scheme, which combines a large Piwinski angle, a vertical IP beta function comparable to the overlap area, and a crab-waist sextupole transformation which shifts the location of the vertical waist as a function of the horizontal position so as to maximize the luminosity [24]. The betatron phase advance from the sextupole to the collision point is $\pi/2$ in the vertical plane, and π horizontally. The "crab waist" scheme was first proposed by P. Raimondi for the SuperB factory [25]. The recently completed DAFNE IR upgrade includes a large crossing angle with crab waist (see Fig. 2). The crab-waist arrangement suppresses X-Y resonances, leading to much reduced sensitivity to the working point and much higher luminosity. The absence of X-Y resonances is intuitively clear, and this as well as the higher luminosity are confirmed in beam-beam simulations. Instead of the X-Y resonances, the crab-waist simulations reveals sets of narrow synchrotron sideband resonances localized around the integer and half integer tunes. Weak strong beam-beam simulations for the DAFNE upgrade indicate a possible luminosity gain by a factor of 10 or more, partly thanks to the crab waist (which alone contributes a factor 2–10 depending on the working point). The luminosity is further raised by shortening bunches, reducing the vertical beam size and increasing the beam current. According to the simulations, the beam-beam limit is well above the reachable current values ($\sim$2 A).

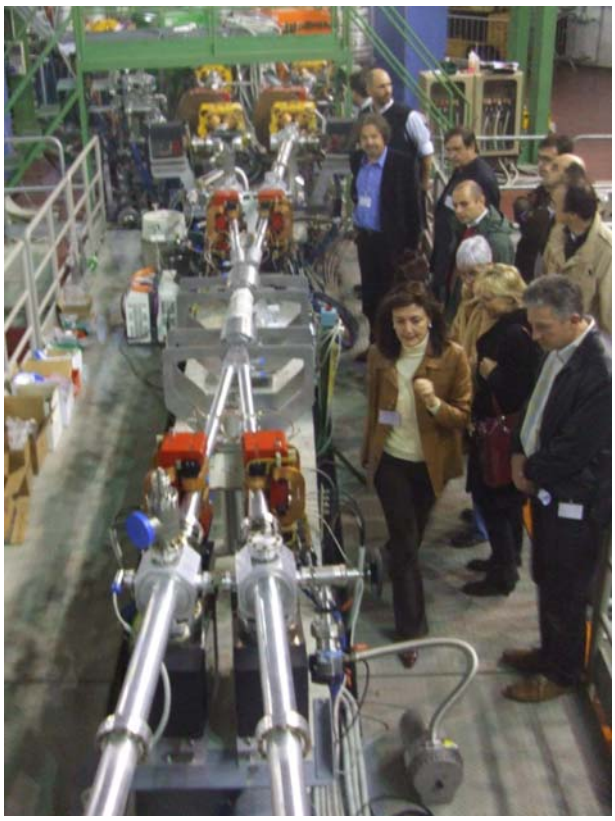

Figure 2: IR07 tour of the new DAFNE IR with large Piwinski angle and crab waist.

IR'07 CONCLUSIONS

The final round table discussion addressed 7 issues: (1) strategy for scenarios, (2) trade off between experiments & accelerator, (3) leveling and large Piwinski angle - where, how, real test?, (4) strategy for magnets, (5) strategy for wires, (6) strategy for crab cavities, and (7) strategy for crab waist in hadron colliders. We now report the answers and comments on each of these issues one by one.

Strategy for Scenarios

The convergence on the triplet-magnet parameters should be easy, which is good since the triplet development also has the longest lead time among all upgrade components. For lowest β^* values, the early separation scheme is not the only option, but full crab crossing would be an interesting alternative not requiring magnets embedded inside the detectors.

The various upgrade components should be decoupled from each other. A possible approach is to wait for the

LHC beam before optimizing phase-2 parameters or even the earlier phase 1; in the words of S. Peggs, "what will beam say?".

Possibly the phase-2 upgrade could consist solely of adding crab cavities.

Trade Off between Experiments & Accelerator

The input from the machine to the experiments should ideally come now. However, the experiments need to wait for the first physics results before being able to conclude on the viability of various upgrade scenarios. It was pointed out that, therefore, we need to take some risk.

Leveling and Large Piwinski Angle - Where, How, Real Test?

Experimental tests of hadron-beam collisions with a large Piwinski angle could be performed either at RHIC or in the LHC itself. Such tests could be decisive for proving the feasibility of the "LPA" upgrade scheme.

For the purpose of luminosity leveling, the orbit angle can be varied either with the early separation dipole or with the crab voltage. Leveling with β^* could be attempted right from the start, even at the nominal LHC. The experiments remarked that they have no interest in luminosity leveling for the nominal LHC, neither for its phase-1 upgrade, but only for phase 2. However, there is yet another reason for leveling with the crossing angle: it may circumvent the beam-beam limit and allow for higher bunch charges, resulting in higher integrated luminosities. An IP feedback will assist in any form of leveling, "or perhaps not" (the example of RHIC was quoted).

Strategy for Magnets

Magnet issues involve cost, technicalities, and even power converters. A large-aperture D1 dipole as a standalone object could be another possibility for US-LARP contributions, with the advantage of being asynchronous with the phase 1 upgrade.

It was asked whether today we already have a definition of D1 for phase 2. However, the D1 parameters will depend on the optics solution adopted. The D1 magnet is by no means trivial, but challenging as well.

Also, the time scale of the phase 2 upgrade must be kept in mind. It is not easy to make a decision now.

The aperture of new triplet quadrupoles should be 130 mm in view of collimator requirements.

Nb_3Sn options and financial aspects were also discussed.

Strategy for Wires

Wire compensators should be installed as soon as possible in the LHC, or, rather, as soon as the beam current requires it. The installation could be paid from the LHC operations budget.

Strategy for Crab Cavities

Different types of crab cavity schemes can be distinguished: global and local ones; small angle vs. large angle crab crossing etc. The recommendation of IR'07 is to gain experience with small-angle crab crossing in phase 1. If successful, one could go to larger angles in phase 2. Feedback from the collimation study concerning the impact of crab cavities on the cleaning efficiency is needed. A global crab cavity scheme might be the most attractive to start with, since it is the cheapest and one could easily adjust in case of problems and e.g. switch back to no-crab collisions. Crab cavities neatly fit into the US program, and they might also be included in the European FP7.

Strategy for Crab Waist in Hadron Colliders

The crab waist could be useful in conjunction with higher brightness from a new injector complex. A "flat" optics with NbTi quadrupoles might provide β^* values of 15 cm $\times$ 30 cm; possibly slightly smaller beam sizes could be reached with Nb_3Sn magnets. Crab waists are well adapted to the large Piwinski angle regime, combined with the lowest possible β^*. The DAFNE experience with crab waist will be an important input for this upgrade option.

SUMMARY OF IR'07 SUMMARY

All auxiliary systems, particularly wires and crab cavities, received a strong boost.

The energy deposition adds an important criterion to the optics requirements; more realistic configurations should be explored. A 2-cm stainless steel linear was considered as a first attempt.

Improved upgrade designs were presented which promise higher and better luminosity than forecast at LUMI'06 in Valencia.

The field quality and temperature margin of Nb_3Sn magnets remain uncertain.

Only two phase-1 IR optics solutions were retained, namely the so-called "low β max" and the "symmetric" optics.

Conflicting time scales were evidenced between the experiment and accelerator upgrades: though the machine input to the experiments is requested now, the experiments need LHC physics results to determine the essential constraints for narrowing down the options of the machine upgrade.

ACKNOWLEDGEMENTS

We acknowledge the support of the European Community-Research Infrastructure Initiative under the FP6 "Structuring the European Research Area" programme (CARE, contract number RII3-CT-2003-506395).

REFERENCES

[1] S. Peggs, "News from LARP," CARE-HHH-APD workshop IR'07, Frascati, 7-9 November 2007, these proceedings.

[2] A. Zlobin, "LARP Joint IR Studies," CARE-HHH-APD workshop IR'07, Frascati, 7-9 November 2007, these proceedings.

[3] E. Todesco, "Design Issues in a 130 mm Aperture Triplet," CARE-HHH-APD workshop IR'07, Frascati, 7-9 November 2007, these proceedings.

[4] G.L. Sabbi, "High Field Nb3Sn Magnets," CARE-HHH-APD workshop IR'07, Frascati, 7-9 November 2007, these proceedings.

[5] D. Tommasini, "CERN Plans on High-Field Magnet Development," CARE-HHH-APD workshop IR'07, Frascati, 7-9 November 2007, these proceedings.

[6] J.-P. Koutchouk, "New Results on the Early Separation Scheme," CARE-HHH-APD workshop IR'07, Frascati, 7-9 November 2007, these proceedings.

[7] J.-P. Koutchouk, "Strong Focusing Insertion Solutions for the LHC Luminosity Upgrade," Proc. CARE-HHH-APD workshop LHC-LUMI-06, CERN Report CERN-2007-002, p. 43 (2007).

[8] P. Limon, "Integrating LHC Upgrades with CMS," CARE-HHH-APD workshop IR'07, Frascati, 7-9 November 2007, these proceedings.

[9] V. Shiltsev, "'CPT Theorem' for Accelerators," Symposium for Alvin Tollestrup, FNAL-Conf-04/126 (2004).

[10] V. Lebedev, "Leveling with β^*," and V. Shiltsev, "Luminosity Performance," CARE-HHH-APD Workshop BEAM'07, CERN October 2007.

[11] P. Limon, "Integration Issues for D0 and Q0," CARE-HHH-APD workshop IR'07, Frascati, 7-9 November 2007, these proceedings.

[12] M. Giovannozzi, "Optics Issues for the Phase 1&2 Upgrades," CARE-HHH-APD workshop IR'07, Frascati, 7-9 November 2007, these proceedings.

[13] S. Fartoukh, "Flat Beam Optics," LHC MAC, 16.06.2006.

[14] R. De Maria, "Phase-1 Optics: Merits and Challenges," CARE-HHH-APD workshop IR'07, Frascati, 7-9 November 2007, these proceedings.

[15] O. Bruning, R. De Maria, R. Ostojic, "Low Gradient, Large Aperture IR Upgrade Options for the LHC compatible with Nb-Ti Magnet Technology," CERN-LHC-Project-Report-1008 (2007).

[16] J.-P. Koutchouk et al, "A Solution for Phase-One Upgrade of the LHC Low-Beta Quadrupoles Based on Nb-Ti," CERN-LHC-Project-Report-1000 (2007).

[17] R. Tomas, "IR Multiplar Correction for the LHC Upgrade," CARE-HHH-APD workshop IR'07, Frascati, 7-9 November 2007, these proceedings.

[18] E. Wildner, "Are Large Aperture NbTi Magnets Compatible with 1e35?," CARE-HHH-APD workshop IR'07, Frascati, 7-9 November 2007, these proceedings.

[19] M. Nessi, "SLHC, ATLAS Considerations," CARE-HHH-APD workshop IR'07, Frascati, 7-9 November 2007, these proceedings.

[20] J. Nash, "CMS Views on SLHC Upgrades," CARE-HHH-APD workshop IR'07, Frascati, 7-9 November 2007, these proceedings.

[21] U. Dorda, "Beam-Beam Issues for Phase 1 and Phase 2," CARE-HHH-APD workshop IR'07, Frascati, 7-9 November 2007, these proceedings.

[22] R. Calaga, "Small Angle Crab Crossing," CARE-HHH-APD workshop IR'07, Frascati, 7-9 November 2007, these proceedings.

[23] U. Dorda, "Wire Compensation Performance, MDs, Pulsed System," CARE-HHH-APD workshop IR'07, Frascati, 7-9 November 2007, these proceedings.

[24] M. Zobov, "Crab Waist Collision Studies for e+e- Factories," CARE-HHH-APD workshop IR'07, Frascati, 7-9 November 2007, these proceedings.

[25] P. Raimondi, 2nd SuperB Workshop, Frascati, 16–18 March 2006.

List of IR'07 Participants

Ambrosio	Giorgio	Fermilab
Biagini	Maria	INFN
Boosteels	Claudine	CERN
Broggi	Francesco	INFN
Calaga	Rama	BNL
Cerutti	Francesco	CERN
De Maria	Riccardo	CERN
Dorda	Ulrich	CERN
Fartoukh	Stephane	CERN
Giovannozzi	Massimo	CERN
Hessey	Nigel	CERN
Kirby	Glyn	CERN
Koutchouk	Jean-Pierre	CERN
Laface	Emanuele	CERN
Levitchev	Evgeni	BINP
Limon	Peter	Fermilab
Lovato	Alessandro	Universita La Sapienza
Milardi	Catia	INFN
Nash	Jordan	CERN
Nessi	Marzio	CERN
Ostojic	Ranko	CERN
Peggs	Steve	BNL
Petracca	Stefania	INFN
Robert-Demolaize	Guillaume	BNL
Sabbi	Gianluca	BNL
Scandale	Walter	CERN
Sterbini	Guido	CERN
Strait	James	Fermilab
Todesco	Ezio	CERN
Tomas Garcia	Rogelio	CERN
Tommasini	Davide	CERN
Tsesmelis	Emmanuel	CERN
Wanderer	Peter	BNL
Wildner	Elena	CERN
Zimmermann	Frank	CERN
Zlobin	Alexander	Fermilab
Zobov	Mikhail	INFN